

## **Dynamics of photosynthetic complexes in the thylakoid membranes from higher plants**

Góral, Tomasz Krzysztof

For additional information about this publication click this link.

<http://qmro.qmul.ac.uk/jspui/handle/123456789/2354>

Information about this research object was correct at the time of download; we occasionally make corrections to records, please therefore check the published record when citing. For more information contact [scholarlycommunications@qmul.ac.uk](mailto:scholarlycommunications@qmul.ac.uk)



# Dynamics of photosynthetic complexes in the thylakoid membranes from higher plants

Author:

Tomasz Krzysztof Góral

A thesis submitted for the degree of  
Doctor of Philosophy

---

London 2011

---

## Declaration

I certify that unless otherwise stated in the text, this thesis is written entirely by myself and the research to which it refers is the product of my own work. Any ideas or quotations from the work of other people, published or unpublished are fully acknowledged in a format which accords with the norms for the discipline.

The research was carried out with guidance and supervision of Professor Conrad Mullineaux and Professor Alexander Ruban.

Tomasz Krzysztof Goral

## Abstract

Photosynthetic machinery in higher plants is localised in the thylakoids enclosed in a chloroplast. To optimise and regulate the photosynthetic efficiency under different, rapidly changeable environmental conditions the dynamics of the thylakoid membrane components is required. It has been invoked in several contexts, for example during assembly and turnover of the photosynthetic apparatus, regulation of light-harvesting and photosynthetic electron transport. In this study, by employing a confocal FRAP technique combined with freeze-fracture electron microscopy, I addressed a fundamental problem of visualising the mobility and distribution of photosynthetic complexes in a direct way close to the situation *in vivo* - the thylakoids of intact chloroplasts isolated from green plants. Firstly, I provided direct evidence that the dynamic changes in the distribution of photosynthetic complexes are involved in two high-light related physiological phenomena, namely photoinhibition and non-photochemical quenching. My study indicates that the photoinhibited membranes exhibit an elevated level of protein mobility accompanied by a decreased spacing between the complexes with the opposite effect observed in the photoprotective state. Secondly, my work allowed the identification of some key elements that are responsible for controlling the mobility under different physiological conditions such as: (1) phosphorylation of PSII core complexes after photoinhibition, (2) PsbS protein enhancing the membrane fluidity in a dark-adapted state and decreasing it after light treatment, (3) different xanthophyll composition of light-harvesting antenna with particular attention being paid to zeaxanthin which decreases the size of mobile fraction, (4) the degree of macromolecular crowding and the organisation of PSII-LHCII supercomplexes in the grana membranes which is dependent strongly on individual light-harvesting proteins, the minor antenna

complexes in particular. Lastly, a completely new approach of visualising the mobility of photosynthetic machinery in intact leaves has been introduced as a useful tool to study different aspects of plant acclimation and physiology under natural conditions.

# Table of contents

Abstract .....	3
List of figures .....	10
List of tables .....	17
Abbreviations .....	19
<b>Chapter I: INTRODUCTION .....</b>	<b>21</b>
1.1. Architecture of the thylakoid membrane network in green plants.....	23
1.2. Organisation of photosynthetic complexes in the thylakoid membranes of higher plants.....	30
1.2.1. Organisation of PSII-LHCII supercomplexes in the grana .....	31
1.2.2. Organisation of photosynthetic complexes in stroma lamellae.....	38
1.3. Flexibility and acclimation of photosynthetic membranes.....	40
1.4. Diffusion of proteins in living cells .....	46
1.5. Current knowledge about the mobility of photosynthetic proteins.....	47
<b>Chapter II: MATERIALS AND METHODS .....</b>	<b>56</b>
2.1. Plant material .....	57
2.2. Isolation of intact chloroplasts.....	59
2.3. Isolation of grana membranes.....	59
2.4. Control experiments with glutaraldehyde and nigericin .....	60
2.5. Experiments with sodium fluoride.....	61
2.6. Induction of different de-epoxidation states of the xanthophyll cycle pool in intact chloroplasts .....	61
2.7. Maintenance of NPQ state in intact chloroplasts.....	62
2.8. Photoinhibitory treatment of intact chloroplasts.....	64
2.9. Photoinhibitory treatment of grana membranes .....	64

2.10.	Sample preparation for FRAP.....	66
2.10.1.	Experiments on isolated intact chloroplasts .....	66
2.10.2.	Experiments on isolated grana membranes .....	66
2.10.3.	Experiments on intact leaves .....	67
2.11.	FRAP measurements .....	67
2.11.1.	Experiments on isolated intact chloroplasts and grana membranes .....	67
2.11.2.	Experiments on intact leaves .....	68
2.12.	Image processing and FRAP data analysis .....	68
2.13.	Thin section electron microscopy .....	72
2.14.	Freeze-fracture electron microscopy .....	72
2.15.	Electron microscopy image analysis .....	72
<b>Chapter III: OPTIMISATION OF FRAP EXPERIMENTS.....</b>		<b>74</b>
3.1.	Theoretical background.....	75
3.2.	Visualisation of chloroplast intactness.....	79
3.3.	FRAP experiments in isolated intact chloroplasts: controls.....	81
<b>Chapter IV: MOBILITY OF CHLOROPHYLL-PROTEINS: EFFECTS OF PHOTOINHIBITION AND PROTEIN PHOSPHORYLATION .....</b>		<b>86</b>
4.1.	Photoinhibition phenomenon.....	87
4.2.	Mobility of chlorophyll-proteins in dark adapted intact spinach chloroplasts 88	
4.3.	Effect of photoinhibition on the mobility of chlorophyll-proteins in intact spinach chloroplasts .....	90
4.4.	Effect of photoinhibition on the mobility of chlorophyll-proteins in isolated grana membranes .....	92

4.5. Mobility of chlorophyll-proteins in intact spinach chloroplasts in the presence of an uncoupler .....	93
4.6. Mobility of chlorophyll-proteins under photoinhibitory conditions: effect of reversible protein phosphorylation.....	94
4.7. Correlation of protein mobility with supramolecular organisation .....	97

**Chapter V: DYNAMICS OF PHOTOSYNTHETIC COMPLEXES DURING PHOTOPROTECTIVE DISSIPATION OF LIGHT ENERGY..... 105**

5.1. Non-photochemical quenching phenomenon .....	106
5.2. Structural changes in the thylakoid membrane network upon formation of the photoprotective state .....	109
5.2.1. Thin section electron microscopy .....	110
5.2.2. Freeze-fracture electron microscopy.....	114
5.2.3. FRAP measurements.....	120
5.3. The role of PsbS protein in modulating the mobility of photosynthetic proteins	123
5.3.1. Freeze-fracture electron microscopy.....	123
5.3.2. FRAP measurements.....	129
5.4. The effect of varying xanthophyll composition within LHCII antenna on the mobility of chlorophyll-proteins in the thylakoid membranes .....	132
5.4.1. FRAP measurements.....	132
5.4.2. Freeze-fracture electron microscopy.....	135

**Chapter VI: THE ROLE OF LIGHT-HARVESTING ANTENNAE IN CONTROLLING THE DYNAMICS AND MACROMOLECULAR ORGANISATION OF PHOTOSYNTHETIC COMPLEXES IN THE GRANA MEMBRANES..... 142**



6.1. Introduction .....	143
6.2. Freeze-fracture electron microscopy in different light-harvesting antenna mutants of <i>Arabidopsis thaliana</i> .....	144
6.2.1. Analysis of PSII particles organised in semi-crystalline arrays ..	145
6.2.2. Analysis of PSII particle sizes .....	154
6.2.3. Distribution of PSII particles in the grana membranes: clustering and density .....	159
6.2.4. Distribution of LHCII particles in the grana membranes: clustering, density and particle sizes .....	165
6.3. Mobility of chlorophyll-proteins in light-harvesting antenna mutants of <i>Arabidopsis thaliana</i> .....	169
6.4. Correlation of protein mobility with macromolecular organisation of photosynthetic complexes in the grana membranes.....	172
6.5. Correlation of protein mobility with the amount of non-photochemical quenching (NPQ) .....	174
6.6. Solubilisation and re-stacking of the thylakoid membranes in light-harvesting antenna mutants of <i>Arabidopsis</i> .....	175

**Chapter VII: PROBING THE DYNAMICS OF PHOTOSYNTHETIC COMPLEXES IN INTACT LEAVES ..... 183**

7.1. Introduction .....	184
7.2. Visualisation of chloroplasts in intact leaves .....	185
7.3. Mobility of chlorophyll-proteins in grana membranes of intact leaves chloroplasts .....	187
7.3.1. FRAP measurements on chloroplasts in different higher plant species .....	187

7.3.2. Probing the mobility of chlorophyll-proteins in intact leaves of tobacco photosystem II mutants.....	190
<b>Chapter VIII: DISCUSSION .....</b>	<b>194</b>
8.1. Introduction .....	195
8.2. Confocal FRAP as a useful tool for probing the dynamics of photosynthetic complexes in the intact thylakoid membrane network.....	196
8.3. Enhancement of the mobility of chlorophyll-proteins under photoinhibitory conditions .....	201
8.4. Dynamic and structural changes of PSII and LHCII protein complexes within the grana membranes during photoprotective energy dissipation: the role of xanthophyll composition and the PsbS protein .....	207
8.5. The role of light-harvesting antennae in controlling the mobility and the organisation of photosynthetic complexes in the thylakoid membranes .....	220
8.6. Mobility of chlorophyll-proteins is dependent on the macromolecular crowding in the thylakoid membranes .....	232
<b>Chapter IX: SUMMARY AND FUTURE WORK.....</b>	<b>235</b>
<b>References .....</b>	<b>239</b>
<b>Appendix 1 .....</b>	<b>264</b>

## List of figures

Figure 1.1. Thin-section electron micrograph of green plant chloroplast.....	23
Figure 1.2. Computer-generated model of a helical arrangement of stroma thylakoids around the granum body.....	26
Figure 1.3. Computer-generated visualization of the Pairwise Organisation Model of the granum.....	27
Figure 1.4. Schematic model showing the key photosynthetic protein machinery involved in oxygenic photosynthesis in higher plants .....	30
Figure 1.5. Schematic diagram showing localization of different components in the core of Photosystem II .....	33
Figure 1.6. Schematic representation of the C <sub>2</sub> S <sub>2</sub> M <sub>2</sub> supercomplex based on the electron microscopy images from spinach .....	35
Figure 1.7. Freeze-fracture electron micrograph showing the PSII complexes in the thylakoid membranes of intact chloroplast from wild-type <i>A.thaliana</i> forming a two-dimensional crystalline array.....	36
Figure 1.8. Schematic representation of PSI-LHCI complex showing location of different proteins composing the core and peripheral antenna system regions.....	39
Figure 1.9. Schematic diagram showing the mechanism of state transitions.....	43
Figure 2.1. PAM chlorophyll fluorescence measurement on intact spinach chloroplast .....	62
Figure 2.2. PAM chlorophyll fluorescence induction trace of intact spinach chloroplast light-treated at 350 $\mu\text{mol photons m}^{-2}\text{s}^{-1}$ at 22°C in a Peltier device temperature-controlled cuvette .....	63

Figure 2.3. Photoinhibition of intact spinach chloroplasts monitored by PAM fluorometry .....	65
Figure 2.4. Deconvolution of confocal images performed by DeconvolutionJ plugin of the NIH ImageJ software.....	70
Figure 3.1. One dimensional FRAP .....	76
Figure 3.2. Two dimensional FRAP .....	77
Figure 3.3. Schematic diagram showing the idea of FRAP experiment performed on the thylakoid membranes in intact chloroplasts.....	79
Figure 3.4. Confocal fluorescence images of intact and broken chloroplasts from spinach.....	80
Figure 3.5. Control FRAP experiments on intact spinach chloroplasts .....	84
Figure 3.6. Control FRAP experiment on a broken spinach chloroplast .....	85
Figure 4.1. Schematic diagram showing the damage, repair and assembly of D1 protein during photoinhibition.....	88
Figure 4.2. FRAP measurements on intact spinach chloroplasts.....	91
Figure 4.3. Effect of sodium fluoride (NaF) on the mobility of chlorophyll-proteins in intact spinach chloroplasts with and without photoinhibition.....	95
Figure 4.4. Chlorophyll-protein mobility in intact Arabidopsis chloroplasts, with and without photoinhibition .....	96
Figure 4.5. Freeze-fracture electron micrographs from intact spinach chloroplasts .....	99
Figure 4.6. Differences in PSII density in the grana regions of dark-adapted and photoinhibited spinach chloroplasts revealed in the EFs faces of freeze-fracture electron micrographs.....	100

Figure 4.7. Freeze-fracture electron micrographs from isolated spinach chloroplasts.....	102
Figure 4.8. Chlorophyll-protein mobility in isolated spinach chloroplasts with stacked and unstacked thylakoid membranes.....	104
Figure 5.1. PAM fluorescence measurement from an <i>Arabidopsis</i> leaf.....	107
Figure 5.2. PAM chlorophyll fluorescence measurement on intact spinach chloroplasts.....	110
Figure 5.3. Thin-section electron micrographs showing the structural effect of illumination on thylakoid membrane structure in intact spinach chloroplasts....	111
Figure 5.4. Analysis of thin-section electron micrographs of intact spinach chloroplasts.....	112
Figure 5.5. Analysis of thin-section electron micrographs of intact spinach chloroplasts.....	113
Figure 5.6. Freeze-fracture electron micrographs from intact spinach chloroplasts .....	115
Figure 5.7. Analysis of PSII particles in the EFs fracture faces from freeze-fracture electron micrographs of intact spinach chloroplasts.....	118
Figure 5.8. Image analysis of PFs fracture faces from intact spinach chloroplasts .....	120
Figure 5.9. Effect of NPQ formation and de-epoxidation state on the mobility of chlorophyll-proteins in intact spinach chloroplasts prepared in four different states .....	122
Figure 5.10. Linear relationship between the mobility of chlorophyll-proteins and PSII nearest-neighbour distances in the grana membranes of intact spinach chloroplasts prepared in different states.....	122

Figure 5.11. Non-linear relationship between the mobility of chlorophyll-proteins and the amount of NPQ formed in intact spinach chloroplasts prepared in different states.....	123
Figure 5.12. Freeze-fracture electron micrographs showing the effect of illumination on the thylakoid membrane structure in <i>Arabidopsis thaliana</i> PsbS mutants.....	125
Figure 5.13. Effect of PsbS protein on the organisation of PSII-LHCII supercomplexes in intact <i>Arabidopsis</i> chloroplasts in the dark and light-adapted states.....	126
Figure 5.14. Effect of PsbS protein on the mobility of chlorophyll-proteins in intact <i>Arabidopsis</i> chloroplasts in dark and light-adapted states.....	129
Figure 5.15. Effect of E122QE226Q mutations in a PsbS gene on the mobility of chlorophyll-proteins.....	130
Figure 5.16. Non-linear relationship between the mobility of chlorophyll-proteins in dark-adapted state and the amount of NPQ formed after light treatment.....	131
Figure 5.17. Mobility of chlorophyll-proteins in intact chloroplasts isolated from different xanthophyll mutants of <i>Arabidopsis thaliana</i> .....	134
Figure 5.18. Freeze-fracture electron micrographs from different xanthophyll mutants of <i>Arabidopsis thaliana</i> .....	136
Figure 5.19. Analysis of PSII particles from EFs fracture faces of electron micrographs obtained for different xanthophyll mutants of <i>Arabidopsis</i> .....	137
Figure 5.20. Analysis of LHCII particles from PFs fracture faces of electron micrographs obtained for different xanthophyll mutants of <i>Arabidopsis</i> .....	138
Figure 6.1. Freeze-fracture electron microscopy experiments performed on the light-harvesting antenna mutants of <i>Arabidopsis</i> .....	147

Figure 6.2. Freeze-fracture electron microscopy experiments performed on the light-harvesting minor antenna mutants of <i>Arabidopsis</i> .....	148
Figure 6.3. Freeze-fracture electron microscopy experiment performed on the <i>chl</i> mutant of <i>Arabidopsis</i> which does not form functional LHC antenna .....	149
Figure 6.4. Freeze-fracture electron microscopy image analysis of the PSII arrays in intact thylakoid membranes of different light-harvesting antenna mutants of <i>Arabidopsis</i> .....	152
Figure 6.5. Analysis of EFs particle sizes in minor antenna mutants of <i>Arabidopsis</i> .....	156
Figure 6.6. Analysis of EFs particle sizes in major antenna mutants of <i>Arabidopsis</i> .....	157
Figure 6.7. Analysis of EFs particle sizes in the <i>chl</i> mutant of <i>Arabidopsis</i> .....	158
Figure 6.8. Analysis of PSII particle macromolecular crowding in the grana membranes of major light-harvesting antenna mutants of <i>Arabidopsis</i> .....	160
Figure 6.9. Analysis of PSII particle macromolecular crowding in the grana membranes of minor light harvesting mutants of <i>Arabidopsis</i> .....	161
Figure 6.10. Analysis of PSII particle macromolecular crowding in the grana membranes of the <i>chl</i> mutant of <i>Arabidopsis</i> .....	163
Figure 6.11. Analysis of LHCII particle distribution in the grana membranes of light-harvesting antenna mutants of <i>Arabidopsis</i> .....	167
Figure 6.12. Mobility of chlorophyll proteins in intact chloroplasts isolated from different light-harvesting antenna mutants of <i>Arabidopsis</i> .....	171
Figure 6.13. Relationships between the mobility of chlorophyll-proteins and the macromolecular crowding of PSII-LHCII supercomplexes in the grana membranes of different light-harvesting antenna mutants of <i>Arabidopsis</i> .....	173

Figure 6.14. Correlation plot showing a linear relationship between the mobility of chlorophyll-proteins in dark-adapted state and the amount of NPQ which is formed after light treatment.....	174
Figure 6.15. Kinetics of solubilisation and re-stacking of the thylakoid membranes of light-harvesting antenna mutants determined by PAM fluorescence measurements .....	178
Figure 6.16. Kinetic parameters of solubilisation and re-stacking of the thylakoid membranes from light-harvesting antenna mutants of <i>Arabidopsis</i> .....	182
Figure 7.1. Visualisation of chloroplasts in mesophyll cells of intact spinach leaf under Leica SP5 confocal microscope .....	186
Figure 7.2. FRAP measurement on individual chloroplast in intact spinach leaf	189
Figure 7.3. Comparison of the sizes of mobile fractions for chlorophyll-proteins in intact chloroplasts which were either isolated or retained within the cells in intact leaves of spinach and <i>Arabidopsis thaliana</i> wild-type plants .....	190
Figure 7.4. Mobility of chlorophyll-proteins in different dark-adapted tobacco mutants impaired in phosphorylation of PSII core proteins or lacking functional PSII photosystems (A20 mutant).....	192
Figure 7.5. Confocal images of dark-adapted chloroplasts in intact leaves of tobacco wild-type and pFM-A20 mutant plants .....	193
Figure 8.1. Model proposing possible explanations for the differences in the mobility of chlorophyll-proteins upon photoinhibitory illumination in intact chloroplasts where grana are interconnected with stoma lamellae vs. isolated grana patches.....	204
Figure 8.2. Model describing the changes in the ultrastructure and the macro-organisation of PSII-LHCII supercomplexes in the thylakoid membranes upon the	



switch from light-harvesting (low light) to the photoprotective state (high light)  
..... 218

Figure 8.3. Confocal images of the intact chloroplast isolated from *chl* mutant of  
*Arabidopsis*..... 229

## List of tables

Table 1. List of <i>Arabidopsis thaliana</i> mutants used in this study .....	58
Table 2. Effect of photoinhibition on the mobility of chlorophyll-proteins in intact spinach chloroplasts and isolated grana membranes .....	92
Table 3. Effect of nigericin (4 $\mu$ M) on the mobility of chlorophyll-proteins in intact spinach chloroplasts .....	94
Table 4. Analysis of EF fracture faces in the stacked and unstacked thylakoid membranes from spinach.....	103
Table 5. Comparison of NPQ values measured for intact spinach chloroplasts prepared in four different states.....	114
Table 6. Comparison of NPQ values in intact chloroplasts of PsbS protein mutants of <i>Arabidopsis thaliana</i> under different conditions.....	124
Table 7. Comparison of chlorophyll <i>a/b</i> ratios in intact chloroplasts of PsbS protein mutants of <i>Arabidopsis thaliana</i> .....	125
Table 8. Analysis of EFs fracture faces from electron micrographs of wild-type and PsbS mutant intact <i>Arabidopsis</i> chloroplasts in dark and light-adapted states ...	128
Table 9. Quantitative analysis of EFs fracture faces from electron micrographs of wild-type and different xanthophyll mutants of <i>Arabidopsis</i> chloroplasts in dark-adapted state .....	140
Table 10. Quantitative analysis of PFs fracture faces from electron micrographs of wild-type and different xanthophyll mutants of <i>Arabidopsis</i> chloroplasts in dark-adapted state .....	141

Table 11. Quantitative analysis of particles from EFs fracture faces from electron micrographs of wild-type and different light-harvesting antenna mutants of <i>Arabidopsis</i> chloroplasts in dark-adapted state .....	164
Table 12. Quantitative analysis of PFs fracture faces from electron micrographs of wild-type and different light-harvesting antenna mutants of <i>Arabidopsis</i> chloroplasts in dark-adapted state.....	169
Table 13. Fluorescence and kinetics parameters of solubilisation and re-stacking of the thylakoid membranes from light-harvesting antenna mutants of <i>Arabidopsis</i> .....	180

## Abbreviations

DCMU - (3-(3,4-dichlorophenyl)-1,1-dimethylurea)

EDTA – ethylenediaminetetraacetic acid disodium salt dihydrate

EF – exoplasmic face

EM – electron microscopy

FLIM – fluorescence lifetime imaging microscopy

FRAP – fluorescence recovery after photobleaching

GFP – green fluorescence protein

LD – linear dichroism

LHCI – light-harvesting antenna of photosystem I

LHCII – light-harvesting antenna of photosystem II

NPQ – non-photochemical quenching

PAM – pulse-amplitude-modulated fluorometry

PF – protoplasmic face

PSI – photosystem I

PSII – photosystem II

qE – energy-dependent quenching

qI – photoinhibitory quenching

qT – state-transition quenching

SD – standard deviation

SE – standard error

SPT – single particle tracking

TAAB resin – low viscosity aliphatic epoxy resin for embedding biological  
specimens for electron microscopy

WT – wild-type

## Acknowledgements

I would like to express my greatest acknowledgements to Prof Conrad Mullineaux and Prof Alexander Ruban, my supervisors, for their invaluable help, strong support, always useful and constructive feedback and omnipresent kindness throughout my PhD studies. I am grateful for giving me this outstanding opportunity to study in London in such a multinational environment and for making it possible to travel around the world to participate in scientific meetings and international conferences.

A big thank-you is given also to Matt Johnson for his immense input in conducting some experiments and the subsequent data analysis. I greatly appreciated his support and constructive feedback as well as his positive attitude in doing science at all times.

Many thanks are sent also to Anja Nenninger, Tchern Lenn, Tony Brain Ahmad Zia, Heike Brinkman and all those who taught me different experimental techniques and growth of plants throughout my project. Without them the progress in my project would not be possible.

Thank-you also to Prof Andrew Leitch and Dr Jon Nield, my panel members, who were always supportive and kind, fairly assessing my progress and giving useful feedback during our panel meetings.

I acknowledge meeting and working with all the current and former members of my both research groups: Giulia, Samantha, Samuel, Joanna, Dennis, Elodie, Liuning, Chris, Erica. Thank you all for creating such great atmosphere in the lab making it a real pleasure to come to work everyday.

I acknowledge Biotechnology and Biological Sciences Research Council for funding my studentship and University of London, Central Research Fund for funding partly my freeze-fracture experiments.

I am grateful so much for the constant support and belief I always received from my family, my Mum and Dad, my brother Piotr, his wife Aga and my nephew Mateusz. This thesis is partly dedicated to you.

Last but not least, a special thank-you and gratefulness is given to my own family, my beloved wife Anna and our son Oskar, who brought in so much happiness and love to my life. This thesis is also dedicated to you.

# **Chapter I**

## **Introduction**

Free energy used by all biological systems comes entirely from sunlight energy which is trapped during the process of photosynthesis. Its occurrence, particularly in an oxygenic form almost 2.6 - 2.7 billion years ago by early prokaryotic cyanobacteria (Buick, 2008) has fundamentally changed the Earth's ecosystem and led to development of much complex forms of life, including human beings. One of the major breakthroughs in the evolution of photosynthetically active organisms is ascribed to the appearance of the first vascular plants in the second half of the Silurian period (about 420 million years ago). It started the era of green plants inhabiting terrestrial ecosystems and produced a dramatic effect on atmospheric chemistry and climate (Berner, 1997). Currently there are over quarter of million discovered higher plant species (and still nearly one-fifth left to discover) that are primarily responsible for the global photosynthetic activity and carbon fixation on land (Barber, 2007; Chapman, 2009). Higher plants are the most complex photosynthetic organisms both structurally and functionally. It is reflected on the photosynthesis efficiency being tightly regulated in response to changeable environmental conditions. This regulation occurs not only at the molecular level (photosynthetic protein complexes embedded in the thylakoid membrane) but also the whole plant organs such as leaves, for example. This study deals comprehensively with the former effect i.e. dynamic changes and mobile properties of photosynthetic complexes in the thylakoid membrane and indicates their significant role in optimising the photosynthesis process in nature.

## 1.1. Architecture of the thylakoid membrane network in green plants

The photosynthetic machinery in vascular plants is localised in specific cellular organelles called chloroplasts within the complex internal membrane network known as thylakoids. The thylakoid membrane system is formed from a continuous membrane that separates the thylakoid lumen from the rest of the chloroplast internal aqueous phase called the stroma. The whole system is surrounded by two bilayers of lipid membranes commonly referred to chloroplast envelope (Figure 1.1). The envelope membranes control the transport of metabolites, lipids and proteins in and out of chloroplasts. The stroma contains the enzymes involved in carbon fixation, DNA attached to the thylakoids, ribosomes, starch granules and plastoglobuli (Rose and Possingham, 1976; Staehelin and van der Staay, 1996).

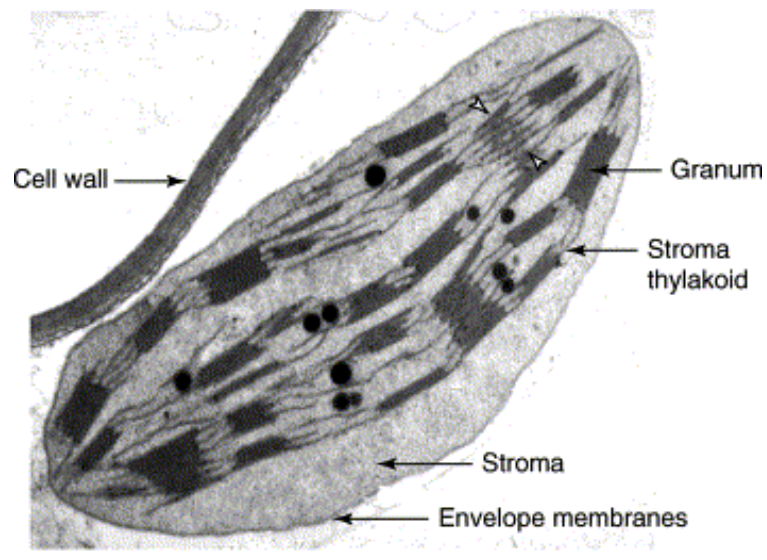


Figure 1.1. Thin-section electron micrograph of green plant chloroplast. Adapted from Mustárdy and Garab (2003).



Chloroplasts are descended from cyanobacteria and in many ways their photosynthetic apparatus resembles the one found in cyanobacterial cells. However, green-plant chloroplasts exhibit a significantly different thylakoid membrane organisation to that of cyanobacteria. The most striking feature is their extensive folding and, as a result, structural heterogeneity. They consist of two major domains, namely the grana (appressed domains) comprising about 80% of the membrane (Kirchhoff, 2008) and the stromal lamellae (non – appressed domains) that connect the grana stacks (Figure 1.1). An ultrastructural organisation of the thylakoid membrane system in higher plants shows, to some extent, a high degree of periodicity: cylindrical grana stacks, typically of 10 – 20 layers and 300 – 600 nm in diameter are interconnected by unstacked stroma lamellae of several hundred nanometers in length. An interesting question arises of the role and evolutionary significance of grana stacks inside land-plant chloroplasts. These structures are not essential for oxygenic photosynthesis as they are not found in present-day cyanobacteria as well as many eukaryotic green algae. According to Mullineaux grana evolved primarily to optimise photosynthesis efficiency in shade environments after plants colonised the land (Mullineaux, 2005). This allowed for recruiting and packing a large quantity of light-harvesting antennae complexes into separate regions of the chloroplast to capture low light and combining it efficiently with electron transport. This requirement was not important in the immediate ancestors of land-plants such as macroalgae since, living mostly on shorelines, they were well adapted to high light conditions and did not need a large photosystem II light-harvesting antenna. Therefore, grana seem to occur as the side-effect product of evolution created under selection pressure to optimise harvesting of photons without restricting the transport of electrons along the photosynthetic membrane (Mullineaux, 2005).

Despite the recent advantages in microscopic techniques and extensive studies in this field, the three-dimensional architecture of the thylakoids, particularly the topography of the granum-stroma lamellae assembly still remains unclear. To date, there are several different models that have been proposed (Mustárды and Garab, 2003), but at present mainly two of them dominate the field:

- **Helical model** that was first formulated by Paolillo (1970) and was based on serial-section electron microscopy (EM) analyses and observations made by von Wettstein (1959), Heslop-Harrison (1963) and Wehrmeyer (1964). In its latest version (Mustárды and Garab, 2003) the model suggests a structure consisting of a cylindrical granum body surrounded by multiple right-handed helices of stroma thylakoids that are connected via junctions at the margins of the grana (Figure 1.2). The helices are tilted at  $\sim 20^\circ$  with respect to grana stacks, and are in contact with successive layers in the grana. The whole structure is achieved by self-assembly, which has been initiated by primary growth layers and then followed by the spiral cyclical overgrowth of the vesicles (Paolillo, 1970). Recently, the helical model has been further refined (Mustárды et al., 2008) suggesting that the helical organisation is far less regular, although the general spiral organisation of the stroma thylakoids around the granum stacks is still retained.

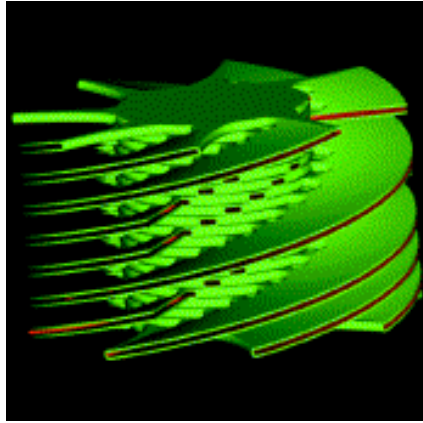


Figure 1.2. Computer-generated model of a helical arrangement of stroma thylakoids around the granum body. See description in the text. Adapted from Mustárdy and Garab (2003).

- **Pairwise Organisation Model** that was put forward by Shimoni et al. (2005). According to that model which was obtained on the basis of electron microscope tomography (EMT), the grana layers are formed by bifurcations and subsequent fusion of the membranes instead of invaginations and folding. Stroma lamellae membranes do not connect granal adjacent layers to each other but, to the contrary, they are interconnected directly through their edges by bending towards and fusing with neighbouring layers as well as through direct membrane bridges (Figure 1.3). The authors of the model claim that such a way of the thylakoid membrane organisation is evolutionarily conservative as it allows for more structural flexibility that is required under rapidly changing environmental conditions (Brumfeld et al., 2008)

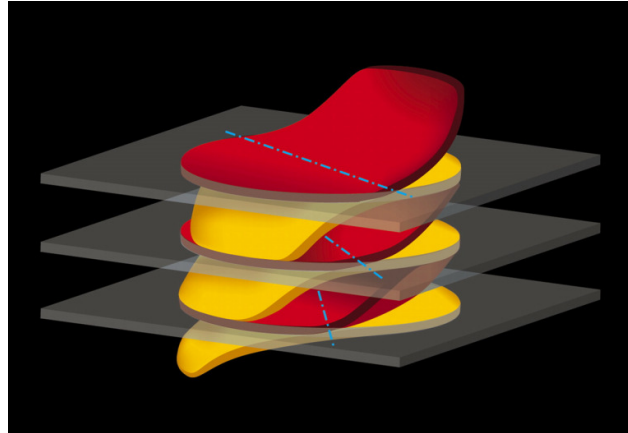


Figure 1.3. Computer-generated visualisation of the Pairwise Organisation Model of the granum. See description in the text. Adapted from Shimoni et al. (2005).

The architecture of thylakoid membranes is highly flexible and undergoes dynamic structural changes in response to different physiological conditions. The most important factors triggering those changes are:

- **Light intensity** – plants grown under low light conditions exhibit more stacking of the grana and increased size of the light-harvesting antennae to maximise capturing of photons, with the opposite effect observed in plants adapted to high light (Ruban, 2009). Moreover, in dark or under very low light intensity the pairs of stacked photosynthetic membranes are more widely spaced, with the thylakoid lumen appearing swollen. However, high light treatment results in the volume of the thylakoid lumen decreasing and, as a consequence, the spacing between the adjacent granal stack is reduced significantly (Murakami and Packer, 1970a, 1970b). This structural change is believed to underlie the photoprotective state of the membrane which is based on a natural phenomenon known as non-photochemical quenching (NPQ). The further details of this effect are widely described in chapter V.

- **Light quality** – during state transitions, a low light phenomenon that is based on the phosphorylation-driven association of light-harvesting antennae with two different photosystems dependent on the spectral quality of the absorbing light, the thylakoid membrane network shows significant macroscopic rearrangements. They involve changes in the granal stacking and can result in even partial disassembly of the granum (Chuartzman et al., 2008). It is worth noticing that those changes are fully reversible on a relatively short timescale.
- **Presence of cations** – monovalent or divalent cations (magnesium cations in particular) are known to play an important role in stabilising the stacking of the grana. Chloroplasts incubated in a low salt medium develop a complete grana-free membrane system while the stacks can be again restored upon re-addition of cations (Izawa and Good, 1966; Murakami and Packer, 1971).
- **Abundance of light-harvesting antennae** – LHCII has been shown to stabilise the granum ultrastructure, and to participate to some extent in the cation-mediated stacking of the thylakoids (Barber, 1982; Dekker and Boekema, 2005). This is achieved by the electrostatic interaction between different LHCII complexes in opposing membranes of the granal stacks, but the lateral organisation of the proteins is also important (Dekker and Boekema, 2005).
- **Phosphorylation of photosynthetic complexes** – LHCII is quickly phosphorylated under low light and dephosphorylated in darkness (Bennett, 1983; Bennett, 1984; Rintamäki et al., 1996), while the PSII core undergoes a rapid phosphorylation with the increase of light intensity which is related to its photoinhibition and turnover (Barber and Andersson, 1992; Aro et al., 1993; Adir et al., 2003; Tikkanen et al., 2008). In the latter case, the high

level of phosphorylation affects also macroscopic structure of thylakoids by increased stacking and decrease in size of thylakoid grana in the leaves (Fristedt et al., 2009; Fristedt et al., 2010).

- **Temperature** – thylakoid membranes subjected to heat treatment at temperatures above 30°C undergo changes in their structural arrangement and functional activity, particularly by reduction of appressed membrane sites and subsequent destacking (Weis, 1985; Dobrikova et al., 2002). A further increase of the temperature above 45 - 55°C results in complete breakdown and vesiculation of the thylakoids (Gounaris et al., 1984).
- **Water content** – some plant species, particularly those which are drought-sensitive exhibit dramatic changes in the thylakoid membrane structure following dehydration such as fractures and extensive swelling (Navari-Izzo et al., 2000).

## 1.2. Organisation of photosynthetic complexes in the thylakoid membranes of higher plants

Thylakoid membranes are enriched in different protein complexes mediating the light phase reactions of photosynthesis (Figure 1.4).

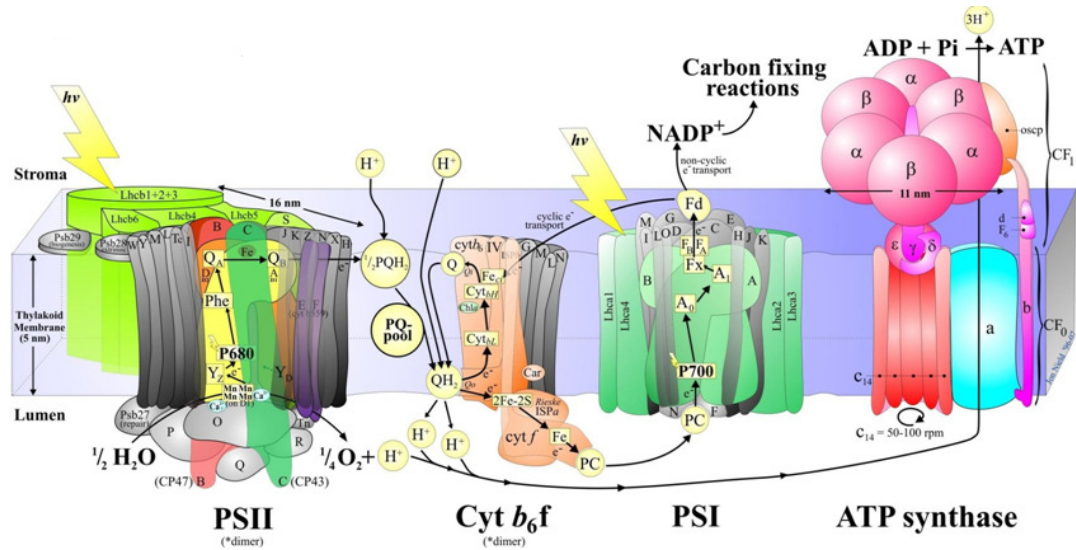


Figure 1.4. Schematic model showing the key photosynthetic protein machinery involved in oxygenic photosynthesis in higher plants. Adapted from Dr. Jon Nield's webpage (<http://www.photosynthesis.sbcs.qmul.ac.uk/nield/psIIimages/oxygenicphotosynthmodel.html>).

However, the clear differentiation into grana and stroma lamellae regions results in spatial segregation and non-uniform distribution of the photosynthetic complexes in the membrane. The stacked domains (grana) contain mostly photosystem II (PSII) and light-harvesting complexes (LHCII), whereas photosystem I (PSI), light-harvesting complex I (LHCI) and the ATPase complexes are localised mainly in the unstacked regions (stroma thylakoids) (Allen and Forsberg, 2001). Cytochrome  $b_6f$  (the complex which receives electrons from PSII by plastoquinol and passes them to PSI by reducing plastocyanin or cytochrome  $c_6$ ) is found in both

types of thylakoid membranes (Allen and Forsberg, 2001) but there are also evidences suggesting that its location could be limited to the granum-stroma assembly under certain conditions (as discussed in Dekker and Boekema, 2005). In the past two decades, a significant progress has been made in elucidating the structure and supramolecular organisation of the protein complexes composing the photosystem machinery involved in energy transduction. Currently there are intermediate (3.5 – 4.2 Å) or high (<2.5 Å) resolution structures available for all these complexes (Dekker and Boekema, 2005, and references therein).

### **1.2.1 Organisation of PSII-LHCII supercomplexes in the grana**

Photosystem II is a large multisubunit chlorophyll-binding protein complex which is evolutionarily highly conserved in both structural and functional terms. It is found in the thylakoid membranes of all major oxygenic photosynthetic organisms such as green plants, algae and cyanobacteria. Because of a pivotal role it played in the course of life evolution on Earth, the protein is sometimes described as the real ‘life engine’ (Barber, 2003). This is the only protein complex capable of splitting water molecules into dioxygen, protons and electrons, the reaction which is thermodynamically the most demanding of all biological processes and which is driven naturally by solar energy. PSII supplies the planet with all the oxygen we breathe, helps to maintain the ozone layer, and provides the reducing agents necessary to fix carbon dioxide to produce sugars.

PSII normally functions as a dimer in both higher plants and cyanobacteria (Dekker and Boekema, 2005). However, in the former group PSII dimers tend to monomerise when they leave the grana membranes, which is related to the repair cycle that takes place in the unstacked regions (Aro et al., 2005). Each monomer of



the protein consists of approximately 27-28 subunits which are organised in two groups: the core complex and the peripheral antenna system (Caffarri et al., 2009). The major components of the core are shown in Figure 1.5 and can be divided into three groups:

- D1 (PsbA) and D2 (PsbD) proteins containing the reaction centre P680 in which the charge separation and primary electron transfer reactions takes place. They both bind six chlorophyll *a* and two pheophytin *a* molecules (Dekker and Boekema, 2005)
- CP47 (PsbB) and CP43 (PsbC) which have inner light-harvesting function and transfer the excitation energy to the reaction centers. They mediate also the transfer of absorbed energy from peripheral antenna system directly to the reaction center. CP47 and CP43 bind 16 and 14 chlorophyll *a* molecules, respectively (Dekker and Boekema, 2005)
- Several low molecular weight transmembrane subunits whose role is still not fully understood together with the oxygen evolving complex (OEC) on the luminal side of the membrane (Caffarri et al., 2009). There are no indications that those proteins can bind chlorophyll (Dekker and Boekema, 2005).

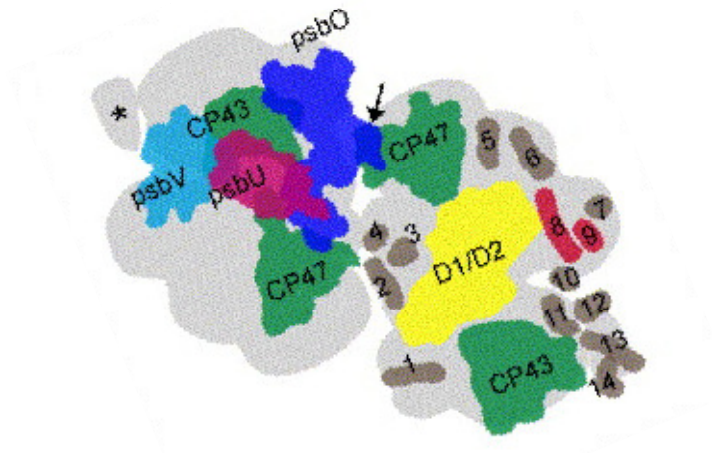


Figure 1.5. Schematic diagram showing localisation of different components in the core of Photosystem II. Right part of the diagram refers to the proteins located in the membrane-intrinsic part of the monomeric core while the monomer on the left shows the luminal exposed membrane-extrinsic part. Adapted from Dekker and Boekema (2005).

The peripheral antenna system plays a crucial role in light-harvesting, transfer of the absorbed energy to the reaction centers and photosynthesis regulation through photoprotective mechanisms which dissipate the excess energy as heat under high-light (non-photochemical quenching). In higher plants the antenna system consists of a number of pigment-protein complexes belonging to the Lhcb multigenic family (Jansson, 1999). They can be divided into two different categories:

- Major antenna complexes that are the most abundant in the photosynthetic membrane binding 60% of the total PSII chlorophyll (Peter and Thornber, 1991). They usually form a heterotrimer composed of the products of *lhcb1*, *lhcb2* and *lhcb3* genes in a ratio of about 8:3:1 (Jansson, 1994).

- Minor antenna complexes which are known as CP29, CP26 and CP24, and are products of the *lhcb4*, *lhcb5* and *lhcb6* genes, respectively. These proteins occur as monomers but they adopt a similar three-dimensional organisation to the one exhibited by the major LHCII antenna (Bassi et al., 1999; Croce et al., 2002).

Another important component of the thylakoid membranes in the grana regions is the PsbS protein which also belongs to the Lhc super-gene family (Funk et al., 1995). Although it is sometimes considered as a part of the PSII core, it has never been found in PSII crystals (Nield et al., 2000a; Dekker and Boekema, 2005; Nield and Barber, 2006), and its exact location is still not fully known. Moreover, it seems that the protein does not bind any chlorophyll molecules since it is one of the very few members of the Lhc gene-like family that is stable in the absence of pigments (Dominici et al., 2002; Dekker and Boekema, 2005). PsbS plays an important role in non-photochemical quenching, the phenomenon that allows plants to dissipate the excess energy into heat (Niyogi et al., 2005). However, the exact mechanism in which the protein acts during this process is still a matter of debate. I addressed this problem in my work and obtained, together with Dr. Matthew Johnson, a set of new data that proposes an explanation of the involvement of PsbS in the process of NPQ. They are presented and discussed in details in chapter V.

In most cases, PSII in stacked grana thylakoids is organised as the so-called PSII-LHCII supercomplex. It is composed of a core dimer ( $C_2$ ) with minor LHCII and two major LHCII trimers (trimers S) strongly bound to the complex on the side of CP43 and CP26 (Boekema et al., 1995; Nield et al., 2000b). This is known as a  $C_2S_2$  supercomplex. However, two more trimers (trimers M) can be moderately bound (the strength of these binding sites was assessed according to the frequency of

occurrence of trimeric LHCII in partially solubilised grana membranes) and get in contact with CP29 and CP24, and thus form the  $C_2S_2M_2$  supercomplex (Figure 1.6) (Boekema et al., 1999). Moreover, several different intermediate versions of those complexes have been discovered with the most recent one described as CS consisting of one monomeric core, one LHCII S trimer and the minor antenna CP26 (Boekema et al., 1999; Caffarri et al., 2009). This indicates that the supercomplex formation is highly flexible and changes upon different environmental conditions.

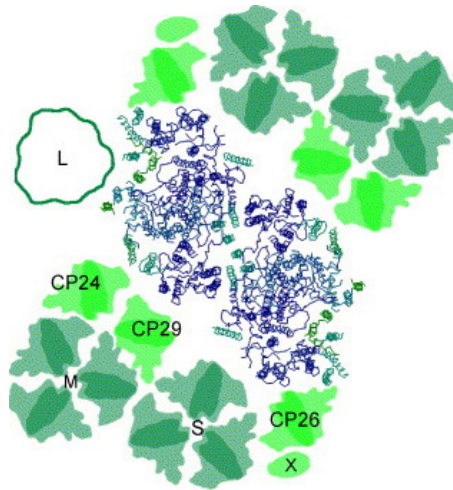


Figure 1.6. Schematic representation of the  $C_2S_2M_2$  supercomplex based on the electron microscopy images from spinach. The 'L' trimer refers to an additional LHCII trimer found only in spinach. Adapted from Dekker and Boekema (2005).

The question arises whether or not the PSII-LHCII supercomplex represents the native organization of PSII in the grana. Several studies have shown that this is a genuine organisational unit which is retained even after detergent solubilisation of complete thylakoid membranes (Eshaghi et al., 1999) and is found also in EM micrographs of partially unfolded membranes (van Roon et al., 2000). What is more, there is also evidence showing that PSII-LHCII supercomplexes can laterally associate to each other forming megacomplexes (dimer of supercomplexes). To date,

five types of such megacomplexes in different organisms have been described (Boekema et al., 1999; Yakushevskaya et al., 2001; Dekker and Boekema, 2005). An important aspect of the organisation of PSII-LHCII supercomplexes in the grana thylakoids is the fact that a small fraction of those complexes forms a regular arrangement, sometimes referred to ‘crystalline arrays’. They have been observed long time ago in the thylakoid membranes of green plants *in vivo* mainly thanks to the freeze-fracture electron microscopy technique (Figure 1.7).

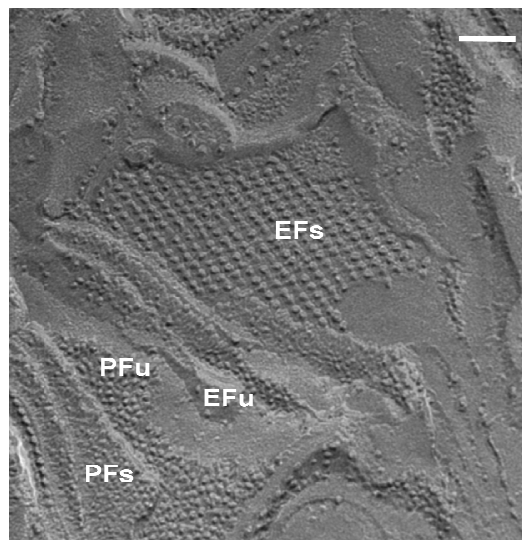


Figure 1.7. Freeze-fracture electron micrograph showing the PSII complexes (EFs face) in the thylakoid membranes of intact chloroplast isolated from wild-type *Arabidopsis thaliana* forming a two-dimensional crystalline array. The fracture faces were labelled according to nomenclature introduced by Branton et al. (1975), and are explained in more details in chapter IV. Scale bar = 100 nm.

It was noted that PSII in such arrays is dimeric and the repeating unit consists mostly of the  $C_2S_2M_2$  supercomplex in *Arabidopsis* and  $C_2S_2M$  in spinach ((Boekema et al., 2000; Dekker and Boekema, 2005). However, it is still not clear if such a structural arrangement represents a fully functional photosystem unit with efficient energy transfer and primary electron transport taking place as normal. For example, a special

long-range plastoquinone diffusion pathway between PSII in rows and cytochrome  $b_6/f$  in another part of the membrane would have to exist, but this has not been proved yet (Dekker and Boekema, 2005). Nonetheless, crystalline arrays of PSII were observed under some physiological conditions, for example after cold acclimation or under different light intensities (Garber and Steponkus, 1976; Kirchhoff et al., 2007). Moreover, their abundance in the grana must have an impact on the dynamic properties of PSII photosystems. This is due to the greater packing of the supercomplexes when they form semi-crystalline arrays as compared to a more random distribution. For that reason, this type of PSII organisation in the grana membranes was investigated also in this study and is discussed in more details in chapters V and VI.

The grana stacks usually consist of approximately 10 – 20 layers of membranes. The stromal side membranes are rather flat and form a pair spaced by about 2 nm whereas at the luminal side the distance between opposite membranes is much larger because of large protrusions from PSII and cytochrome  $b_6/f$  complexes. The vertical distance from one pair of membranes to the next varies from 14 to 24 nm. This would be just sufficient for the vertical height of two PSII or cytochrome  $b_6/f$  on top of each other, because each PSII or cyt  $b_6/f$  has about 10.5 nm (Dekker and Boekema, 2005). This means that the organisation of the PSII-LHCII supercomplexes in one membrane affects the organisation of complexes in the opposing membrane not only at the stromal sides but also in opposing membranes in the lumen. It has been proposed that most PSII-LHCII supercomplexes face the LHCII-only regions in the opposing membrane because of a very pronounced handedness that these complexes exhibit (Dekker and Boekema, 2005). This is possible due to the fact that within the grana regions not all of the LHCII antennae

are bound in the supercomplexes. In fact, it has been proved that LHCII can form aggregates *in vivo* and occupy some parts of the grana without PSII (see chapter V for details). Furthermore, at the luminal sides of the stacks, PSII complexes cannot be located directly opposed to each other as it would restrict their diffusion and limit the space for the luminal proteins as well.

In summary, the organisation of photosynthetic complexes in the appressed granal regions of higher plants is, on one hand extremely complex with a lot of protein- protein and protein-lipid interactions (Tremmel et al., 2005; Kirchhoff, 2008), but on the other hand is highly flexible and sensitive to external environmental conditions. This is an extremely important ability which allows for optimal photosynthesis efficiency in natural ever-changing environment.

### **1.2.2 Organisation of photosynthetic complexes in stroma lamellae thylakoids**

Non-appressed regions of the thylakoid membranes known as stroma lamellae interconnect grana and can reach several micrometers in length as compared to the maximal diameter of about 600 nm in the grana discs. They contain most of the photosystem I (PSI) and ATPase complexes and are the place where the monomeric PSII diffuses into after escaping the grana during the repair cycle (Barber and Andersson, 1992; Adir et al., 2003; Aro et al., 2005).

PSI structure (similarly to PSII) can be divided into two major groups: the core complex and the peripheral antenna system (Figure 1.8)

- The core of PSI is evolutionarily related to that of the PSII core (Dekker and Boekema, 2005, and references therein). In green plants it consists of two

sequence related large subunits (PsaA and PsaB), four extrinsic subunits (PsaC-E and PsaN), and a number of small intrinsic subunits (PsaF, PsaI-PsaL, PsaG-H and PsaO) (Dekker and Boekema, 2005). In green plants this complex probably only occurs in a monomeric state as opposed to cyanobacteria where it occurs in trimers. This results from the fact that in green plants the PsaH subunit binds to PsaL (which is known to play a role in the trimerisation in cyanobacteria) and completely encircles the membrane – exposed part of it, thus prevents from trimerisation.

- The peripheral antenna system is composed of membrane-bound light harvesting complexes called LHCI. This antenna consists of four different polypeptides called Lhca1-4 which also belong to the Lhc super-gene family. Lhca1 and Lhca4 form a heterodimer. Each Lhca protein binds 10 chl *a* or chl *b* molecules, as well as few xanthophylls. These subunits bind in a cluster at one side of the PSI core complex with a sequence of Lhca1 - Lhca4 - Lhca2 - Lhca3 (from the PsaG to PsaK side of the complex, respectively) (Ben-Shem et al., 2003; Nelson and Ben-Shem, 2004).

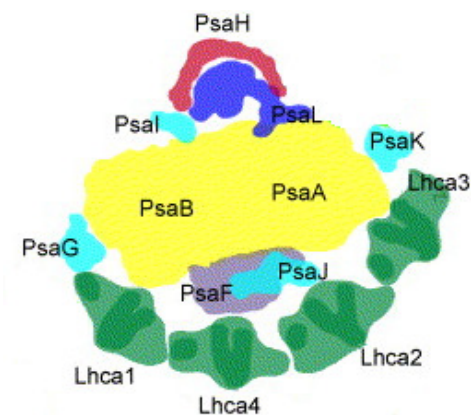


Figure 1.8. Schematic representation of PSI-LHCI complex showing location of different proteins composing the core and peripheral antenna system regions. Adapted from Dekker and Boekema (2005) with modifications.



### **1.3. Flexibility and acclimation of photosynthetic membranes**

Natural environmental conditions are highly variable which has great implications for higher plants in terms of their ability to grow and reproduce, to compete with neighbours for light and nutrients, and biotic and abiotic stress resistance. This variability has a particular impact on the photosynthetic machinery as it is a major source of energy and fixed carbon and, at the same time, it is a place where most damage occurs under stress conditions. This makes the photosynthetic apparatus extremely vulnerable to any changes in the environment. Plants have evolved many methods of responding to changes in their growth conditions, with particular attention being paid to the responses to incident light as an elusive substrate for the function of photosynthetic light reactions in the thylakoid membranes. However, acclimation to the environment could also involve responses to temperature, drought, atmospheric CO<sub>2</sub> levels, pathogen infection etc. They can occur on different timescales – from long-term developmental processes operating at the level of the whole plant or individual leaves to slight alterations in functioning of photosynthetic complexes taking place in a range of seconds to hours. Acclimation in a way serves as a homeostatic mechanism which reverses the consequences of environmental change and maintains efficient photosynthesis. A special case is given to photosynthetic acclimation – a process involving adjustments in the composition of the photosynthetic apparatus within individual cells or even chloroplasts (Walters, 2005). Therefore structural and functional dynamics of the thylakoid membrane components is required to occur during this process.

The majority of studies on photosynthetic acclimation in higher plants have focused on the effects of different growth light conditions relating both to light quantity and quality. These differences are the key factors influencing some of the physiological phenomena occurring on relatively short timescales, the most important of them being:

- 1. State transitions.** This short-term adaptation (it occurs on a timescale of minutes) is a consequence of frequent spectral quality changes of light environment and the fact that in higher plants the photosystems I and II have different chlorophyll excited state energies, 700 and 680 nm, respectively. The red shift of the photosystem I results from a decreased amount of chlorophyll b (most abundant in the LHCII light-harvesting antenna) compared to photosystem II and a number of red-shifted chlorophyll a forms (Ruban and Johnson, 2009). Any fluctuations in the quality of absorbed photons can strongly alter the ratio between the excitation energy flows into reaction centres of both photosystems. This might affect substantially the linear electron transfer flow from water (occurring at the level of PSII) to ferredoxin (occurring at the level of PSI) and, as a consequence, the whole photosynthetic processes would become inefficient. State transitions are therefore an essential adaptation allowing for harvesting every photon and utilising them when light becomes a limiting factor. However, it seems that they are not completely indispensable for plant survival, as deduced from *Arabidopsis* mutants lacking this acclimation response (Mullineaux and Emlyn-Jones, 2005). The mechanism of this phenomenon is based on LHCII reversible phosphorylation and a quick redistribution between PSI and PSII dependent on changing illumination energy. Over-excitation of PSII relative

to PSI (commonly referred as light 2) causes a reduction of plastoquinone pool (PQ) which in turn triggers phosphorylation of LHCII, its detachment from PSII and migration towards PSI where it serves as an additional antenna for this photosystem (state 2 is achieved). However, excess excitation of PSI (under the so-called light 1) results in the oxidised plastoquinone bringing about dephosphorylation of LHCII and its reversible movement to PSII leading to occurrence of state 1. The whole cycle and reversible switching between states 1 and 2 is summarised in Figure 1.9 (Allen, 2003). Non-homogenous distribution of photosynthetic complexes in the thylakoid membranes in higher plants gives a clear implication that LHCII undergoing phosphorylation during state transitions must be dynamic and subject to a long-range diffusion between grana and stroma lamellae regions of the thylakoids. These observations have been made by various microscopy and biochemistry experiments and are discussed in more details in the next sections. Moreover, as mentioned before, these movements can lead also to structural rearrangements of the entire thylakoid membrane network (Chuartzman et al., 2008).

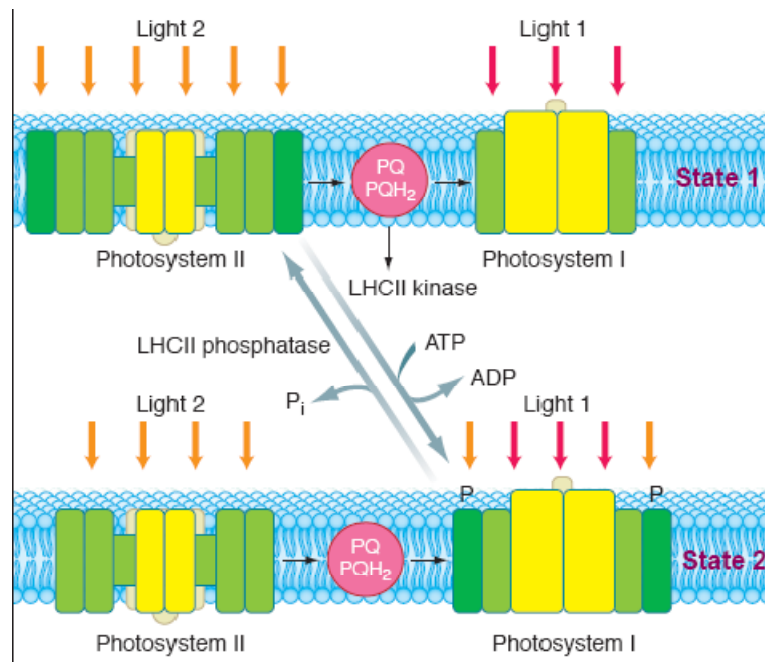


Figure 1.9. Schematic diagram showing the mechanism of state transitions. See description in the text. Adapted from Allen (2003).

**2. Non-photochemical quenching (NPQ).** At high light, the transition to state 2 is completely inhibited, but photosynthetic light harvesting is regulated by a process known as the non-photochemical quenching of chlorophyll fluorescence (NPQ) or the energy-dependent quenching (qE). This mechanism of adaptation can be induced within a timescale of seconds to minutes, and involves harmless thermal dissipation of excess energy, thus preventing from photo-oxidative stress that is known to be damaging on the photosynthetic apparatus. This dissipation is relatively efficient with over 75% of the absorbed photons able to be eliminated in this way (Kanervo et al., 2005). NPQ is mainly triggered by a  $\Delta\text{pH}$  across the photosynthetic membrane and is controlled by the regulatory role of the xanthophyll-cycle

carotenoids such as violaxanthin, antheraxanthin and zeaxanthin as well as the PsbS protein (Horton et al., 1996; Robert et al., 2004). These carotenoids were suggested to allosterically regulate a quenching process that is intrinsic to LHCII and requires its dynamics and structural changes (Horton et al., 1991; Horton et al., 2005; Horton et al., 2008) However, the exact mechanism of NPQ and any direct structural changes of the thylakoid membrane components related to this process still remain unclear. A part of the current study aimed to investigate these problems in more depth and, for that reason, a detailed description of the dynamic aspects of non-photochemical quenching in higher plants is presented in chapter V.

**3. Photoinhibition.** Oxygenic photosynthesis requires light as a substrate of energy but light can be also harmful when present in excess amount. Because the oxidative chemistry of PSII resulting from water splitting can generate highly reactive radicals, plants have evolved a potent adaptation mechanism protecting their photosynthetic apparatus especially under strong illumination (Barber and Andersson, 1992). Under these conditions accumulation of radicals, such as triplet chlorophyll and singlet oxygen is greatly increased, which in turn can be damaging and induce inactivation of PSII, the reaction-center core protein D1 being the most vulnerable for this damage. As a result, the D1 protein has to undergo a complex turnover and repair process. This repair involves reversible phosphorylation of damaged D1 subunits and is combined with the shuttling of these proteins between grana and stroma thylakoid domains (Aro et al., 1993; Baena-Gonzalez et al., 1999; Tikkanen et al., 2008). As a consequence, both structural and dynamic changes in the photosynthetic membranes are required to occur. The study of those changes

has been one of the main goals of my project. For that reason, the detailed analysis of photoinhibition and its influence on the physiology of the thylakoid membranes is presented in chapter IV.

Apart from short-term responses operating on timescales from seconds to minutes, plants have developed various adaptation mechanisms lasting for a longer time period. This is the case when plants are subjected to stable light irradiances during their growth, which induces much more profound alterations in the composition and physiology of the thylakoids and photosynthetic apparatus when compared to the fast changes mentioned above. The key difference here is that short-term acclimation is purely a post-translational event while long-term adaptation involves changes in the expression of photosynthetic genes and in the accumulation of photosynthetic pigments. Various long-term responses to different growth irradiances have already been described, such as for example: adjustments in reaction centre stoichiometry, altered antenna size or altered levels of Rubisco (Bailey et al., 2001; Bailey et al., 2004). As mentioned before, light intensity can change significantly not only the number of minor and major LHC antenna, shift the amounts of reaction centres and the organisation of photosynthetic complexes in the thylakoid membranes but also alter the structure of the membranes themselves.

In summary, constant exposure to fluctuations in natural environment forced plants to evolve numerous strategies enabling them to deal with the effects of such variation. Equipped with such adaptation mechanisms these organisms can optimise their photosynthetic abilities to the existing environmental conditions. Thus, acclimation responses contribute significantly to plant fitness and survival, and provide a genuine evolutionary advantage which allows for inhabiting even the most extreme niches around the globe.

## 1.4. Diffusion of proteins in living cells

Proteins inside living cells localise to two fundamentally different environments. They are either embedded in, or peripherally associated with biological membranes or they are in an aqueous phase such as the cytoplasm, nucleoplasm or organelle lumen. Within these environments, a protein can freely diffuse, be anchored to the membrane or be actively transported. These dynamic properties have crucial roles in determining what function a protein serves within the cell. The diffusion constant for a particle in a free volume is described by the Stokes-Einstein formula:

$$D = kT / 6\pi\eta R$$

where  $D$  is the diffusion constant,  $T$  is the absolute temperature,  $\eta$  is the viscosity of the solution,  $k$  is the Boltzmann constant and  $R$  is the hydrodynamic radius of the particle. Because absolute temperature is usually constant within cells, the most important factors underlying  $D$  are the size of a protein and the viscosity of the medium within which it is diffusing. Biological membranes have a much higher viscosity than cytoplasm, so the lateral diffusion of a protein assembled within a membrane is considerably slower than that of a soluble protein which is reflected by a lower  $D$  value (Lippincott-Schwartz et al., 2001). Moreover, owing to the higher viscosity of membrane, the radius of the transmembrane fragment dominates the  $D$  value of a membrane protein (Cole et al., 1996). Even though viscosity and size are key factors underlying the diffusion rate of a protein, other factors also have a role in determining protein dynamics inside cells. These include protein-protein interactions or binding to a matrix that might slow or immobilise a protein, and collisions with other molecules, which hinder free diffusion (Lippincott-Schwartz et

al., 2001). Such factors are likely to prevent proteins from diffusing at their theoretical limit within the crowded thylakoid membranes inside chloroplasts.

## **1.5. Current knowledge about the mobility of photosynthetic proteins**

Thylakoid membranes are enriched with different photosynthetic protein complexes creating all together a specific and tightly regulated machinery performing photosynthetic energy conversion. This enrichment is reflected at the level of high molecular crowding and dense packing of these proteins within the thylakoid membrane network. It is a common feature of all photosynthetic membranes present even in purple bacteria and cyanobacteria as well as in the inner mitochondrial membrane (Kirchhoff, 2008). However, the thylakoids from vascular plants exhibit the most extreme case and belong to the most densely-packed biological membranes known (Kirchhoff et al., 2008). It is estimated that proteins occupy nearly 70% of the total area in the thylakoid membrane of a chloroplast with almost 80% of the area in grana regions (Kirchhoff, 2008). On one hand, such macromolecular crowding has obvious physiological advances. For example, it concentrates the chromophores and electron transport complexes in a limited membrane area increasing significantly the probability that the light photons will be absorbed with greatest possible efficiency. Moreover, it clearly enhances the ultra-fast energy transfer from peripheral light-harvesting antennae to the reaction centers of photosystems. It has been shown before that the 'dilution' of the membrane with additional lipids reduces the fraction of absorbed light quanta used for charge separation and slows down the rate of photosynthetic activity (Haferkamp and



Kirchhoff, 2008). On the other hand, this dense macromolecular crowding may also cause problems. Recent observations made by Haferkamp et al. (2010) suggest that the overcrowded membrane (protein packing more than 80% of the grana area) results in the decreased efficiency in light-harvesting due to excited state quenching in LHCII. Furthermore, as mentioned before, physiological function of the thylakoids involves their rapid structural response to variable environmental conditions, and thus the dynamics of different components that are present there. However, the more densely packed the membrane, the slower is the diffusion of proteins. According to the percolation theory, with the increasing macromolecular obstructions the movements of any particle become significantly limited and after reaching a certain threshold they are practically impossible (Kirchhoff, 2008). Such a drastic restriction on protein mobility within the thylakoid membranes would have a detrimental effect on a whole range of processes. For example, assembly and turnover of photosynthetic complexes, electron transport carriers such as plastoquinone or plastocyanin, shuttling of LHCII between PSII and PSI during state transitions, PSII repair during photoinhibition – all these processes require significant fluidity in the membrane system and lateral diffusion of the involved proteins. The image that emerges from recent observations is that plants need to retain an optimised protein packing density in the thylakoid membrane at the level of about 70% in order to photosynthesise efficiently (Haferkamp et al., 2010). At the same time they need to overcome problems with high molecular crowding allowing for some lateral diffusion to occur. According to Kirchhoff (2008) this is achieved by non-random distribution and molecular order of photosynthetic complexes that is present to some extent in the grana thylakoids. Firstly, the existence of supercomplexes, as described before, minimises the number of obstacles that would impair protein movements

during its lateral diffusion. As the supercomplexes themselves need to be flexible and dynamic, particularly during acclimation their size must be small enough to ensure rapid response upon changes in the natural environment. Secondly, the supramolecular organisation (with the particular attention being paid to a parallel alignment of PSII complexes and the presence, under some conditions, highly ordered two-dimensional arrays of parallel-oriented complexes) ensures that the mobile proteins can migrate in a kind of diffusion channels. They could be formed temporarily and promote diffusion of particular proteins when it is necessary (Kirchhoff, 2008).

Although we know that the mobility of photosynthetic complexes has to occur under some conditions, still very little is known about the dynamics in real time. Over the years, different approaches have been used to probe mobility of photosynthetic proteins. They can be divided into two groups:

- **Indirect methods.** They are based on non-invasive techniques for monitoring photosynthetic light-harvesting and electron transport by measuring chlorophyll fluorescence or with using oxygen electrode. The data obtained from such measurements can be combined with structural data and some estimates about diffusion rates can be done. For example, the diffusion of plastoquinone and plastocyanin has been estimated with electron transfer kinetics (Mitchell et al., 1990; Kirchhoff et al., 2002) or the pyrene fluorescence quenching technique (Blackwell et al., 1994), and the diffusion coefficient for phospho-LHCII was obtained using a biochemical approach (Drepper et al., 1993). Although the data showed that a redistribution of LHCII occurred on a timescale of a few minutes but they failed to indicate for example how far the complexes migrated. One of the main drawbacks of the

biochemical approach is that it does not distinguish between two possibilities with regard to the relationship between grana structure and protein movement: (1) whether diffusion of proteins in and out of the grana requires any structural change or (2) the dynamic properties of complexes migrating to and from stroma lamellae does not affect the membrane structure, especially at the grana margins.

A more complex, but still indirect approach has been also implemented to study protein mobility which involved a combination of experimental data with Monte Carlo simulations (Drepper et al., 1993; Kirchhoff et al., 2004). This method can give a rough indication about diffusion rates, but because it is based on some indirect assumptions sometimes tends to give completely wrong results when compared to more direct measurements. For example, the estimated mobility of chlorophyll-proteins in grana thylakoids calculated from Monte Carlo simulations suggested that it would be severely restricted leading to an escape time from the grana of about 1 hour (Kirchhoff et al., 2004). However, the recent direct measurements using confocal microscopy combined with fluorescence recovery after photobleaching (FRAP) showed that at least a fraction of these proteins can escape the grana within a few seconds (Kirchhoff et al., 2008). It proves that the initial assumption of a pure random distribution of complexes made in the simulation turned out to be untrue as the real supramolecular organisation facilitated the rapid diffusion of the mobile population. For that reason, direct measurements of protein mobility in photosynthetic membranes are necessary.

- **Direct methods.** Several light and electron microscopy based techniques have already been used to study the distribution and structural changes in the organisation of photosynthetic complexes such as, for example freeze fracture (Staehelin, 2003, and references therein) or recently atomic force microscopy and electron tomography (Chuartzman et al., 2008). Application of these techniques allowed to see quantitative differences in the distribution of complexes and structural changes under specific conditions, for instance upon state transitions (Staehelin and Arntzen, 1983; Chuartzman et al., 2008). However, due to sample preparation any real time membrane rearrangements and dynamic tracking of protein movements would be excluded following such techniques. To resolve these issues, it seems that the most appropriate approach would include application of fluorescent microscopy to visualise the dynamics in real time. Although the spatial resolution is much lower compared to the one obtained with electron microscopy fluorescent techniques offer much less invasive way of looking into the distribution of some protein complexes, simply by visualising the natural fluorescence of the chlorophylls. It has its disadvantage in a sense that does not provide specific fluorescence signal emitting from particular protein of interest but, on the other hand such a way of observation will certainly not perturb the system. Fluorescent tagging of GFP or fluorescent antibodies is theoretically possible but due to their bulkiness it would not allow for investigation of native membranes such as tightly appressed grana regions of the thylakoids (Consoli et al., 2005). Among different fluorescent microscopy techniques three of them have recently been proved to be efficient in probing mobility of proteins in the thylakoid membranes:

- **Fluorescent lifetime imaging microscopy (FLIM)** that is based on confocal microscopy but it produces the image of fluorescent lifetimes of the fluorophore signal rather than its intensity. Iwai et al. (2010) took advantage of it and using FLIM technology recorded live-cell imaging of dissociation of phospho-LHCII from PSII during state transitions in *Chlamydomonas reinhardtii*. The experiments showed clearly that within a few minutes the chlorophyll lifetime fluorescence increased from 170 ps to 250 ps upon transition from state 1 to state 2 (dissociation of phospho-LHCII from PSII and its migration to PSI). In this way, the dynamic movements of LHCII under those specific conditions could be first detected in vivo in real time.
- **Single particle tracking (SPT)** which allows for detecting dynamic behaviour of individual particles. The fluorescence microscope used in this approach must be sensitive enough to detect the fluorescent tag attached to a single complex and the rate of imaging must allow for visualisation of its movement trajectory on a fast timescale. The technique provides better spatial resolution than conventional fluorescence techniques and allows to obtain the position of the particle to within a few nanometers. However, it has its own limitations. Firstly, the native fluorescence from the photosynthetic pigments cannot be used for SPT in intact systems. This is due to dense packing of the complexes in the photosynthetic membranes which does not allow for separating individual particles and following their movements. Secondly, an artificial fluorescent tag must be introduced which, as mentioned before, may perturb the system in native membranes. Despite these drawbacks, the SPT technique has been successfully implemented in the photosynthetic research. Consoli et al. (2005) used an antibody to link LHCII to a fluorescent

bead. Because of its size the bead must have been excluded from the appressed grana regions but even though the diffusion coefficients of individual LHCII in different phosphorylation states could be obtained.

- **Fluorescent recovery after photobleaching (FRAP).** This is a classic method for measuring diffusion in biological systems and has already been used to probe the mobility of protein complexes in some photosynthetic membranes (Mullineaux et al., 1997; Mullineaux and Sarcina, 2002). In favourable cases, FRAP is fully quantitative and can be used to measure the diffusion coefficients of photosynthetic complexes. However, this requires a simple, predictable membrane topography, and a membrane that can be assumed to be homogeneous over a distance of a micron or more. This is the case with the thylakoid membranes of some cyanobacteria (Mullineaux et al., 1997; Mullineaux and Sarcina, 2002). The experimental data obtained from *in vivo* measurements on the cyanobacterial photosynthetic membranes showed that PSII is normally completely immobile (Sarcina and Mullineaux, 2004). However, it is not clear if this is due to interactions within the membrane, or the thylakoid lumen, or both. It was also showed that under specific conditions (exposure to intense red light) almost half of the PSII population can be mobilised and move relatively fast in the membrane (Sarcina et al., 2006). It is perhaps due to a large-scale redistribution of PSII which may be required for the repair cycle. Green plant thylakoid membranes are much more difficult systems for FRAP because of their lateral heterogeneity and their complex three-dimensional architecture, which is still not fully understood (Garab and Mannella, 2008). Kirchhoff et al. recently used FRAP to measure the mobility of chlorophyll–protein

complexes in isolated grana membranes from spinach (*Spinacia oleracea* L.), taking advantage of the tendency of these membranes to fuse laterally into larger membrane patches *in vitro* (Kirchhoff et al., 2008). There, most of the chlorophyll proteins are completely immobile, at least on timescales of a few minutes. In this case it is clear that the immobility can be ascribed to protein-protein or protein-lipid interactions within the thylakoid membrane since the stromal and luminal proteins have been washed away during sample preparation (Kirchhoff et al., 2008). However, despite great reduction in the lateral diffusion abilities the membrane must retain some fluidity since a subpopulation accounting for about 25% of chlorophyll fluorescence is still able to diffuse surprisingly fast. It has been suggested that the mobile fraction probably consists only of a subpopulation of LHCII antennae which might be involved in state transitions phenomenon (Kirchhoff et al, 2008).

In this thesis I present the extension of the FRAP approach to probe the mobility of chlorophyll proteins in a more physiologically relevant system: the thylakoid membranes of intact spinach (*Spinacia oleracea*) and *Arabidopsis thaliana* chloroplasts under different physiological conditions. Although I could not measure exact diffusion coefficients in these systems because of the complex architecture of the membrane, I was able to determine ‘mobile fractions’ and track, for the first time, the mobility of chlorophyll-proteins that can exchange between grana via connecting stroma lamellae regions. I used a number of different control measurements to ensure that the results genuinely come from protein diffusion. They are presented, along with the detailed description of the FRAP method in chapter III.

Part of the work presented in this thesis has been published in the following journal article:

**Goral, T.K.**, Johnson, M.P., Brain, A.P., Kirchhoff, H., Ruban, A.V., and Mullineaux, C.W. (2010). Visualizing the mobility and distribution of chlorophyll proteins in higher plant thylakoid membranes: effects of photoinhibition and protein phosphorylation. *Plant J* **62**, 948-959.

This article is reprinted in Appendix 1.



# **Chapter II**

## **Materials and methods**

## 2.1. Plant material

Spinach leaves (*Spinacia oleracea* (L.)) were purchased fresh from a local supermarket and kept overnight at 4°C in the dark prior to use. Wild-type *Arabidopsis thaliana* (L.) ecotype Columbia (Col-0) plants (Nottingham Arabidopsis Stock Centre, UK) and all the mutants used in this study (Table 1) were grown in a Conviron plant growth room with an 8-h photoperiod at a light intensity of 200  $\mu\text{m photons m}^{-2} \text{sec}^{-1}$  and a day/night temperature 22/18°C, respectively. Mature rosette leaves from 10- to 12-week-old plants were dark adapted for 30 min prior to isolation of intact chloroplasts.

For *in vivo* FRAP experiments (chapter VII) the intact leaves of wild-type spinach (*Spinacia oleracea* (L.)), wild-type *Arabidopsis thaliana* (L.) and tobacco (*Nicotiana tabacum* (L.)) mutants were used. The latter plants were obtained from Mr. Franck Michoux working towards his PhD in Prof. Peter Nixon's research group at Imperial College, London. Transplastomic tobacco mutants were created by bombarding chloroplast transformation vectors pFM-T2Wt, pFM-T2A, pFM-T2S, pFM-T2D and pFM-A20 onto 4 weeks old *Nicotiana tabacum* petit havana leaves. The vectors consisted of a chloroplast DNA fragment containing the MatK and PsbA gene of the tobacco plastome. The *aadA* cassette conferring spectinomycin resistance was inserted in the unique BglIII restriction site located just before the PsbA promoter. In addition, a silent NdeI site was introduced at the start of the PsbA gene (pFM-T2Wt mutant), and the first threonine, T2, was changed to an alanine (pFM-T2A), aspartate (pFM-T2D) and serine (pFM-T2S). Finally, pFM-A20 mutant was created by removing the first 20 aa of photosystem II core protein D1. After biolistic bombardment, resistant shoots growing on spectinomycin-containing

media were subcultured 5 times onto RMOP media (Svab and Maliga, 1993) supplemented with spectinomycin. Homoplastomy was verified by southern blot.

**Table 1. List of *Arabidopsis thaliana* mutants used in this study.**

<b>Mutant</b>	<b>Reference</b>	<b>Seeds obtained from</b>
<b>stn7</b>	Bonardi et al., (2005)	Prof. D. Leister (LMU, Germany)
<b>stn8</b>	Bonardi et al., (2005)	Prof. D. Leister (LMU, Germany)
<b>stn7/stn8</b>	Bonardi et al., (2005)	Prof. D. Leister (LMU, Germany)
<b>npq4</b>	Li et al. (2002a)	Dr. Kris Niyogi (Berkeley, USA)
<b>L17</b>	Li et al. (2002b)	Dr. Kris Niyogi (Berkeley, USA)
<b>E122QE226Q</b>	Li et al. (2004)	Dr. Kris Niyogi (Berkeley, USA)
<b>npq1</b>	Niyogi et al. (1998)	Nottingham Stock Centre (UK)
<b>npq2</b>	Niyogi et al. (1998)	Nottingham Stock Centre (UK)
<b>lut2npq1</b>	Niyogi et al. (2001)	Dr. Kris Niyogi (Berkeley, USA)
<b>lut2npq2</b>	Havaux et al. (2004)	Dr. Kris Niyogi (Berkeley, USA)
<b>lut1</b>	Pogson et al. (1996)	Prof. Peter Horton (Sheffield, UK)
<b>lut2</b>	Pogson et al. (1996)	Prof. Peter Horton (Sheffield, UK)
<b>asLhcb2</b>	Andersson et al. (2003)	Prof. S. Jansson (Umeå, Sweden)
<b>koLhcb3</b>	Damkjaer et al. (2009)	Prof. S. Jansson (Umeå, Sweden)
<b>asLhcb4</b>	Andersson et al. (2001)	Prof. S. Jansson (Umeå, Sweden)
<b>asLhcb5</b>	Andersson et al. (2001)	Prof. S. Jansson (Umeå, Sweden)
<b>koLhcb6</b>	Kovács et al. (2006)	Prof. S. Jansson (Umeå, Sweden)
<b>ch1</b>	Murray and Kohorn (1991)	Nottingham Stock Centre (UK)

## **2.2. Isolation of intact chloroplasts**

Intact chloroplasts were isolated from spinach and Arabidopsis leaves using a modification of the procedure described by Crouchman et al. (2006). Fresh, dark-adapted leaves were homogenized in ice-cold grinding buffer (450 mM sorbitol, 20 mM Tricine, 10 mM EDTA, 10 mM NaHCO<sub>3</sub>, 5 mM MgCl<sub>2</sub> and 0.1% BSA at pH 8.4) with a Polytron (Kinematica GmbH, <http://www.kinematica.ch>). The homogenate was then filtered through four layers of muslin followed by four layers of muslin and one layer of cotton wool. The filtrate was centrifuged for 30 sec at 4000 g and 4°C. The chloroplast-enriched pellet was then washed twice and finally resuspended with a small volume of the buffer containing 300 mM sorbitol, 20 mM Tricine, 5 mM MgCl<sub>2</sub> and 2.5 mM EDTA, pH 7.6, and put on ice until use. The washing step was carried out with the resuspension medium. Chlorophyll concentration was determined according to the method described by Porra et al. (1989). The typical preparation contained approximately 50-70% of intact chloroplasts as judged from their visualisation under a confocal microscope (see section 2.11.1 for details). For unstacking of the thylakoid membranes MgCl<sub>2</sub> was removed from all buffers used for isolation of intact chloroplasts.

## **2.3. Isolation of grana membranes**

**(work done by Prof. Helmut Kirchhoff)**

Isolated grana membranes were prepared from spinach leaves following a procedure described previously (Kirchhoff et al., 2008). In brief, spinach leaves were ground in a grinding buffer (0.4 M sucrose, 25 mM Hepes, pH = 7.5, 1 mM EDTA, 15 mM

NaCl, 5 mM MgCl<sub>2</sub>, 5 mM CaCl<sub>2</sub>, BSA (2g/l), Ascorbate (1g/l) for 10 sec. The homogenate was then filtered through 2 layers of muslin and 2 x 4 layers of muslin with cotton wool. After centrifugation (5000 g for 6 min) the pellet was resuspended in the resuspending buffer (25 mM Hepes, pH = 7.5, 150 mM NaCl and 8 mM MgCl<sub>2</sub>). After the next centrifugation (5000 g for 10 min) the pellet was resuspended in a small amount of another buffer (1 M betaine, 25 mM Mes, pH = 6.2, 15 mM NaCl, 10 mM MgCl<sub>2</sub>, 5 mM CaCl<sub>2</sub>) and then diluted to a final chlorophyll concentration of 4 mg/ml. 10% Triton X-100 (diluted in a buffer containing 25 mM Mes, pH = 6.2, 15 mM NaCl, 10 mM MgCl<sub>2</sub> and 5 mM CaCl<sub>2</sub>) was then added in a stoichiometry of 1 : 1. After 2 min incubation the starch was pelleted (1800 g for 2 min) followed by the centrifugation of the supernatant (48000 g for 20 min). The resulting pellet was washed once in a cryo-buffer containing 1 M betaine, 25 mM Mes, pH = 6.2, 15 mM NaCl, 5 mM MgCl<sub>2</sub> and 5 mM CaCl<sub>2</sub> and then pelleted for another 12 min at 48000 g. The final pellet was resuspended in 200 µl the cryo-buffer and shock frozen in liquid nitrogen and stored at - 20°C until use.

#### **2.4. Control experiments with glutaraldehyde and nigericin**

For the glutaraldehyde control, chloroplasts were resuspended in resuspending buffer containing 2% glutaraldehyde (Agar Scientific Ltd., <http://www.agarscientific.com>) and incubated for 30 min at 4°C in the dark, followed by centrifugation (60 sec at 5000 g). The clean pellet was then resuspended in the resuspending buffer, and chlorophyll content was measured. For the nigericin control, 4 µM nigericin (Sigma-

Aldrich, <http://www.sigmaaldrich.com>) was added to the chloroplast suspension at a chlorophyll concentration of  $10 \mu\text{g ml}^{-1}$  prior to FRAP measurements.

## **2.5. Experiments with sodium fluoride**

Intact spinach chloroplasts were isolated as described above in the presence of 10mM NaF (Sigma-Aldrich) in both grinding and resuspension buffers.

## **2.6. Induction of different de-epoxidation states of the xanthophyll cycle pool in intact chloroplasts**

Isolated intact spinach chloroplasts were resuspended in the reaction medium (450 mM sorbitol, 10 mM NaCl, 10 mM KCl, 5 mM  $\text{MgCl}_2$ , 10 mM Tricine pH 8.0, 1 mM  $\text{KH}_2\text{PO}_4$  and 0.2% BSA) at a chlorophyll concentration of  $12 \mu\text{M}$  and put in a quartz cuvette with a continuous stirring. Chlorophyll fluorescence was monitored by pulse-amplitude-modulated (PAM) chlorophyll fluorometer (Walz-101 PAM, <http://www.walz.com>) and actinic lamp with attached fiber optic in conjunction with a Peltier sample cooler (Jobin Yvon) operated by a LFI-3751 temperature control unit (Wavelength electronics). Prior to measurements  $100 \mu\text{M}$  methyl viologen (Sigma-Aldrich) was added to the reaction medium as a terminal electron acceptor which allows for the built-up of transmembrane proton gradient during photosynthetic electron transport. Additionally, 30 mM sodium ascorbate (Sigma-Aldrich) was also present to mediate violaxanthin de-epoxidation.  $F_o$  (the fluorescence level with PSII reaction centers open) was measured in the presence of a  $10 \mu\text{mol photons m}^{-2} \text{s}^{-1}$  measuring beam. The maximum fluorescence in the dark-adapted state ( $F_m$ ), during the course of actinic illumination ( $F_m'$ ) and in the subsequent dark relaxation periods was determined using a 0.8 s saturating light

pulse ( $4000 \mu\text{mol photons m}^{-2} \text{s}^{-1}$ ). The actinic light intensity used was  $350 \mu\text{mol photons m}^{-2} \text{s}^{-1}$  for about 5 minutes. The light treated samples were either maintained in the NPQ state or allowed a further 5 minute period of darkness to relax NPQ. The quantum yield of PSII was defined as  $F_v/F_m = ((F_m - F_o)/F_m)$  and NPQ as  $((F_m - F_m')/F_m')$ .

## 2.7. Maintenance of NPQ state in intact chloroplasts

Induction and maintenance of NPQ state was performed in two alternative ways. First approach, based on observations made by Rees et al. (1992), involved addition of acid at the end of light treatment in order to collapse the transmembrane proton gradient ( $\Delta\text{pH}$ ) and prevent relaxation of NPQ in dark (Figure 2.1).

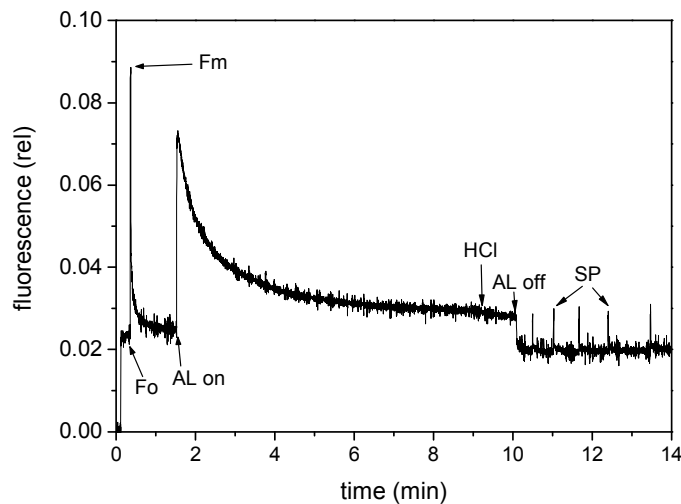


Figure 2.1. PAM chlorophyll fluorescence measurement on intact spinach chloroplast. Prior to illumination with the actinic light ( $AL = 350 \mu\text{mol photons m}^{-2} \text{s}^{-1}$ ) a saturating light pulse was applied to the chloroplast suspension to determine  $F_v/F_m$  value. At the end of the illumination period a small amount of 1M HCl (point marked by the arrow) was added to the sample resulting in acidification of thylakoid lumen ( $\text{pH} = 5.5$ ). After AL was switched off the saturating pulses ( $SP = 4000 \mu\text{mol photons m}^{-2} \text{s}^{-1}$ ) were applied to determine irreversibility of NPQ state under these conditions.  $F_o$ ,  $F_m$  – fluorescence levels when all PSII reaction centers are open or closed, respectively.

The second approach was based on observations made by Lambrev et al. (2007) and used low temperature to trap the NPQ state following light adaptation. In brief, at the end of light treatment the temperature of the reaction medium was rapidly cooled (~ 60s) by the Peltier device from 22°C to 4°C. This resulted in no reversal of fluorescence quenching upon removal of actinic light as presented in Figure 2.2.

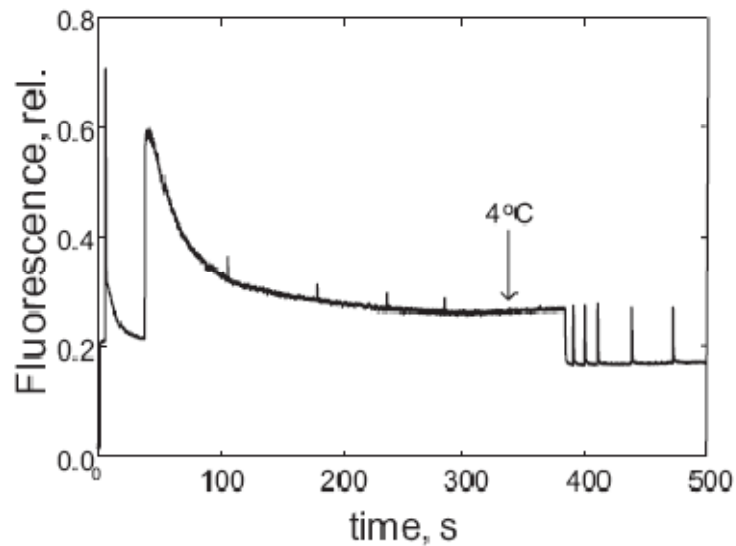


Figure 2.2. PAM chlorophyll fluorescence induction trace of intact spinach chloroplast light-treated at  $350 \mu\text{mol photons m}^{-2} \text{s}^{-1}$  at 22°C in a Peltier device temperature-controlled cuvette. At the point marked by the arrow the temperature was lowered to 4°C, cooling was complete within 60 seconds, after which the actinic light was removed. Note lack of reversal of fluorescence quenching at low temperature in dark.

As shown above, both mentioned approaches could lead to induction and maintenance of NPQ state following light adaptation. However, the low temperature treatment (Figure 2.2) turned out to be more stable and reproducible, and for that reason only the chloroplasts treated in such a way were used for FRAP and electron microscopy analysis as described below.



## **2.8. Photoinhibitory treatment of intact chloroplasts**

Photoinhibition in intact chloroplasts was induced by high light exposure and monitored by pulse-amplitude-modulated (PAM) fluorescence measurements (Walz-101 PAM fluorometer), as presented in Figure 2.3. In brief, the chloroplast suspension (at a chlorophyll concentration of  $10 \mu\text{g ml}^{-1}$ ) was illuminated with a high intensity of light ( $3000 \mu\text{mol photons m}^{-2} \text{sec}^{-1}$ ) for approximately 10–15 min at room temperature following saturating light pulses at 30-sec intervals for about 5 min. Prior to illumination,  $25 \mu\text{M}$  3-(3,4-dichlorophenyl)-1,1-dimethylurea (DCMU) (Sigma-Aldrich) was added to eliminate the photochemical contribution to fluorescence quenching (Figure 2.3.A). The decrease in variable fluorescence  $F_v/F_m$  after photoinhibitory treatment was more than 50%, and did not recover significantly, even after 2 h (Figure 2.3.B). Photoinhibited chloroplasts were immediately used for FRAP measurements.

## **2.9. Photoinhibitory treatment of grana membranes**

**(work done by Prof. Helmut Kirchhoff)**

Photoinhibition in grana membranes (at a chlorophyll concentration of  $40 \mu\text{g ml}^{-1}$ ) was induced and monitored by PAM fluorescence measurements in a similar way as for intact chloroplasts. Photoinhibited grana membranes were immediately used for FRAP measurements.

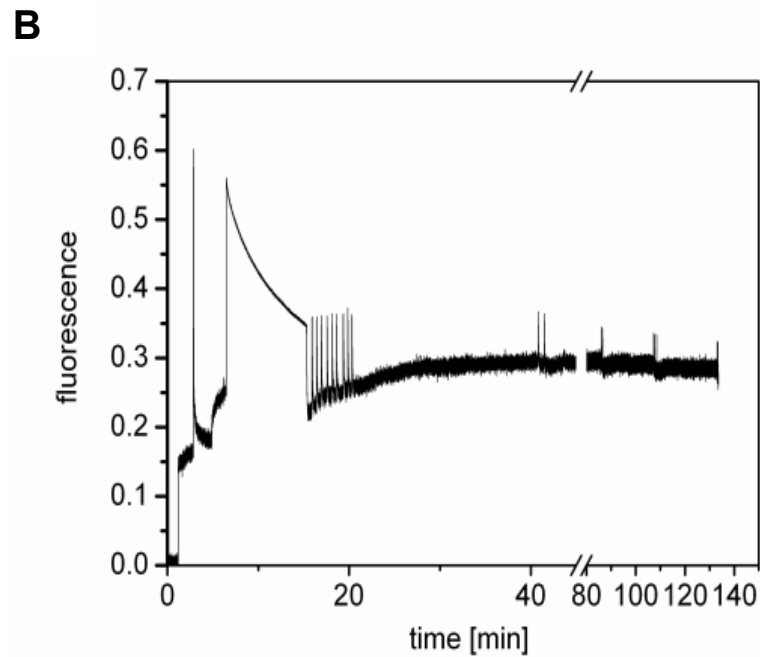
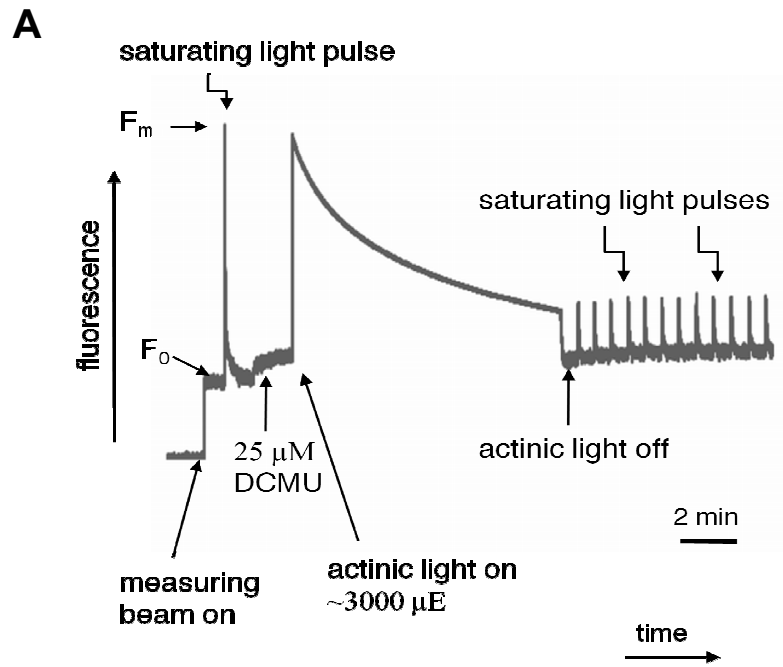


Figure 2.3. Photoinhibition of intact spinach chloroplasts monitored by PAM fluorometry. (A). Typical fluorescence trace during photoinhibitory treatment. A sample was withdrawn and used for FRAP measurements at the end of the actinic illumination. (B). Fluorescence trace during photoinhibitory treatment at the extended timescale showing irreversibility of PSII damage within a few hours.

## **2.10. Sample preparation for FRAP**

### **2.10.1. Experiments on isolated intact chloroplasts**

Prior to experiments, chloroplast suspensions were diluted in resuspension buffer containing 5  $\mu\text{M}$  BODIPY FL C<sub>12</sub> (Invitrogen, <http://www.invitrogen.com>) to a final chlorophyll concentration of 10  $\mu\text{g ml}^{-1}$ . A glass slide was sealed with a coverslip using vacuum grease, so as to form a flow chamber. A 60- $\mu\text{l}$  volume of 0.5% aqueous solution of polylysine (Sigma-Aldrich) was applied to the chamber, washed with the resuspension buffer, followed by the application of 60  $\mu\text{l}$  of the chloroplast suspension. After 5 min of incubation the chloroplasts that were not immobilized were washed out with resuspension buffer.

### **2.10.2. Experiments on isolated grana membranes**

(Work done by Prof. Helmut Kirchhoff)

Isolated grana membranes were immobilised by adsorption onto an artificial lipid layer, as described previously (Kirchhoff et al., 2008). In brief, 20  $\mu\text{l}$  of 2,2,2-trifluoroethanol (Sigma-Aldrich) containing 10 mM phosphatidylcholine (PC) and 10  $\mu\text{M}$  4,4-difluoro-5,7-dimethyl-4-bora-3a,4a-diaza-s-indacene-3-dodecanoic acid (BODIPY FL C<sub>12</sub>; Invitrogen) was spotted onto a glass slide. The lipid film was dried under a stream of nitrogen for 1 h and then rehydrated in anaerobic buffer (5 mM MgCl<sub>2</sub>, 40 mM NaCl, 30 mM MES [pH 6.5], 11 units mL<sup>-1</sup> Glc oxidase, 800 units/mL catalase, and 4 mM Glc) at 40°C for 2 min. This generated stacks of PC bilayers labeled with BODIPY FL C<sub>12</sub>. 30  $\mu\text{l}$  of membrane suspension in anaerobic buffer at a chlorophyll concentration of 10  $\mu\text{g ml}^{-1}$  were placed on the glass-PC

support, incubated for at least 10 min in the dark, sealed with a coverslip, and used for FRAP measurements.

### **2.10.3. Experiments on intact leaves**

Leaf discs (about 5 mm in diameter) were cut out from fresh mature intact leaves of spinach, *Arabidopsis* and tobacco mutant plants. The discs were then allowed to float in 0.9 M aqueous solution of sucrose for 2 hours in dark to prevent from chloroplast movements that occur naturally within plant cells in response to light illumination (McCain, 1998). Prior to FRAP experiments, the leaf discs were placed onto a glass slide and sealed with a coverslip using vacuum grease.

## **2.11. FRAP measurements**

### **2.11.1. Experiments on isolated intact chloroplasts and grana membranes**

The FRAP measurements were carried out with a Nikon PCM2000 laser-scanning confocal microscope using a 60× oil-immersion objective (numerical aperture 1.4). Images were recorded with pixel dimensions of 28 nm. The 488-nm line of a 100-mW Argon laser (Spectra-Physics, part of Newport, <http://www.newport.com>) was used for exciting both chlorophyll and BODIPY FL C-12 fluorescence. BODIPY FL C-12 fluorescence was selected with a 505-nm dichroic mirror and an interference filter with a transmission range of 500–527 nm. Chlorophyll fluorescence was selected with a Schott RG665 red glass filter transmitting above about 665 nm. Chloroplasts were visualised using a 20- $\mu\text{m}$  confocal pinhole giving a point-spread in the *z*-direction of about 1.3  $\mu\text{m}$  (full width at half maximum). For FRAP, a line was bleached across the sample by withdrawing neutral density filters

to increase the laser power by a factor of 32. The laser was then scanned repeatedly in one dimension for 5–7 sec. Laser power was then reduced again, and 10 post-bleaching images were recorded at 60-sec intervals. For the total bleaching control, the entire sample was bleached out by increasing the laser power and scanning across the entire field of view in *xy* mode for 15–20 sec.

### **2.11.2. Experiments on intact leaves**

These FRAP measurements were carried out with a Leica SP5 laser-scanning confocal microscope (Leica Microsystems, Germany) using a 63× glycerol-immersion objective (numerical aperture 1.3) with a working distance of 0.28 mm. Images were recorded with pixel dimensions in a range of 68 - 96 nm. The 488-nm line of a 100-mW Argon laser was used for exciting chlorophyll fluorescence. Chlorophyll fluorescence was selected with a green/red emission filter with emission bandwidth between 653 – 695 nm. Chloroplasts were visualised using a confocal pinhole size of 1 AU (airy units) giving an optical thickness of about 0.73  $\mu\text{m}$  (full width at half maximum). For FRAP, a two-dimensional bleaching spot was bleached in the region of interest by increasing the laser power from 30% to 100% and scanning in two-dimensions for 2 sec. Laser power was then reduced again, and 20 post-bleaching images were recorded at 30-sec intervals.

### **2.12. Image processing and FRAP data analysis**

In the intact chloroplast measurements, confocal images were converted to greyscale and deconvolved using the DeconvolutionJ plug-in of the public domain NIH ImageJ software (<http://rsb.info.nih.gov/ij>) using 2D deconvolution based on the Wiener filter (Figure 2.4). The regularisation parameter ( $\gamma$ ) was 0.0001. The point-

spread function was determined by the visualisation of 0.175- $\mu\text{m}$  diameter fluorescence microspheres (PS-Speck Microscope Point Source kit; Invitrogen, Molecular Probes, <http://www.invitrogen.com>) with the same microscope set-up (Figure 2.4.B). The point-spread function in the  $xy$  plane was 0.76  $\mu\text{m}$  (full width at half-maximum), and was reduced to 0.68  $\mu\text{m}$  after deconvolution. The images were aligned to correct for the slight drift with time during the FRAP series using ImagePro Plus software (Media Cybernetics, <http://www.mediacy.com>), and then analysed with ImageJ. An individual granum was selected as a region of interest and the fluorescence intensity of that region was measured in pre- and post-bleach images. Simultaneously, the fluorescence in unbleached regions in post-bleach images was normalised to the same total fluorescence as in pre-bleach images. Mobile fractions were determined by fluorescence recovery curves according to the following equation (Reits and Neefjes, 2001):

$$R = (F_{\infty} - F_0) / (F_i - F_0)$$

where  $R$  is the mobile fraction,  $F_{\infty}$  is the fluorescence intensity in the bleached region after full recovery,  $F_0$  is the fluorescence intensity just after bleaching (time 0) and  $F_i$  is the fluorescence intensity in the pre-bleach image.  $F_0$  values were normalised to 0 in all measurements, and an exponential curve was plotted to the experimental points using Origin software (OriginLab, <http://www.originlab.com>).

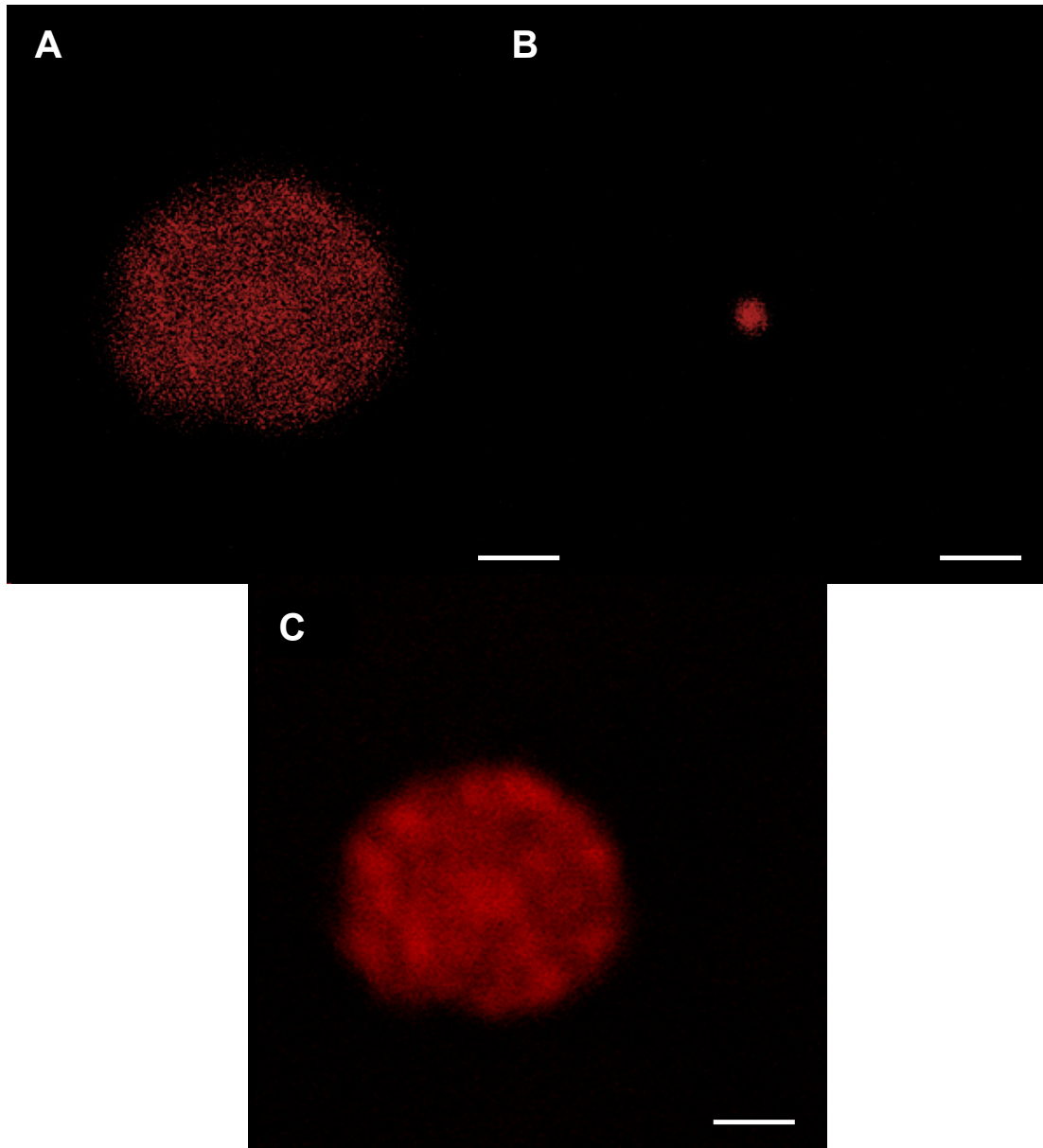


Figure 2.4. Deconvolution of confocal images performed by DeconvolutionJ plug-in of the NIH Image J software. (A). Raw confocal image of intact chloroplast isolated from *Arabidopsis thaliana* wild-type plants. (B). Raw confocal image of 0.175- $\mu\text{m}$  diameter fluorescence microsphere used for point-spread function calculations. (C). Deconvolved confocal image of the same chloroplast as in image (a). Notice removal of the blurring and improvement in contrast so that individual grana (bright fluorescent spots within the chloroplast) could be visualised. Scale bars = 2  $\mu\text{m}$ .

(Work done by Prof. Helmut Kirchhoff) Mathematical analysis and calculation of mobile fractions for isolated grana membranes were conducted as described below. One-dimensional fluorescence profiles were extracted from each image in the Y-direction (i.e. perpendicular to the line-bleach), summing fluorescence across the membrane patch in the X-direction. Because the membrane patches are small, bleaching results in a significant decrease in the total fluorescence from the sample. To compare fluorescence distributions before and after the bleach, the profiles were normalised to the same total fluorescence. The postbleach profiles were then subtracted from the prebleach profile to generate a set of difference profiles. The mobile fraction was estimated by comparing the first postbleach profile with the profiles obtained at the longest time points (Kirchhoff et al., 2008).

For FRAP experiments performed on chloroplasts in intact leaves the raw confocal images were used for mobile fraction calculations (as described for the isolated chloroplasts). The fluorescence intensity in the bleaching spot was recorded for each image and then normalised. Normalisation was necessary to correct for the changes in the total fluorescence intensity caused by the bleaching of chlorophyll occurring on the timescale of FRAP series. This was achieved by normalising the fluorescence intensity of neighbouring chloroplasts with respect to the one where the bleaching spot was generated in post-bleach images to the same total fluorescence as in pre-bleach images.



## **2.13. Thin section electron microscopy**

**(work done by Dr. Matthew Johnson and Dr. Anthony Brain)**

Chloroplasts were centrifuged and the pellets fixed in 2.5% glutaraldehyde in 0.1 M sodium cacodylate buffer (pH 7.2), post-fixed in osmium tetroxide in 0.1 M sodium cacodylate buffer (pH 7.2) and embedded in TAAB resin (TAAB Laboratories Equipment Ltd, United Kingdom). Ultrathin sections (~ 70 nm thickness) were cut and stained with uranyl acetate and lead citrate. Thin sections were examined with an FEI Tecnai T12 BioTWIN and a Hitachi H7600 electron microscope.

## **2.14. Freeze-fracture electron microscopy**

**(work done in collaboration with Dr. Anthony Brain)**

Freshly prepared spinach or *Arabidopsis* chloroplast suspensions were concentrated and rapidly frozen as a thin film by rapid immersion in slushy liquid nitrogen (-210°C) using Bal-Tech double replica carriers, and were then fractured at -150°C in a Polaron E7000 freeze-fracture device. Replicas were prepared by shadowing with platinum and carbon, cleaned with bleach and examined with an FEI Tecnai T12 BioTWIN and a Hitachi H7600 electron microscope at 120 000× magnification.

## **2.15. Electron microscopy image analysis**

PSII and LHCII particles were selected from the freeze-fracture electron micrographs using either Pixcavator IA 4.2 software (Intelligent Perception, <http://inperc.com>) or manually by ImagePro Plus software. Nearest neighbour distances (center-to-center) were conducted using the Delaunay Voronoi plug-in of the ImageJ software and

a bespoke programme created on request by Dr. Christopher Duffy. The latter programme was used also for calculations of particle clustering based on the coordinates from each particle. Nearest neighbour distance analysis allows for measuring the distances with about 0.72 nm accuracy which is the spatial resolution (single pixel size in xy direction) of the electron micrographs obtained. If there is a change in the distance between any two particles the programme would only detect the difference at the level of at least one single pixel size. Measurements of particle sizes were carried out with ImagePro Plus software. The percentage of semi-crystalline PSII arrays was quantified as the total amount of ordered PSII from the total of all EFs fracture faces in all micrographs obtained. Thin section samples were analysed by using autocorrelation functions performed on typical densitometry traces with the use of web based software: Wessa P., (2009), (Partial) Autocorrelation Function (v1.0.7) in Free Statistics Software (v.1.1.23-r5), Office for Research Development and Education, [http://www.wessa.net/rwasp\\_autocorrelation.wasp/](http://www.wessa.net/rwasp_autocorrelation.wasp/).

# **Chapter III**

## **Optimisation of FRAP experiments**

### 3.1 Theoretical background

The technique of fluorescence recovery after photobleaching (FRAP) is one of the direct methods for observing the dynamics and diffusion in biological systems, including the dynamics of membrane components. Nowadays, FRAP measurements are normally performed with a laser-scanning confocal microscope. This requires the tagging of the component whose diffusion is to be observed with a fluorophore so that it can be visualised under the confocal microscope. The principle underlying FRAP is that by transiently increasing the laser power illuminating a particular region of the sample will lead to photobleaching of that region probably due to photo-oxidation mechanism (Xie and Trautman, 1998). This will generate a 'black hole' in the region of fluorescence signal. After bleaching, the laser power is decreased again and the whole sample is imaged in a series of subsequent post-bleach scans. If the fluorophore is mobile then one can observe a characteristic change in the bleached region. The migration of fluorescent molecules from the surrounding area into the bleaching spot will cause recovery of fluorescence in its center, and the bleach will become broader and shallower. In that case, provided the membrane topology is known and the membrane environment is fairly uniform on a large scale, it is possible to analyse quantitatively the dynamic properties of the fluorophore by calculating its diffusion coefficient. In principle, there are two forms of the FRAP method dependent on the equipment used and the type of sample which is to be investigated:

- **One dimensional FRAP** which involves bleaching a line across the sample by scanning the confocal spot in one dimension (Figure 3.1). After decreasing the laser power, the confocal spot is scanned in two dimensions and a series of post-bleach images is recorded. Diffusion of the bleached fluorophore causes the bleached line to become broader and shallower in time. This variant of FRAP was performed on intact chloroplasts that I used in this study.

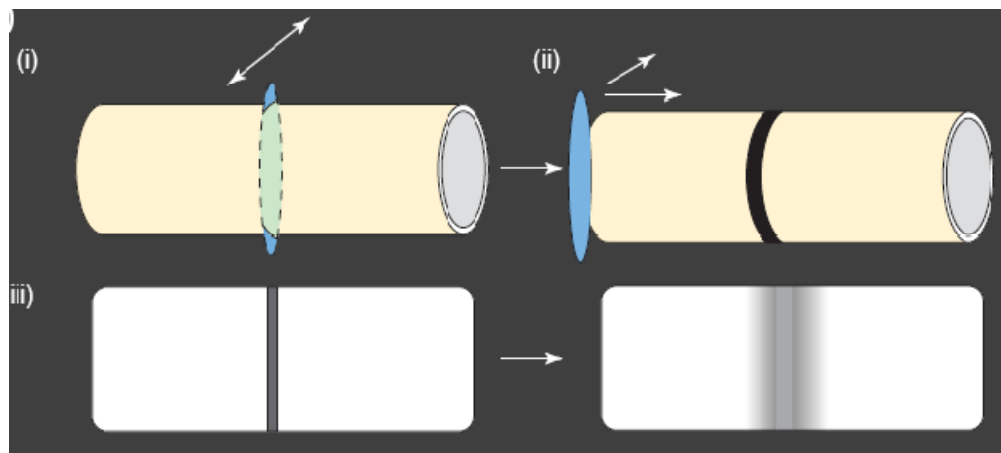


Figure 3.1. One dimensional FRAP. The confocal laser spot is shown in blue. (i) Bleaching a line in one dimension, (ii) Recording a series of post-bleach scans in two dimensions. (iii) Change of the bleaching spot over time. See description in the text for further orientation. Adapted from Mullineaux and Sarcina (2002).

- **Two-dimensional FRAP** which requires the confocal spot to be kept stationary for the moment of bleaching or alternatively the bleaching spot is created by scanning the laser over a small area (Figure 3.2). After decreasing the laser power, the confocal spot is scanned in two dimensions and a series of post-bleach images is recorded. Diffusion of the bleached fluorophore causes the bleached spot becoming broader and shallower with time. This

form of FRAP was performed in experiments on chloroplasts in intact leaves (chapter VII).

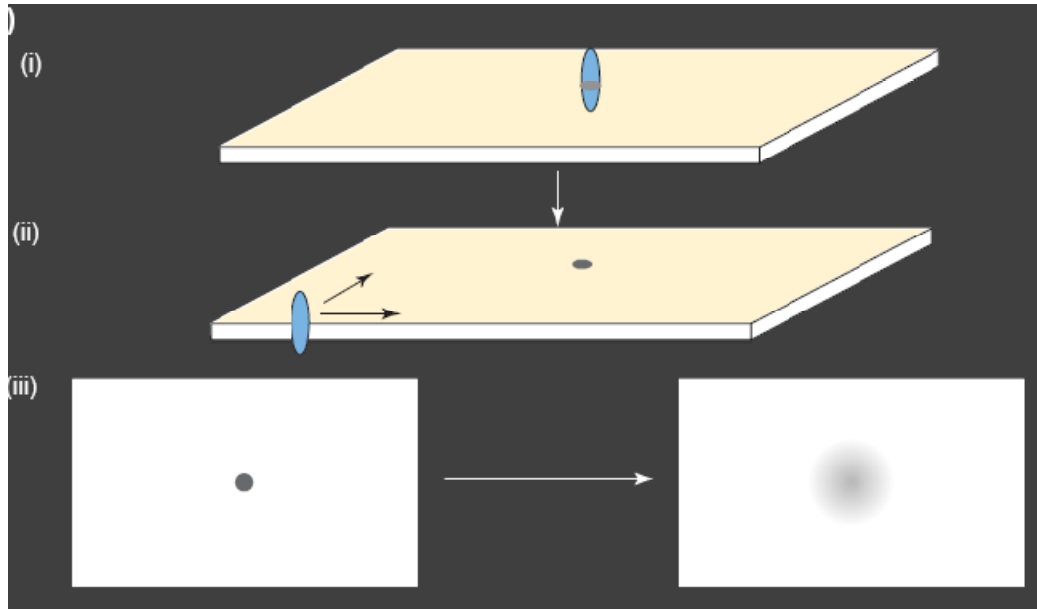


Figure 3.2. Two dimensional FRAP. Blue colour indicates the confocal laser spot. (i) Bleaching the confocal spot in two dimensions. (ii) Recording a series of post-bleach scans in two dimensions. (iii) Change of the bleaching spot over time. See description in the text for further details. Adapted from Mullineaux and Sarcina (2002).

FRAP as an optical technique has a limited spatial resolution (theoretically at a diffraction limit which depends on the emitted light wavelength and the numerical aperture of the objective used for imaging according to the following equation:  $\text{resolution}_{\text{spatial}} = 0.6 \lambda / \text{NA}$  where  $\lambda$  is the emitted light wavelength and NA is the numerical aperture of the objective). *In vivo* experiments decrease the resolution even further because of light scattering during imaging. As a consequence, in experimental conditions the confocal spot and a resulting bleaching area usually appear much larger than predicted.

Thylakoid membranes of green plants are far from being ideal model systems for FRAP experiments. Apart from being enclosed in a small area of a chloroplast, they are never flat and have a complicated three-dimensional topography. On the other hand, they are packed with proteins with natural fluorophores attached such as chlorophylls. This eliminates the necessity for specific fluorophore binding or GFP gene fusions. What is more, thylakoid membranes represent a much more physiologically relevant system than isolated flat grana membranes that have been investigated previously (Kirchhoff et al., 2008). This study provides strong evidence that FRAP can still be successfully applied to probe mobility of membrane components in such a complex system. The method has to be carefully controlled and optimised but it allows to observe the genuine dynamics of chlorophyll-proteins in different plant species under different environmental conditions. The FRAP experiments performed in this study (except for those presented in chapter VII) involve using isolated intact chloroplast with the internal thylakoid membrane network untouched. Because of the complex membrane architecture, I cannot measure diffusion coefficients in this system. However, I can accurately measure the ‘mobile fraction: in this case the proportion of chlorophyll-proteins escaping from one granum and diffusing through stroma lamellae to another granum. This leads to recovery of fluorescence in a bleached granum (Fig. 3.3).

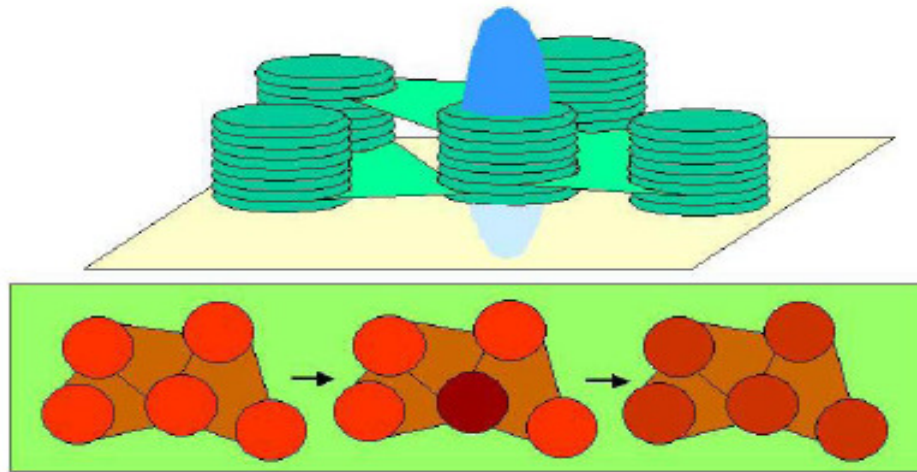


Figure 3.3. Schematic diagram showing the idea of FRAP experiment performed on the thylakoid membranes in intact chloroplasts. Confocal laser spot is shown in blue. Chlorophyll fluorescence from a single granum is bleached out. Diffusion of chlorophyll-proteins from neighbouring grana via interconnecting stroma lamellae leads to recovery of fluorescence in the bleached granum.

### 3.2. Visualisation of chloroplast intactness

To determine mobility of chlorophyll-proteins in the thylakoid membranes of intact chloroplasts it is of crucial importance to have an efficient method to distinguish chloroplasts possessing the outer envelope in an intact form from those which have the outer membrane broken. To date, several standard procedures have been developed for isolating intact chloroplasts from different species, most of them involving centrifugation on a Percoll cushion to separate intact and broken organelles (Napier and Barnes, 1995). However, I never managed to obtain 100% intact organelles in the preparation. As the confocal FRAP measurements are made on individual chloroplasts it is important to assess whether the chloroplast under examination is broken or intact. I found that this could be achieved by staining the preparation with the green lipophilic fluorophore BODIPY FL C<sub>12</sub>, which was



previously used to stain membranes in the cells of cyanobacteria (Sarcina et al., 2003). In intact chloroplasts the dye can incorporate specifically into the chloroplast envelope, and does not enter the chloroplast interior. It is visualised as a continuous halo of green fluorescence surrounding the red chlorophyll fluorescence from the thylakoid membranes (Figure 3.4). However, when the outer membrane is broken the distribution of green fluorescence is very different: there is only fragmentary staining outside the thylakoid membranes and considerable staining of the thylakoid membranes themselves (Figure 3.4). Hence, confocal imaging of isolated chloroplasts can serve as a direct, rapid and efficient method to probe their intactness. I used this method to select intact chloroplast for the FRAP experiments.

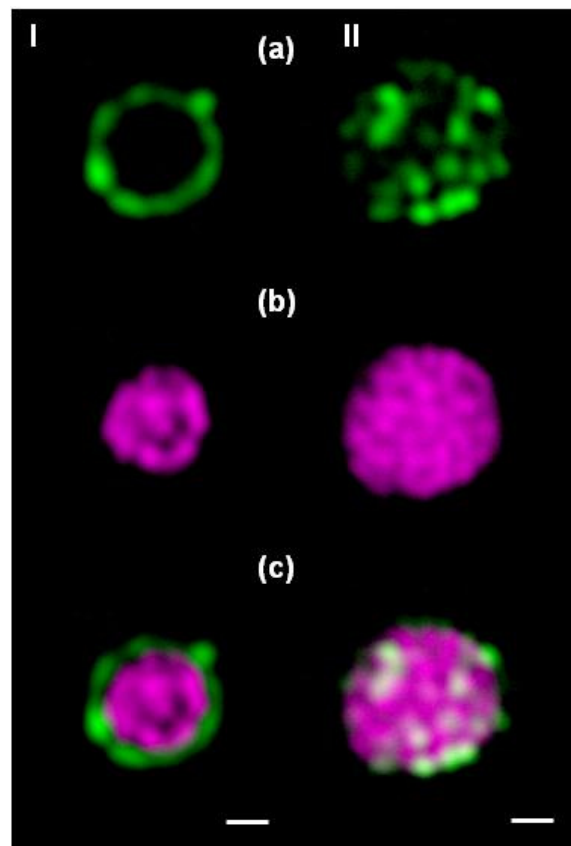


Figure 3.4. Confocal fluorescence images of intact (I) and broken (II) chloroplasts from spinach (*Spinacia oleracea* L.). Scale bars = 2  $\mu\text{m}$ . (a) Green fluorescence from the BODIPY FL C<sub>12</sub> stain, (b) Chlorophyll fluorescence, (c) Merged pseudocolour images (chlorophyll fluorescence shown in magenta; BODIPY FL C<sub>12</sub> fluorescence shown in green).

### **3.3. FRAP experiments in isolated intact chloroplasts: controls**

For FRAP it is important that the sample is immobilised to ensure that any fluorescence recovery is the result of diffusion within the sample rather than movement of the sample as a whole. Slides coated with polylysine are often used to immobilise bacterial cells (e.g. Lenn et al., 2008) and I found this method to be effective with intact chloroplasts. Most chloroplasts adhered to the polylysine-coated slide and remained immobile during the experiment. Presumably, the negatively charged outer membrane (Stocking and Franceschi, 1982) interacts electrostatically with the positively charged polylysine film. It is worth noticing that in this system there is no direct interaction between the thylakoid membranes and the support, and thus no danger that such interactions might perturb membrane conformation and the mobility of membrane proteins.

For FRAP measurements I first selected intact, immobilized chloroplasts as described above, and then visualised chlorophyll fluorescence by scanning in two dimensions (see Methods for details). At the fixed imaging laser intensity, chlorophyll fluorescence was stable: repeated scans across the same chloroplast did not lead to detectable photobleaching. The grana within the chloroplasts appeared as bright fluorescent spots (as shown in Figures 3.5-3.6 and 4.2). For the measurements it was important to resolve the fluorescence from individual grana as cleanly as possible. Because the grana are tightly packed together, this is problematic at optical resolution.

I used a routine deconvolution procedure taking into account the measured point-spread function (see Methods for further details) to improve the resolution of

individual grana. To photobleach a region of the chloroplast I increased the laser power by a factor of 32 and then scanned the confocal laser spot repeatedly in one dimension across the sample for 5-7 s (one dimensional FRAP). This resulted in bleaching a line across the chloroplast which could be visualised by subsequent imaging at lower laser power (Figures 3.5 – 3.6 and 4.2). Under some conditions I could then observe a partial recovery of fluorescence in the bleached zone over a timescale of a few minutes (Figure 4.2).

It was necessary to establish whether or not this fluorescence recovery was due to the diffusion of chlorophyll-protein complexes into the bleached area. Since the differences in mobile fractions are not dependent on the bleaching efficiency (Kirchhoff et al., 2008) the most probable source of changes in fluorescence intensity in the bleached region unrelated to dynamics of fluorophores would be some sort of reversible fluorescence quenching of the chlorophylls. This could be achieved by formation of states which are temporarily bleached but eventually reemit the fluorescence spontaneously (Mullineaux, 2004). In geometrically simpler systems (for example isolated, laterally fused grana membranes and the quasi-cylindrical thylakoid membranes of some cyanobacteria) fluorescence redistribution can clearly be visualised. The recovery of fluorescence in the bleached area is matched by loss of fluorescence in the neighbouring regions of the membrane, leading to a characteristic "blurring" of the bleached line which is a clear indication of diffusion (Mullineaux et al. 1997; Kirchhoff et al., 2008). However, the situation is more complex in intact chloroplasts due to the lateral heterogeneity and intricate geometry of the membrane (Andersson and Anderson, 1980), combined with the small extent of fluorescence recovery. To test the possibility of reversible fluorescence quenching I bleached entire chloroplasts, rather than just a line across the chloroplast

(Figure 3.5.A). If recovery were due to reversible fluorescence quenching, I would still expect to observe it in this experiment. If recovery were to diffusion I would expect not to see it, since bleaching the entire chloroplast removes the pool of unbleached complexes whose diffusion into the bleached area causes the recovery. Fluorescence recovery was very slight in this experiment (Figure 3.5.A). This is strong evidence against any significant reversible fluorescence quenching under conditions that I used.

As a second control I used treatment with glutaraldehyde, a very effective protein cross-linker (Habeeb and Hiramoto, 1968). If fluorescence recovery were due to protein diffusion I would expect it to be strongly inhibited by glutaraldehyde treatment, and indeed I observed very little fluorescence recovery in glutaraldehyde-treated chloroplasts (Fig. 3.5.B). Both of the controls shown in Figure 3.5 suggest that the fluorescence recovery I observe is due to protein diffusion, as it is in isolated grana membranes (Kirchhoff et al., 2008).

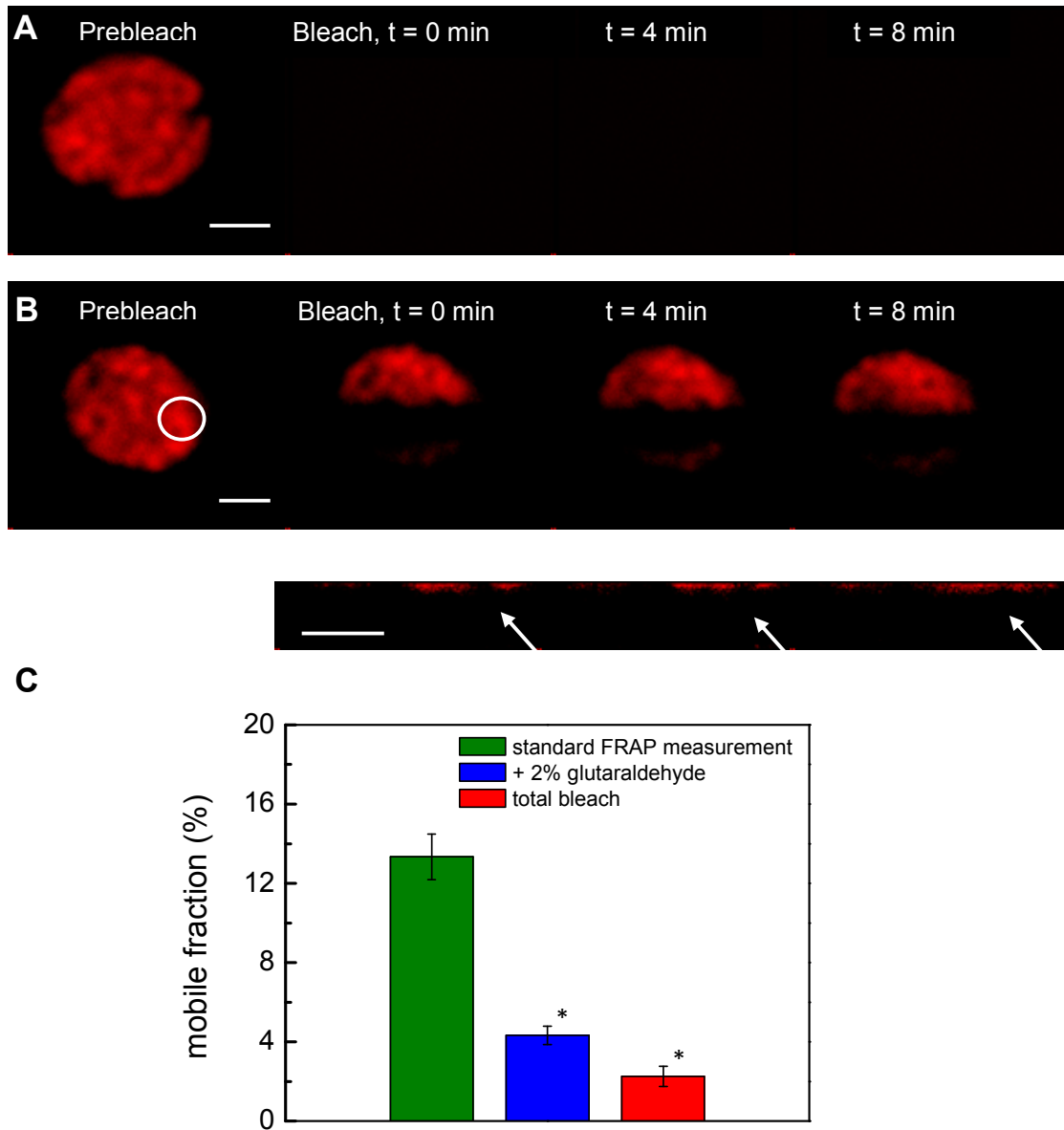


Figure 3.5. Control FRAP experiments on intact spinach (*Spinacia oleracea* L.) chloroplasts. Scale bars = 3  $\mu$ m. (A) ‘Total bleach’ experiment, bleaching out the entire membrane area. Note the lack of fluorescence recovery. (B) Bleaching a line across a chloroplast fixed with glutaraldehyde. The circle in the prebleach image shows the region of interest selected for quantitative analysis, and the panel below shows enlarged and contrast-enhanced images of the bleached area (with the position of the granum indicated by the arrow). Fluorescence recovery is minimal. (C) Mobile fractions in experiments of the type shown in (A) and (B), compared with experiments of the type shown in Figure 4.2. Bars represent means of 10 experiments  $\pm$  SEs. Asterisks indicate values significantly different from the control (analysed by a one-way ANOVA with Tukey’s post hoc test,  $P < 0.05$ ).

For my purposes it was also important to assess the effect of the bleach on the grana membrane structure. To do this I carried out FRAP measurements on broken chloroplasts in which the thylakoid membrane system was stained with the BODIPY FL C<sub>12</sub> dye as in Figure 3.4. Following the bleaching, fluorescence recovery was observed simultaneously in the red channel (monitoring chlorophyll fluorescence) and the green channel (monitoring BODIPY fluorescence) (Figure 3.6). The recovery of chlorophyll fluorescence in the bleached granum is slow and incomplete (Figure 3.6.A). However, there is a complete recovery of BODIPY fluorescence on a timescale of a few minutes (Figure 3.6.B). This indicates relatively rapid lipid mobility within the thylakoid membrane system, and it indicates that the basic structure of the granum is not destroyed by photobleaching.

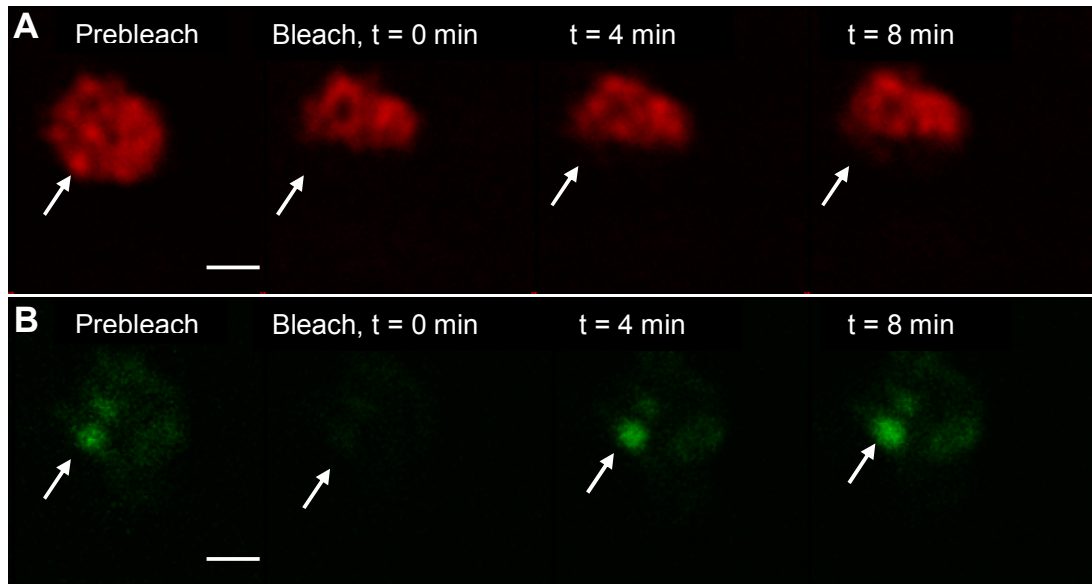


Figure 3.6. Control FRAP experiment on a broken spinach (*Spinacia oleracea* L.) chloroplast. Scale bars: 3  $\mu$ m. The chloroplast was stained with the green lipophilic fluorophore BODIPY FL C<sub>12</sub>. Following photobleaching, fluorescence was monitored simultaneously in (A) red channel (chlorophyll fluorescence) and (B) the green channel (BODIPY fluorescence). The arrowed granum shows only partial chlorophyll fluorescence recovery, but complete BODIPY fluorescence recovery.

# **Chapter IV**

**Mobility of chlorophyll-proteins:  
effects of photoinhibition and  
protein phosphorylation**

## 4.1. Photoinhibition phenomenon

The term 'photoinhibition' is generally referred to high-light induced inactivation of photosystem II caused by oxidative damage of its reaction centers, in particular D1 subunits. This seems to be an inevitable consequence of the complicated redox chemistry which uses water as a source of electrons and liberating molecular oxygen as a side product. However, highly reactive oxygen species (ROS) such as singlet oxygen can also be generated during water splitting and thus pose a real threat to the photosynthetic machinery. At high light intensities the production of ROS is greatly increased. This leads to irreversible damage of PSII which slows down the rate of photosynthesis and in extreme cases after prolonged treatment may result in the death of the whole organism (Barber and Andersson, 1992). For this reason, a number of protective systems have evolved in the thylakoid membrane and surrounding stroma to dissipate excess light energy and to scavenge various radicals effectively (Müller et al., 2001; Horton et al., 2008). However, when the damage of PSII occurs during photoinhibition another mechanism exists to efficiently degrade and replace the damaged D1 polypeptide in the photosynthetic machinery. This repair process involves reversible phosphorylation of PSII core proteins and monomerisation of photodamaged reaction centres (Baena-Gonzalez et al., 1999). This is combined with their migration from the grana where they are normally located to the stroma lamellae where a highly specific proteolysis of the damaged D1 protein occurs. A new D1 polypeptide is then synthesised *de novo* and assembled back into the photosynthetic apparatus of PSII in the grana membranes (Figure 4.1).



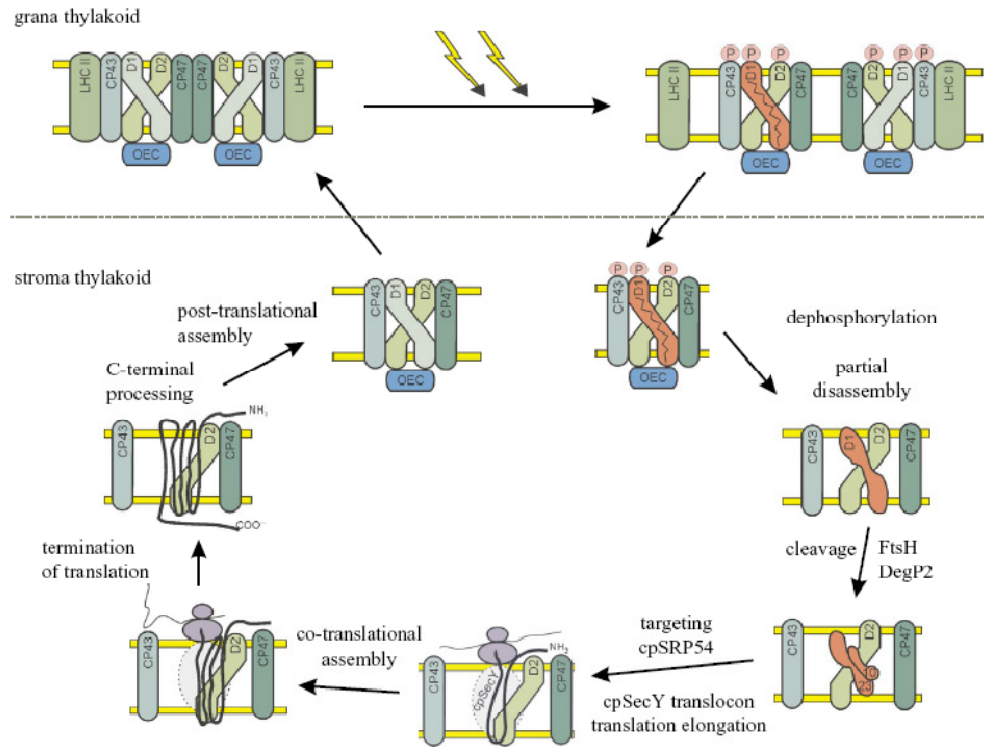


Figure 4.1. Schematic diagram showing the damage, repair and assembly of D1 protein during photoinhibition. Adapted from Baena-González and Aro (2002).

This mechanism is extremely effective and operates even at low light intensities. Hence, the turnover of D1 subunit of PSII belongs by far to the fastest among all photosynthetic complexes (Baena-González and Aro, 2002).

## 4.2. Mobility of chlorophyll-proteins in dark adapted intact spinach chloroplasts

Figure 4.2.A shows an example of a FRAP measurement in an intact spinach chloroplast. After 8 min the bleached line remains clearly visible with only small

partial recovery of chlorophyll fluorescence in the bleached granum. This recovery is attributed to the long-range diffusion of chlorophyll-proteins within the thylakoid membrane system. Analysis of the fluorescence recovery curve (Figure 4.2.C: blue curve), which is obtained by selecting a region of interest in the images corresponding roughly to one individual granum whose fluorescence is bleached out during the experiment, shows about 17% of fluorescence recover over about 10 min. Thus, the mobile fraction of chlorophyll fluorescence is small, but measurable, and fairly consistent under these dark-adapted conditions. There is some variation between measurements, but the mean mobile fraction from measurements on 10 individual chloroplasts is about 13% (Table 2). The controls described in chapter III and shown in Figures 3.5 and 3.6 indicate that this partial fluorescence recovery results from protein diffusion. I considered the possibility that this diffusion might be ‘vertical’ movements between the different membrane layers of the granum, which according to the pairwise model (see chapter I for further details), may be interconnected (Shimoni et al., 2005). However, the limited resolution in my experiments in the  $x$ ,  $y$  and  $z$  directions (see Materials and Methods) will ensure that the full depth of the granum is bleached. It also means that ‘any’ vertical movement within the granum will not affect the fluorescence signal observed in my measurements. This means that the mobility of photosynthetic complexes that is reported here does not relate to ‘vertical’ diffusion within a granum. However, it cannot be excluded that such movements can also occur. The diffusion I observe must result from exchange between grana, with complexes escaping one granum and diffusion to another granum via interconnecting stroma lamellae thylakoids. This is the first evidence showing that a limited pool of chlorophyll-protein complexes is able to exchange between grana on a timescale of a few minutes.

### **4.3. Effect of photoinhibition on the mobility of chlorophyll-proteins in intact spinach chloroplasts**

As mentioned already most models indicate that photoinhibition results in the migration of photodamaged D1 protein from grana to stroma lamellae regions for repair (Figure 4.1). Therefore, the repair cycle might be expected to cause an increase in the mobility of the chlorophyll-protein complexes within the thylakoid membrane system. To test this possibility I decided to carry out FRAP experiments on photoinhibited spinach chloroplasts (Figure 4.2.B). Photoinhibition was induced by illuminating for 10 – 15 min the suspension of intact chloroplasts with strong actinic light at approximately  $3000 \mu\text{mol photons m}^{-2} \text{sec}^{-1}$ . During photoinhibition, chlorophyll fluorescence was monitored with a pulsed-amplitude modulation (PAM) fluorometer (see Methods for details). Photoinhibited chloroplasts were immediately adhered to polylysine-coated slides, and FRAP measurements were carried out as described above. The experiments revealed that under photoinhibitory conditions chlorophyll fluorescence recovery was faster and more complete on the timescale of 10 min (Figure 4.2.B) in comparison with the chloroplast that had not been photoinhibited (Figure 4.2.A). This is reflected on the fluorescence recovery curve (Figure 4.2.C: red curve) indicating a greater mobile fraction of chlorophyll-proteins in the bleached granum. The mean mobile fraction in photoinhibited chloroplasts was significantly increased, as compared with chloroplasts that were dark-adapted prior to experiments (Table 2).

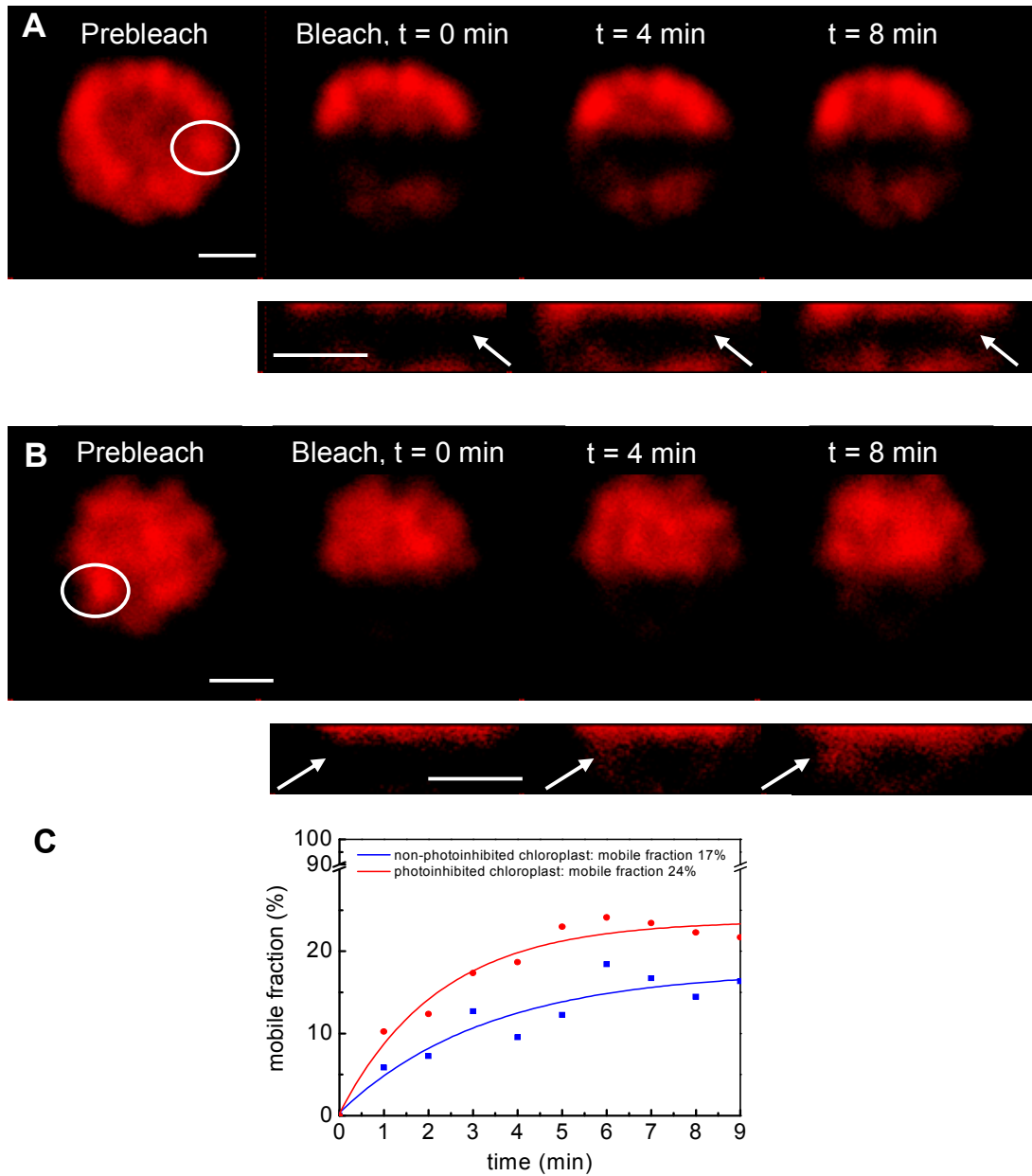


Figure 4.2. FRAP measurements on intact spinach (*Spinacia oleracea* L.) chloroplasts. (A) Chlorophyll fluorescence image sequence for a dark-adapted chloroplast. The circle indicates the position of an individual granum (used as a region of interest for quantitative data analysis). Scale bars = 2  $\mu$ m. The lower panel shows enlarged and contrast-enhanced images of the bleached area (granum indicated by an arrow). (B) Similar image sequence for a photoinhibited chloroplast. (C) Fluorescence recovery curves for the bleached granum in (A) and the bleached granum in (B) (blue and red curves, respectively). Note the greater mobile fraction and faster recovery of fluorescence in the photoinhibited chloroplast.

**Table 2. Effect of photoinhibition on the mobility of chlorophyll-proteins in intact spinach chloroplasts and isolated grana membranes.**

Data are presented as mean values ( $\pm$  S.E.) from 10 FRAP measurements on individual chloroplasts and 16-18 measurements on isolated grana membranes. Mean mobile fraction in photoinhibited chloroplasts (PI) is significantly higher than in dark adapted chloroplasts (D) as indicated by an asterisk (T test,  $P = 0.014$ ) while in isolated grana membranes the difference is not statistically significant (T test,  $P = 0.86$ ).

Sample	Mobile fraction (%)	
	D	PI
Intact chloroplast	$13.3 \pm 1.1$	$18.0 \pm 1.3^*$
Isolated grana membrane	$28.0 \pm 3.0$	$27.0 \pm 5.0$

#### **4.4 Effect of photoinhibition on mobility of chlorophyll-proteins in isolated grana membranes**

I compared my results from FRAP experiments on intact chloroplasts with the measurements of mobility of chlorophyll-proteins in isolated grana membranes from spinach performed by Prof. Helmut Kirchhoff. These experiments used the system previously described in which isolated grana membranes are adsorbed onto an artificial lipid bilayer support. Under those conditions, membrane patches tend to fuse together, forming patches large enough for quantitative FRAP measurements of mobile fraction and diffusion coefficient (Kirchhoff et al., 2008). As previously reported (Kirchhoff et al., 2008), grana membranes show a mobile fraction of chlorophyll fluorescence of about  $28 \pm 3\%$  (S.E.). This is much higher than I observed in intact chloroplasts. However, upon photoinhibition there is no significant increase in the mobility of chlorophyll-proteins in contrast to the result in intact chloroplasts (Table 2).

#### **4.5. Mobility of chlorophyll-proteins in intact spinach chloroplasts in the presence of an uncoupler**

As an additional control for my FRAP measurements I repeated the measurements in the presence of nigericin which is an effective uncoupler that prevents the formation of a transmembrane pH gradient ( $\Delta\text{pH}$ ).  $\Delta\text{pH}$  formation serves an indispensable trigger for the induction of qE, a reversible quenching mechanism that dissipates excess energy into heat under high light (Horton et al., 1996; Ruban et al., 2007). The addition of nigericin completely abolishes the occurrence of qE which has been shown previously in PAM fluorescence measurements (Johnson and Ruban, 2010). Mobile fractions calculated from this control did not differ significantly from the corresponding measurements on chloroplasts where nigericin was not added (Table 3). It is worth noticing that I still could observe a significant increase in the mobile fraction in chloroplasts that were photoinhibited in the presence of nigericin (Table 3) as with chloroplasts where nigericin was not added (Figure 4.2, Tables 2 and 3). These measurements confirm that changes in the extent of qE are not involved in the fluorescence bleaching and recovery that I observe in FRAP measurements. They also show that the increase in the mobility of chlorophyll-proteins that I observed following photoinhibition (Table 2) is not dependent on the induction of qE.

**Table 3. Effect of nigericin (4  $\mu$ M) on the mobility of chlorophyll-proteins in intact spinach chloroplasts.** Data represent mean mobile fractions out of 10 measurements ( $\pm$  S.E.). Significant differences (T-test,  $P < 0.05$ ) are marked with an asterisk. D = dark adapted chloroplasts, PI = photoinhibited chloroplasts, N = nigericin.

Mobile fraction (%)					
D	D + N	D + N	PI + N	PI	PI + N
13.3 $\pm$ 1.1	12.3 $\pm$ 1.5	12.3 $\pm$ 1.5	16.4 $\pm$ 1.0*	18.0 $\pm$ 1.3	16.4 $\pm$ 1.0

#### **4.6. Mobility of chlorophyll-proteins under photoinhibitory conditions: effect of reversible protein phosphorylation**

Upon photoinhibition, the PSII core proteins, in particular D1 polypeptide, undergo a rapid light-induced phosphorylation cycle that is connected to the regulation of PSII protein turnover and the repair of damaged proteins (Rintamäki et al., 1996). To investigate the effect of the reversible phosphorylation cycle on the mobilisation of chlorophyll-proteins I performed FRAP experiments on intact chloroplasts isolated in the presence of sodium fluoride (NaF). NaF is known to act as an effective inhibitor of thylakoid protein phosphatases and completely blocks the dephosphorylation and degradation of the damaged D1 polypeptide (Bennett, 1980; Rintamäki et al., 1996). The results clearly show that dephosphorylation of the damaged D1 proteins does not influence the mobility of chlorophyll-proteins following photoinhibition (Figure 4.3). A small but significant increase in the mobile fraction was still observed in intact chloroplast subjected to photoinhibitory illumination even in the presence of NaF (Figure 4.3).

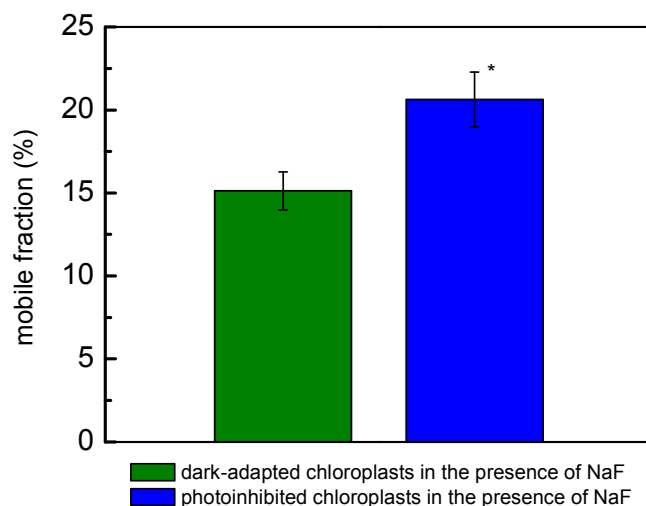


Figure 4.3. Effect of sodium fluoride (NaF) on the mobility of chlorophyll-proteins in intact spinach chloroplasts with and without photoinhibition. Bars represent mean mobile fractions ( $\pm$  SE) from 10 measurements. Note an increase in the mobility of chlorophyll-proteins in photoinhibited chloroplasts denoted by an asterisk and determined by unpaired Student's t-test ( $P = 0.014$ ).

Since dephosphorylation of the damaged D1 proteins does not prevent from greater mobilisation of chlorophyll-proteins upon photoinhibition I took a different approach to further investigate this noticeable change in the mobile fractions as shown in Figures 4.2 - 4.3 and Table 2. Rintamäki et al. (1996) showed previously that high-light-induced photoinhibition of PSII, although not being a prerequisite for phosphorylation of D1, occurs *in vivo* in PSII complexes containing D1 polypeptides in phosphorylated form. To test a possibility that mobilisation of chlorophyll-proteins is triggered by phosphorylation of the PSII core, I carried out FRAP measurements on intact chloroplasts isolated from *Arabidopsis thaliana* wild-type (Col-0), and *stn8* and *stn7stn8* double mutants. *Arabidopsis thaliana stn7* and *stn8* mutants lack the protein kinases required for the phosphorylation of thylakoid membrane proteins (Bonardi et al., 2005). The STN8 protein kinase appears to be primarily responsible for phosphorylation of the PSII core proteins (Bonardi et al., 2005). However, the *stn7stn8* double mutant shows a more complete loss of capacity for PSII



phosphorylation at high light intensities (Tikkanen et al., 2008). The results that I obtained from wild-type plants were comparable to those obtained on spinach. After photoinhibition a small but significant increase in the mobility of chlorophyll-proteins could be observed (Figure 4.4). However, in the *stn8* and *stn7stn8* mutants the mobility of chlorophyll-proteins was significantly lower than in the wild-type, and there was no increase in the mobile fraction following photoinhibition (Figure 4.4).

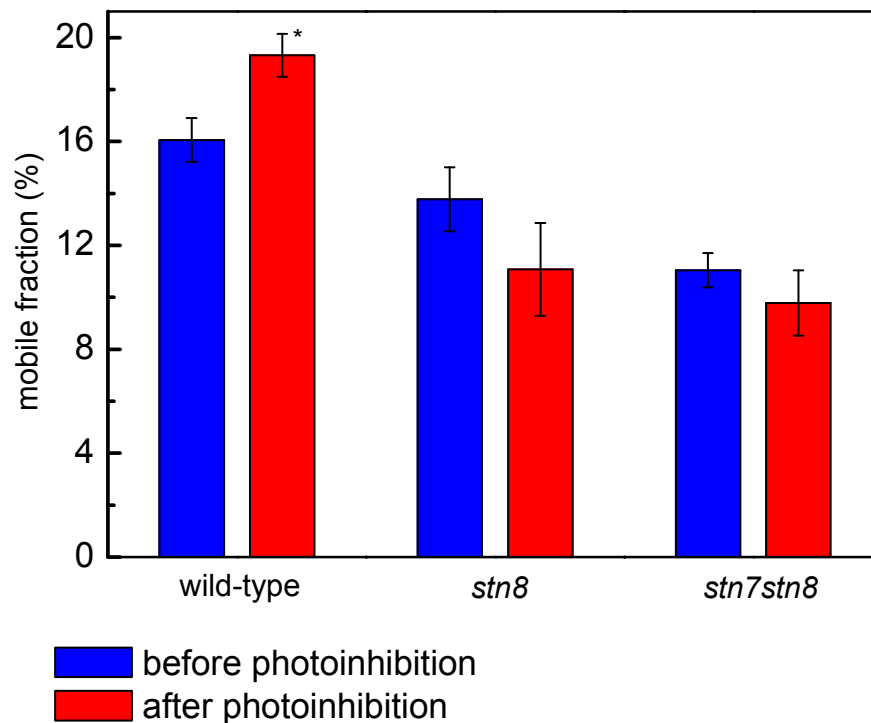


Figure 4.4. Chlorophyll-protein mobility in intact *Arabidopsis* chloroplasts, with and without photoinhibition. Bars represent mean mobile fractions ( $\pm$  SE) from 10 measurements. P-values are from unpaired Student's t-tests. (a) Wild-type (Col-0). Photoinhibition induces a significant increase in the mobile fraction as indicated by an asterisk ( $P = 0.013$ ). (b) *stn8* mutant. Photoinhibition does not increase the mobile fraction. (c) *stn7stn8* mutant. Photoinhibition does not increase the mobile fraction, and mobility in non-photoinhibited chloroplasts is significantly lower than in the wild-type ( $P = 0.0001$ ).

#### **4.7. Correlation of protein mobility with supramolecular organisation**

In order to find out whether changes in the mobility of chlorophyll-proteins observed during photoinhibition result from the changes in the supramolecular organisation of photosynthetic complexes in the grana membranes I decided to obtain freeze-fracture electron micrographs from intact spinach chloroplasts that were either dark-adapted or photoinhibited prior to freezing (Figure 4.5). Freeze-fracture electron microscopy (FFEM) is a well established technique which provides a useful means for visualising the lateral distribution of integral protein complexes in thylakoid membranes such as PSI, PSII, LHCII cytochrome  $b_6f$  and the  $F_0$ -subunit of the ATP synthase (Staelin, 2003). The process of freeze-fracturing of frozen thylakoid membranes at  $-100^{\circ}\text{C}$  causes the membranes to be split along the central hydrophobic plane of their bilayer and results in production of two complementary fracture faces. The structural details of these frozen fracture faces are preserved for viewing in the transmission electron microscope by means of high resolution platinum/carbon replicas (Chapman and Staelin, 1986). Because the integral protein complexes are not split during the fracturing process, the individual complexes are seen as discrete particles that rise above the smooth fracture face of the bilayer (as seen in Figure 4.5). The exoplasmic fracture face of the stacked membranes (EFs) is dominated by PSII particles of  $\sim 16\text{-}18$  nm (Staelin, 1976; Armond et al., 1977). The complementary protoplasmic fracture face of the stacked membranes (PFs) contains the  $\sim 8$  nm LHCII particles (Miller et al., 1976; Simpson, 1979). The protoplasmic fracture face of the unstacked membranes (PFu) is distinguished on the basis of its slightly larger asymmetric  $\sim 10$  nm Photosystem I particles (Simpson, 1982). Finally the complementary exoplasmic fracture face of the

unstacked membranes (EFu) is largely smooth and marked by generally more widely spaced ~10-16 nm PSII particles (Staehelin, 1976; Armond et al., 1977).

The micrographs revealed that there were no dramatic changes in PSII organisation as a result of photoinhibition (Figure 4.5). However, quantitative analysis of the images indicates that photoinhibition results in a significant decrease in the density of PSII particles in the granal regions, with a concomitant increase in the mean distance between particles (Figure 4.6). What is more, photoinhibition also induced a small but significant decrease in the mean size of granal PSII particles. Mean PSII dimensions in dark-adapted samples were  $(16.0 \pm 2.4) \times (10.8 \pm 2.0)$  nm, decreasing to  $(14.2 \pm 2.6) \times (9.2 \pm 1.8)$  nm in photoinhibited samples ( $\pm$  SDs,  $P \leq 0.0002$  from a Student's t-test).

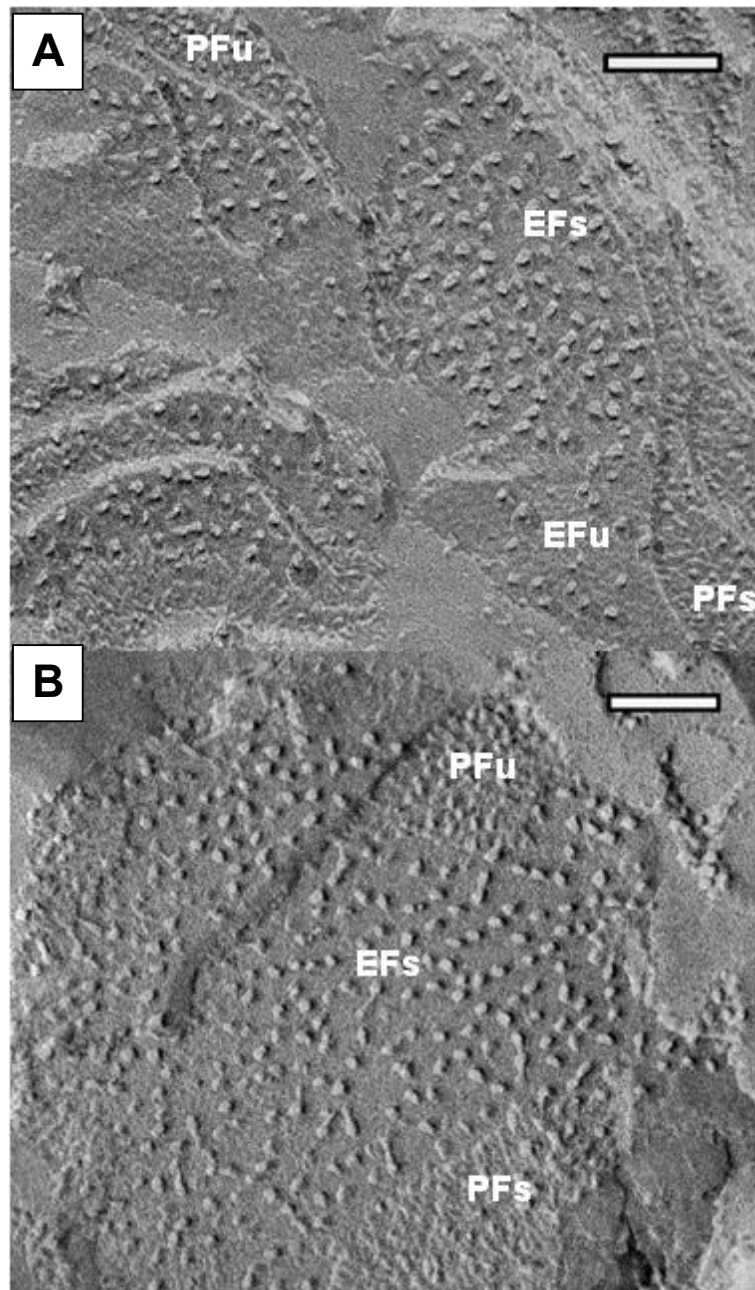


Figure 4.5. Freeze-fracture electron micrographs from intact spinach chloroplasts. Scale bars = 100 nm. (A) Dark-adapted sample. The thylakoid fracture faces EFs, EFu, PFs and PFu have been labelled according to the nomenclature of Branton et al. (1975) and stand for: EFs – exoplasmic face in the stacked regions of the thylakoids containing PSII particles, EFu – exoplasmic face in the unstacked regions of the thylakoids containing PSII particles (mostly monomers) of stroma lamellae, PFs – protoplasmic face in the stacked regions of the thylakoids containing LHCII particles, PFu – protoplasmic face in the unstacked regions of the thylakoids containing PSI particles of stroma lamellae. (B) Photoinhibited sample.

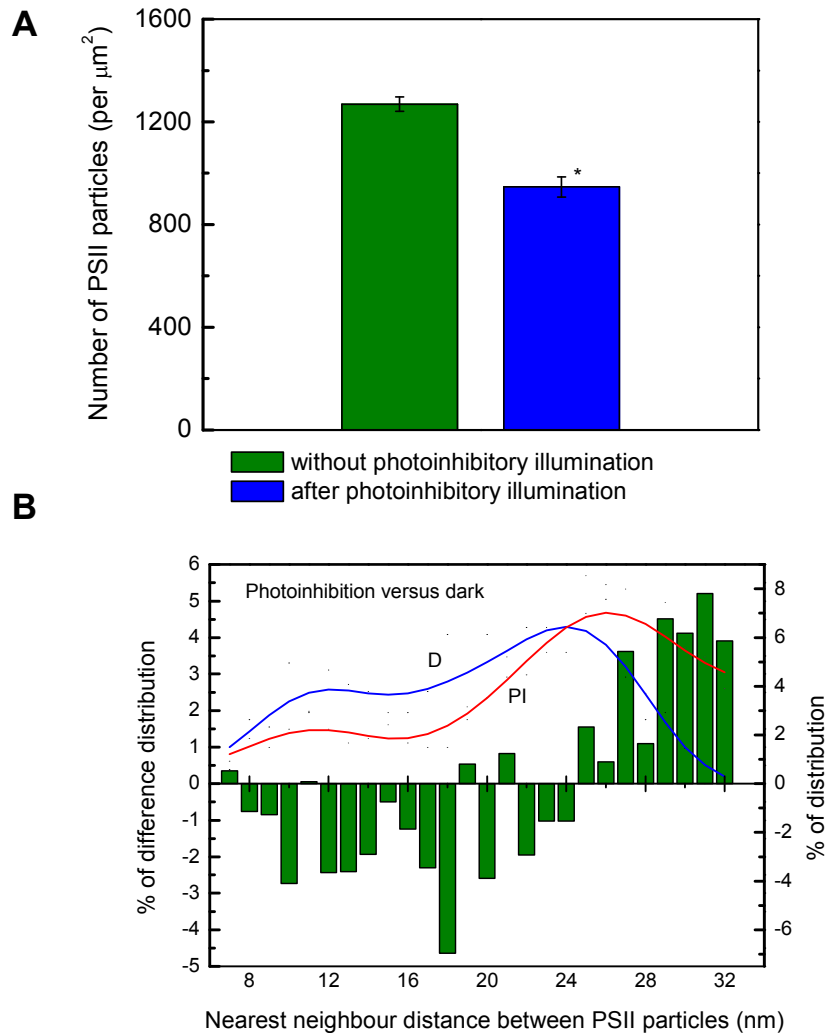


Figure 4.6. Differences in PSII density in the grana regions of dark-adapted and photoinhibited spinach chloroplasts revealed in the EFs faces of freeze-fracture electron micrographs, such as those shown in Figure 4.5. (a) Mean PSII density in  $\mu\text{m}^{-2}$ . Mean  $\pm$  SE ( $n = 30$ ) is shown, and the difference is significant as indicated by an asterisk and determined by Student's *t*-test ( $P < 0.001$ ). (b) Nearest-neighbour distances between PSII particles in photoinhibited (PI) and dark (D) states. The lines show the smoothed distributions of nearest-neighbour distances, and the histogram shows the difference between the distributions (PI - D). Note the shift towards greater nearest-neighbour distance in the photoinhibited state.

The results presented here suggest that the mobility of chlorophyll-proteins is directly related to the density and supramolecular organisation of PSII complexes in the grana regions. To further investigate this observation, I decided to probe the mobility of chlorophyll-proteins in a system where the optimal protein density and

supramolecular organisation of photosynthetic complexes in the grana is clearly disrupted. I chose to unstack the thylakoid membranes by removing  $Mg^{2+}$  cations from the buffers used for isolation of intact spinach chloroplasts (see Methods for details). Under these conditions, the grana regions made of stacked appressed membrane domains are no longer present, and as a result, the distribution of photosynthetic complexes is no longer spatially segregated (Izawa and Good, 1966, Murakami and Packer, 1971). This was confirmed by freeze-fracture electron micrographs (Figure 4.7) and is in agreement with similar observations made originally by Staehelin (1976). The distribution of PSII particles in the unstacked membranes is significantly different as compared to their normal distribution in the grana and stroma lamellae (Figure 4.7 and Table 4). In the chloroplasts with the stacked thylakoids there is a clear distinction between the grana membranes (EFs faces) with high density of PSII particles and short distances between them and the stroma lamellae regions (EFu faces) with much lower density of PSII particles and greater nearest-neighbour distances (Figure 4.7.A and Table 4). After unstacking all particles on the fracture faces appear randomly distributed, and no distinction between formerly stacked and unstacked membrane regions can be made (Figure 4.7.B). Quantitative analysis of the images revealed that the PSII particle density on the EF faces is intermediate between EFs and EFu faces with the same pattern observed for the analysis of nearest-neighbour distances (Table 4). Furthermore, the mean size of PSII particles in the unstacked membranes also appeared to be somewhat in between the mean sizes calculated separately for EFs and EFu faces (Table 4).

This is strong evidence showing that unstacking of the thylakoid membranes results in intermixing of the EFs and EFu particles and significantly changes their supramolecular organisation within the membrane network.

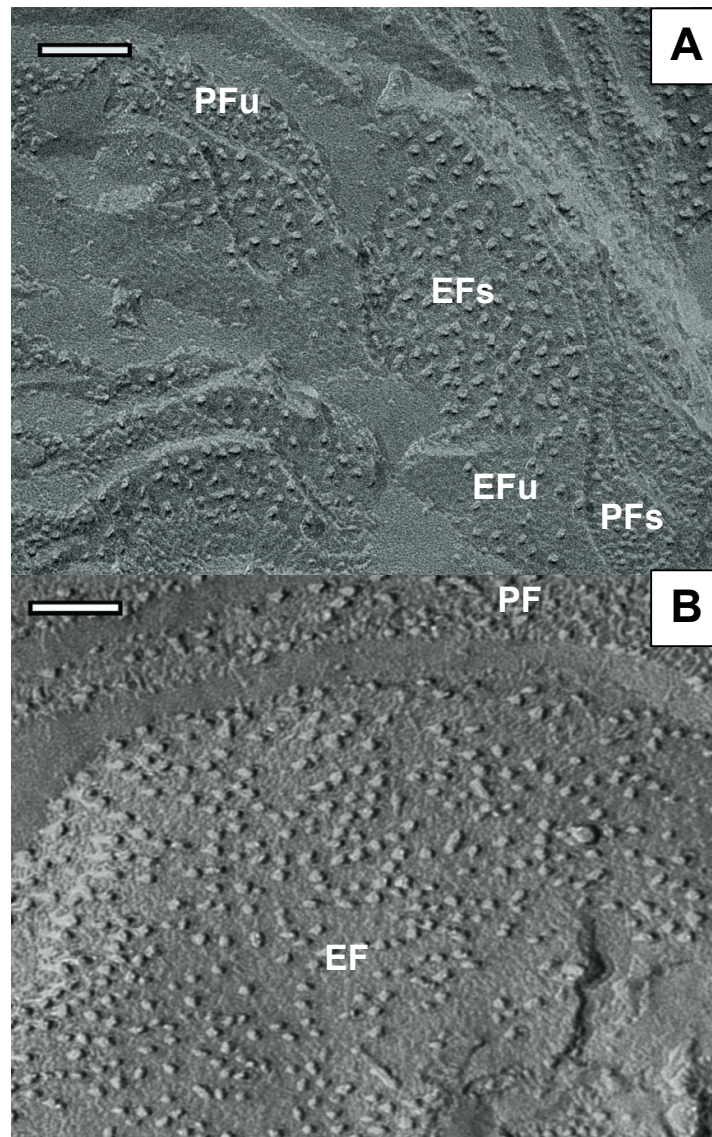


Figure 4.7. Freeze-fracture electron micrographs from isolated spinach chloroplasts. Scale bars = 100 nm. (A) Chloroplast with the stacked thylakoid membranes as in Figure 4.5.A. (B) Chloroplast with the unstacked thylakoid membranes. The fracture face labels stand for exoplasmic and protoplasmic faces for EF and PF, respectively. Note the lack of grana stacks and the randomised distribution of PSII particles with the lower density as compared to the EFs face as in image (A).

**Table 4. Analysis of EF fracture faces in the stacked and unstacked thylakoid membranes from spinach.**

Data show mean values  $\pm$  SE. n = number of particles analysed. \* = statistically significant difference with respect to the stacked EFs face using unpaired Student's t test ( $P < 0.05$ ).

<b>Sample</b>	<b>n</b>	<b>PSII nearest neighbour distance (nm)</b>	<b>PSII particle size (long axis) (nm)</b>	<b>PSII particle size (width axis) (nm)</b>	<b>PSII particles density (per <math>\mu\text{m}^2</math>)</b>
<b>stacked EFs face</b>	343	24.7 $\pm$ 1.5	16.0 $\pm$ 0.33	10.8 $\pm$ 0.28	1268 $\pm$ 28.0
<b>stacked EFu face</b>	57	35.3 $\pm$ 1.38	11.1 $\pm$ 0.32	7.1 $\pm$ 0.24	525 $\pm$ 51.2
<b>unstacked</b>	2684	27.2 $\pm$ 0.9*	12.4 $\pm$ 0.17*	8.3 $\pm$ 0.12*	978 $\pm$ 31.9*

Given the fact that the unstacking of thylakoid membranes results in lower density of the PSII particles and greater nearest-neighbour distances, the effect similar to the one observed for photoinhibited chloroplasts (Figures 4.5 – 4.7 and Table 4), it might be expected that the mobility of chlorophyll-proteins would also be increased as noticed before (Figure 4.2 and Table 2). Indeed, FRAP experiments performed on the chloroplasts with unstacked thylakoid membranes confirmed these assumptions (Figure 4.8). Firstly, in line with observations derived from freeze-fracture electron micrographs the confocal images revealed the presence of hardly any grana stacks in the investigated chloroplasts (Figure 4.8.A). Secondly, the calculated mean mobile fraction was significantly higher when compared to the mobile fraction obtained from the chloroplasts with stacked thylakoids (Figure 4.8.B). Therefore, the results presented here suggest strongly that the mobility of chlorophyll-proteins is directly dependent on the density of



photosynthetic complexes in the membrane. These findings were confirmed even further in the experiments carried out on the spinach chloroplasts prepared in different NPQ state and the chloroplasts isolated from *Arabidopsis thaliana* light-harvesting antenna mutants (see chapters V and VI for details, respectively).

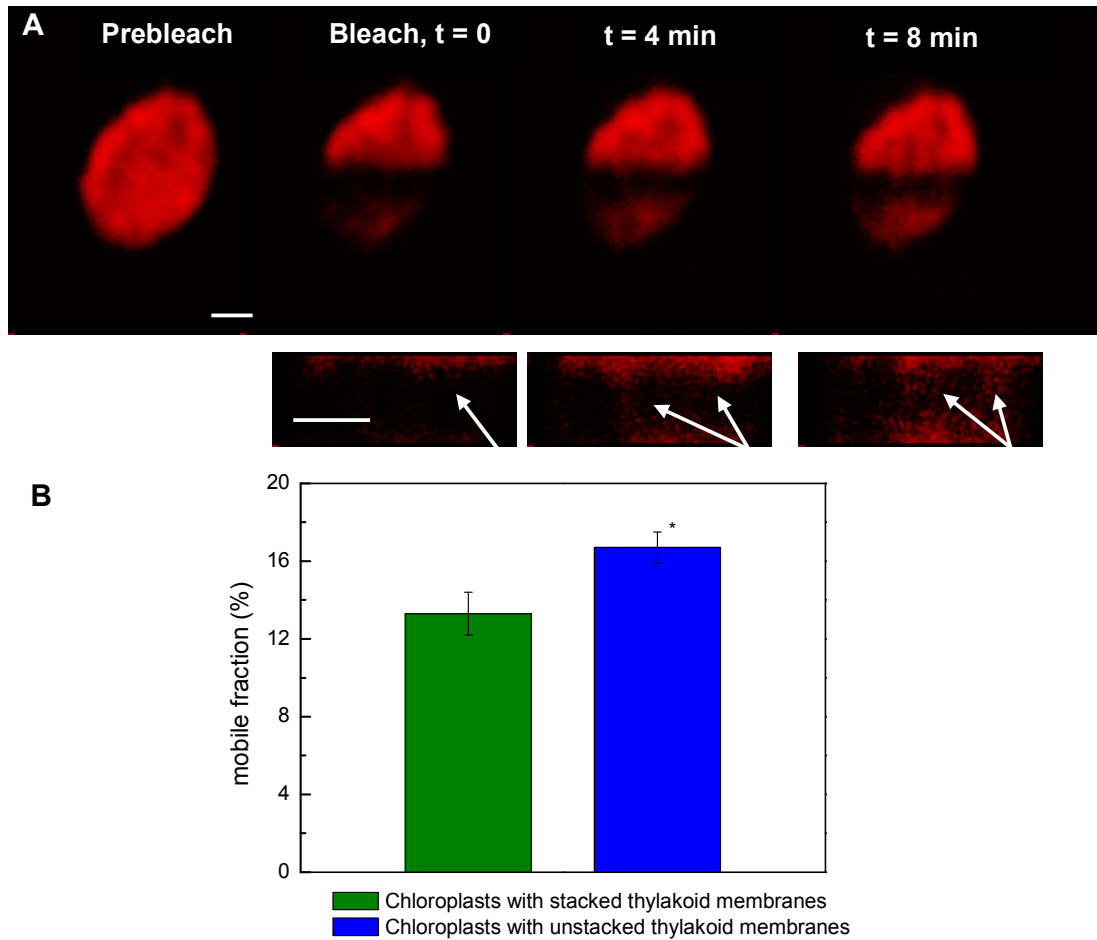


Figure 4.8. Chlorophyll-protein mobility in isolated spinach chloroplasts with stacked and unstacked thylakoid membranes. (a) FRAP measurement on the chloroplast isolated without  $Mg^{2+}$ . Note the presence of hardly any grana stacks as compared to the chloroplast with stacked thylakoid membranes (Figure 4.2.A). Chlorophyll fluorescence image sequence is presented in similar way as in Figure 4.2. For quantitative data analysis the whole bleached region was used instead of an individual granum as presented in Figure 4.2. Note greater fluorescence recovery as compared to the example shown in Figure 4.2.A. Scale bars: 2  $\mu m$  (B). Effect of thylakoid membrane unstacking on the mobility of chlorophyll-proteins. Bars represent mean values ( $\pm$  SE) from 10 experiments. Note significant increase in the mean mobile fraction for chloroplasts with unstacked thylakoid membranes as indicated by an asterisk and determined by Student's t-test ( $P < 0.05$ ).

# **Chapter V**

**Dynamics of photosynthetic  
complexes during photoprotective  
dissipation of light energy**

## 5.1. Non-photochemical quenching phenomenon

When light energy absorption exceeds the capacity for its utilisation the light-harvesting antenna of photosystem II (LHCII) undergoes a rapid and reversible switch into a photoprotected quenched state in which the absorbed excitation energy is efficiently dissipated as heat (the quenching of singlet-excited chlorophylls occurs) (Horton et al., 1996; Szabó et al., 2005; Horton et al., 2008). This process is known as non-photochemical quenching (NPQ), and has evolved to protect plants from potentially damaging effect of too much light. NPQ has multiple components but the major and most rapid is the  $\Delta\text{pH}$ -, or energy-dependent component referred commonly to qE. The induction of qE is fully reversible on a short timescale (seconds to minutes) (Müller et al., 2001), and can be monitored by PAM fluorescence measurements (Figure 5.1). The other components such as qT (state-transition quenching caused by separation of LHCII from PSII, see chapter I for details) and qI (photoinhibitory quenching caused by damage of PSII reaction centers, see chapter IV for details) relax on a much slower timescale and do not seem to be important for photoprotection in the context of dissipation of excess energy. Hence, all the information referring to NPQ described in this chapter will consider only the qE component of this phenomenon.

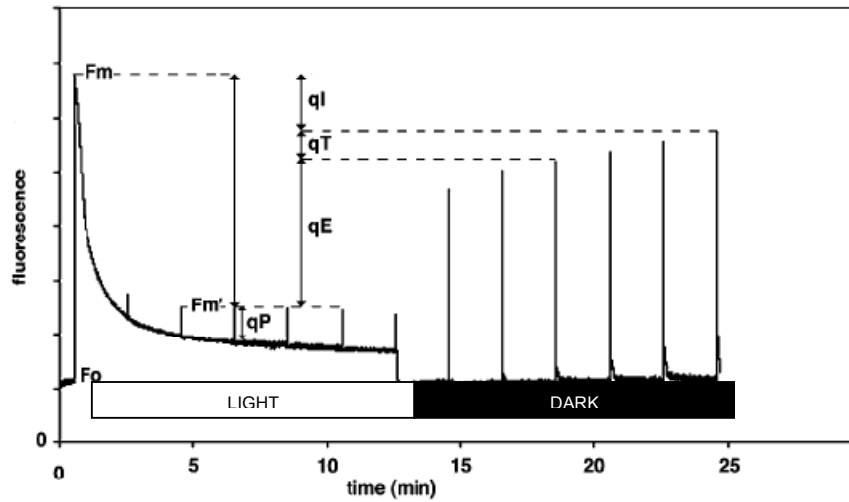


Figure 5.1. PAM fluorescence measurement from an *Arabidopsis* leaf. Upon continuous illumination ( $750 \mu\text{mol photons m}^{-2} \text{s}^{-1}$ ), a combination of photochemical quenching (qP) and NPQ lowers the fluorescence yield. After switching off the light, a rapid relaxation of qE component of NPQ is observed. The other components (qT and qI) relax much slower, and will not be considered here. Adapted from (Müller et al., 2001) with modifications.

qE is triggered by the increased acidification of the thylakoid lumen that results from protonomotive electron transport (Pérez-Bueno et al., 2008). The decrease in lumen pH activates the violaxanthin de-epoxidase enzyme (VDE) that converts the carotenoids violaxanthin into zeaxanthin via the intermediate antheraxanthin (the xanthophyll cycle) (Johnson et al., 2007). These carotenoids are bound to the LHCII proteins, mostly at the peripheral V1 site (Liu et al., 2004; Pascal et al., 2005). Apart from violaxanthin or zeaxanthin, LHCII antenna bind internally the other xanthophylls with the most important *lutein1* shown recently to act as a potent quencher of excited chlorophylls (Ruban et al., 2007). It has been postulated that the xanthophyll cycle allosterically regulates a quenching process – de-epoxidation of violaxanthin into zeaxanthin occurring upon pre-illumination of leaves shifts the  $\Delta\text{pH}$  requirement for qE but does not change its maximum capacity (Noctor et al.,

1991). Additionally, light adaptation results also in the faster rate of qE formation and its slower relaxation in dark which is supported by observations showing that the rate of quenching in isolated LHCII is accelerated by addition of zeaxanthin and slowed down by violaxanthin (Ruban et al., 2001). This effect is linked with enhancement of the formation of LHCII aggregates that favour the quenched conformation when zeaxanthin is present and the stabilization of the unquenched conformation upon the presence of violaxanthin (Horton et al., 2008).

Apart from xanthophylls and  $\Delta pH$ , the PsbS protein has also been shown to influence the level of qE. PsbS is a small 22 kDa protein belonging to one of the subunits of photosystem II but its precise location within thylakoid membranes is still a matter of debate. It is not located either in the  $C_2S_2$  supercomplex (Nield et al., 2000) or near the additional M-LHCII and CP24 minor antenna (Yakushevskaya et al., 2001). In fact, it is postulated that this protein is localized in the LHCII-enriched regions of the grana membranes. However, the mechanism of its action has not been fully determined up to date. It has been suggested that the protein is involved in sensing the formation of  $\Delta pH$  and could have a facilitating role in the conformational change of LHCII which underlies qE (Horton et al., 2005).

There are growing evidences suggesting that qE arises from a conformational change within LHCII antenna leading to a strong prediction that NPQ would change the entire macrostructure of the PSII-LHCII supercomplexes in the thylakoid membranes (Ruban et al., 2007; van Oort et al., 2007). Indeed, some experiments are consistent with this hypothesis showing for example, that any perturbations in the macrostructure alter qE characteristics (Horton et al., 2008). The same authors proposed that in order to create a qE locus the specific assembly of the LHCII-PSII supercomplexes into organised arrays is needed. For that reason, it is clear that the

overall dynamics of chlorophyll-proteins might be strongly affected under these conditions. This is why in my project I decided to investigate, for the first time, the structural and dynamic aspects of the NPQ state in intact photosynthetic membranes. I employed the FRAP method to probe the mobility of chlorophyll-proteins under NPQ conditions and tried to elucidate the role of different xanthophylls and the PsbS protein in controlling this process. My results, which are presented here, are combined with structural data obtained by thin-section and freeze-fracture electron microscopy analysis. The latter work (especially for the samples trapped in the NPQ state and different mutants of PsbS protein) was done primarily by Dr. Matthew Johnson.

## **5.2. Structural changes in the thylakoid membrane network upon formation of the photoprotective state**

The first indication suggesting that structural changes within the photosynthetic membrane are involved in a formation of NPQ comes from the observation that relaxation of fluorescence quenching in the dark (as in Figure 5.1) can be inhibited by a protein crosslinker such as glutaraldehyde, even in the presence of the uncoupler nigericin (Figure 5.2). This observation was made by Dr. Matthew Johnson and stimulated us to address this problem in more depth.

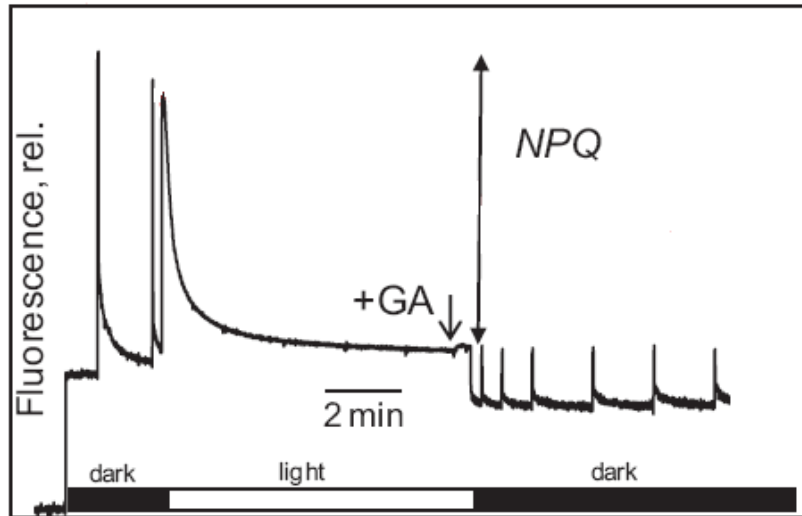


Figure 5.2. PAM chlorophyll fluorescence measurement on intact spinach chloroplasts as described in Methods. At the end of the illumination period 2% glutaraldehyde (GA) was added to the chloroplast suspension as indicated by the arrow. Note lack of fluorescence recovery in the dark and maintenance of NPQ state under these conditions. Figure obtained from Dr. Matthew Johnson, with permission.

### 5.3.1. Thin section electron microscopy

Intact chloroplasts isolated from spinach leaves were subjected to light adaptation and investigated under electron microscope as described in Methods. Firstly, thin-section electron micrographs of dark-adapted intact chloroplasts (referred to Dark Vio) were compared to those light-treated for 5 minutes in the absence (Light Vio) or presence (Light Zea) of ascorbate to mediate de-epoxidation of violaxanthin to zeaxanthin. The light-treated samples were either maintained in the NPQ state (see Methods for details) or allowed a further 5 minute period of darkness to relax NPQ (Dark Zea) (Figure 5.3). The electron micrographs revealed that the pairs of stacked photosynthetic membranes are more widely spaced in the dark-adapted sample (Dark Vio), with the thylakoid lumen appearing swollen (Figure 5.3.A). In contrast, in the samples treated for 5 minutes in the light (Light Vio and Light Zea) the volume of the thylakoid lumen was reduced resulting

in a decreased spacing between thylakoid membranes (Figure 5.3.B-C). This suggests that formation of  $\Delta\text{pH}$  during light adaptation is sufficient for the observed phenomenon. Relaxation of NPQ for 5 minutes in the dark (Dark Zea) restored the lumen to the swollen state characteristic of the Dark Vio sample, with an increased spacing between thylakoid membranes, thus demonstrating that the effect was reversible (Figure 5.3.D). The quantitative measurements confirmed these observations (Figure 5.5.A).

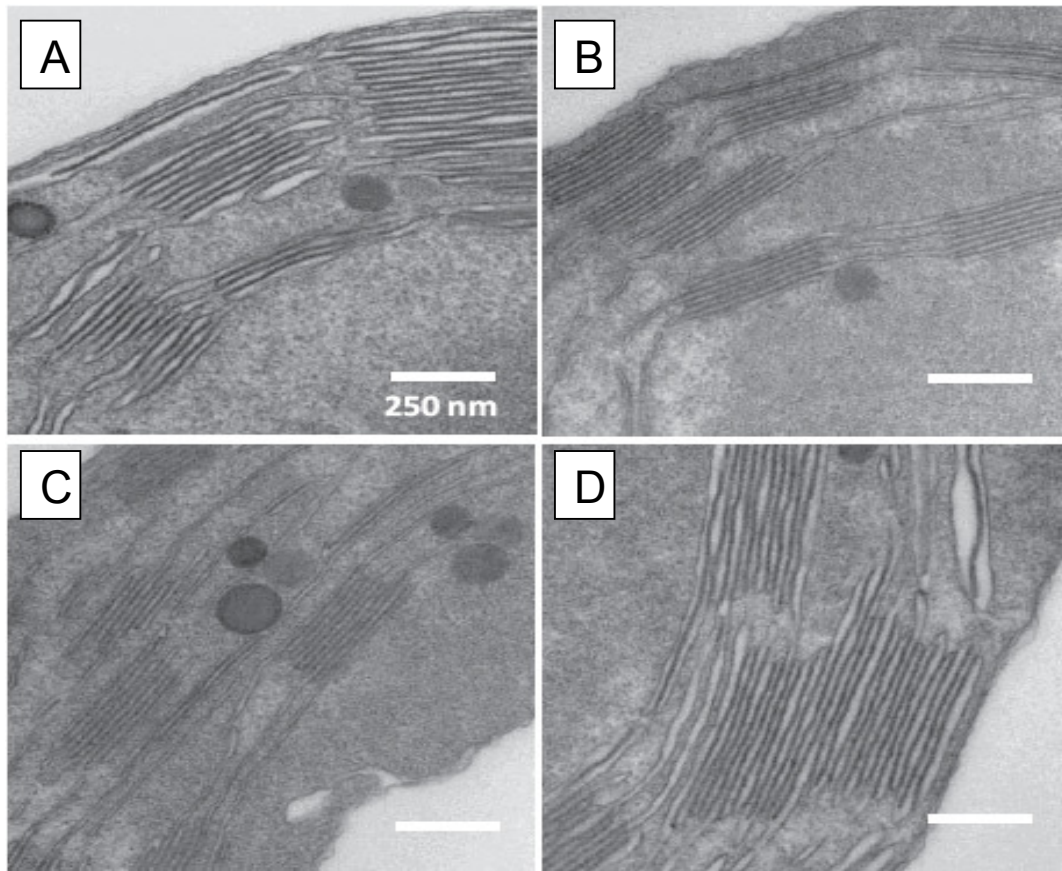


Figure 5.3. Thin-section electron micrographs showing the structural effect of illumination on thylakoid membrane structure in intact spinach chloroplasts. (A). dark-adapted sample (Dark Vio). (B). light-adapted sample in the absence of zeaxanthin (Light Vio). (C). light-adapted sample in the presence of zeaxanthin (Light Zea). (D). Sample light-adapted for 5 minutes in the presence of zeaxanthin followed by 5 minutes dark recovery (Dark Zea). Figure obtained from Dr. Matthew Johnson, with permission.



The thickness of the membranes was also investigated by analysing densitograms recorded for a set of images from each sample (Figure 5.4.A and B), and then processed using an autocorrelation function (Figure 5.4.C) (see Methods for details).

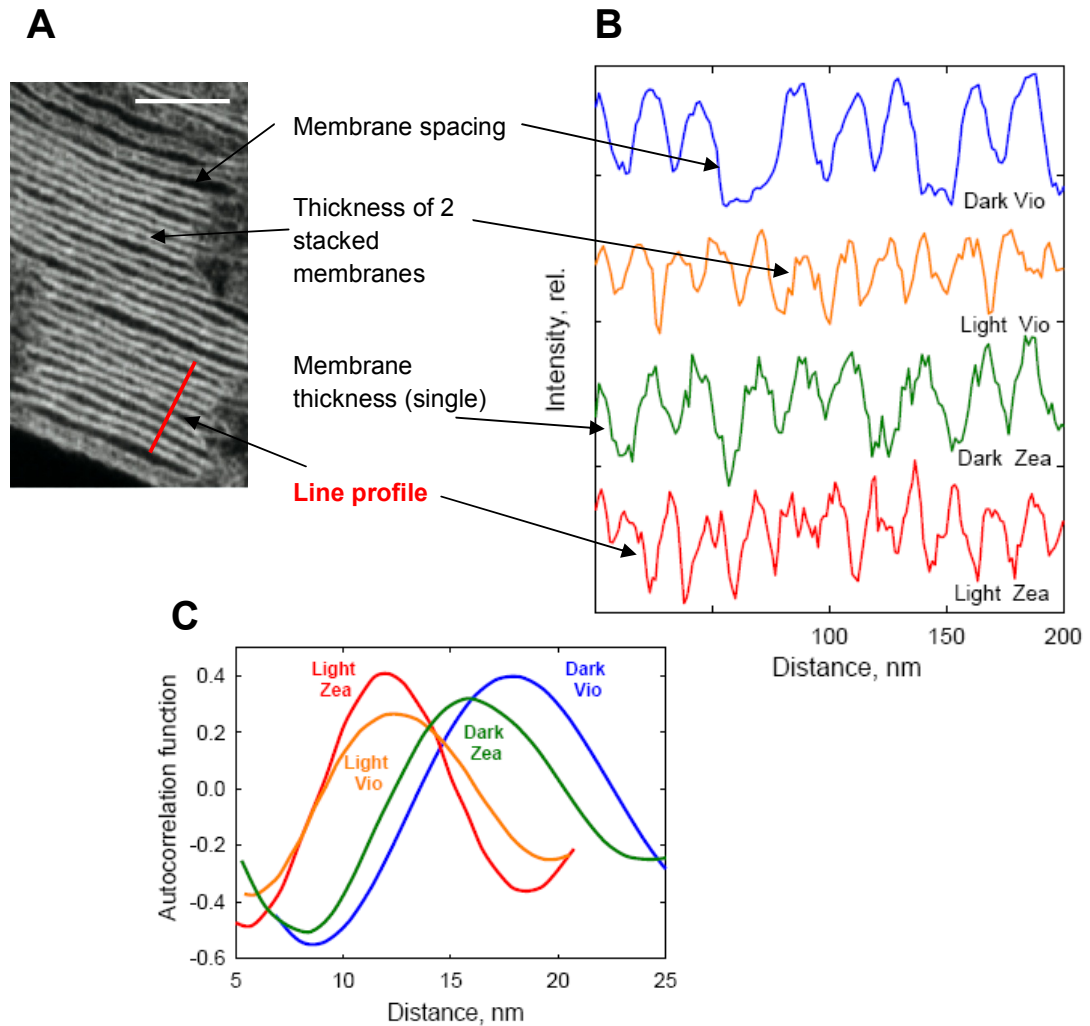


Figure 5.4. Analysis of thin-section electron micrographs of intact spinach chloroplasts. (A). Negative-stain thin-section images of spinach thylakoid grana membranes within intact spinach chloroplasts (in which the contrast was inverted) were analysed by densitometry, to yield measurements of the thickness of two stacked thylakoid membranes within a grana stack, the distance between two pairs of stacked membranes and the thickness of the single grana end membranes (located at top and bottom of grana stacks). Scale bar = 250 nm. (B) Typical line profile densitograms of grana stacks from Dark Vio (blue), Light Vio (orange), Dark Zea (green) and Light Zea (red) chloroplasts. (C) Averaged autocorrelation functions of densitograms of thylakoid grana membranes from Dark Vio (blue), Light Vio (orange), Dark Zea (green) and Light Zea (red) chloroplasts. Figure obtained from Dr. Matthew Johnson, with modifications.

The data confirmed that the thickness of membrane stacks (the thickness of two stacked membranes) also decreased following light-adaptation for 5 minutes (Figure 5.5.B). However, while the spacing between membranes was similar in both Light Vio and Light Zea chloroplasts (Figure 5.5.A), the membrane thickness was significantly different (Figure 5.5.B). This was particularly seen in the Light Zea chloroplasts which had the thickness of thylakoid membranes reduced by ~ 16% compared to Light Vio chloroplasts and by almost 30% with respect to Dark Vio samples. Moreover, the same tendency was observed when it comes to the amount of NPQ which was present in the investigated samples (as measured by Dr. Matthew Johnson and shown in Table 5). Since the Light Zea chloroplasts had the greatest reduction in membrane thickness in the grana, and at the same time the greatest amount of NPQ (Table 5), it indicates that de-epoxidation of violaxanthin to zeaxanthin is associated with an enhancement of the structural change occurring in the membrane that accompanies NPQ.

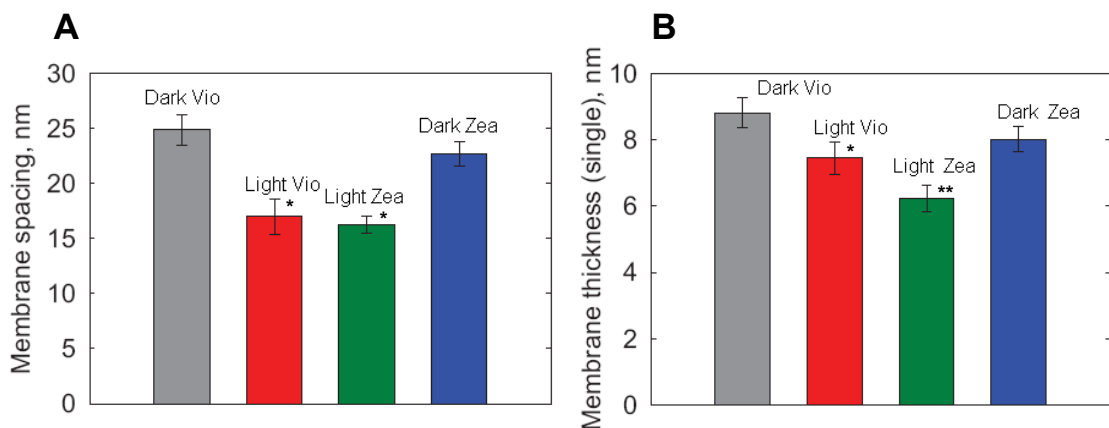


Figure 5.5. Analysis of thin-section electron micrographs of intact spinach chloroplasts. (A) Average spacing between pairs of stacked grana membranes from Dark Vio (grey), Light Vio (red), Light Zea (green) and Dark Zea (blue) chloroplasts  $\pm$  S.E.M.,  $n=20$ . (B) Average thickness of single thylakoid membranes in the grana from Dark Vio (grey), Light Vio (red), Light Zea (green) and Dark Zea (blue) chloroplasts  $\pm$  S.E.M.,  $n=20$ . \*= significantly different from Dark Vio sample, \*\*= significantly different from Dark Vio, Dark Zea and Light Vio samples (Anova analysis with Tukey contrast,  $p < 0.01$ ).

**Table 5. Comparison of NPQ values measured for intact spinach chloroplasts prepared in four different states as described in section 2.1.** Data show mean values  $\pm$  S.E. (n = 4). \* = values significantly different with respect to Dark Vio sample (one-way ANOVA followed by Dunnett contrast,  $p < 0.01$ )

	<b>Dark Vio</b>	<b>Light Vio</b>	<b>Light Zea</b>	<b>Dark Zea</b>
<b>NPQ</b>	0	0.6 $\pm$ 0.1*	2.1 $\pm$ 0.1*	0.3 $\pm$ 0.03*

### 5.2.2. Freeze-fracture electron microscopy

To investigate whether the NPQ-related alterations in photosynthetic membrane thickness were accompanied by any changes in the macroorganisation of PSII-LHCII supercomplexes freeze-fracture electron microscopy (FFEM) was performed on intact chloroplasts prepared in the four states outlined above. Four distinct fracture faces are observed in FFEM images (Staehelin, 2003) allowing information on the organization of individual protein complexes within the membrane to be determined as already mentioned in chapter IV. In the Dark Vio chloroplasts PSII particles on the EFs fracture faces are well spaced (Figure 5.6.A). However, in the light-adapted sample (Light Vio) there was a noticeable tendency for the PSII particles to become more tightly clustered together (Figure 5.6.B) with this effect being even more pronounced in the Light Zea chloroplasts (Figure 5.6.C, Arrow 1). The samples subjected to 5 minute relaxation period in the dark (Dark Zea) exhibited a partial restoration of the dark-like organisation, although some smaller clusters of PSII did remain (Figure 5.6.D).

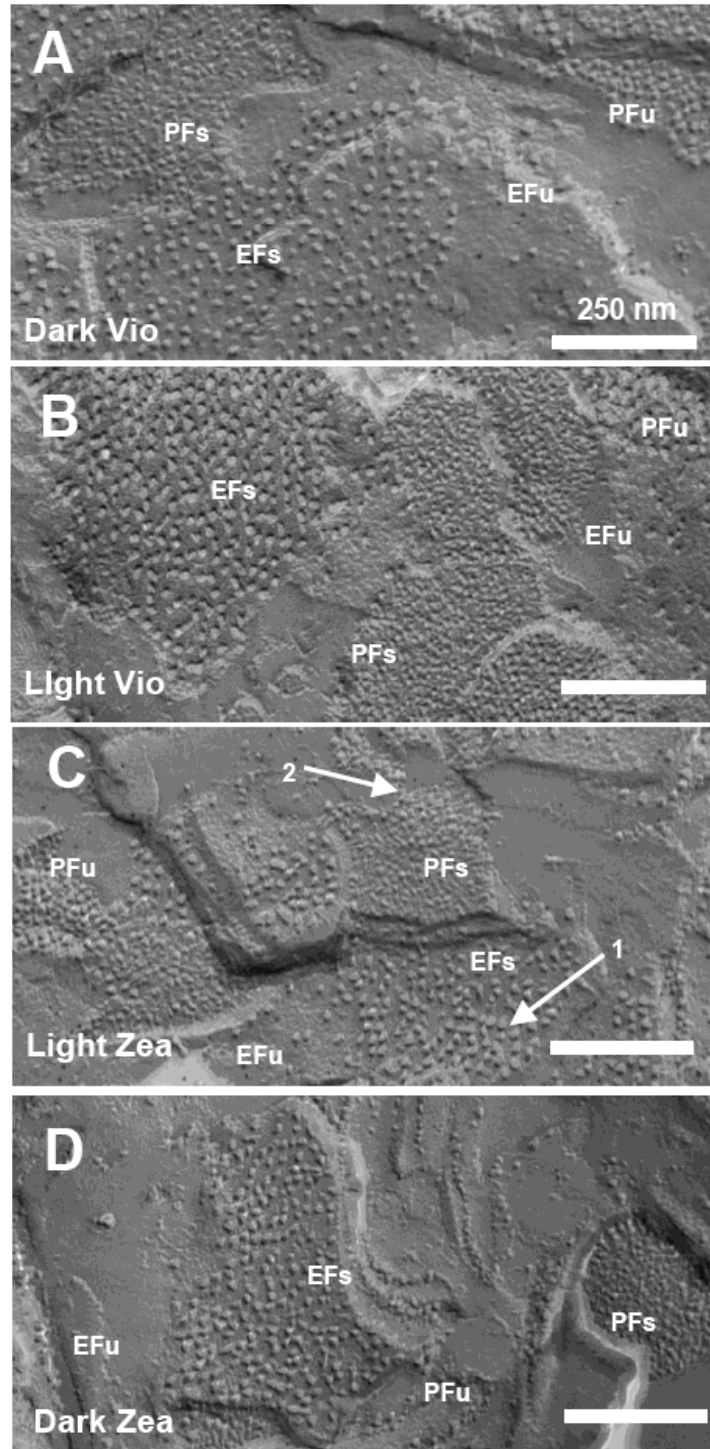


Figure 5.6. Freeze-fracture electron micrographs from intact spinach chloroplasts. (A) Dark Vio. (B). Light Vio. (C). Light Zea. (D). Dark Zea samples. Fracture faces were labelled as described in text and shown in Figure 4.5. For explanation of arrows see text. Figure obtained from Dr. Matthew Johnson, with permission.

Image analysis allowed to quantify the changes in PSII clustering, nearest-neighbour distance and particle size in each type of sample. The clustering of PSII particles was quantified by calculating the number of EFs particles within a 50 nm radius of any given EFs particle, with normalisation to account for variation in the area of EFs fracture faces from one image to another. The normalisation was necessary to remove edge effects, or the tendency for particles at the edge of a fracture face to have fewer neighbours than those nearer to the center. The average PSII clustering was significantly increased in the Light Vio chloroplasts compared to the Dark Vio chloroplasts (Figure 5.7.A), and these changes were further enhanced in the Light Zea sample. The clustering was partially reversed upon dark recovery (Dark Zea) as compared to the Light Zea chloroplasts, with the distribution similar to that found in the Light Vio chloroplasts (Figure 5.7.A). A similar pattern was observed in the analysis of the nearest-neighbour distances between PSII particles as a measure of their association (Kirchhoff et al., 2007). Again, in the Light Zea chloroplasts there is a significant shift towards shorter distances between PSII particles (Figure 5.7.B). It is worth noticing that I observed the exact opposite tendency i.e. increased spacing between PSII particles in the photoinhibited chloroplasts (Figures 4.5 and 4.6), suggesting that light damage and photoprotection work in opposing ways with regards to PSII organisation. The third parameter calculated during FFEM analysis was PSII particle size. In this case, significant differences were also observed. The average PSII particle size decreased from  $\sim 200 \text{ nm}^2$  in the Dark Vio chloroplasts to  $\sim 125 \text{ nm}^2$  in the Light Zea sample (Figure 5.7.C) with a clear increase of average size in a range of  $100 - 150 \text{ nm}^2$  at the expense of those above  $200 \text{ nm}^2$  (Figure 5.7.C). The average size of the EFs fracture face PSII particles in the dark is too large to represent a PSII core dimer ( $145 \text{ nm}^2$ ) (Hankamer et al.,

1997). On the other hand, the calculated sizes are far too small to represent a C<sub>2</sub>S<sub>2</sub> type PSII-LHCII supercomplex (310 nm<sup>2</sup>) (Boekema et al., 1995). Rather, the size of the PSII particles is most consistent with a PSII core dimer and 2-3 minor antenna proteins (~220 nm<sup>2</sup>) (Boekema et al. 1995), which is in agreement with previous observations suggesting that a part of the attached LHC complexes may also fracture with the EFs face under some conditions (Armond et al., 1977). The observations which I made and present in this thesis (see chapter VI for details) that *Arabidopsis* mutants lacking certain minor antenna complexes contained smaller PSII particles in the EFs fracture face compared to the wild-type confirm this view. Thus, it indicates that during NPQ the affinity of the minor LHC antenna for the PSII core dimer is weakened, resulting in them now fracturing with the PFs face.

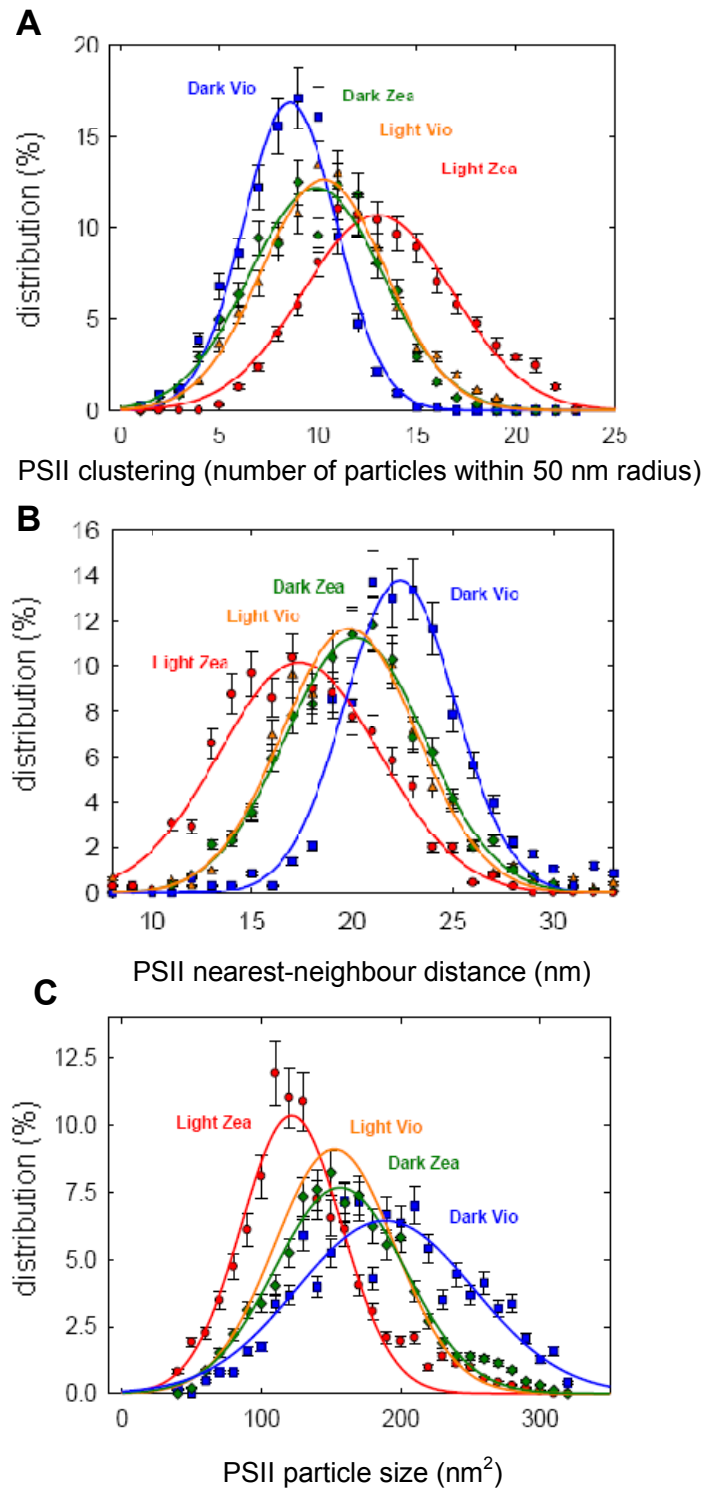


Figure 5.7. Analysis of PSII particles in the EFs fracture faces from freeze-fracture electron micrographs of intact spinach chloroplasts. (A). Distribution of PSII clustering (number of neighbouring PSII particles within a 50 nm radius of a given PSII particle). (B). Distribution of PSII nearest-neighbour (center-to-center) distances. (C) Distribution of PSII particle sizes in Dark Vio (blue squares), Light Vio (orange triangles), Light Zea (red circles), and Dark Zea (green diamonds) intact spinach chloroplasts. Data are averaged from 3 independent experiments;  $\pm$  S.E..

The PFs fracture face containing LHCII particles is complementary to the EFs PSII face (Staehelein, 2003). Image analysis of PFs faces revealed that, similar to the EFs face, there was an increase in the packing of LHCII complexes in the Light Zea sample (Figure 5.6. C. Arrow 2) compared to the Dark Vio sample (Figure 5.6.A). In the Dark Vio chloroplasts the LHCII particles were quite evenly distributed across the fracture face with the clear ‘gaps’ between the particles (Figure 5.8.A. Arrows) which presumably correspond to the space occupied in the membrane by the PSII particles which fracture with the EFs face. However, in the Light Zea samples the LHCII particles appeared to form aggregates (Figure 5.8.B. Arrow 1) while areas of lower density where LHCII particles are more sparse were also observed (Figure 5.8.B. Arrow 2). The increased clustering of LHCII in the Light Zea chloroplasts could be measured from the number of neighbouring LHCII particles within a 25 nm radius of a given LHCII particle (Figure 5.7.C). In the Light Vio chloroplasts the changes in LHCII clustering were smaller than in the Light Zea chloroplasts (Figure 5.8.C), whereas in the Dark Zea samples there was a partial recovery from the LHCII aggregation state compared to the Light Zea chloroplasts (Figure 5.8.C). Thus, as with the effect on membrane thickness zeaxanthin was associated with an enhancement of the clustering of LHCII and PSII particles observed in chloroplasts exhibiting the NPQ state. The relative size of the LHCII particles was  $\sim 50 \text{ nm}^2$ , which is consistent with the size of an LHCII trimer (Dekker and Boekema, 2005) (Figure 5.8.D). Unlike for the PSII particles on the EFs fracture faces the size of the LHCII particles on the PFs fracture faces was observed to be fairly constant in all four chloroplast samples (Figure 5.8.D), suggesting the LHCII trimer remains intact.



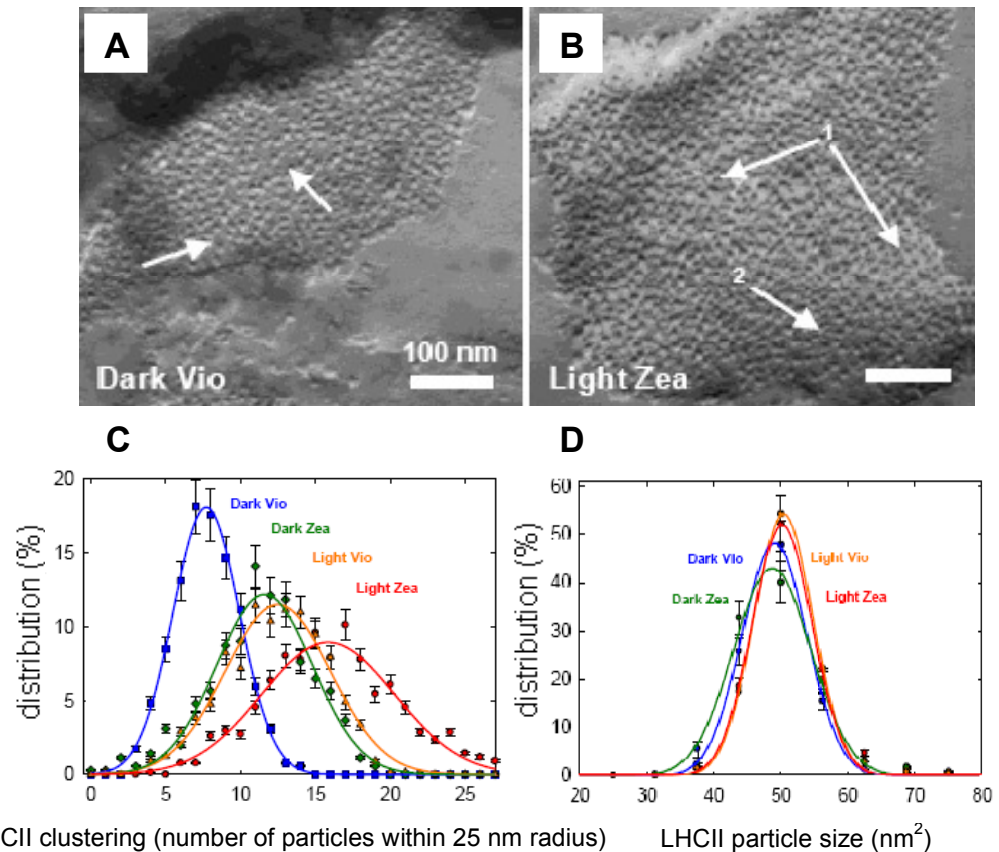


Figure 5.8. Image analysis of PFs fracture faces from intact spinach chloroplasts. (A) Higher magnification view of LHCII PFs fracture face in freeze-fracture electron micrographs of Dark Vio chloroplasts and (B) Light Zea intact spinach chloroplasts. (C) Distribution of LHCII clustering (number of neighbouring LHCII particles within a 25 nm radius of a given LHCII particle). (D) Distribution of LHCII particle sizes (area) in Dark Vio (blue squares), Light Vio (orange triangles), Light Zea (red circles), and Dark Zea (green diamonds) chloroplasts. Data are averaged from 3 independent experiments;  $\pm$  S.E. For explanation of arrows see text. Electron micrographs were obtained from Dr. Matthew Johnson, with permission.

### 5.2.3. FRAP measurements

The structural data presented in sections 2.1. and 2.2. obtained primarily by Dr. Matthew Johnson revealed that NPQ formation involves some alterations in the thylakoid membrane thickness and the organisation of PSII-LHCII complexes in the grana. However, as observed before for the photoinhibited samples (Chapter IV), these structural changes are likely to affect also the dynamic properties of chlorophyll-proteins. By taking these considerations into account, I decided to probe

the mobility of chlorophyll-proteins in the chloroplasts which were prepared in the four, already described different states. I followed the same procedure as mentioned in chapter IV. The mobile fraction in the Dark Vio spinach chloroplasts is the same as already obtained for dark-adapted chloroplasts (Table 2) and accounts for about 13% of fluorescence recovery. However, in the Light Zea chloroplasts the mobility decreased by almost 35% when compared to the Dark Vio samples (Figure 5.9). A similar, although less pronounced effect, was also observed for the Light Vio chloroplasts (Figure 5.9). Interestingly, upon 5 minute recovery in the dark (Dark Zea) the mobility of chlorophyll-proteins increased to about 60% of the initial value as in the Dark Vio samples (Figure 5.9). This suggests that the observed re-organisation of the PSII macrostructure and aggregation of LHCII in the NPQ state decreases the size of mobile fraction of chlorophyll-proteins. Moreover, the incomplete recovery of the size of mobile fraction in the Dark Zea samples compared to Dark Vio chloroplasts is consistent with the incomplete recovery of the LHCII clustering (Figure 5.8.C) suggesting that de-epoxidation preserves a part of the light-induced structural change. The data also confirmed the previous observation made on both photoinhibited chloroplasts and the chloroplasts with unstacked thylakoid membranes (section 7, chapter IV) that the mobility of chlorophyll-proteins is strongly related to the degree of macromolecular crowding in the membrane. This is reflected on a strong linear correlation which exists between these two parameters (Figure 5.10). Moreover, a non-linear correlation was also found to exist between the mobility of chlorophyll-proteins and the amount of NPQ present in the investigated samples (Figure 5.11). This suggests that formation of the NPQ state impairs the diffusion of photosynthetic complexes, most likely due to observed enhanced clustering and macromolecular crowding in the thylakoid membrane.

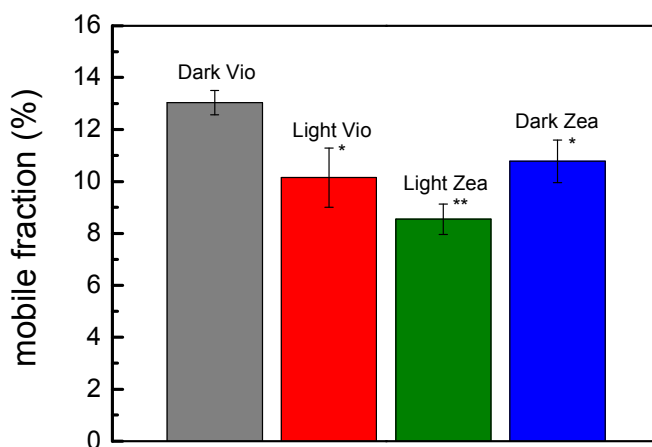


Figure 5.9. Effect of NPQ formation and de-epoxidation state on the mobility of chlorophyll-proteins in intact spinach chloroplasts prepared in four different states. Bars represent means  $\pm$  S.E. (n = 10). \* = significantly different from Dark Vio sample, \*\* = significantly different from Dark Vio, Dark Zea and Light Vio samples (one-way ANOVA followed by Tukey contrast,  $p < 0.01$ ).

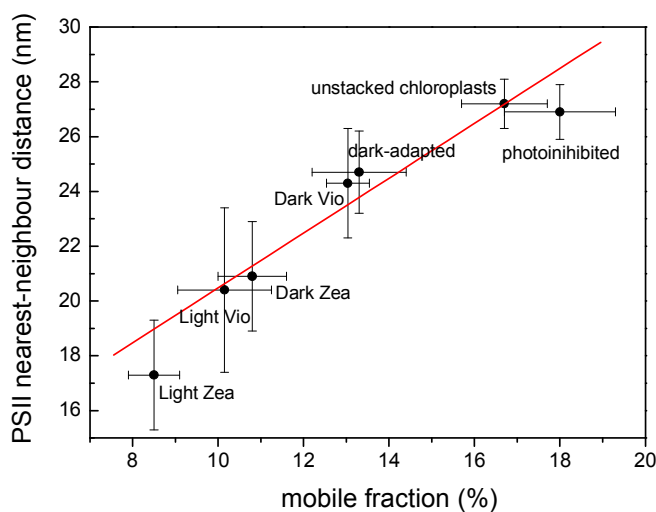


Figure 5.10. Linear relationship between the mobility of chlorophyll-proteins and PSII nearest-neighbour distances in the grana membranes of intact spinach chloroplasts prepared in different states as described above and in chapter IV. The mean values of mobile fractions are those shown in Table 1 and Figures 4.8.B and 5.9. The mean values for PSII nearest-neighbour distances are calculated from all analysed particles as shown in Table 4 and Figure 5.7.B in the distribution graph. Error bars = S.E. Note a strong correlation which exists between the two analysed parameters (Pearson coefficient (R) = 0.96,  $p < 0.001$ ).

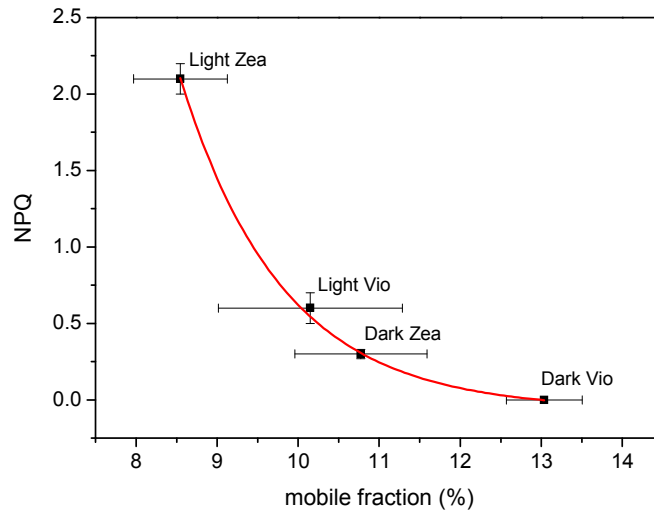


Figure 5.11. Non-linear relationship between the mobility of chlorophyll-proteins and the amount of NPQ formed in intact spinach chloroplasts prepared in different states as described in section 2.1. Each data point represents a mean value ( $\pm$  SE) as calculated in Figure 5.9 and Table 5. Non-linear exponential curve was fitted to the data points ( $R^2 = 0.99$ ). Note a decrease in mobility of proteins upon formation of NPQ state.

### 5.3. The role of PsbS protein in modulating the mobility of photosynthetic proteins

#### 5.3.1. Freeze-fracture electron microscopy

An identical freeze-fracture experiment to the one described above for spinach was undertaken using wild-type (WT) intact *Arabidopsis thaliana* chloroplasts and those from plants either lacking PsbS (*npq4*) or overexpressing the protein (*L17*) (Li et al., 2002a; Li et al., 2002b). The PsbS protein is required for photoprotective qE to be formed rapidly: *npq4* chloroplasts therefore have low levels of NPQ following 5 minutes illumination (Li et al., 2002a, Table 6), while the *L17* chloroplasts have higher levels compared to the wild-type (Li et al., 2002b, Table 6). Analysis of freeze-fracture electron micrographs revealed that the organisation of

PSII-LHCII supercomplexes was significantly different in the three types of chloroplasts in dark-adapted state (Figure 5.12, left panel). The quantitative analysis confirmed that the clustering of PSII and LHCII particles was substantially higher in the *L17* compared to the *npq4* mutant plants (Figure 5.13.A-B). The wild-type samples possessed the level of clustering of PSII and LHCII in between *npq4* and *L17* (Figure 5.13.A-B). What is important, these differences were not caused by an altered LHC antenna size in *L17* and *npq4* chloroplasts as the chlorophyll *a/b* ratios were not significantly different than in the wild-type (Table 7).

**Table 6. Comparison of NPQ values in intact chloroplasts of PsbS protein mutants of *Arabidopsis thaliana* under different conditions.** Intact chloroplasts were prepared from wild-type (WT), PsbS overexpressor *L17*, PsbS-deficient mutant *npq4*, and *E122QE226Q Arabidopsis* leaves, either dark-adapted or light treated for 5 minutes at 350  $\mu\text{mol photons m}^{-2} \text{s}^{-1}$  in the presence of 35 mM sodium ascorbate (light). An additional *npq4* sample was light treated with the same intensity for 1 hour. Data show mean values  $\pm$  S.E. (n = 4). \* = values significantly different with respect to dark-adapted sample (one-way ANOVA with Dunnett contrast, p < 0.01).

Sample	WT dark	WT light	<i>L17</i> dark	<i>L17</i> light	<i>npq4</i> dark	<i>npq4</i> light (5 min)	<i>npq4</i> light (1 h)	<i>E122QE226Q</i> dark
NPQ	0	1.8 $\pm$ 0.11*	0	2.8 $\pm$ 0.08*	0	0.2 $\pm$ 0.08*	1.6 $\pm$ 0.08*	0

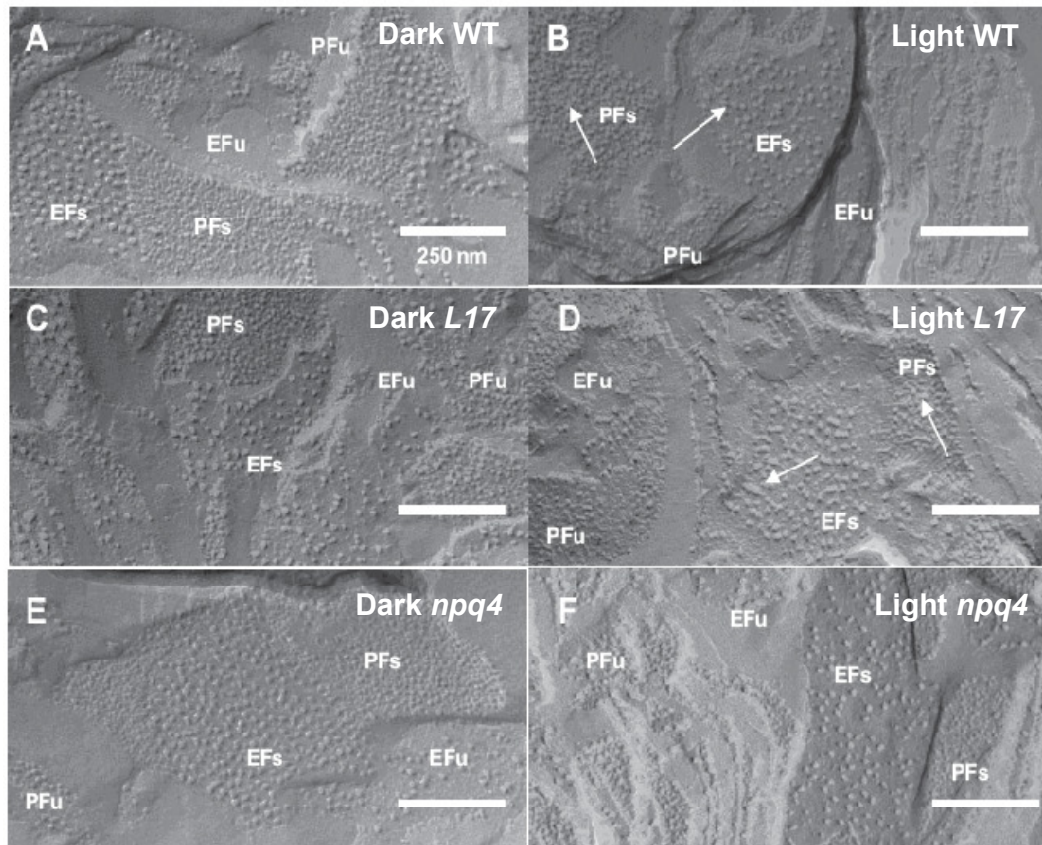


Figure 5.12. Freeze-fracture electron micrographs showing the effect of illumination on the thylakoid membrane structure in *Arabidopsis thaliana* PsbS mutants. Panel on the left shows samples in the dark-adapted state (wild-type (A), *L17* (C), *npq4* (E)) . Panel on the right shows the same samples after 5 minute illumination period ( $350 \mu\text{mol photons m}^{-2} \text{s}^{-1}$ ) ((wild-type (B), *L17* (D), *npq4* (F)). Fracture faces were labelled as described previously in Figure 4.5. For explanation of arrows see text. Figure obtained from Dr. Matthew Johnson, with permission.

**Table 7. Comparison of chlorophyll *a/b* ratios in intact chloroplasts of PsbS protein mutants of *Arabidopsis thaliana*.** Data show mean values  $\pm$  S.D. (n = 3)

Sample	wild-type	<i>npq4</i>	<i>L17</i>
Chlorophyll <i>a/b</i> ratio	$3.7 \pm 0.31$	$3.7 \pm 0.61$	$3.8 \pm 0.49$

As observed in spinach, light treatment of the wild-type *Arabidopsis* chloroplasts resulted in an increased clustering of both PSII and LHCII particles (Figures 5.12.B, Arrows and 5.13.C-D). This effect was further enhanced in *L17* (Figures 5.12.D, Arrows and 5.13.C-D) but in *npq4* chloroplasts there was no significant difference between the dark and light-adapted samples (Figures 5.12.F and 5.13.C-D). Thus while zeaxanthin appeared to amplify the structural changes associated with NPQ formation, in the absence of PsbS it has little effect on the structural parameters analysed here.

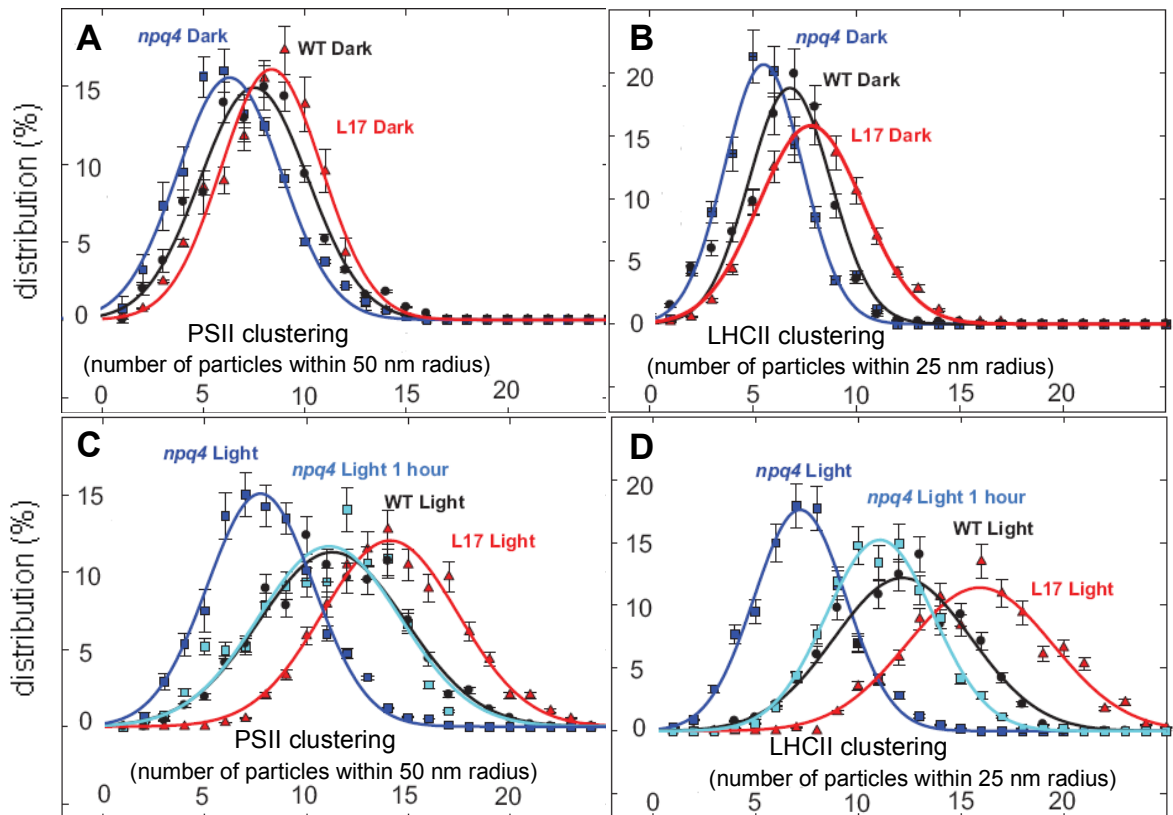


Figure 5.13. Effect of PsbS protein on the organisation of PSII-LHCII supercomplexes in intact *Arabidopsis* chloroplasts in the dark (left panel) and light-adapted states (right panel). (A) and (C) Distribution of PSII clustering (number of neighbouring particles within 50 nm radius) (B) and (D) Distribution of LHCII clustering (number of neighbouring particles within 25 nm radius). Data represent means from 3 independent experiments. Error bars = S.E.

The differences observed in the clustering of PSII particles in the various PsbS mutants were also confirmed by nearest-neighbour distance and particle density analysis (Table 8). As for spinach, the sizes of PSII particles were also investigated. The analysis revealed that in contrast to the wild-type, the size of PSII particles in *L17* mutant was already reduced in the dark and no significant decrease was seen in the light (Table 8). The average size of PSII particles in the light was consistent in *Arabidopsis* and spinach at about 130 nm<sup>2</sup> (Figure 5.7.C and Table 8). Thus, the data suggest that the decrease in PSII particle size is alone insufficient to trigger NPQ. In the *npq4* chloroplasts the PSII particle size was similar to the wild-type dark sample (Table 8). However, unlike the wild-type, no light associated decrease was observed (Table 8).

It has been shown previously that *npq4* chloroplasts can form (within about 1 hour of illumination) up to 85% of NPQ formed by the wild-type in 5 minutes (Johnson and Ruban, 2010, Table 5). In this study such chloroplasts were also prepared and investigated under freeze-fracture electron microscopy. Image analysis revealed that after 1 hour light treatment the same symptoms of the NPQ-related re-organisation of PSII-LHCII supercomplexes observed in the wild-type samples were also present, with a decrease in PSII particle size, nearest-neighbour distance and PSII and LHCII clustering (Table 8 and Figure 5.13.C-D). The amount of PSII arranged in semi-crystalline arrays (see chapter VI for further orientation) was also affected by the level of PsbS protein. The PSII arrays accounted for ~7% of the total EFs fracture faces in the dark-adapted wild-type chloroplasts, while they were almost doubled in the *npq4* mutants and completely absent in the *L17* samples (Table 8). This is consistent with the view that the arrays do not contain PsbS (Dekker and Boekema, 2005). Upon light treatment the percentage of semi-crystalline PSII arrays



was reduced in both the wild-type and *npq4* samples (Table 8). This indicates that the array formation is disrupted by PsbS itself and also by the structural re-organisation occurring upon transition to NPQ state.

**Table 8. Analysis of EFs fracture faces from electron micrographs of wild-type and PsbS mutant intact *Arabidopsis* chloroplasts in dark and light-adapted states.**

Data show mean values  $\pm$  SE. n = number of particles analysed. \* = statistically significant difference with respect to the dark-adapted wild-type sample using one-way ANOVA analysis followed by Dunnett contrast ( $P < 0.05$ ). The fraction of PSII particles organised into arrays was calculated out of the total fraction of EFs fracture faces obtained in all electron micrographs ( $n \approx 30$ ).

Sample	n	PSII nearest neighbour distance (nm)	PSII particle size (nm <sup>2</sup> )	PSII particle density (per $\mu\text{m}^2$ )	% PSII present as semi-crystalline arrays
<b>Wild-type dark</b>	1602	20.4 $\pm$ 0.12	178 $\pm$ 3.7	1120 $\pm$ 37.9	6.8
<b>Wild-type light</b>	1856	17.6 $\pm$ 0.13*	131 $\pm$ 11.7*	1255 $\pm$ 30.7*	0
<b><i>L17</i> dark</b>	1952	18.6 $\pm$ 0.15*	139 $\pm$ 14.4*	1218 $\pm$ 32.8*	0
<b><i>L17</i> light</b>	1759	17.1 $\pm$ 0.13*	132 $\pm$ 14*	1328 $\pm$ 36.6*	0
<b><i>npq4</i> dark</b>	1802	21.3 $\pm$ 0.15*	191 $\pm$ 17.1*	982 $\pm$ 22.4*	12.4
<b><i>npq4</i> light</b>	1859	21.1 $\pm$ 0.09*	190 $\pm$ 3.5*	1001 $\pm$ 18.1*	10.4
<b><i>npq4</i> light (1 hour)</b>	1774	18.3 $\pm$ 0.16*	156 $\pm$ 20.9*	1147 $\pm$ 44.4	4.2
<b><i>E122QE226Q</i> dark</b>	1855	20.9 $\pm$ 0.16	174 $\pm$ 14.4	1077 $\pm$ 27.7	0

### 5.3.2. FRAP measurements

To better understand the relationship between the mobility of chlorophyll-proteins, the rate of NPQ formation and the amount of semi-crystalline domains of PSII present in the thylakoid membrane, I decided to perform FRAP experiments on the wild-type, *npq4* and *L17* chloroplasts in the dark and light-adapted states. In the dark-adapted state the mobility of chlorophyll-proteins was increased of about 30% in the *L17* chloroplasts when compared to the wild-type (Figure 5.14). However, in the *npq4* mutant the mobility was decreased by a similar amount (Figure 5.14). The mobile fraction of chlorophyll-proteins in the light-treated wild type chloroplasts was reduced by ~30%, while in *L17* it was reduced by almost 60% (Figure 5.14) which is consistent with the higher amplitude of NPQ in the overexpressor mutant (Li et al., 2002b, Table 6). In contrast, the size of mobile fraction in the *npq4* chloroplasts was not significantly different in the light compared to the dark-adapted state (Figure 5.14).

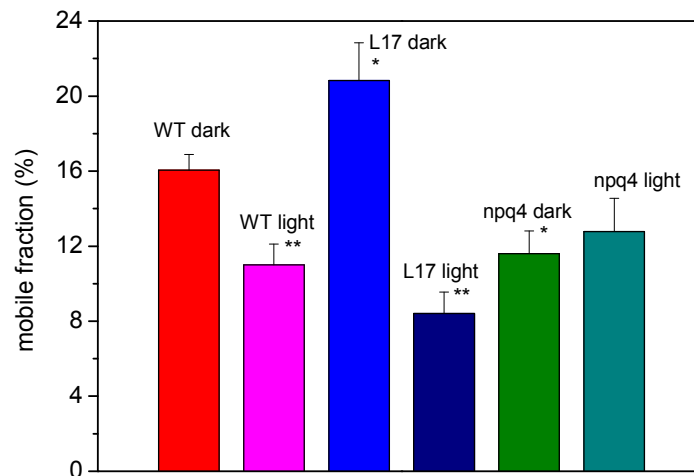


Figure 5.14. Effect of PsbS protein on the mobility of chlorophyll-proteins in intact *Arabidopsis* chloroplasts in dark and light-adapted states. Bars represent mean values out of 10 independent experiments ( $\pm$  S.E.). \* = differences statistically significant from the wild-type dark (Anova analysis with Dunnett contrast,  $p < 0.05$ ) \*\* = differences statistically significant between dark and light-adapted states for each type of samples (Student's t-test,  $p < 0.05$ ).

To confirm that the size of the mobile fraction in the dark was related to the ability to undergo the NPQ-related change in PSII-LHCII macro-organisation I examined the *E122QE226Q Arabidopsis* mutant, which has enhanced content of PsbS protein like *L17* mutant but an NPQ phenotype like that of *npq4* plants (Li et al., 2004). The *E122QE226Q* plants overexpress a mutated PsbS gene in which two acidic glutamate residues, predicted to be in the extrinsic luminal domain of the protein, are mutated to glutamines (Li et al., 2004). Interestingly, the size of the mobile fraction and the PSII organisation in the *E122QE226Q* chloroplasts was not significantly different to the *npq4* plants (Figure 5.15 and Table 8). Hence, the enhancement in the size of the mobile fraction of chlorophyll-proteins in another overexpressor of the PsbS (*L17*) requires the protein to be ‘active’ with respect to NPQ. The data therefore provides a strong link between the size of the mobile fraction in the dark and the ability to undergo the rapid change in PSII-LHCII macro-organisation that underlies NPQ.

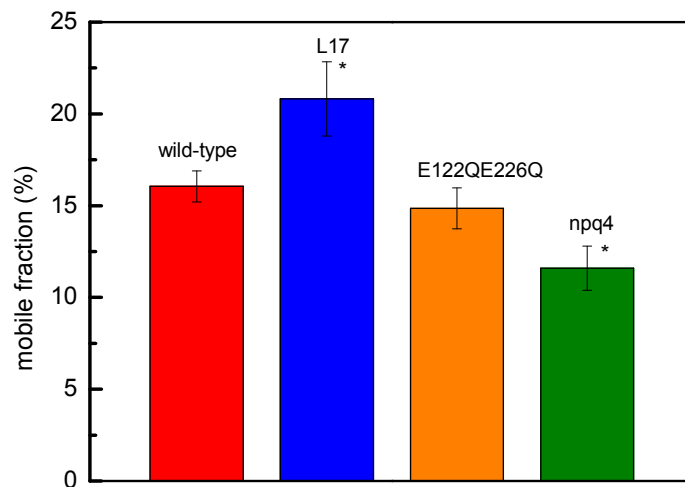


Figure 5.15. Effect of *E122QE226Q* mutations in a PsbS gene on the mobility of chlorophyll-proteins. Data are presented in the same way as in Figure 5.13. \* = differences statistically significant from the wild-type (ANOVA followed by Dunnett test,  $p < 0.05$ ). Note a lack of significant difference in the *E122QE226Q* mutant as compared to the *npq4* plant (Student's t-test,  $P = 0.07$ ).

As noticed previously in the case of spinach chloroplasts a non-linear relationship between the mobility of chlorophyll-proteins and the capacity for NPQ formation was also observed in the PsbS *Arabidopsis* mutant plants (Figure 5.16). This again suggests that the higher the dynamics of photosynthetic complexes in the dark the greater the ability for the LHCII antenna to switch into the photoprotective state in the light (Figure 5.16).

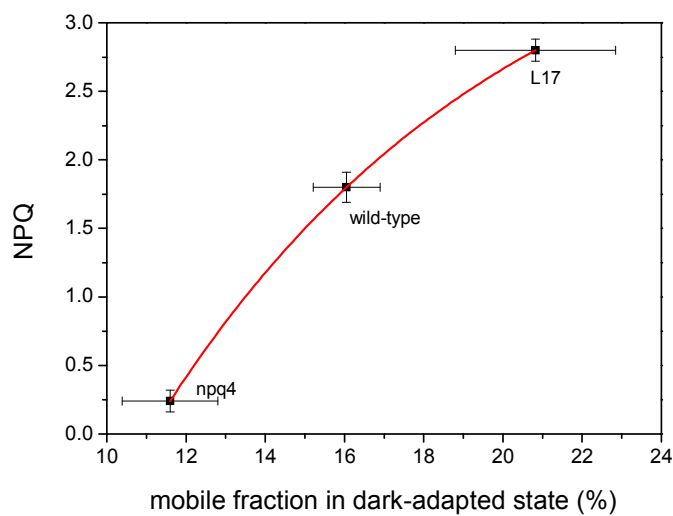


Figure 5.16. Non-linear relationship between the mobility of chlorophyll-proteins in dark-adapted state and the amount of NPQ formed after light treatment. Each data point represents a mean value ( $\pm$  SE) as calculated in Figure 5.14 and Table 5. Non-linear exponential curve was fitted to the data points ( $R^2 = 1$ ).

## **5.4. The effect of varying xanthophyll composition within LHCII antenna on the mobility of chlorophyll-proteins in the thylakoid membranes**

### **5.4.1. FRAP measurements**

Recently it has been shown that differences in the rates of NPQ formation and relaxation could result also from different composition of xanthophylls that are bound both externally (violaxanthin or zeaxanthin binding to the peripheral V1 site of LHCII monomer) and internally (two luteins and one neoxanthin per LHCII trimer) to the light-harvesting antenna (Ruban and Johnson, 2010). It was found that these differences are caused by different hydrophobicity parameters for each xanthophyll with more hydrophobic xanthophylls accelerating development of NPQ but, at the same time, drastically decreasing its relaxation (Ruban and Johnson, 2010). To further investigate the role of de-epoxidation of violaxanthin into zeaxanthin (complementary to the results presented in sections 2.1 – 2.3 of this chapter) as well as the role of internally bound xanthophylls on the NPQ-related changes in the organisation and dynamics of photosynthetic complexes in the thylakoid membranes I performed FRAP experiments on intact chloroplasts isolated from a range of dark-adapted *Arabidopsis* mutants with the altered composition of xanthophyll molecules in the LHCII antenna. The mutants of externally bound xanthophylls were *npq1* and *npq2* with violaxanthin or zeaxanthin bound to the peripheral V1 site, respectively. The mutants of internally bound xanthophylls were *lut2npq1* (replacement of lutein by violaxanthin), *lut2npq2* (replacement of lutein by zeaxanthin), *lut1* (deficiency in lutein synthesis resulting in reduction by ~ 80% of

lutein content) and *lut2* (synthesis of lutein blocked completely with violaxanthin occupying the lutein-binding site) (Pogson et al., 1996; Johnson et al., 2008).

FRAP measurements revealed that the mobility of chlorophyll-proteins in the grana membranes was unchanged in the *npq1*, *lut2npq1* and *lut1* mutants whereas a significant decrease in the size of mobile fraction by about 25 – 30% was observed in the *npq2*, *lut2npq2* and *lut2* xanthophyll mutants of *Arabidopsis* (Figure 5.17). The observed effect is similar to the light-induced de-epoxidation of violaxanthin to zeaxanthin (Figure 5.9) suggesting that the elevated level of zeaxanthin, particularly in the *npq2* and *lut2npq2* mutants decreases fluidity of the membrane even in the dark-adapted state. This might serve as a prerequisite for the formation of NPQ state and aggregation of LHC antenna as observed in intact spinach chloroplasts subjected to light adaptation (Figure 5.8).

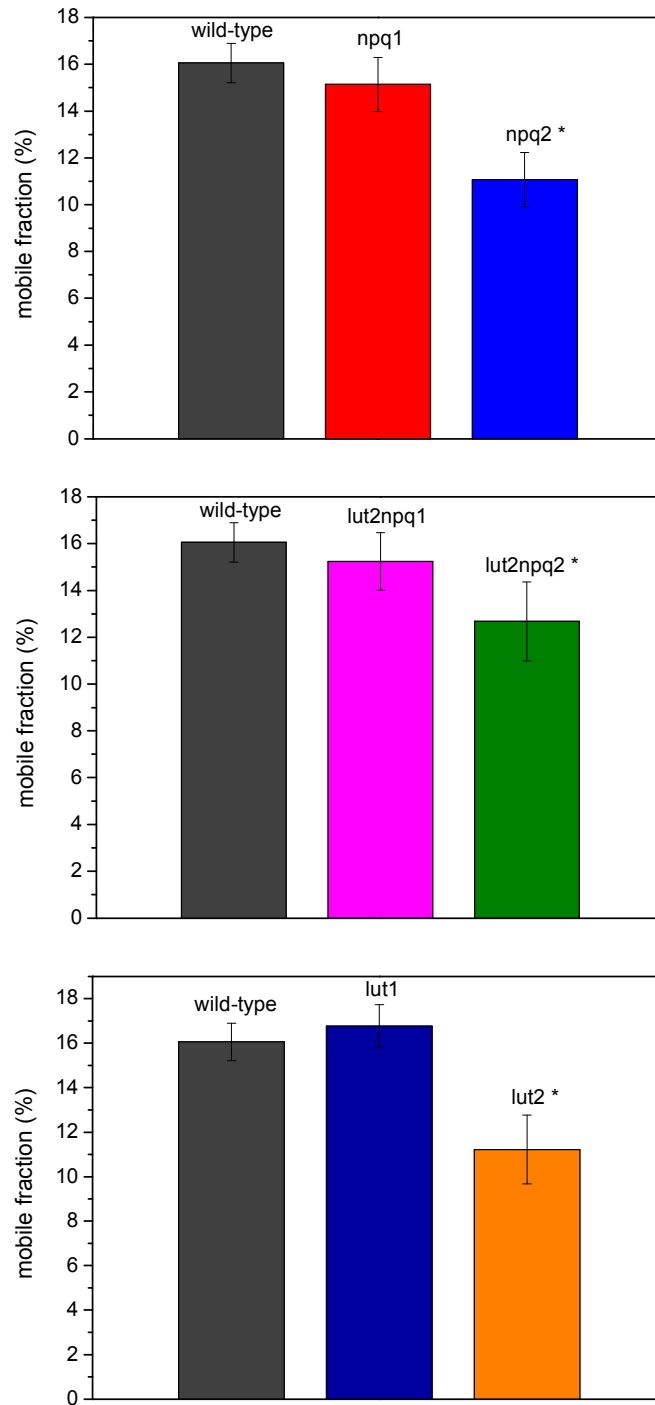


Figure 5.17. Mobility of chlorophyll-proteins in intact chloroplasts isolated from different xanthophyll mutants of *Arabidopsis thaliana*. Bars represent mean values out of 10 independent experiments  $\pm$  S.E. Statistically significant differences are indicated by asterisks (one-way ANOVA followed by Dunnett contrast,  $p < 0.05$ ).

#### 5.4.2. Freeze-fracture electron microscopy

To find out whether the observed differences in mobility were accompanied by the structural rearrangement of PSII-LHCII supercomplexes in the thylakoid membranes the intact chloroplasts from different xanthophyll mutants were investigated by means of freeze-fracture electron microscopy. The electron micrographs revealed no substantial changes in the macro-organisation of PSII-LHCII supercomplexes with respect to the wild-type, except for the *npq2*, *lut2npq2* and *lut2* mutants. These samples exhibited a noticeable tendency for PSII particles to become more clustered together (Figure 5.18, Arrows). These observations were further confirmed by quantitative analysis of both EFs and PFs fracture faces, as shown in Figures 5.19 - 5.20 and Tables 9 - 10. The enhanced clustering between PSII particles was noticed for the three mentioned mutant plants while the clustering in the other samples (*npq1*, *lut2npq1* and *lut1*) were not significantly different from the wild-type (Figure 5.19.A, C, E and Table 9). The similar pattern, although less pronounced, was observed in the measurements of PSII nearest-neighbour distances (Figure 5.19.B, D, F and Table 9). Analysis of PFs fracture faces revealed the same tendency of increased LHCII clustering in the *npq2*, *lut2npq2* and *lut2* mutants which was also reflected in shortening of nearest-neighbour distances between LHCII particles (Figure 5.20 and Table 10). Interestingly, a significant clustering of LHCII particles was also observed in the *lut1* mutant, similarly to the effect shown in the *lut2* sample (Figure 5.20. E, F and Table 10).



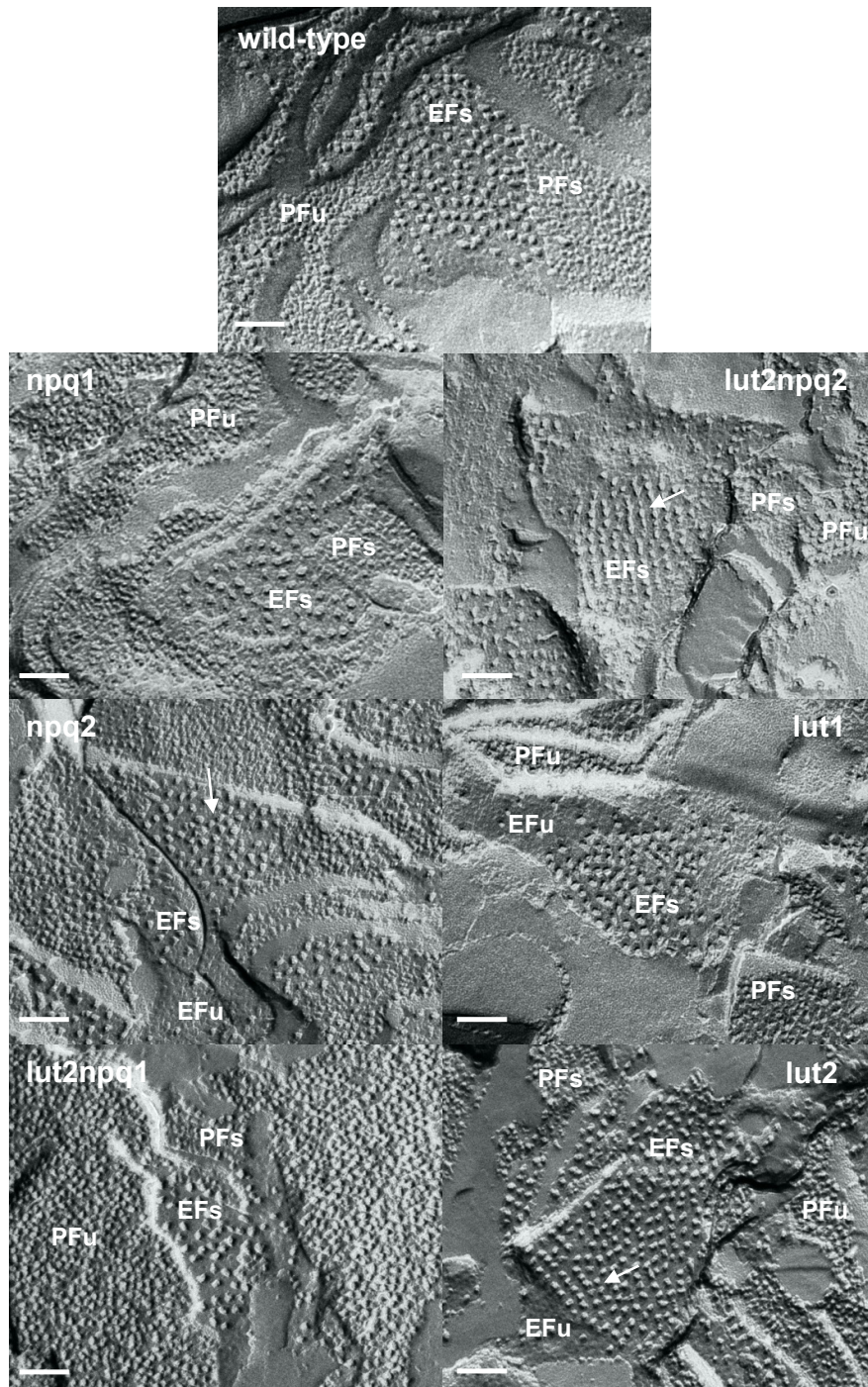


Figure 5.18. Freeze-fracture electron micrographs from different xanthophyll mutants of *Arabidopsis thaliana*. Fracture faces are labelled as described in section 2.2 and Figure 4.5. Scale bars = 100 nm. For explanation of arrows see text.

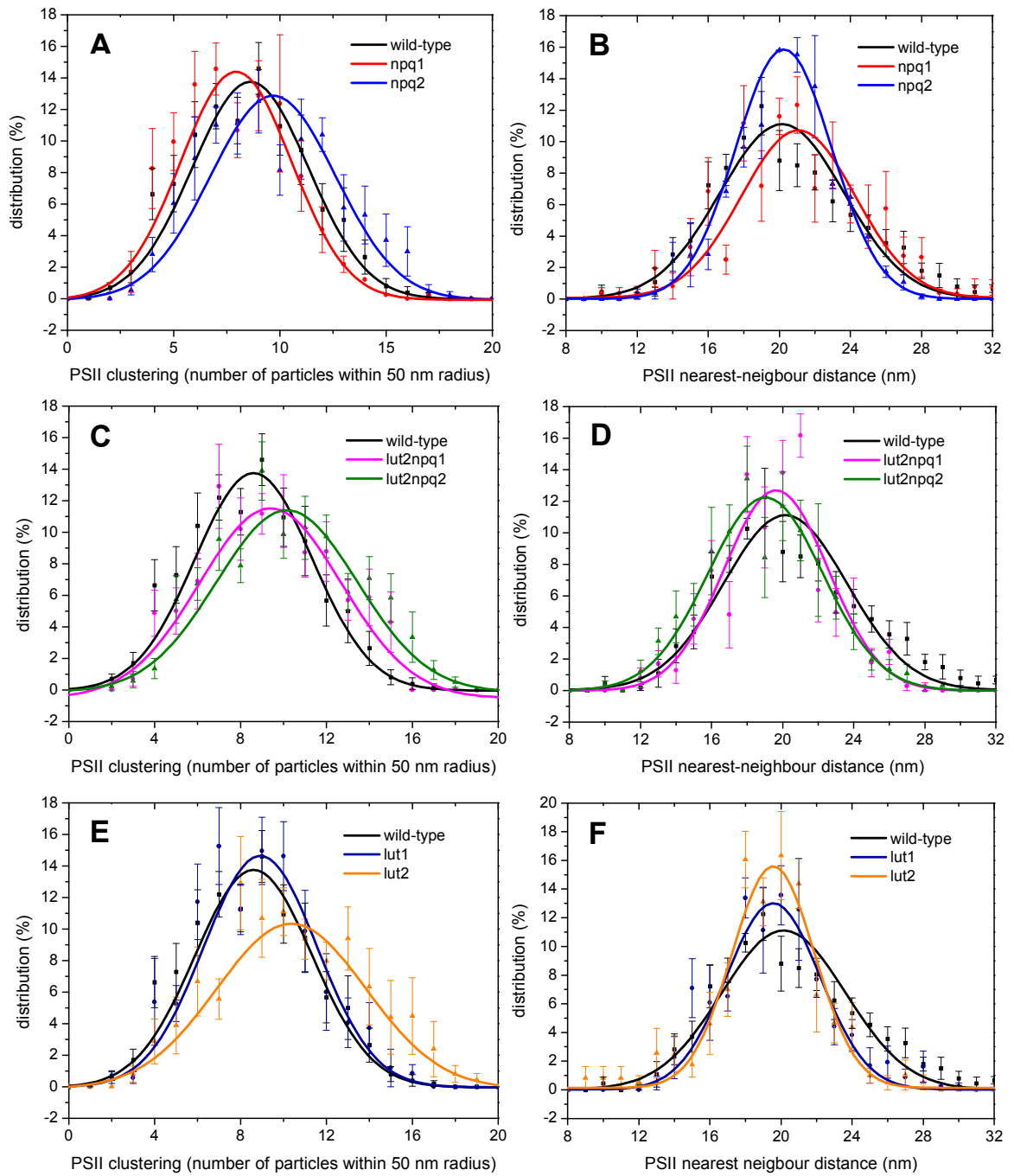


Figure 5.19. Analysis of PSII particles from EFs fracture faces of electron micrographs obtained for different xanthophyll mutants of *Arabidopsis*. (A), (C), (E). Distribution of PSII clustering measurements for externally and internally bound xanthophyll mutants as compared to the wild-type. (B), (D), (F). Distribution of nearest-neighbour distances between PSII particles. Each data point represents a mean value ( $\pm$  SE) calculated out of all EFs fracture faces analysed ( $n = 10 - 15$ ).

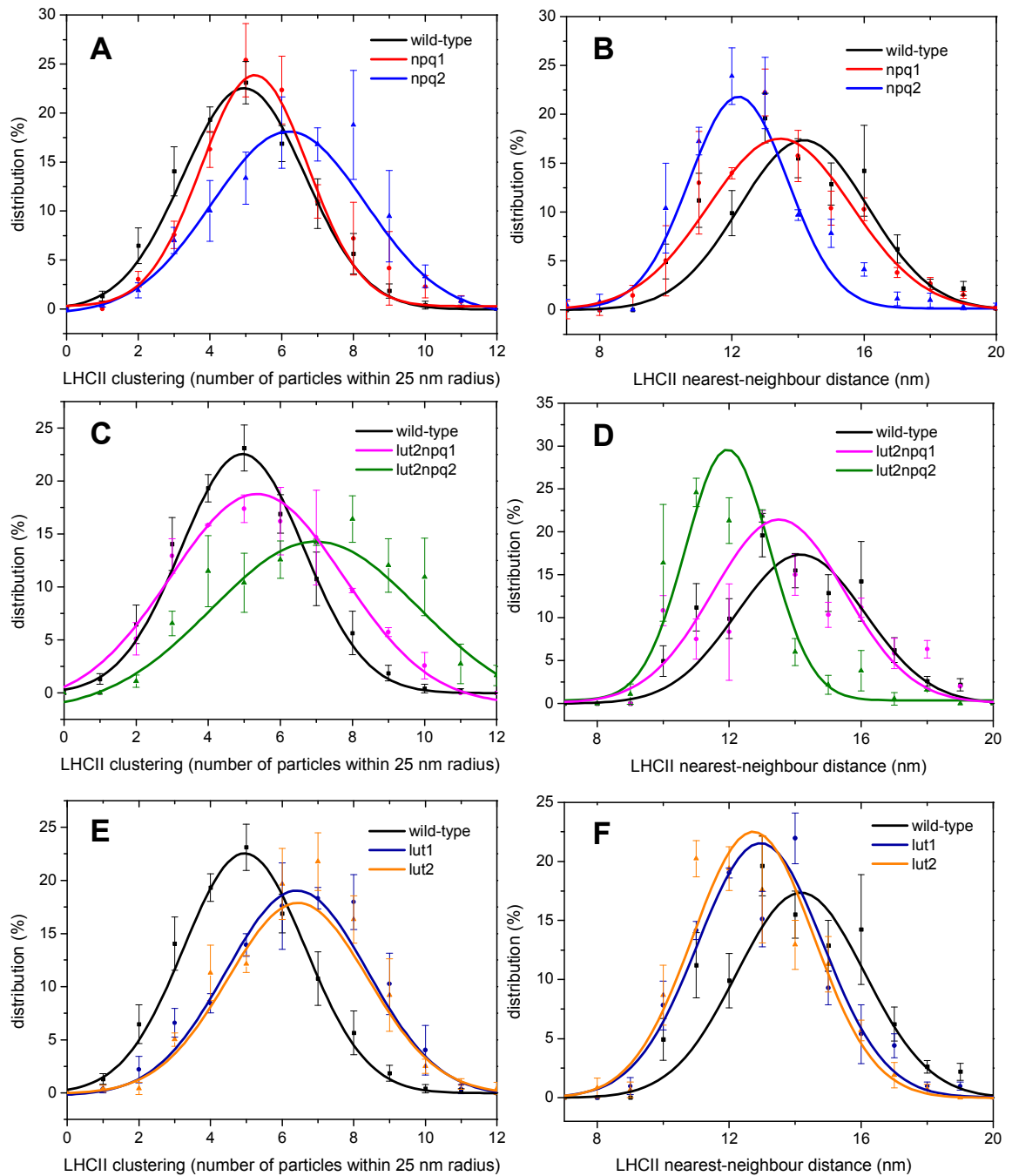


Figure 5.20. Analysis of LHCII particles from PFs fracture faces of electron micrographs obtained for different xanthophyll mutants of *Arabidopsis*. (A), (C), (E). Distribution of LHCII clustering measurements for externally and internally bound xanthophyll mutants as compared to the wild-type. (B), (D), (F). Distribution of nearest-neighbour distances between LHCII particles. Each data point represents a mean value ( $\pm$  SE) calculated out of all PFs fracture faces analysed ( $n = 7 - 10$ ).

The sizes of PSII and LHCII particles were also investigated but in all cases they did not differ from the particles present in the wild-type chloroplasts (Tables 9 - 10). However, it is worth noticing that the amount of PSII particles organised into semi-crystalline arrays was affected in the samples with different composition of xanthophylls in the LHCII antenna (Table 9). This was the case in the *npq2*, *lut2npq2* and *lut2* mutants which exhibited 30 – 50% increase in the total amount of semi-crystalline arrays present in the grana membranes (Table 9).

The results obtained from freeze-fracture experiments are fully consistent with the FRAP measurements (section 4.1) indicating that the presence of more hydrophobic xanthophylls (i.e. zeaxanthin) within LHCII antenna results *per se* in a greater packing of PSII-LHCII supercomplexes and a decreased fluidity of chlorophyll-proteins in the thylakoid membranes – the effect which is similar to the one observed in intact spinach chloroplasts after de-expoxidation of violaxanthin to zeaxanthin upon light treatment and formation of NPQ state (section 2.2).

**Table 9. Quantitative analysis of EFs fracture faces from electron micrographs of wild-type and different xanthophyll mutants of *Arabidopsis* chloroplasts in dark-adapted state.**

Data show mean values  $\pm$  SE. n = number of particles analysed. \* = statistically significant difference with respect to the dark-adapted wild-type sample using one-way ANOVA analysis followed by Dunnett contrast ( $P < 0.05$ ). The fraction of PSII particles present as arrays was calculated as described in Table 7.

Sample	n	PSII nearest neighbour distance (nm)	PSII particle size (nm <sup>2</sup> )	PSII particle density (per $\mu\text{m}^2$ )	PSII clustering (number of particles within 50 nm radius)	% PSII present as semi-crystalline arrays
Wild-type	1602	20.4 $\pm$ 0.12	178 $\pm$ 3.7	1120 $\pm$ 37.9	8.7 $\pm$ 0.09	6.8
<i>npq1</i>	413	20.3 $\pm$ 0.19	171 $\pm$ 9.0	1160 $\pm$ 46.4	7.9 $\pm$ 0.13	6.8
<i>npq2</i>	508	19.9 $\pm$ 0.13	169 $\pm$ 3.23	1341 $\pm$ 51.8*	10.8 $\pm$ 0.19*	8.2
<i>lut2npq1</i>	397	19.3 $\pm$ 0.20	168 $\pm$ 3.6	1325 $\pm$ 43.5*	9.1 $\pm$ 0.19	5.8
<i>lut2npq2</i>	465	18.4 $\pm$ 0.16*	169 $\pm$ 3.8	1329 $\pm$ 52.0*	10.2 $\pm$ 0.15*	8.2
<i>lut1</i>	365	19.2 $\pm$ 0.16*	169 $\pm$ 7.8	1272 $\pm$ 36.8*	9.6 $\pm$ 0.15*	7.3
<i>lut2</i>	387	18.5 $\pm$ 0.14*	165 $\pm$ 3.3	1644 $\pm$ 47.3*	11.6 $\pm$ 0.19*	9.5

**Table 10. Quantitative analysis of PFs fracture faces from electron micrographs of wild-type and different xanthophyll mutants of *Arabidopsis* chloroplasts in dark-adapted state.**

Data show mean values  $\pm$  SE. n = number of particles analysed. \* = statistically significant difference with respect to the dark-adapted wild-type sample using one-way ANOVA analysis followed by Dunnett contrast ( $P < 0.05$ ).

Sample	n	LHCII nearest neighbour distance (nm)	LHCII particle size (nm <sup>2</sup> )	LHCII particle density (per $\mu\text{m}^2$ )	LHCII clustering (number of particles within 25 nm radius)
Wild-type	643	13.4 $\pm$ 0.09	70 $\pm$ 1.3	3197 $\pm$ 69.4	4.9 $\pm$ 0.07
<i>npq1</i>	417	12.8 $\pm$ 0.14	66 $\pm$ 2.7	3236 $\pm$ 88.6	5.6 $\pm$ 0.11
<i>npq2</i>	410	12.0 $\pm$ 0.10*	71 $\pm$ 3.8	3500 $\pm$ 121.4*	6.5 $\pm$ 0.1*
<i>lut2npq1</i>	421	13.0 $\pm$ 0.21	76 $\pm$ 5.1	3111 $\pm$ 162.0	5.8 $\pm$ 0.16
<i>lut2npq2</i>	384	11.6 $\pm$ 0.14*	64.0 $\pm$ 6.4	3833 $\pm$ 186.3*	6.9 $\pm$ 0.17*
<i>lut1</i>	473	12.6 $\pm$ 0.14*	71 $\pm$ 3.2*	3416 $\pm$ 103.6*	6.4 $\pm$ 0.12*
<i>lut2</i>	540	12.2 $\pm$ 0.13*	70 $\pm$ 4.0*	3381 $\pm$ 148.2*	6.5 $\pm$ 0.12*

# **Chapter VI**

**The role of light-harvesting antenna  
in controlling the dynamics and  
macromolecular organisation of  
photosynthetic complexes in the  
grana membranes**

## 6.1. Introduction

In higher plants the peripheral light-harvesting antenna system of photosystem II plays a crucial role not only in efficient light harvesting and transfer of the absorbed energy to the reaction centers of PSII but it is also indispensable in photosynthesis regulation through photoprotective mechanisms, which dissipate the excess energy into heat under high light (non-photochemical quenching) (see chapter V for details). In green plants the antenna system consists of number of pigment-protein complexes belonging to the Lhcb multigenic family (Jansson, 1999). They include major antenna complexes, usually forming a heterotrimer which are the products of *lhcb1*, *lhcb2* and *lhcb3* genes. The second group includes minor monomeric antenna complexes which are known as CP29, CP26 and CP24 (the genes encoding them are referred to *lhcb4*, *lhcb5* and *lhcb6*, respectively) (Jansson, 1999). Both minor and major antenna proteins form, together with PSII photosystems, structural units of higher degree known as PSII-LHCII supercomplexes which are specifically organised and distributed within the grana membranes. There are numerous reports indicating that different antenna proteins are important for stabilising and controlling the macromolecular organisation of supercomplexes in the membrane (reviewed in Dekker and Boekema, 2005). The data presented in chapters IV and V suggest strongly that the way protein complexes are organised in the thylakoid membranes influences their dynamic properties. In this chapter I aim at investigating the role of individual light-harvesting antennae in controlling structural and dynamic changes of PSII-LHCII supercomplexes in the grana membranes.



## **6.2. Freeze-fracture electron microscopy in different light-harvesting antenna mutants of *Arabidopsis thaliana***

To study the effect of loss of individual light-harvesting antenna proteins on the macromolecular organisation of photosynthetic complexes in the grana I performed freeze-fracture electron microscopy analysis on the intact thylakoid membranes isolated from a collection of light-harvesting antenna mutants of *Arabidopsis* created either by antisense inhibition (*as*) or ‘knockout’ mutagenesis (*ko*). The former approach involves the use of a sequence, complementary by virtue of Watson-Crick base pairing to a specific mRNA, which can inhibit its expression and then induce a blockade in the transfer of genetic information from DNA to protein. This inhibition of gene expression is believed to occur by a combination of two mechanisms: RNase H-dependent mechanism which induces the degradation of mRNA and steric hindrance preventing or inhibiting the progression of splicing or the translational machinery (Dias and Stein, 2002). The knockout mutations are generated by insertion of a transposon or the transferred DNA (T-DNA) into a structural gene (either into an exon or an intron) which results in a complete disruption of gene expression (Thornycroft et al., 2001). In this case one can have complete confidence that a particular protein is totally absent from all cells throughout a homozygous plant. The *Arabidopsis* mutants used in the current study included the mutants of major antenna proteins such as *asLhcb2* and *koLhcb3* which lack major trimeric LHCII antenna or they do not form “moderately bound (M)” trimers of LHCII, respectively (Dekker and Boekema, 2005) and the mutants lacking minor antenna complexes CP29, CP26 and CP24 (*asLhcb4*, *asLhcb5* and *koLhcb6*, respectively). In addition, the *chl* mutant was also used in this study which possesses a recessive mutation on chromosome 1 leading to a complete block in the synthesis

of chlorophyll *b* which, in turn, has severe implications on the formation and stability of all major and minor LHCII antenna complexes (Murray and Kohorn, 1991; Havaux et al., 2007). In fact the latter mutant exhibits the most extreme case as, although possessing functional *lhcb* genes, it does not form functional LHCII that could efficiently harvest light energy and transfer it to the PSII core reaction centers (Murray and Kohorn, 1991). As a result of a reduced level of chlorophyll the leaves of the mutant plant appear light green in colour and the growth rate is much slower than in the wild-type. Moreover, the PSII core proteins become more abundant in the mutant plants in comparison to the wild-type suggesting that more photosystems are produced to compensate for the lack of light-harvesting antenna (Murray and Kohorn, 1991; Havaux et al., 2007). Freeze-fracture electron micrographs revealed considerable differences in the appearance of the thylakoid fracture faces upon mutations in some of the light-harvesting antenna genes and in the *chl* mutant (Figures 6.1 – 6.3). Although in all investigated samples (except for the *chl* mutant) the different fracture faces (as described in chapter IV) could be clearly distinguished (Figures 6.1 – 6.2), the organisation of the particles occupying these faces (macromolecular crowding) plus their individual characteristics (size and shape) were significantly different when compared to the wild-type chloroplasts. This was confirmed by the quantitative measurements which are described below in detail.

### **6.2.1. Analysis of PSII particles organised in semi-crystalline arrays**

The amount of PSII particles ordered in semi-crystalline arrays (as shown in Figure 1.7) has changed significantly, especially in the minor antenna mutants (Figure 6.2). In the dark-adapted wild-type chloroplasts the PSII-array like organisation accounted for ~ 7% of the total PSII complexes present in the grana (Figure 6.1). This almost doubled in the *asLhcb5* mutant and tripled in the *koLhcb6*

resulting in the quarter of all PSII complexes organised into semi-crystalline arrays in the latter sample (Figure 6.2). In contrast, the *asLhcb4* samples showed no presence of PSII arrays at all (Figure 6.2). Major antenna mutants exhibited the amount of PSII arrays comparable to the one found in the wild-type chloroplasts (Figure 6.1).

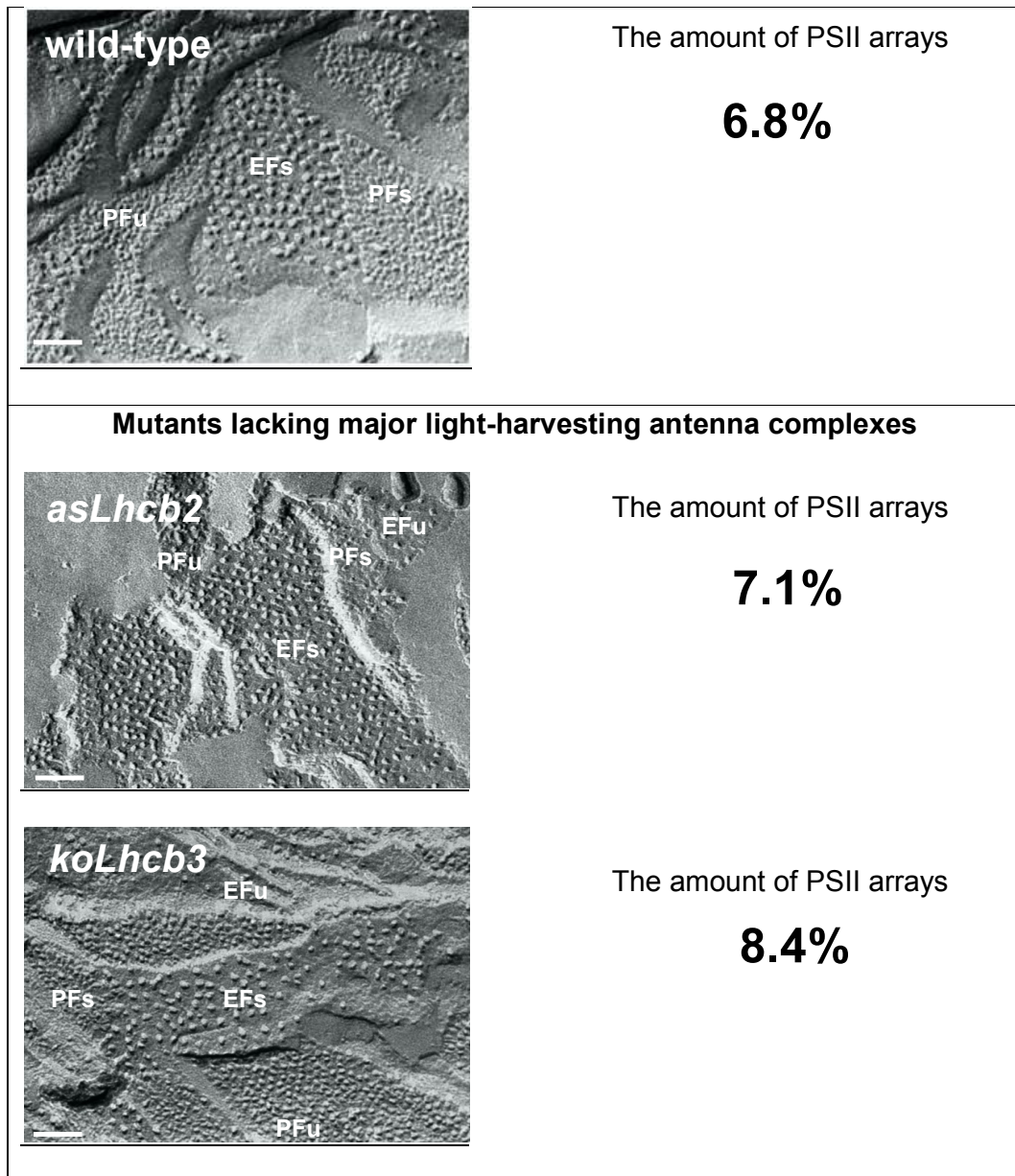
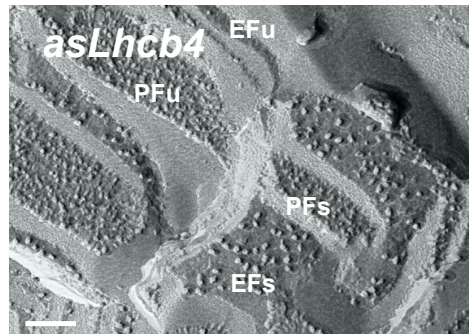


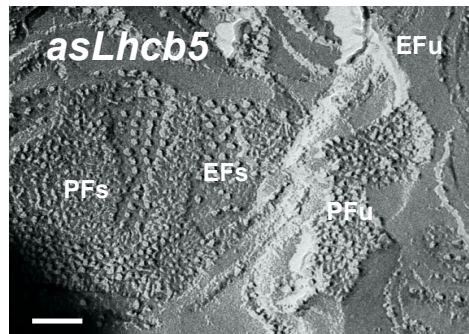
Figure 6.1. Freeze-fracture electron microscopy experiments performed on the light-harvesting antenna mutants of *Arabidopsis*. (Panel on the left). Electron micrographs showing typical appearance of the thylakoid fracture faces in the dark-adapted wild-type and the major antenna mutant samples. Scale bar = 100 nm. (Panel on the right). Comparison of the amount of PSII particles organised into semi-crystalline arrays. The fractions were calculated as described in Table 6.

**Mutants lacking minor light-harvesting antenna complexes**



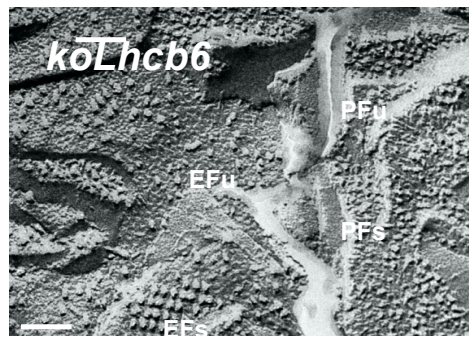
The amount of PSII arrays

**0 %**



The amount of PSII arrays

**11.1%**



The amount of PSII arrays

**22.3%**

Figure 6.2. Freeze-fracture electron microscopy experiments performed on the light-harvesting minor antenna mutants of *Arabidopsis*. The figure is presented in an identical way as Figure 6.1. Scale bars = 100 nm.

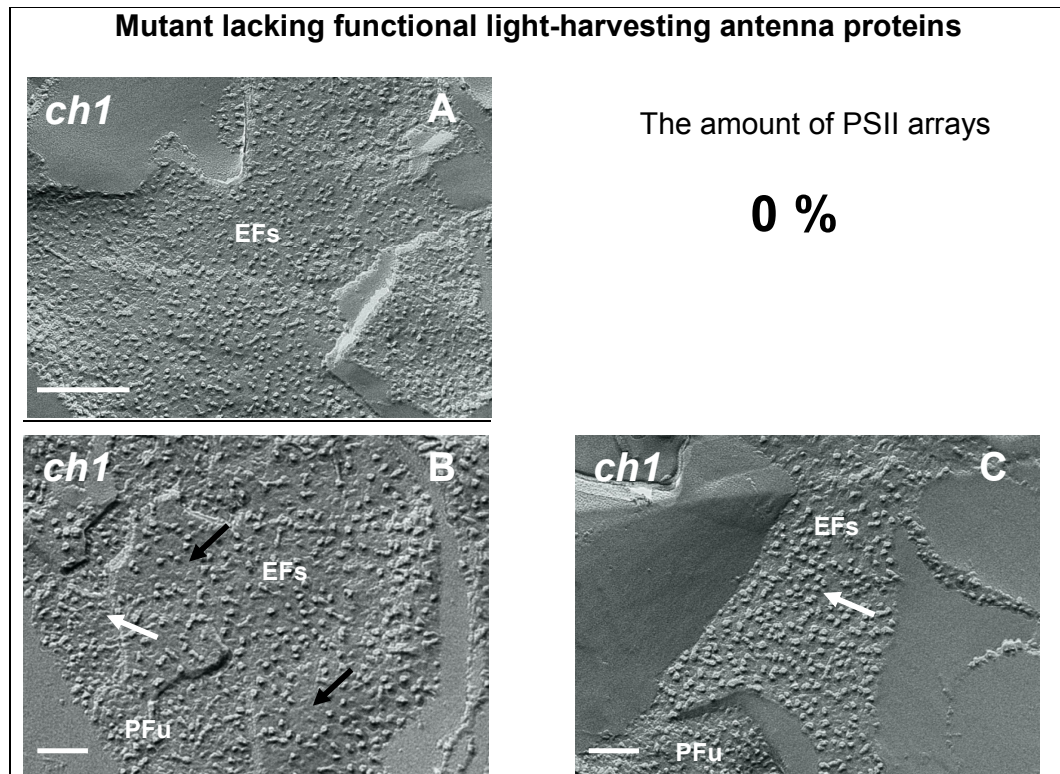


Figure 6.3. Freeze-fracture electron microscopy experiment performed on the *chl* mutant of *Arabidopsis* which does not form functional LHC antenna. Note large EFs fracture faces present in the mutant plants (A) and a specific appearance of the PSII particles in the EFs fracture faces in (B) and (C) as described in the text. For explanation of arrows see text again. Scale bars in (A) = 200 nm, in (B) and (C) = 100 nm.

A special appearance of the thylakoid fracture faces was observed in the *chl* mutant (Figure 6.3). First and foremost, the EFs faces were much larger than in the wild-type (Figure 6.3.A) suggesting that the mutant plants might form bigger grana as was already observed in chlorophyll b-deficient mutants of barley (Simpson, 1979). Moreover, the PSII particles were distributed in a much more random way leading to existence of large spaces in the grana completely free of particles (Figure 6.3.B. Black arrows). In addition, the PFs fracture faces which normally contain the LHCII particles were hardly seen in the *chl* mutant confirming the findings that these plants do not form functional LHCII (Murray and Kohorn, 1991; Havaux et al., 2007). Instead, these spaces were again almost completely devoid of

any particles (Figure 6.3.B. White arrow). However, some EFs fracture faces showed the PSII particles which remained more densely packed and clustered together than in the wild-type (Figure 6.3.B.White arrows). As predicted, such specific appearance and organisation of PSII resulted in a complete lack of semi-crystalline arrays formation (Figure 6.3). The observed characteristics were further confirmed in the quantitative analysis of freeze fracture electron micrographs (section 2.3).

Single-particle studies performed previously on the detergent-solubilised membrane fragments suggested that the loss of individual light-harvesting antenna proteins not only changes the amount of PSII arrays present in the grana membranes but also alters the structural features of the ordered arrays of PSII (Ruban et al., 2003; Yakushevska et al., 2003; Kovács et al., 2006; Damkjaer et al., 2009). In my study I investigated the samples prepared by the freeze-fracture technique which eliminates the need for detergent treatment, and therefore has an advantage over the previous work since the thylakoid membrane still remains intact under these conditions. Hence, I decided to probe carefully the structural features of the PSII arrays formed in different light-harvesting antenna mutants of *Arabidopsis*. Similarly to the mentioned studies, I recognised the repeating unit in the array organisation and measured its dimensions and the angle between the axes (Figure 6.4). Although my calculations were not based on the averaged projections of the PSII-LHCII supercomplexes like for the single-particle analysis the results obtained are in a good agreement with the published data.

In the wild-type plants the typical array-like domain consists of  $C_2S_2M_2$  supercomplexes which are organised in rows in a head-to-tail arrangement along the rows (as shown in Figure 1.7) (Kovács et al., 2006). The repeating unit in the wild-type plants has dimensions of  $26.3 \times 20.7$  nm with the angle between the axes of  $73^\circ$

(Figure 6.4). This has changed in the *asLhcb2* mutant where the spacing between the rows is slightly reduced whereas the spacing in a row has slightly increased (Figure 6.4). However, no change in the angle between the axes was observed suggesting that only slight difference in packing of the complexes exists in the antisense mutant. In fact, the structural analysis of the PSII arrays confirms the finding that plants lacking the major trimeric light-harvesting antenna retain the PSII macro-organisation normally found in the wild-type samples (Ruban et al., 2003).



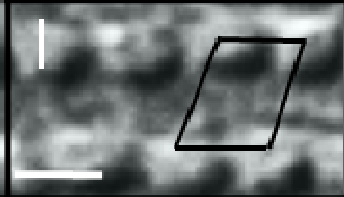
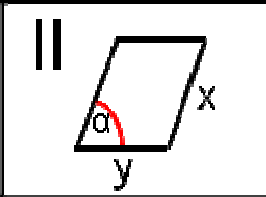
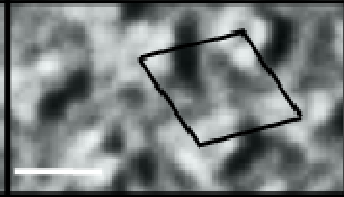
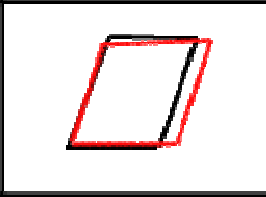
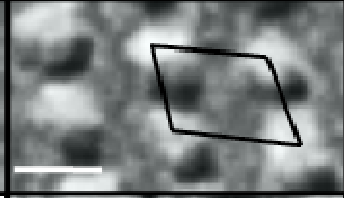
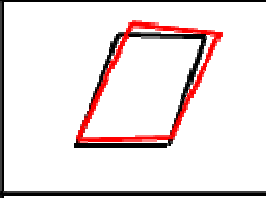
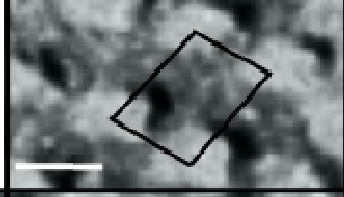
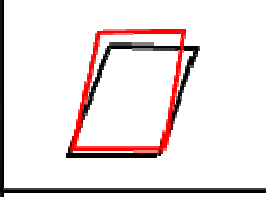
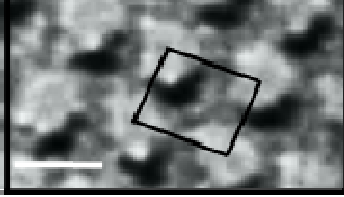
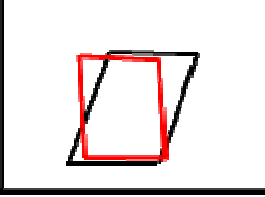
		<b>III wild-type</b> n = 96 x = 26.3 ± 1.63 y = 20.7 ± 1.08 α = 73° ± 7.9
		<b>asLhcb2</b> n = 87 x = 23.9 ± 1.75* y = 21.8 ± 1.98* α = 70° ± 3.9
		<b>koLhcb3</b> n = 103 x = 28.3 ± 1.80* y = 19.9 ± 1.55 α = 65° ± 4.9*
		<b>asLhcb5</b> n = 70 x = 26.6 ± 2.01 y = 19.9 ± 1.95 α = 84° ± 8.5*
		<b>koLhcb6</b> n = 83 x = 22.6 ± 2.22* y = 16.1 ± 2.11* α = 90° ± 5.0*

Figure 6.4. Freeze-fracture electron microscopy image analysis of the PSII arrays in intact thylakoid membranes of different light-harvesting antenna mutants of *Arabidopsis*. (Panel I). Enlarged images of PSII semi-crystalline arrays formed in the investigated mutants. The individual particles were selected followed by the center-to-center distance measurements between two neighbouring particles in one row (y axis) and two opposing particles from neighbouring rows (x axis) leading to formation of the repeating crystalline unit (dark diamond). Note that all images are in the same scale. Scale bar = 20 nm. (Panel II). The selected repeating units from Panel I are presented alone for better visualisation. The x and y measurements (shown in the wild-type sample) correspond to distances between neighbouring particles from the opposing rows and within the same row, respectively. The angle between these axes is indicated as *alpha*. The repeating units obtained for each mutant are superimposed onto the repeating unit from the wild-type to visualise differences in the measured distances and angles. (Panel III). The calculated averaged values ( $\pm$  SE) for x, y and angle measurements are shown for each mutant. n = number of repeating units used for calculations. Values which are significantly different from the wild-type are indicated by the asterisks (one-way ANOVA with Dunnett contrast,  $p < 0.05$ ).

Analysis of PSII arrays in the *koLhcb3* mutant samples revealed also slight alterations in the overall organisation of the repeating unit. Its size was somewhat larger in the mutant plants when compared to the wild-type which was particularly visible in the spacing between the rows increasing by about 2 nm (Figure 6.4). In addition, the angle between the axes has slightly decreased in the repeating unit of the knockout mutant (Figure 6.4). Nonetheless, the observed changes were still relatively insignificant and the main PSII macro-organisation is again still retained in the mutant plants with  $C_2S_2M_2$  supercomplexes predominantly present in the arrays. This confirms the view that depletion of M trimers of LHCII encoded normally by the *lhcb3* gene leads to a compensatory response in which Lhcb1 and Lhcb2 subunits replace the missing Lhcb3 subunit in the M trimer (Damkjaer et al., 2009).

Among the minor antenna mutants only *asLhcb5* and *koLhcb6* samples retained the array-like organisation of PSII particles but its abundance in the grana and the structural features of the repeating units were significantly different than in the wild-type chloroplasts (Figures 6.2 and 6.4). The loss of CP26 proteins (*asLhcb5* samples) resulted in a slight tendency for the shortening of the spacing between particles in the same row while the spacing between the rows remained the same (Figure 6.4). However, there was a noticeable increase in the angle between the axes replacing the diamond-shape like repeating unit in the wild-type with almost perfect rectangular shape. This results in a formation of the PSII array where two opposing particles from neighbouring rows face each other perpendicularly to the particles within the same row (Figure 6.4). Such type of macro-organisation leads to the particles being packed closer together which in the *asLhcb5* mutant is a consequence of the removal of CP26 minor antenna from the tips of the  $C_2S_2M_2$  supercomplexes (Yakushevskaya et al., 2003). This effect is even more pronounced in the *koLhcb6*

mutant where the angle measurement is equal to  $90^\circ$ , and both spatial measurements are substantially reduced in comparison to the wild-type arrays (Figure 6.4). Since the spatial distance between the rows decreases to about 16 nm which is the width of the  $C_2S_2$  supercomplex (Kovács et al., 2006) the arrays in the *koLhcb6* mutant are likely to contain only this type of complexes. In fact, the lack of CP24 minor antenna prevents from the association of the major LHCII M-trimer into the supercomplex (Kovács et al., 2006) which leads to much greater packing of the particles forming the array-like organisation in the grana membranes.

### **6.2.2. Analysis of PSII particle sizes**

Some previous observations made after examination of the freeze-fracture electron micrographs of plastid membranes from plants grown under intermediate light suggested that the particles on EFs fracture faces do not consist only of PSII dimeric cores but a part of the attached light-harvesting antenna complexes may also fracture with the EFs face under these conditions (Armond et al., 1977). Now equipped with a range of different light-harvesting antenna mutants I decided to verify this suggestion by analysing quantitatively the sizes of EFs particles and find out which, if any, of the LHC complexes remain associated with the PSII core after freeze-fracture treatment. The average size of EFs particles in the wild-type plants is about  $175 \text{ nm}^2$  (Figure 6.5) which is larger than the size of a PSII core dimer ( $145 \text{ nm}^2$ ) (Hankamer et al., 1997). On the other hand, a ‘standard’  $C_2S_2$  PSII-LHCII supercomplex has size of about  $310 \text{ nm}^2$  (Boekema et al., 1995) – far larger than the calculated size of the EFs particles. A PSII core dimer plus 2-3 minor antenna proteins with a size of about  $220 \text{ nm}^2$  (Boekema et al., 1995) would be the most consistent with the calculated sizes. Indeed, the average sizes in all investigated minor antenna mutants confirmed this view. The average sizes of EFs particles

decreased to about 120 – 130 nm<sup>2</sup> after removal of either CP29, CP26 or CP24 proteins (Figure 6.5). Thus, the reduction in size would be enough to fit at least 2-3 minor antenna of approximate individual size of 7 nm<sup>2</sup> at each tip of PSII core dimer (Caffari et al., 2009). This is a strong evidence confirming that minor antenna complexes are strongly associated with the PSII core dimers and are integral components of the particles present in EFs fracture faces.

An interesting observation was made for the EFs particle sizes in the major antenna mutants. While the average sizes in the *koLhcb3* samples were identical to the wild-type supporting the view that the EFs particles do not contain major LHCII associated with a PSII core dimer, the antisense mutant of major LHCII (*asLhcb2*) exhibited a similar decrease in the size (from 178 nm<sup>2</sup> in the wild-type to about 145 nm<sup>2</sup> in the *asLhcb2* samples) as observed in the minor antenna chloroplasts (Figure 6.6). This is perhaps the consequence of replacement of the major LHCII antenna with the CP26 minor complexes which are able to form trimers and in this way preserve the native macro-molecular organisation of photosynthetic complexes even when the major LHCII are missing (Ruban et al., 2003). Under these conditions it seems likely that CP26 minor antenna loses its strong association with a PSII core and fractures in the protoplasmic PFs face as major trimeric LHCII usually do.

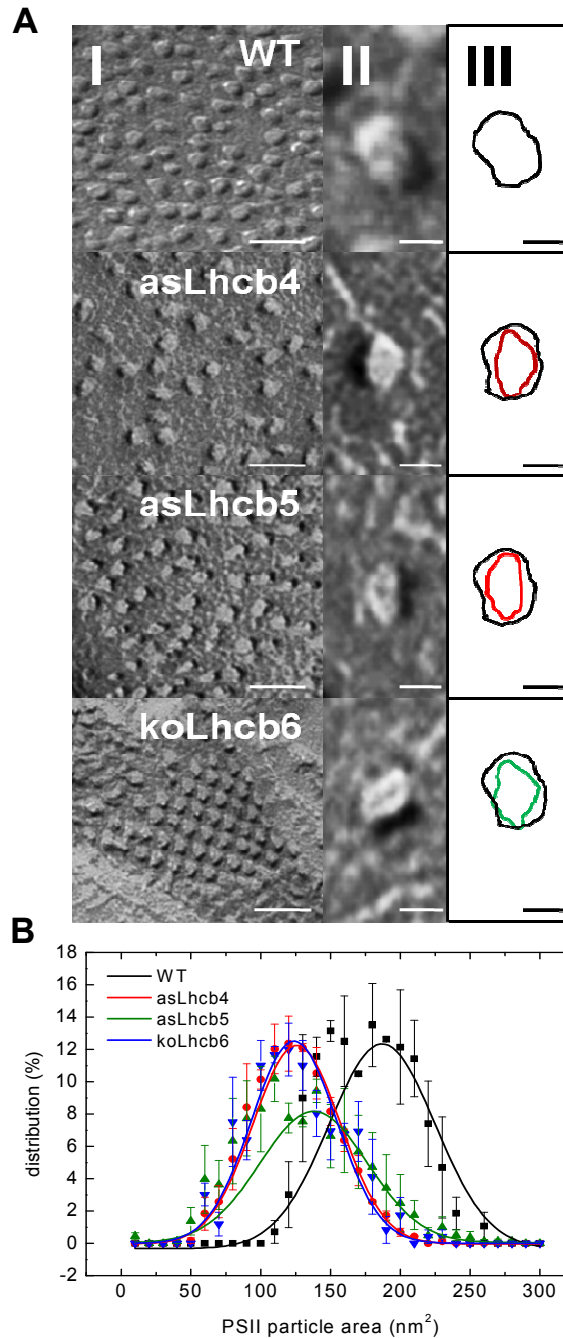


Figure 6.5. Analysis of EFs particle sizes in minor antenna mutants of *Arabidopsis*. (A, Panel I). Electron micrographs showing the particles on EFs fracture faces. Scale bars = 50 nm. (A, Panel II). Enlarged electron micrographs of representative individual EFs particles with the sizes close to the mean values calculated for the whole population as in graph B. Scale bars = 10 nm (A, Panel III). The contour images of the particles from panel II in the mutant samples were superimposed on the particle characteristic for the wild-type sample. Note that in all three mutants the average particles were smaller when compared to the wild-type. (B). Graph showing distribution of the calculated sizes of PSII particles in the wild-type and minor antenna mutants. Note a clear decrease in the average particle sizes in all investigated mutants. Each data point represents a mean value ( $\pm$  SE) out of all EFs fracture faces analysed ( $n = 10 - 15$ ).

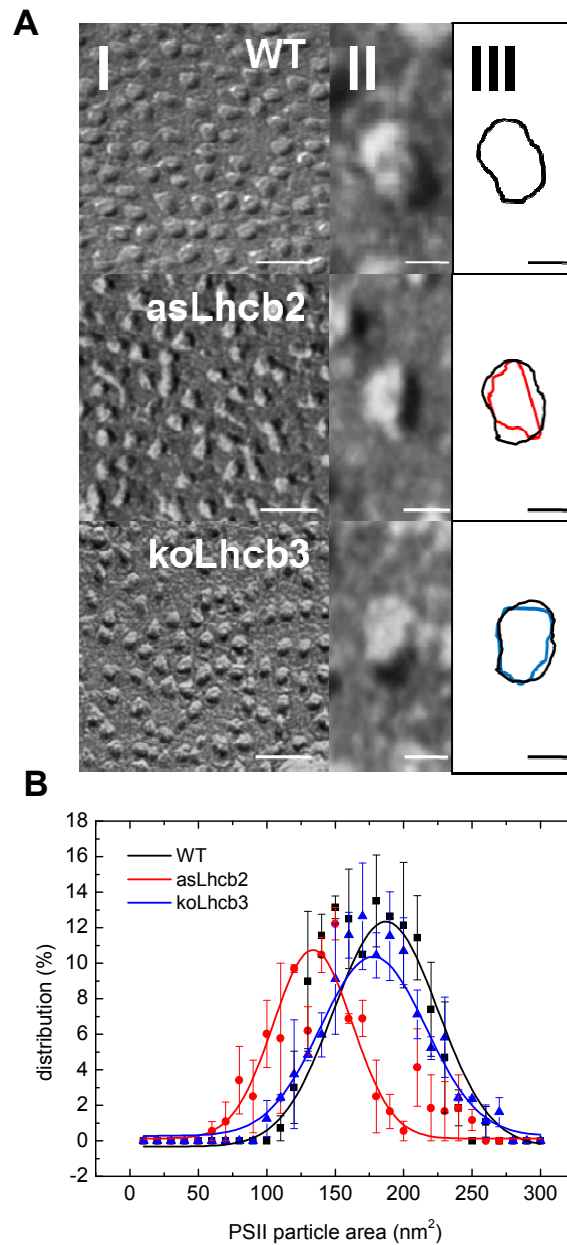


Figure 6.6. Analysis of EFs particle sizes in major antenna mutants of *Arabidopsis*. The figure is presented in the identical way as the Figure 6.5. Note the same average sizes of EFs particles in the *koLhcb3* mutant and the reduced mean sizes in the *asLhcb2* sample.

Analysis of the EFs particle sizes was also performed on the electron micrographs obtained from the *chl* mutant of *Arabidopsis*. The data revealed that the average sizes of the particles were slightly smaller in the mutant than in the wild-type

decreasing from about 175 nm<sup>2</sup> to approximately 140 nm<sup>2</sup>, respectively (Figure 6.7). This again suggests that the mutant plants which are not forming stable major LHCII antenna might detach a part of monomeric LHC proteins, mainly CP26 (Havaux et al., 2007; Dall'Osto et al., 2010), from a PSII core resulting in the observed reduction in the average PSII particle size.

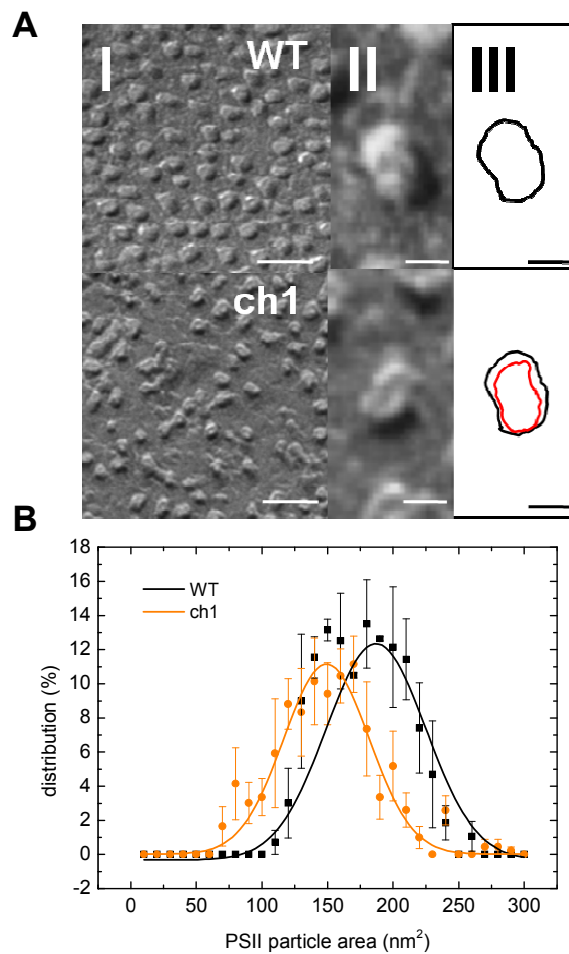


Figure 6.7. Analysis of EFs particle sizes in the *chl* mutant of *Arabidopsis*. The figure is presented in the identical way as the Figure 6.5. Note a shift towards smaller sizes of the particles in the mutant plants.

### **6.2.3. Distribution of PSII particles in the grana membranes: clustering and density**

Given the fact that some of the light-harvesting mutants change significantly the macromolecular organisation of photosynthetic complexes in the grana membranes (e.g. by changing the amount of PSII arrays present in the membrane and their structural features) (Figures 6.1 – 6.4) it is clear that the macromolecular crowding in the investigated mutants would be also substantially changed. In fact, this turned out to be the case as the quantitative measurements of the PSII clustering, density and nearest-neighbour distances revealed (Figures 6.8 – 6.10, Table 11).

In the major antenna mutants there seemed to be a slight tendency for more clustering of PSII particles in the *asLhcb2* samples while the opposite trend was observed in the case of *koLhcb3* chloroplasts (Figure 6.8.A, Table 11). This effect, although less pronounced, was also seen in the measurements of the PSII nearest-neighbour distances and PSII density (Figure 6.8.B, Table 11). These slight differences are in line with the previous observations revealing small alterations in the structural features of the PSII arrays formed in the mutant plants (Figure 6.4).

In the minor antenna mutants the most significant changes in macromolecular crowding of PSII particles was observed in the *asLhcb4* and *koLhcb6* samples. The former plants exhibited a noticeable decrease in PSII clustering and density (Figure 6.9.A, Table 11) which was reflected on a slight increase in the mean nearest neighbour distances between the particles (Figure 6.9.B, Table 11). This is fully in agreement with the fact that the loss of CP29 minor antenna prevents the formation of stable PSII-LHCII supercomplexes (Yakushevskaya et al., 2003)



and leads to disruption in the organisation of particles into semi-crystalline arrays (Figure 6.2).

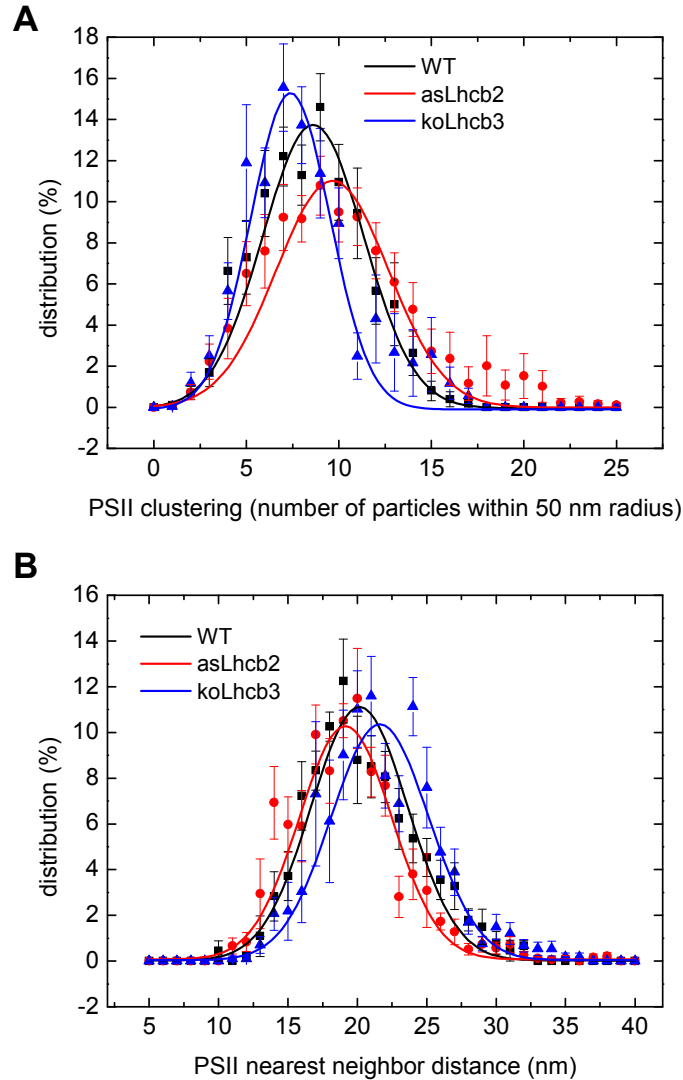


Figure 6.8. Analysis of PSII particle macromolecular crowding in the grana membranes of major light-harvesting antenna mutants of *Arabidopsis*. (A). Distribution of PSII clustering measurements (expressed as the number of particles within 50 nm radius of a given particle) in the wild-type (black line), *asLhcb2* mutant (red line) and *koLhcb3* mutant (blue line). (B). Distribution of PSII nearest neighbour distances in the wild-type (black line), *asLhcb2* mutant (red line) and *koLhcb3* mutant (blue line). Each data point represents a mean value ( $\pm$  SE) calculated out of all EFs fracture faces analysed ( $n = 10 - 15$ ).

The opposite tendency was detected in the case of the *koLhcb6* samples. There was a significant increase in the PSII clustering and density (Figure 6.9.A, Table 11) together with a shortening of the nearest neighbour distances between the particles (Figure 6.9.B, Table 11). This is reflected on the amount of PSII arrays and their structural features characteristic for these mutants (Figures 6.2 and 6.4).

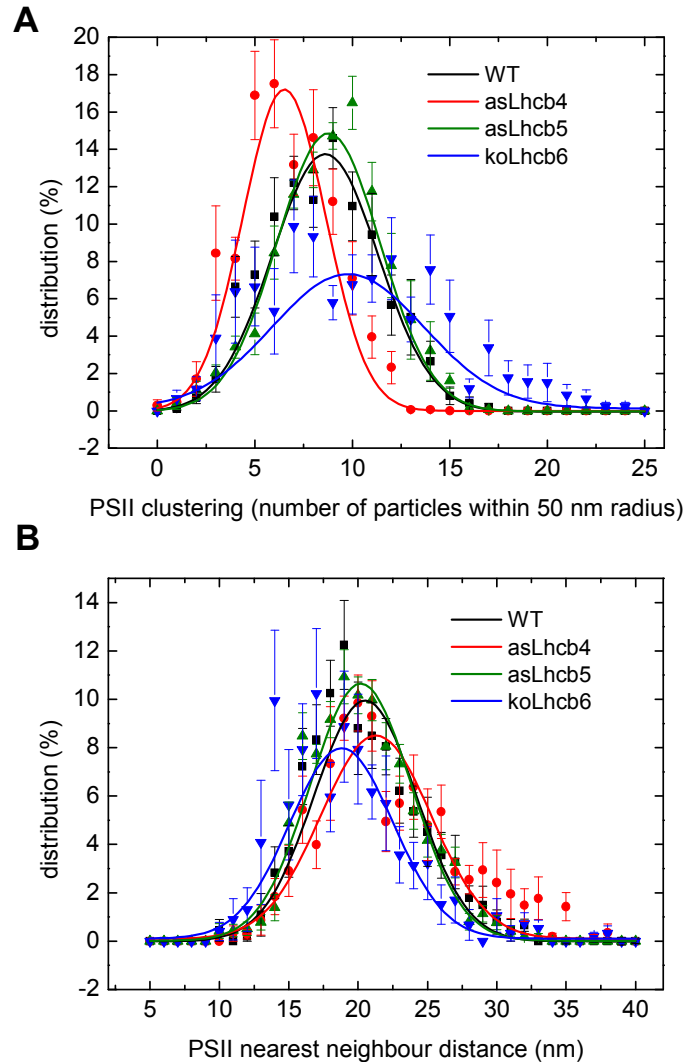


Figure 6.9. Analysis of PSII particle macromolecular crowding in the grana membranes of minor light harvesting mutants of *Arabidopsis*. (A). Distribution of PSII clustering measurements (expressed as the number of particles within 50 nm radius of a given particle) in the wild-type (black line), *asLhcb4* (red line) *asLhcb5* (green line) and *koLhcb3* mutant (blue line). (B). Distribution of PSII nearest neighbour distances in the wild-type (black line), *asLhcb4* (red line) *asLhcb5* (green line) and *koLhcb3* mutant (blue line). Each data point represents a mean value ( $\pm$  SE) calculated out of all EFs fracture faces analysed ( $n = 10 - 15$ )

The *asLhcb5* samples showed no such dramatic changes as the *koLhcb6* mutant but a slight tendency of more clustering and a decreased nearest neighbour distances between the PSII particles could still be observed (Figure 6.9, Table 11). This was particularly the case in the measurements of PSII density (per  $\mu\text{m}^2$  of the membrane) which was noticeably increased when compared to the wild type plants (Table 11). Again, this is in agreement with the fact that the CP26-depleted plants form more of the PSII semi-crystalline arrays with their altered structural features leading to the particles being more packed together (Figures 6.2 and 6.4).

The quantitative measurements of the PSII particle macromolecular crowding was also performed on the freeze-fracture electron micrographs from the *chl* mutant. Since this mutant possesses only PSII complexes and some of the monomeric LHC antenna (mainly CP26) (Havaux et al., 2007; Dall'Osto et al., 2010) it is clear that under these conditions the macromolecular crowding would be somehow affected (as already seen in the Figures 6.3 and 6.7.A). Indeed, there was a slight tendency of shortening of PSII nearest-neighbour distances in the mutants when compared to the wild-type samples (Figure 6.10.B, Table 11). However, the measurements of PSII density and clustering did not reveal significant changes to the wild-type chloroplasts (Figure 6.10.A, Table 11). This suggests that although on average the particles become closer together but their overall density remains unchanged which can be explained given the fact that the mutant plants presumably possess bigger grana membranes and some regions of the grana could be free of any photosystems as seen for example in Figure 6.3.B.

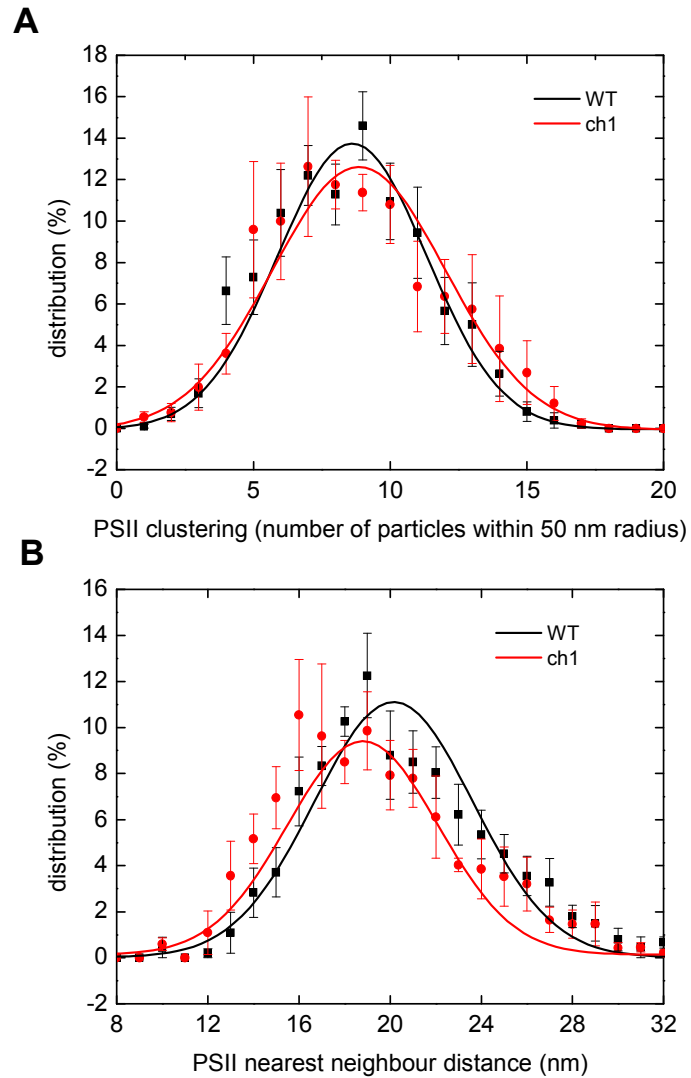


Figure 6.10. Analysis of PSII particle macromolecular crowding in the grana membranes of the *chl* mutant of *Arabidopsis*. (A). Distribution of PSII clustering measurements (expressed as the number of particles within 50 nm radius of a given particle) in the wild-type (black line) and *chl* (red line) mutant. (B). Distribution of PSII nearest neighbour distances in the wild-type (black line) and *chl* (red line) mutant. Each data point represents a mean value ( $\pm$  SE) calculated out of all EFs fracture faces analysed ( $n = 10 - 15$ ).

All quantitative measurements performed on PSII particles from freeze-fracture electron micrographs of different light-harvesting antenna mutants are summarised in Table 11.

**Table 11. Quantitative analysis of particles from EFs fracture faces from electron micrographs of wild-type and different light-harvesting antenna mutants of *Arabidopsis* chloroplasts in dark-adapted state.**

Data show mean values  $\pm$  SE. n = number of particles analysed. \* = statistically significant difference with respect to the dark-adapted wild-type sample using one-way ANOVA analysis followed by Dunnett contrast ( $P < 0.05$ ).

Sample	n	PSII nearest neighbour distance (nm)	PSII particle size (nm <sup>2</sup> )	PSII particle density (per $\mu\text{m}^2$ )	PSII clustering (number of particles within 50 nm radius)
Wild-type	1602	20.4 $\pm$ 0.12	178 $\pm$ 3.7	1120 $\pm$ 37.9	8.7 $\pm$ 0.09
<i>asLhcb2</i>	842	19.0 $\pm$ 0.14*	146 $\pm$ 4.2*	1238 $\pm$ 40*	9.4 $\pm$ 0.12*
<i>koLhcb3</i>	872	21.1 $\pm$ 0.14	168 $\pm$ 3.5*	1097 $\pm$ 45.2	8.3 $\pm$ 0.11
<i>asLhcb4</i>	828	21.2 $\pm$ 0.20	119 $\pm$ 1.2*	1023 $\pm$ 32.6*	7.0 $\pm$ 0.08*
<i>asLhcb5</i>	895	19.3 $\pm$ 0.21*	127 $\pm$ 1.6*	1298 $\pm$ 36.4*	9.1 $\pm$ 0.14
<i>koLhcb6</i>	949	17.8 $\pm$ 0.26*	120 $\pm$ 2.2*	1655 $\pm$ 74.5*	11.0 $\pm$ 0.24*
<i>ch1</i>	832	18.9 $\pm$ 0.17*	138 $\pm$ 2.7*	1070 $\pm$ 38.7	9.0 $\pm$ 0.11

#### **6.2.4. Distribution of LHCII particles in the grana membranes: clustering, density and particle sizes**

Similarly to the analysis of PSII particles on the EFs fracture faces I performed the quantitative measurements of particle distribution in the complementary PFs faces containing LHCII antenna proteins in both major and minor LHC antenna-deficient mutants. Such analysis was not possible in the case of *chl1* mutant which, as mentioned already, produced hardly any particles in the PFs faces (Figure 6.3. White arrow) confirming the fact that inhibition of chlorophyll *b* synthesis prevents from the formation of stable LHCII complexes (Murray and Kohorn, 1991).

In the dark-adapted wild type samples the LHCII particles are distributed with the average nearest-neighbour distances of about 13 nm (Figure 6.11.H and Table 12). This measurement was significantly decreased in the *asLhcb2* mutant where the major trimeric LHCII are replaced mostly by the CP26 minor complexes (Ruban et al., 2003). This resulted in the particles being more clustered together (Figure 6.11.B, G-H and Table 12), similarly to the effect observed in the PSII particle analysis (Figure 6.8 and Table 11). However, in the *koLhcb3* chloroplasts there was a noticeable tendency for slightly reduced LHCII clustering when compared to the wild-type (Figures 6.11.C, G and Table 12). This was also reflected in the nearest-neighbour distance measurements, although this effect was much less pronounced (Figure 6.11.H and Table 12).

The analysis of PFs faces from minor antenna mutant plants revealed even more radical changes in the distribution of LHCII particles. In both *asLhcb5* and particularly *koLhcb6* mutant plants there was a considerable increase in the particle clustering confirmed by the shortening of nearest neighbour distances

(Figure 6.11.E-F, I-J, Table 12). This effect was not observed in the case of the *asLhcb4* mutant where the measurements were quite similar as in the wild-type plants (Figure 6.11.D, I-J, Table 12).

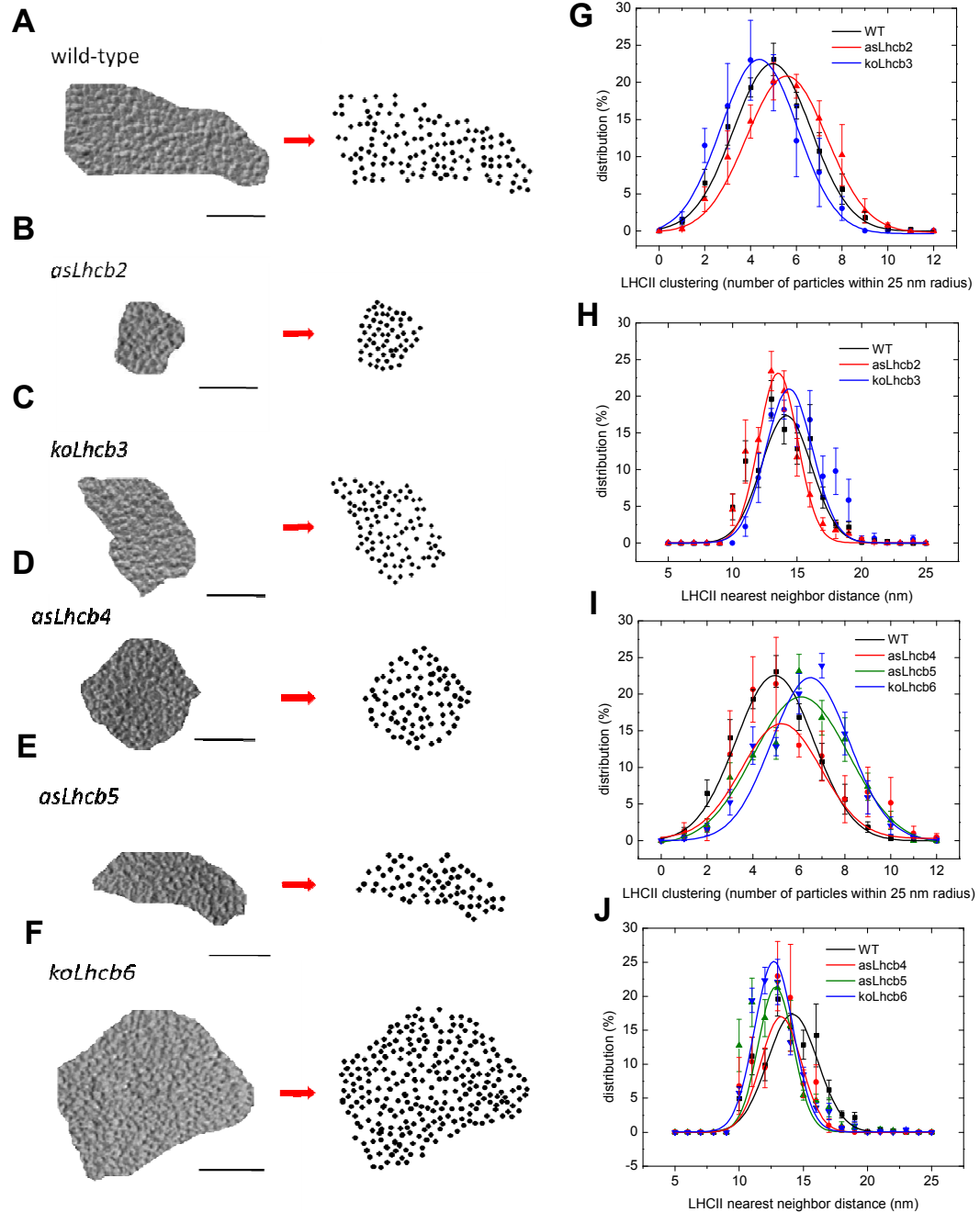


Figure 6.11. Analysis of LHCII particle distribution in the grana membranes of light-harvesting antenna mutants of *Arabidopsis*. (Panel A-F). Fragments of PFs fracture faces were cut out from the electron micrographs and the individual LHCII particles were picked manually in the ImagePro software to produce a mask for better visualisation of particle distribution. Scale bars = 100 nm. (G-H). Quantitative measurements of LHCII clustering (calculated as a number of particles within 25 nm radius of a given particle) and LHCII nearest-neighbour distances for wild-type (black line), *asLhcb2* (blue line) and *koLhcb3* mutants (red line), respectively. (I-J). Quantitative measurements of LHCII clustering (calculated as a number of particles within 25 nm radius of a given particle) and LHCII nearest-neighbour distances for wild-type (black line), *asLhcb4* (red line), *asLhcb5* (green line) and *koLhcb6* mutants (blue line), respectively. Each data point in graphs G-J represents a mean value ( $\pm$  SE) calculated out of all PFs fracture faces analysed ( $n = 7 - 10$ ).



An interesting observation was made in the analysis of LHCII particle sizes. In all investigated mutants the average sizes were close to 70 nm<sup>2</sup> which is similar to the mean size already measured in the wild-type LHCII particles (Table 12). This suggests strongly that even without the presence of specific antenna proteins the LHCII complexes retain the major trimeric type of organisation. This was especially the case in the *asLhcb2* mutant where the monomeric CP26 minor antenna together with the products of the *lhcb3* gene could compensate for the loss of major LHCII and form trimers under these specific conditions (as confirmed by Ruban et al., 2003).

**Table 12. Quantitative analysis of PFs fracture faces from electron micrographs of wild-type and different light-harvesting antenna mutants of *Arabidopsis* chloroplasts in dark-adapted state.**

Data show mean values  $\pm$  SE. n = number of particles analysed. \* = statistically significant difference with respect to the dark-adapted wild-type sample using one-way ANOVA analysis followed by Dunnett contrast ( $P < 0.05$ ).

Sample	n	LHCII nearest neighbour distance (nm)	LHCII particle size (nm <sup>2</sup> )	LHCII particle density (per $\mu\text{m}^2$ )	LHCII clustering (number of particles within 25 nm radius)
Wild-type	643	13.4 $\pm$ 0.09	70 $\pm$ 1.3	3197 $\pm$ 69.4	4.9 $\pm$ 0.07
<i>asLhcb2</i>	546	12.3 $\pm$ 0.08*	67 $\pm$ 2.4	3348 $\pm$ 103.0*	5.7 $\pm$ 0.07*
<i>koLhcb3</i>	376	14.2 $\pm$ 0.20*	68 $\pm$ 2.2	3057 $\pm$ 104.2*	4.4 $\pm$ 0.12
<i>asLhcb4</i>	430	12.8 $\pm$ 0.10	66 $\pm$ 3.3	3256 $\pm$ 78.4	5.4 $\pm$ 0.21
<i>asLhcb5</i>	386	12.1 $\pm$ 0.20*	69 $\pm$ 2.6	3389 $\pm$ 98.7*	6.1 $\pm$ 0.10*
<i>koLhcb6</i>	537	12.3 $\pm$ 0.08*	62 $\pm$ 4.0	3407 $\pm$ 48.6*	6.3 $\pm$ 0.08*

### 6.3. Mobility of chlorophyll-proteins in light-harvesting antenna mutants of *Arabidopsis thaliana*

Identical FRAP experiments to the ones described previously (Chapters IV and V) were performed also on intact chloroplasts isolated from all investigated light-harvesting antenna mutant plants, including the *chl* samples. The data revealed that the loss of major antenna complexes resulted in a decrease of the calculated

mobile fractions only in the case of *asLhcb2* mutant where a reduction in mobility by ~25% was observed when compared to the wild-type chloroplasts (Figure 6.12.A). By contrast, the *koLhcb3* mutant exhibited the amount of mobile fraction that remained at the same level as found in the wild-type (Figure 6.12.A). The same effect was observed in the minor *asLhb4* mutant plants where no changes in the mobility of chlorophyll-proteins with respect to the wild-type could be detected (Figure 6.12.B). However, this was not the case in the other minor antenna mutants, namely *asLhcb5* and *koLhcb6* which showed a dramatic reduction in the amount of mobile fractions in comparison to the wild-type plants by ~30% and almost 40%, respectively (Figure 6.12.B). An interesting observation was made in the *chl1* mutant which exhibited a completely opposite effect and revealed a considerable increase in the mobility of chlorophyll-proteins by about 50% allowing for almost a quarter of the bleached chlorophyll fluorescence to recover (Figure 6.12.C).

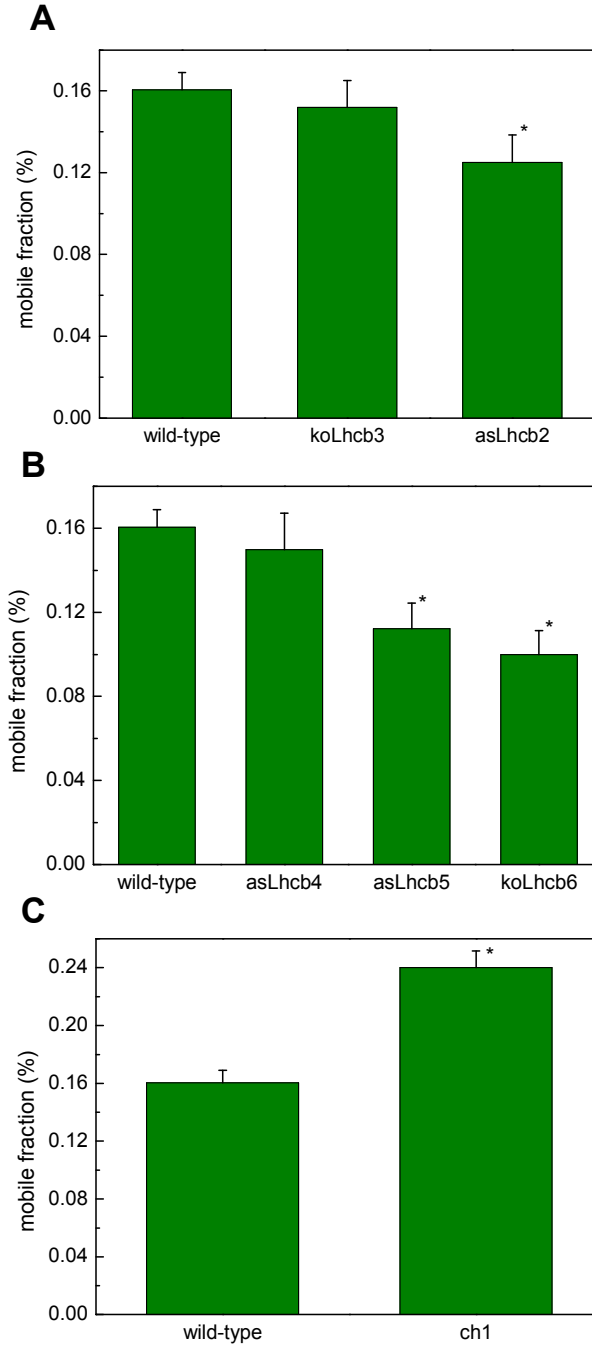


Figure 6.12. Mobility of chlorophyll proteins in intact chloroplasts isolated from different light-harvesting antenna mutants of *Arabidopsis*. The mobile fraction in the wild-type was compared to the mobile fractions in (A) major antenna mutants, (B) minor antenna mutants, and (C) *chl* mutant. Bars represent mean mobile values ( $\pm$  SE) calculated out of 10 independent experiments. \* = statistical difference with respect to the wild type as determined by one-way ANOVA followed by Dunnett contrast,  $p < 0.05$ .

#### **6.4. Correlation of protein mobility with macromolecular organisation of photosynthetic complexes in the grana membranes**

I noticed previously that the size of mobile fractions of chlorophyll-proteins as deduced from FRAP experiments could be directly correlated with the packing of the photosynthetic complexes in the grana membranes as determined from freeze-fracture electron micrographs (Chapters IV and V). To further validate this observation I decided to find out if such correlation genuinely exists in the light-harvesting antenna mutants where the macromolecular organisation of photosynthetic proteins is severely affected upon the loss of some antenna proteins (section 2) followed by the significant changes detected in the mobility of chlorophyll-proteins (section 3). Indeed, the correlation plots revealed a strong linear relationship which exists between these two measured parameters (Figure 6.13). Hence, this data support strongly the previous observations made on both spinach and *Arabidopsis* chloroplasts under different conditions (chapters IV and V) that the diffusion of photosynthetic complexes is dependent directly on the extent of their packing, changes in their distribution and a degree of macromolecular order which is present in the thylakoid membranes.

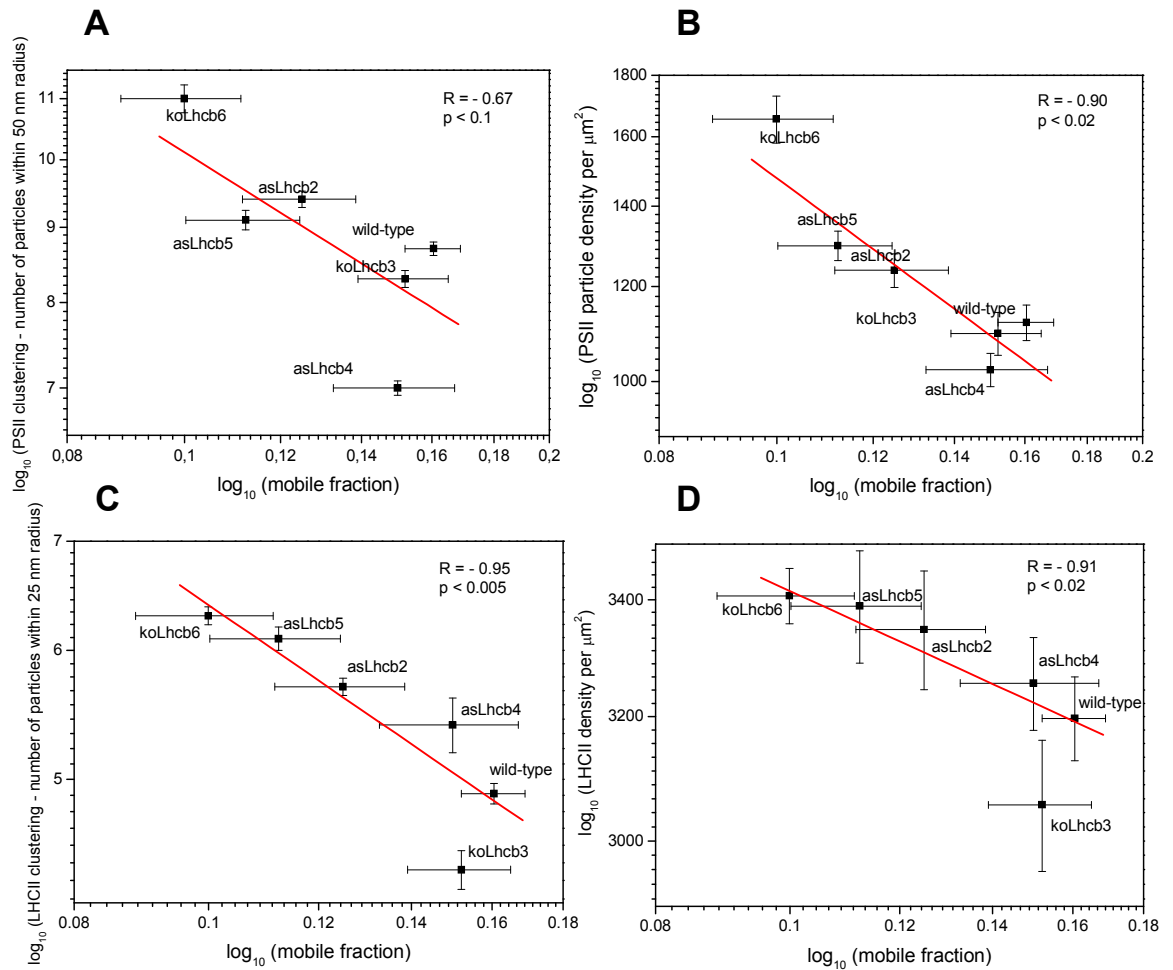


Figure 6.13. Relationships between the mobility of chlorophyll-proteins and the macromolecular crowding of PSII-LHCII supercomplexes in the grana membranes of different light-harvesting antenna mutants of *Arabidopsis*. (A-B). Linear correlations between the amount of mobile fractions and PSII clustering and density, respectively. (C-D). Linear correlations between the amount of mobile fractions and LHCII clustering and density, respectively. Each data point represents a mean value ( $\pm$  SE) as shown in Figure 6.12 and Tables 8-9. In each graph a linear regression was fitted to the data points and the Pearson correlation coefficient (R) was calculated with its statistical significance (p) as shown in the upper right corner of each graph. Note that the axes of the graphs were transformed into logarithmic scale.

## **6.5. Correlation of protein mobility with the amount of non-photochemical quenching (NPQ)**

As mentioned already in chapter V the NPQ phenomenon which evolved to protect plants from the damaging effects of too much light occurs in light-harvesting antenna proteins and involves the structural change of photosynthetic membranes (reflected in a decreased spacing between the thylakoid membranes in the grana and a greater packing of PSII-LHCII supercomplexes upon transition to NPQ state) (Chapter V, section 2). Since this chapter concentrates entirely on different light-harvesting antenna mutants it seems likely that the loss of particular antenna proteins will affect the amount of NPQ which is formed in these mutants. Indeed, the detailed analysis of light-harvesting antenna mutants confirmed that this is the case (Ruban et al., 2003; Yakushevskaya et al., 2003; Damkjaer et al., 2009). A correlation plot revealed that, similarly to the relationships found in spinach chloroplasts and *Arabidopsis* PsbS mutants (chapter V), the size of mobile fractions in different LHC mutant samples in dark-adapted state is directly related to the amount of NPQ which they form after light treatment (Figure 6.14). This finding confirms the previous suggestions that the ability to undergo structural changes characteristic for NPQ state (Chapter V) are dependent on the overall dynamic properties of photosynthetic complexes and their macromolecular organisation in the thylakoid membranes.

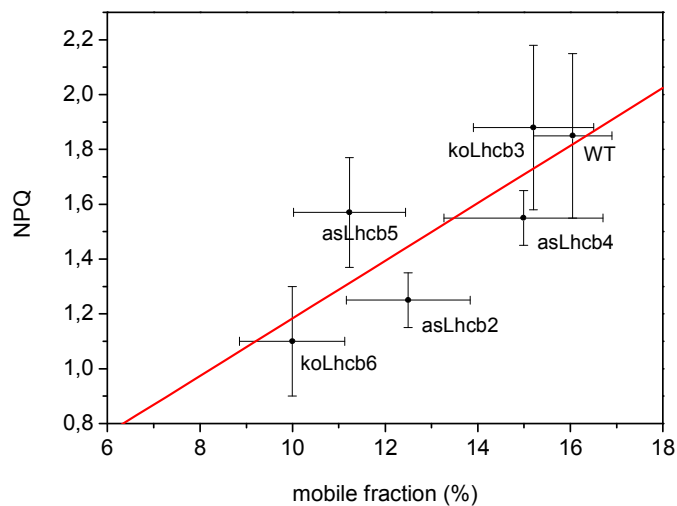


Figure 6.14. Correlation plot showing a linear relationship between the mobility of chlorophyll-proteins in dark-adapted state and the amount of NPQ which is formed after light treatment. Each data point represents a mean value ( $\pm$  SE) calculated as shown in Figure 6.12 with regards to mobile fractions. NPQ values (in triplicates) were measured by PAM fluorescence as described in Figure 5.1 and Table 5 (actinic light at  $350 \mu\text{mol photons m}^{-2} \text{s}^{-1}$  for 5 minutes followed by 5 min relaxation in dark). A linear regression was fitted to the data points and the Pearson correlation coefficient ( $R = 0.82$ ) with its statistical significance ( $p < 0.05$ ) were obtained.

## 6.6 Solubilisation and re-stacking of the thylakoid membranes in light-harvesting antenna mutants of *Arabidopsis*

Light-harvesting antenna proteins are known to participate in stabilising the granum ultrastructure, and to some extent in the cation-mediated stacking of the thylakoids (Barber, 1982; Dekker and Boekema, 2005). It has been suggested that this is achieved by the electrostatic interactions between different LHCII complexes in opposing membranes of the granal stacks, but the lateral organisation of the proteins is also important (Dekker and Boekema, 2005). To investigate the role and the influence of different light-harvesting antenna in controlling this process I decided to perform PAM fluorescence measurements on isolated chloroplasts to



monitor the kinetics of solubilisation and re-stacking of the thylakoid membranes in the LHC mutant plants of *Arabidopsis*.

It has been found previously that the addition of a mild detergent e.g.  $\beta$ -dodecyl maltoside ( $\beta$ -DM) to the chloroplast suspension causes solubilisation of the thylakoid membranes and dissociation of chlorophyll-binding proteins from each other without release of chlorophyll from their protein moiety (Dall'Osto et al., 2005). This can be monitored by PAM fluorescence measurements as shown in Figure 6.15.A. For these experiments the chloroplasts of different light-harvesting antenna mutants were isolated in the presence of  $MgCl_2$  to allow stacking of the thylakoid membranes. This was confirmed by the high  $F_v/F_m$  values which were close to 0.8 indicating the maximum photochemical efficiency of PSII (Table 13). However, the minor antenna mutants exhibited a slight reduction in the  $F_v/F_m$  values which is in agreement with the findings reported e.g. by Andersson et al. (2001) and Kovács et al. (2006). As predicted, this was also seen in the *chl* mutant (Table 13) given its inability to synthesise chlorophyll *b* and form stable LHClI antenna (Murray and Kohorn, 1991). Prior to illumination 10  $\mu$ M DCMU was added to the chloroplast suspension to inhibit electron transport and prevent from the occurrence of photochemical quenching (Figure 6.15.A). Moreover, the low actinic light intensity used during illumination period ( $80 \mu\text{mol photons m}^{-2} \text{s}^{-1}$ ) ensured that no significant non-photochemical quenching was formed under these conditions. As a result, the fluorescence level in the light was not changed until 0.1%  $\beta$ -DM was added to the chloroplast suspension (Figure 6.15.A). This caused a rapid increase in the fluorescence level which reached its maximum within a few minutes resulting from the disruption of protein-protein and lipid-protein interactions in the membrane (Figure 6.15.A).

Similar PAM fluorescence experiments were also performed to monitor the dynamics of grana stacking in the thylakoid membranes of LHC mutant plants. In this case, the chloroplasts were isolated in Mg-free buffers (see Methods for details) to allow unstacking of the grana. This was confirmed by a great reduction in the  $F_v/F_m$  values when compared to the stacked thylakoids (Table 13). The addition of 5 mM  $MgCl_2$  resulted in the fast restoration of the fluorescence level indicating the restacking of the grana membranes (Figure 6.15.B). In the presence of this saturating amount of  $MgCl_2$  the fluorescence level recovered almost completely to the level present in the stacked membranes in the wild-type samples (Figure 6.15.B, Table 13).

Figure 6.15.C-D shows the kinetic growths of fluorescence signal after the addition of  $\beta$ -DM or  $MgCl_2$  to the chloroplast suspension in different light-harvesting antenna mutants, respectively. The results revealed that within 6 minutes the amount of thylakoid membranes solubilised in all investigated mutants was significantly higher than in the wild-type (as judged from the maximum fluorescence level reached after the addition of detergent to the chloroplast suspension) (Figure 6.15.C, Table 13). This was particularly visible in the *asLhcb2* and *chl1* mutants where this amount was almost twice as high as in the wild-type chloroplasts (Figure 6.15.C, Table 13). Among the minor antenna mutants the greatest amount of solubilised membranes was observed in the *asLhcb4* samples while there was almost no difference with regard to the wild-type in the *koLhcb6* chloroplasts (Figure 6.15.C, Table 13). The *koLhcb3* and *asLhcb5* mutants showed the same amount of solubilised membranes which was only slightly higher than in the wild-type (Figure 6.15.C, Table 13).

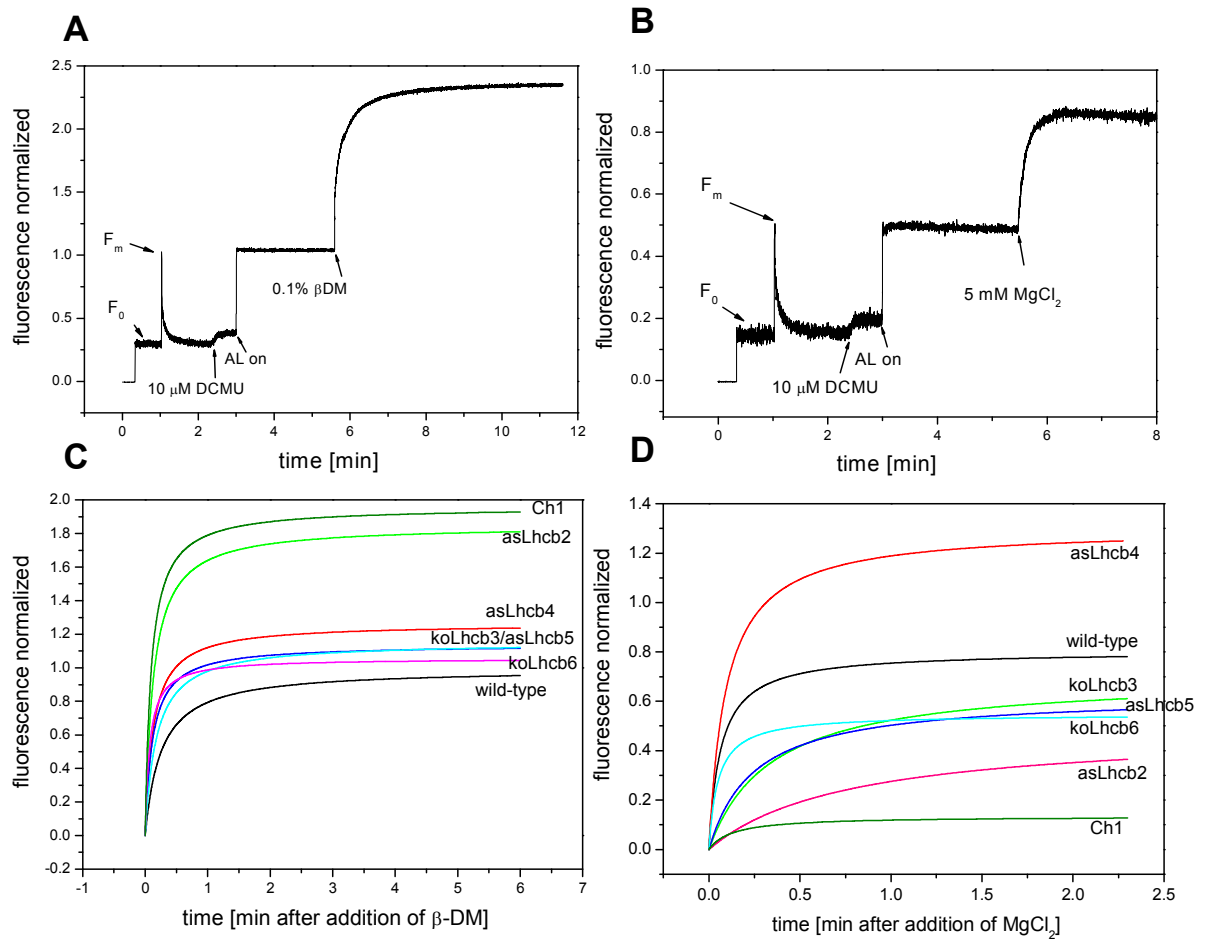


Figure 6.15. Kinetics of solubilisation and re-stacking of the thylakoid membranes of light-harvesting antenna mutants determined by PAM fluorescence measurements. **(A and B)**. PAM fluorescence traces for solubilisation and re-stacking experiments, respectively. For description of the traces see text. Note a rapid increase of fluorescence signal upon addition of  $\beta$ -DM and  $Mg^{2+}$  as indicated by arrows. Fluorescence signal in graphs A-B was normalised to the  $F_m$  values obtained for the stacked chloroplasts (as in graph A). **(C and D)**. Kinetic growth of fluorescence signal after the addition of  $\beta$ -DM and  $Mg^{2+}$  to the chloroplast suspension in different light-harvesting antenna mutants (chlorophyll concentration = 10  $\mu$ g/ml), respectively. Experimental data were fitted to the hyperbolic growth curves and averaged ( $n = 3-4$ ). Note that the timescales were normalised to the point where  $\beta$ -DM or  $MgCl_2$  were added to the chloroplast suspension.

These observations were further confirmed in the kinetic parameters that were obtained during the solubilisation experiments. In the wild-type samples the average time required for the increase in fluorescence signal by 50% after the addition of detergent was  $\sim 16$  seconds (Figure 6.16.A). This was reduced by almost a half in

both major antenna mutants suggesting that the mutations in the LHCII trimeric proteins loosen the protein-protein and lipid-protein interactions resulting in a much faster disassembly of chlorophyll-proteins during solubilisation. This was also the case in the minor antenna mutants where the half-time of solubilisation decreased significantly when compared to the wild-type thylakoids with the fastest half-time of about 4 seconds observed in the *koLhcb6* plants (Figure 6.16.B). A similar value was also obtained in the solubilisation of the thylakoid membranes of *chl* mutant (Figure 6.16.C).

The re-stacking experiments revealed also considerable differences between different light-harvesting antenna mutants reflected in the level of fluorescence signal recovery after the addition of  $Mg^{2+}$  to the chloroplast suspension. The major antenna mutants both showed a reduction in the amount of re-stacked thylakoids when compared to the wild-type (Figure 6.15.D, Table 13). This was particularly observed in the *asLhcb2* mutant which exhibited a decrease in the fluorescence level upon re-stacking by nearly 40% in comparison to the trace recorded for the wild-type (Figure 6.15.D, Table 13). The kinetic parameters calculated for the re-stacking process confirmed these tendencies. While in the wild-type samples the average time required for the increase in fluorescence signal by 50% after the addition of  $MgCl_2$  was ~4 seconds (Figure 6.16.D) this time was about 5 times slower in the *koLhcb3* mutant and over 10 times slower in the *asLhcb2* chloroplasts (Figure 6.16.D). These observations confirm the previous suggestions that major trimeric LHCII antenna play an important role in controlling the stacking of the thylakoid membranes in green plants (Dekker and Boekema, 2005).

**Table 13. Fluorescence and kinetics parameters of solubilization and re-stacking of the thylakoid membranes from light-harvesting antenna mutants of *Arabidopsis*.**

Abbreviations:  $F_v$  – variable fluorescence ( $F_m - F_o$ ),  $F_{max_{sol}}$  – maximum fluorescence level reached after solubilisation with 0.1%  $\beta$ -DM (as in Figure 6.15.A),  $F_{max_{res}}$  – maximum fluorescence level reached after restacking upon addition of 5 mM  $MgCl_2$  (as in Figure 6.15.B), Data represent mean values ( $\pm$  SE) out of 3-4 experiments. \* = statistical confidence levels significantly different with respect to wild-type sample,  $P < 0.05$ , using an ANOVA analysis followed by Dunnett contrast.

Sample	Chl a/b	$F_v/F_m$ stacked	$F_{max_{sol}}$	$F_v/F_m$ unstacked	$F_{max_{res}}$
<b>Wild-type</b>	3.65 $\pm$ 0.311	0.85 $\pm$ 0.017	1.00 $\pm$ 0.047	0.63 $\pm$ 0.03	0.80 $\pm$ 0.037
<i>asLhcb2</i>	4.53 $\pm$ 0.267	0.87 $\pm$ 0.021	1.85 $\pm$ 0.096*	0.68 $\pm$ 0.02	0.49 $\pm$ 0.027*
<i>koLhcb3</i>	3.62 $\pm$ 0.552	0.84 $\pm$ 0.012	1.14 $\pm$ 0.052	0.68 $\pm$ 0.03	0.70 $\pm$ 0.020
<i>asLhcb4</i>	3.4 $\pm$ 0.563	0.74 $\pm$ 0.018*	1.26 $\pm$ 0.226*	0.60 $\pm$ 0.06	1.30 $\pm$ 0.207*
<i>asLhcb5</i>	3.48 $\pm$ 0.049	0.80 $\pm$ 0.021	1.16 $\pm$ 0.018	0.58 $\pm$ 0.04	0.63 $\pm$ 0.072*
<i>koLhcb6</i>	3.67 $\pm$ 0.245	0.74 $\pm$ 0.016*	1.06 $\pm$ 0.042	0.62 $\pm$ 0.03	0.55 $\pm$ 0.080*
<i>chl1</i>	22.27 $\pm$ 5.51	0.74 $\pm$ 0.040*	1.96 $\pm$ 0.045*	0.63 $\pm$ 0.05	0.13 $\pm$ 0.033*

An interesting observation was made in the re-stacking experiments of the minor antenna mutants. Both *asLhcb5* and *koLhcb6* samples exhibited a significant reduction in the amount of re-stacked membranes after  $Mg^{2+}$  cations were added to the chloroplast suspension (Figure 6.15.D, Table 13). However, the re-stacking of the thylakoid membranes in the *asLhcb4* mutant was much greater when compared to the

wild-type (Figure 6.15.D, Table 13). The kinetic parameters of the re-stacking process in minor mutants did not reveal significant differences with respect to the wild-type, except for the *asLhcb5* chloroplasts which showed almost a fourfold slower time needed for the fluorescence level to increase by 50% upon the MgCl<sub>2</sub> addition (Figure 6.16.E). These results suggest therefore that the minor antenna complexes might also participate in the process of cation-mediated stacking of the thylakoid membranes.

The most extreme case regarding the amount of the re-stacked membranes was detected in the *chl* mutant which showed only a slight increase in the fluorescence signal after the addition of MgCl<sub>2</sub> (Figure 6.15.D, Table 13). Moreover, the half-time required for this increase was about two times slower when compared to the wild-type (Figure 6.16.F). Nevertheless, this observation confirms the previous suggestion that even without the presence of stable LHCII antenna the stacking of the thylakoid membranes can still occur (Murray and Kohorn, 1991).

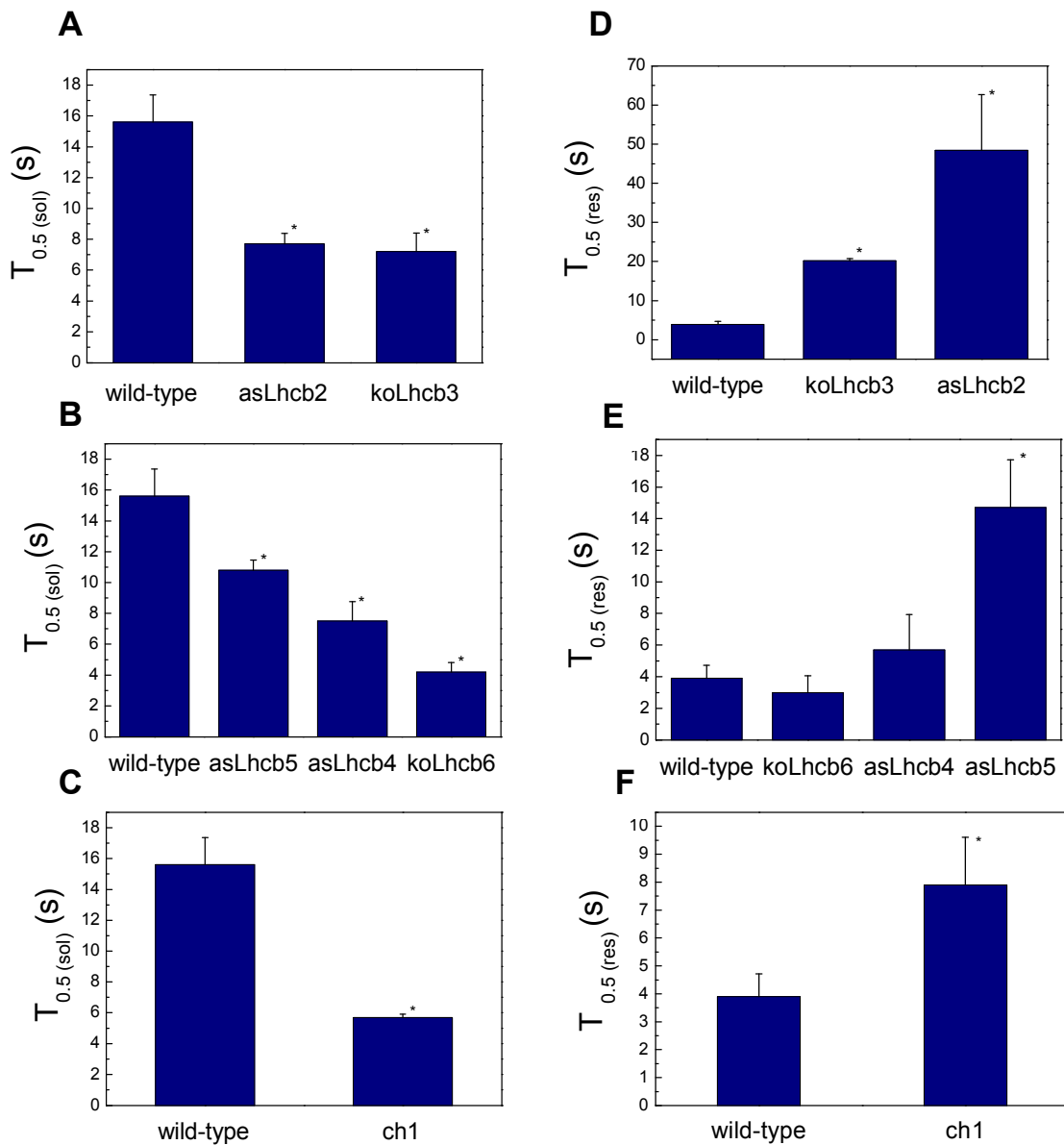


Figure 6.16. Kinetic parameters of solubilisation and re-stacking of the thylakoid membranes from light-harvesting antenna mutants of *Arabidopsis* calculated from PAM fluorescence measurements as shown in Figure 6.15.C-D. (A-C). Comparison of the average times required for the increase in fluorescence level by 50% during solubilisation of the thylakoid membranes in the major, minor and the *chl* light harvesting antenna mutants, respectively. (D-F). Comparison of the average times required for the increase in fluorescence level by 50% during re-stacking of the thylakoid membranes in the major, minor and the *chl* light harvesting antenna mutants, respectively. Bars represent mean values ( $\pm$  SE) calculated out of 3-4 experiments. Differences statistically significant with respect to the wild-type were indicated by asterisks and determined by one-way ANOVA with Dunnett contrast,  $p < 0.05$ .

# **Chapter VII**

**Probing the dynamics of  
photosynthetic complexes in  
intact leaves**



## 7.1. Introduction

The previous chapters of this thesis describe the first application of FRAP technique to study the mobility of chlorophyll-proteins in a system which is close to the situation *in vivo*: the isolated intact chloroplasts. On one hand this approach has a great advantage over the previous method which used only the isolated grana membranes (Kirchhoff et al., 2008). This is because it allows to probe, for the first time, the dynamic properties of photosynthetic complexes in the fully intact thylakoid membrane network where individual grana membranes are interconnected via stroma lamellae regions. On the other hand, it has still its own drawbacks. Firstly, isolation of chloroplasts from their native environment as found in the plant cell might affect their physiological properties. Secondly, isolated chloroplasts have to be stained with the artificial lipophilic dye (BODIPY FL C<sub>12</sub>) in order to select the organelles possessing their unbroken envelope membrane and to ensure that FRAP measurements are performed on truly intact systems (see Figure 3.4). Thirdly, isolated chloroplasts need to be immobilised on a polylysine support prior to FRAP experiments (see Methods for details) to ensure that the observed changes in fluorescence recovery do not result from the sample movements as a whole. Lastly, FRAP measurements need to be done always on freshly isolated chloroplasts which, in addition, cannot be examined under a confocal microscope for longer than 2-3 hours to avoid the loss of their intactness over time.

To eliminate all these difficulties I decided to go one step forward and try out the best possible system for probing the mobility of photosynthetic complexes in intact thylakoid membranes: an intact leaf. It was made possible using a new, highly improved confocal microscope with high-resolution confocal optics and a long-

working objective which could penetrate deep into a leaf tissue (see Methods for details). This chapter presents some potential applications for this approach which can be further developed to address different important aspects of the dynamics of photosynthetic protein complexes (as discussed in Chapter IX).

## **7.2. Visualisation of chloroplasts in intact leaves**

Plant cells contain a number of individual chloroplasts which maintain all together the optimal photosynthetic efficiency under specific environmental conditions. They are usually localised along the cell wall and have an elongated shape, although it can vary in different cell types and different plant species (Figure 7.1.A). The great abundance of chloroplasts inside the cells as well as the number of naturally fluorescent chlorophyll-containing proteins present in the thylakoid membranes makes it fairly straightforward for their visualisation under a confocal microscope. However, while it was quite difficult to distinguish between the individual grana in the isolated chloroplasts (see e.g. Figures 3.5 and 4.2) the confocal images from intact leaves allowed for visualisation of these regions with a much greater resolution, even without a need for image deconvolution (Figure 7.1.B). This is a consequence of a better optics of the microscope that was used for imaging making it extremely interesting to perform FRAP experiments which allow to probe the exchange of chlorophyll-proteins between individual grana membranes more accurately, and at the same time in a completely *in vivo* situation.

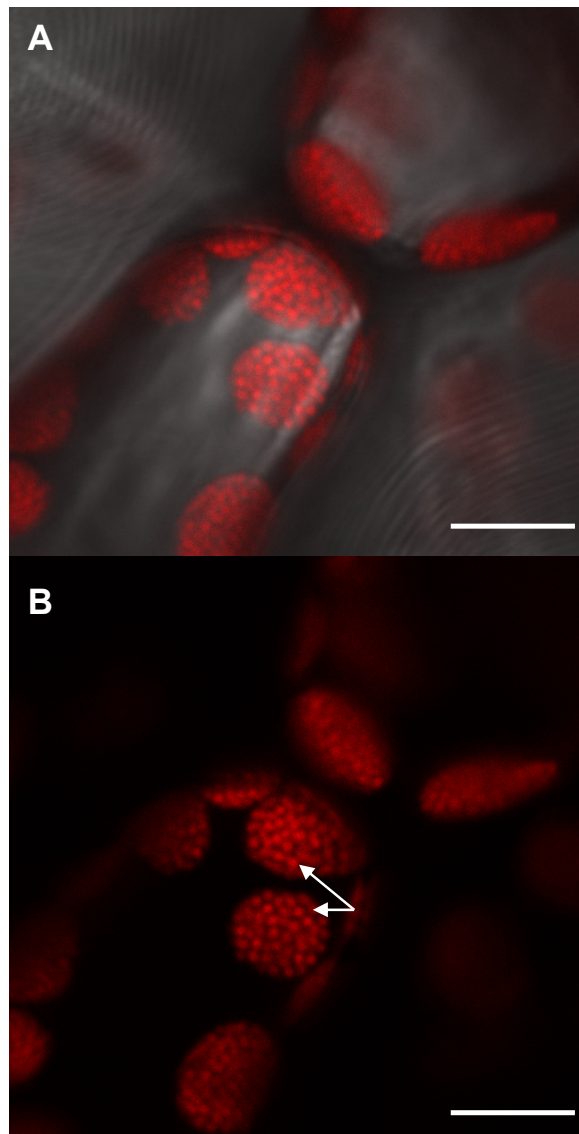


Figure 7.1. Visualisation of chloroplasts in mesophyll cells of intact spinach leaf under Leica SP5 confocal microscope. (A). Confocal image (red autofluorescence of chlorophyll-containing chloroplasts) was overlaid with a bright field image of the same region showing the localisation of chloroplasts within the cells. (B). Confocal image (chlorophyll channel only) showing the chloroplasts inside the cells with individual grana regions (white arrows) clearly distinguished. The image was averaged out of 6 scans. Scale bars = 7.5  $\mu\text{m}$

## **7.3. Mobility of chlorophyll-proteins in grana membranes of intact leaves chloroplasts.**

### **7.3.1. FRAP measurements on chloroplasts in different higher plant species**

The calculated mobile fractions of chlorophyll-proteins in dark-adapted wild-type spinach and *Arabidopsis* isolated intact chloroplasts were ~13% and ~16%, respectively (Table 1 and Figure 4.4). Here I decided to repeat these measurements but instead of using the isolated chloroplasts I performed FRAP experiments on the intact leaves of these two higher plant species (Figure 7.2). The experimental idea was the same as shown already for the FRAP series in isolated chloroplasts (see e.g. Figure 4.2.) and consisted of the following steps: (1) recording a prebleach image, (2) photobleaching irreversibly a region of the chloroplast that corresponds to a few grana, and (3) recording a series of post-bleach images to observe any fluorescence recovery in the bleached zone. However, given the fact that the last step required a timescale of at least a few minutes an additional treatment of intact leaves needed to be performed prior to FRAP measurements (see Methods for details). This was to impede the movements of chloroplasts that occur naturally inside the cells and serve as one of the physiological phenomena evolved to protect the photosynthetic apparatus from photodamage under high light conditions (Kasahara et al., 2002). This could be achieved by the dense packing or ‘crowding’ of the chloroplasts in the cytoplasm in the leaves which are subjected to low water potentials (McCain, 1998). Indeed, I found this treatment to be effective in reducing the chloroplast movements during FRAP measurements allowing for post-bleach imaging on timescales ranging from 5 to 10 minutes. However, while in the case of isolated chloroplasts

a one-dimensional variant of the FRAP technique was performed (resulting in a bleached line visible across the chloroplast e.g. Figures 3.1 and 4.2) in the case of intact leaves measurements a two-dimensional variant of the method (as described in Figures 3.2 and 3.3) could be applied. This resulted in a small two-dimensional bleaching spot to be generated which, concerning the high-resolution optics of the confocal microscope, corresponded accurately to a few individual grana within the single chloroplast (Figure 7.2). The subsequent post-bleach imaging allowed to track, for the first time, the recovery of chlorophyll fluorescence in this region and thus enabled to calculate the degree of mobility of chlorophyll-proteins in a completely *in vivo* situation (Figure 7.3). The experiments performed on spinach and *Arabidopsis* leaves revealed that on a timescale of a few minutes the average mobile fractions were lower than 20% in both cases which is fully in agreement with the results obtained for isolated chloroplasts (Figure 7.3). It indicates therefore that the FRAP measurements on chloroplasts in intact leaves are possible and can be used as a reliable tool to study different aspects of the dynamics of photosynthetic complexes *in vivo*.

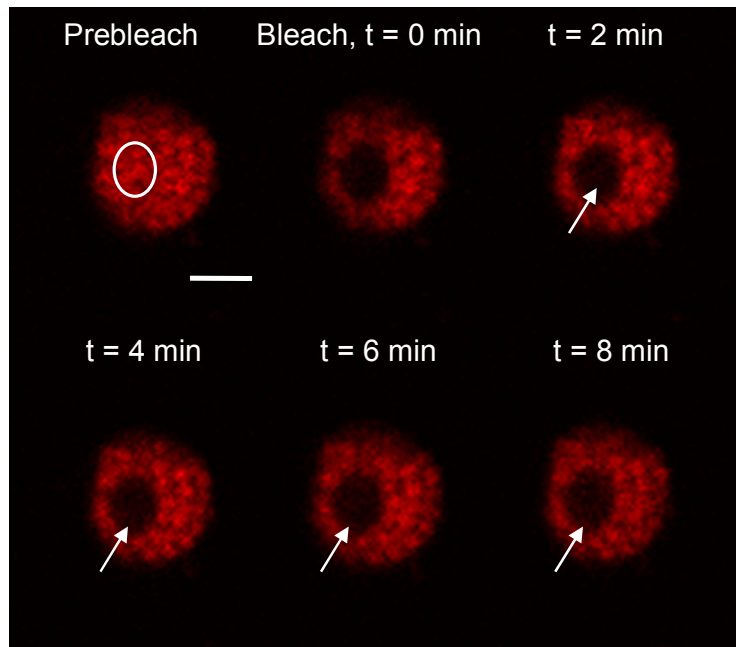
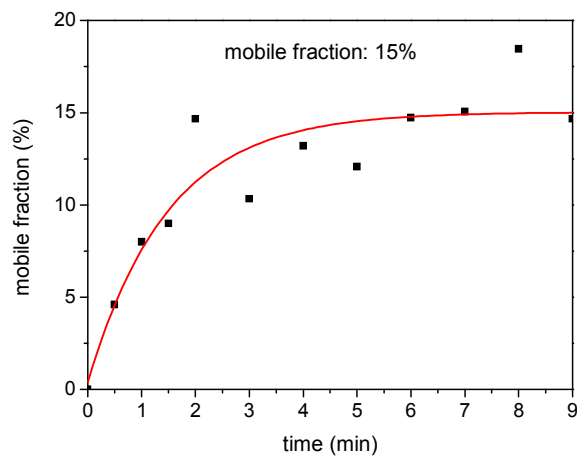
**A****B**

Figure 7.2. FRAP measurement on individual chloroplast in intact spinach leaf. (A). Chlorophyll fluorescence image sequence. Each image represents a raw single scan of a confocal laser in two-dimensions. The circle indicates the position of a few individual grana (used as a region of interest where the two-dimensional bleaching spot was generated). The arrows indicate a partial recovery of fluorescence in the bleaching spot. Scale bar = 2.5  $\mu\text{m}$ . (B) Fluorescence recovery curve for the bleaching spot in (A).

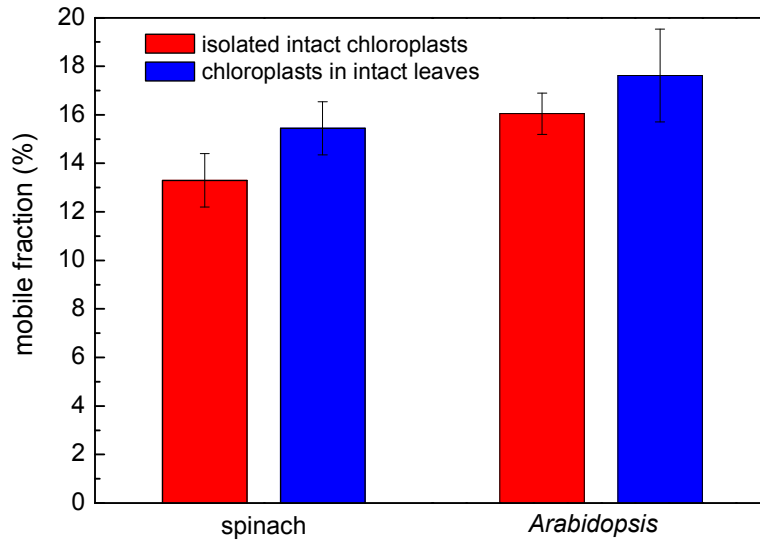


Figure 7.3. Comparison of the sizes of mobile fractions for chlorophyll-proteins in intact chloroplasts which were either isolated (red bars) or retained within the cells in intact leaves (blue bars) of spinach and *Arabidopsis thaliana* wild-type plants. Note a lack of significant differences between the investigated samples indicating that the results obtained from FRAP measurements in intact leaves reflect the physiological level of mobility of chlorophyll-proteins in a dark-adapted state. Data represent mean mobile fractions ( $\pm$  SE) out of 10 independent experiments.

### 7.3.2. Probing the mobility of chlorophyll-proteins in intact leaves of tobacco photosystem II mutants

One of the potential applications of the approach presented here is the use of various higher plant mutants which could be deficient in different aspects of photosynthetic activity e.g. light-harvesting, PSII repair process, photosynthetic electron transport etc. The use of intact leaves rather than isolated chloroplasts is not only beneficial in terms of a more physiological system used but it also requires much less material for sample preparation (a small leaf fragment) compared to at least a couple of leaves (dependent on their size) in the latter case. This is especially important in mutant plants where their growth might be much slower than in normal wild-type plants. This was the case in the tobacco (*Nicotiana tabacum*) mutants which had the altered amino-acid composition in photosystem II reaction centers.

The mutants, created by Mr. Franck Michoux from Imperial College London, were as follows: pFM-T2Wt, pFM-T2A, pFM-T2D, pFM-T2S, and pFM-A20. The first four mutant plants had a silent NdeI site introduced at the start of the PsbA gene of photosystem II reaction centers (pFM-T2Wt) together with the first threonine, T2, replaced by alanine, aspartate and serine, respectively. Such mutations lead to impairment (to a different degree) in PSII core phosphorylation under high-light conditions as the N-terminal threonine residues were found to be the phosphorylation sites in the D1 and D2 reaction centre proteins and the CP43 protein of the PSII core (Bennett, 1977; Bennett, 1984). As mentioned already in chapter IV the phosphorylation of PSII core proteins is performed primarily by the specific STN8 kinase (Vainonen et al., 2005) which plays an important role in the PSII repair cycle after photoinhibition (Tikkanen et al., 2008). The results I present in this thesis (chapter IV) indicate that this specific phosphorylation triggers the increased mobility of chlorophyll-proteins during photoinhibition as judged from the FRAP measurements performed on different *Arabidopsis thaliana* mutants that lack the protein kinases involved in this process (Figure 4.4). Here, I was interested in confirming these observations by performing FRAP experiments on intact leaves of tobacco mutants which possessed both kinases (STN7 and STN8) but lacked the phosphorylation sites required for their activity. In addition, I investigated also the pFM-A20 mutant which lacked the first 20 amino-acids in the D1 core protein of PSII leading to a deficiency in formation of functional PSII complexes. This resulted in a much slower photosynthetic activity and growth rate when compared to the wild-type plants (personal communication with Mr. Franck Michoux). FRAP measurements revealed that in the wild-type dark-adapted tobacco chloroplasts the mobile fraction of chlorophyll-proteins was about 20% (Figure 7.4) which is close to



the values obtained for spinach and *Arabidopsis* chloroplasts (Figure 7.3). This was not significantly changed in the wtF, T2D and T2S samples whereas T2A mutants exhibited a slight tendency of reduced mobility of chlorophyll-proteins (although it was not confirmed statistically most likely due to a small number of experiments performed). Additionally, the pFM-A20 samples showed also a considerable decrease in the size of mobile fraction (Figure 7.4). The results presented here confirm the previous observations showing that in a dark-adapted state the phosphorylation of PSII core does not generally affect the overall dynamics of photosynthetic complexes (Figure 4.4).

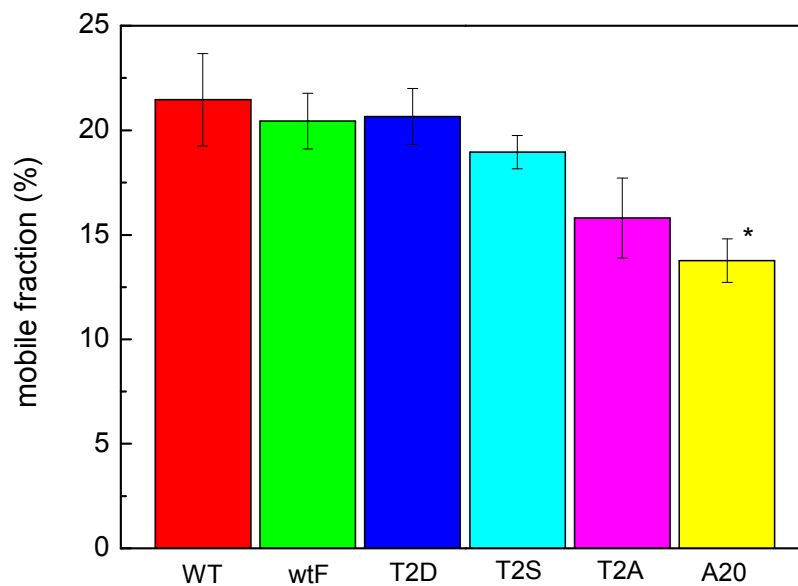


Figure 7.4. Mobility of chlorophyll-proteins in different dark-adapted tobacco mutants impaired in phosphorylation of PSII core proteins or lacking functional PSII photosystems (A20 mutant). FRAP experiments were performed on the chloroplasts in intact leaves in a similar way as presented in Figure 7.2. Data represent mean mobile fractions ( $\pm$  SE) calculated out of 6-10 independent experiments. Note a slight tendency of reduced mobility in T2A mutants (P value = 0.8) and a significant decrease in the size of mobile fraction in the A20 mutant (P = 0.01) as indicated by an asterisk and determined by one-way ANOVA with Dunnett contrast,  $p < 0.05$ .

The next experimental step would be to probe the mobility of chlorophyll-proteins in the investigated mutants following photoinhibition treatment in order to verify the observations made in *Arabidopsis* STN mutants suggesting that under high light intensities the PSII core phosphorylation switches the membrane into more fluid state which facilitates the diffusion of damaged D1 into the stroma lamellae regions (Figure 4.4.).

Apart from the decreased mobility of chlorophyll-proteins another interesting observation was made in the pFM-A20 mutant regarding the appearance of the thylakoid membranes inside the chloroplasts. Instead of individual grana observed clearly in the wild-type samples (Figure 7.5.A, white arrows) the mutant plants exhibited large spots (much bigger than individual grana) of bright chlorophyll fluorescence (Figure 7.5.B, green arrows). This suggests that the organisation of the thylakoid membranes might be somehow impaired upon the loss of functional PSII complexes but more detailed structural studies are necessary to prove this hypothesis.

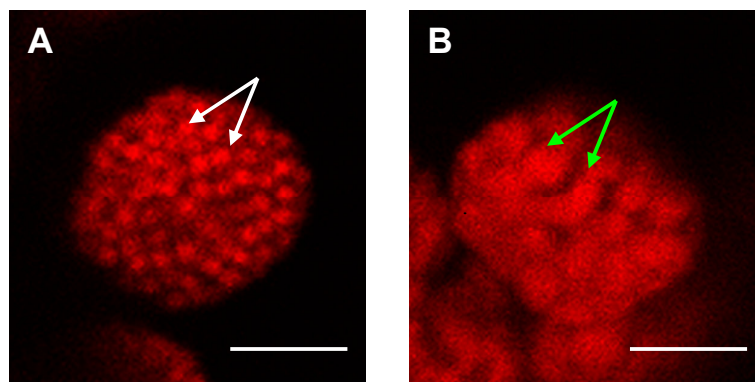


Figure 7.5. Confocal images of dark-adapted chloroplasts in intact leaves of tobacco (A) wild-type and (B) pFM-A20 mutant plants. Note a specific appearance of the thylakoid membranes in the mutant chloroplasts suggesting some alterations in their structural organisation. For explanation of arrows see text. Each image represents a single scan of a confocal laser. Scale bars = 3  $\mu$ m.

# **Chapter VIII**

## **Discussion**

## 8.1 Introduction

The exchange of photosynthetic complexes between the grana and the stroma lamellae regions within the thylakoid membrane network has been a subject of debate since it was discovered that these two distinct regions have a different protein composition (Anderson, 1975). The results obtained from a various biochemical approaches, fluorescence spectroscopy and immunoelectron microscopy techniques clearly indicated that some changes in the protein composition occur in both grana and stroma lamellae regions upon different physiological events such as state-transitions or photoinhibition, for example (Kyle et al., 1983; Barbato et al., 1992; Aro et al., 2005; Ruban and Johnson, 2009). Although these studies shed some light into the dynamic properties of some photosynthetic complexes they did not provide any direct information on the kinetics of protein movements. For instance, it has remained unclear how far the phosphorylated LHCII complexes migrate during state transitions and how the membrane architecture changes upon this physiological phenomenon. Recent discoveries based on a number of microscopic techniques revealed that protein redistribution induces significant structural alterations in both granal and stroma lamellar domains (Chuartzman et al., 2008). This might suggest that the stability of the thylakoid membrane network is dependent on the kinetics of protein diffusion. However, to resolve these specific issues some direct approaches allowing for the movements of photosynthetic complexes in the intact thylakoid membrane system to be observed need to be implemented. In this thesis such direct approaches as fluorescence recovery after photobleaching technique (confocal FRAP) combined with freeze-fracture electron microscopy have been developed and used for the first time for direct visualisation of the mobility and distribution of chlorophyll-proteins in higher plant thylakoid membranes.

## **8.2. Confocal FRAP as a useful tool for probing the dynamics of photosynthetic complexes in the intact thylakoid membrane network.**

In this study I extended the Fluorescence Recovery after Photobleaching technique used previously for probing the mobility of chlorophyll-proteins in isolated grana patches (Kirchhoff et al., 2008) to a much more physiologically relevant system – the thylakoid membranes from intact chloroplasts which were either isolated (chapters III-VI) or still retained inside the cells of intact leaves (chapter VII). I visualised the proteins using the native fluorescence from the chlorophylls. This has the advantage that I do not perturb the membrane structure. This might be the only way to track proteins through the grana, where the tight appression of the membranes (Dekker and Boekema, 2005) is likely to exclude any extrinsic fluorescent tags such as GFP and antibody-linked fluorophores (Consoli et al., 2005). However, it should be stressed that this approach still has its own limitations and brings some difficulties with regards to the information one can obtain:

1. It is impossible to distinguish the different chlorophyll-protein complexes (e.g. PSII, LHCII etc.) under a confocal microscope. This puts an obvious limit on the assessment of contributions of the mobility of these proteins to the overall mobility calculated from FRAP measurements.
2. Emission of chlorophyll fluorescence competes with two other physiological ways of dissipation of absorbed light energy: photochemical quenching (by the reaction centres) and non-photochemical quenching (NPQ) that dissipates excitation energy as heat. For this reason, I needed to carefully control the experiments to ensure that the fluorescence

recovery that I observed genuinely resulted from the mobility of chlorophyll-proteins rather than reversible quenching, for example.

3. Lateral heterogeneity and the complex three-dimensional structure of the thylakoid membrane network prevented me from quantifying diffusion coefficients as it was possible in cyanobacteria (Mullineaux, 2004) and in isolated, flat grana membranes (Kirchhoff et al., 2008). Additionally, it makes it hard to determine if fluorescence changes are due to protein diffusion. This can be visualised as the characteristic redistribution of fluorescence, which is typical for homogenous membranes, for example in cyanobacteria (Mullineaux, 2004), but it is not detectable in the laterally-segregated thylakoid membranes of intact chloroplasts.

Despite these problems, I am confident that FRAP experiments presented in this work do reveal protein movements within the intact thylakoid membrane system. This can be concluded on the basis of the control experiments which are described in chapter III. Bleaching out chlorophyll fluorescence from the whole chloroplast so that there is no reservoir of unbleached fluorophores that can diffuse into the bleached region resulted in a significant loss of fluorescence recovery (Figure 3.5). This clearly indicates that the photobleaching caused by an intense, highly-focused confocal laser spot is not reversible on the timescale of my measurements, and it is diffusion of proteins that is responsible for the observed recovery of chlorophyll fluorescence. Moreover, I found that the addition of nigericin that inhibits NPQ formation, a major rapidly-reversible fluorescent quenching mechanism, does not affect that rate of fluorescence recovery (Table 3). The third control that involved cross-linking the membrane and its components with glutaraldehyde which inhibits

protein diffusion (Habeeb and Hiramoto, 1968) revealed a markedly reduced level of fluorescence recovery compared to the untreated chloroplasts (Figure 3.5).

It is obvious that FRAP measurements are somewhat disruptive. Photobleaching will inevitably damage fluorophores in the bleached region of the membrane and likely to perturb the processes that are taking part there. This is especially the case in the thylakoid membranes where the bleaching of chlorophyll fluorescence would destroy photosynthetic proteins at the same time. However, it would not do any harm in the unbleached remainder of the chloroplast if we take into account the fact that the bleaching is very localised. The line bleach or two-dimensional bleaching spot (as shown in chapter VII) used in my experiments is generally targeted to hit only a single granum, while leaving neighbouring grana practically unaffected. The fact that I observe fluorescence recovery in the bleached region clearly indicates that unbleached chlorophyll-complexes are still functional and must be able to diffuse within those neighbouring, undamaged regions of the membrane, and escape from unbleached grana.

FRAP measurements performed on isolated spinach and *Arabidopsis* chloroplasts as well as the chloroplasts from intact tobacco leaves show in all cases a partial recovery of chlorophyll fluorescence. Although I could not quantify the diffusion coefficients in such complex systems, but I could accurately measure the sizes of mobile fractions. There was a great variation from chloroplast to chloroplast, but on average the mobile fractions for these three different plant species remained generally at the similar level with approximately 15% - 20% of chlorophyll fluorescence being mobile in a dark-adapted state (Figures 4.4 and 7.3, Table 2). Since the FRAP technique has a very limited spatial resolution and can detect only long-range diffusion on a scale of at least a micron (Mullineaux, 2004) I do believe

that this small proportion of chlorophyll-proteins accounting for the observed mobile fraction is able to diffuse not only within the appressed region of a single granum but can also escape from the granum and enter another granum via the unappressed stroma thylakoids that connect grana each other. It would then indicate that a limited fraction of chlorophyll-protein complexes is relatively loosely associated with the grana. This also suggests that the capability of diffusing out of those regions and exchange between the neighbouring grana occurs on a timescale of a few minutes. This result can be compared to the previous studies in isolated spinach grana membranes, which revealed a proportion of chlorophyll-proteins accounting for about 25% of chlorophyll fluorescence that is able to diffuse within the grana regions while the remaining fraction appeared to be completely immobile (Kirchhoff et al., 2008). Here, I extended this finding to the system which is much more physiologically-related and report the ability of some of the photosynthetic complexes to move out of the grana and diffuse into the stroma lamellae regions. Although the precise three-dimensional architecture of the granum-stroma assembly remains still unknown and controversial (Mustárdy et al., 2008) it is clear that these regions are connected by a continuous membrane system. My results show directly for the first time, that the protein movement through these connections is possible and most likely it is facilitated once in the stroma lamellae (Figure 4.8). There has been one study using single particle tracking for direct visualisation of the dynamics of LHCII antenna tagged with antibody-linked fluorophore (Consoli et al., 2005). However, because of the large size of the labelled complex, the visualised LHCII was most probably excluded from the appressed membranes and was localised mainly in the stroma thylakoids. The tagged LHCII exhibited a random movement confined to a limited membrane area, with a mean diffusion coefficient of about  $0.008 \mu\text{m}^2\text{s}^{-1}$ ,



increasing more than three times to about  $0.027 \mu\text{m}^2\text{s}^{-1}$  for phospho-LHCII (Consoli et al., 2005). My data confirm that some long-range diffusion of photosynthetic complexes within the intact membrane system is possible. This is in a strong agreement with the commonly accepted models for state transitions and PSII repair cycle which involve migration of the phosphorylated LHCII and damaged PSII complexes out of the grana into the unstacked region of the stroma lamellae thylakoids (Allen and Forsberg, 2001; Baena-González and Aro, 2002).

My experiments indicate that grana are relatively stable structures *in vivo*. Even after considerable photodamage (photobleaching an entire granum), some chlorophyll-proteins diffuse back into the same region of the sample, and there is rapid and complete diffusion of a lipophilic fluorophore back into the granum (Figure 3.6). This indicates that the location of the granum does not change during my experiments. High-resolution studies using cryo-electron tomography suggest considerable effects of illumination and adaptation on grana structure (Chuartzmann et al., 2008). Such changes would probably not be detectable at optical resolution. However, this study indicates that grana remain in place: they do not totally disintegrate or reform, even after drastic light exposure.

To further investigate the mobility of chlorophyll-proteins in intact chloroplasts I measured the effects of pre-illumination to induce either photoinhibition (chapter IV) or non-photochemical quenching (chapter V). I probed also the mobility of photosynthetic complexes upon the unstacking of the thylakoid membranes (chapter IV), upon the loss of individual light-harvesting antenna proteins (chapter VI) and assessed the effect of different xanthophyll composition within the antenna complexes (chapter V). All these results are discussed in details in sections 8.3 – 8.6.

### **8.3. Enhancement of the mobility of chlorophyll-proteins under photoinhibitory conditions**

Intact chloroplasts subjected to high-light treatment for a prolonged time are likely to develop photoinhibition of photosynthesis leading to photooxidative destruction of the photosynthetic apparatus which will initiate the PSII repair cycle (Barber and Andersson, 1992). This phenomenon is of the major importance when it comes to the effective maintenance of photosynthesis under most conditions in most photosynthetic organisms (Long et al., 1994). The model of the PSII repair cycle involves the migration of the photodamaged PSII core proteins (with D1 polypeptides being the most susceptible to this damage) from the grana membranes where there are normally localized to the stroma lamellae where the repair and turnover take place (Aro et al., 1993). Thus, we might expect a photoinhibitory pre-treatment to mobilize the thylakoid membrane system, causing an increase in the mobile fraction in my FRAP measurements. I found this to be the case: the chloroplasts' exposure to excess light resulted in the significant increase of the calculated mobile fractions in both spinach and *Arabidopsis* wild-type plants, although the effect in spinach was more enhanced as shown in Figure 4.2, Table 2 and Figure 4.4, respectively. This indicates that under photoinhibitory conditions the additional fraction of chlorophyll fluorophores becomes more mobile and diffuses out of the grana. Since the chlorophylls in the grana regions are mostly bound to the light-harvesting antenna proteins (~60% of total chlorophyll population (Luciński and Jackowski, 2006)) a simple interpretation of this result would be that under low light intensities most of the observed mobile population belongs to the LHCII complexes, especially those undergoing state transitions (Allen and Forsberg, 2001; Kirchhoff et al., 2008). This is in agreement with the observation made in the A20

mutant of tobacco which is deprived of PSII reaction centers (see Methods for details) but still exhibits the mobility of chlorophyll-proteins of about 14% as compared to ~20% found in the wild-type plants (Figure 7.4). The observed decrease might be either a consequence of a structural change within the thylakoid membrane network (as shown in Figure 7.5) which impairs the diffusion of the mobile LHCII antenna or this might suggest that in a dark-adapted state a small fraction of PSII can still escape the grana regions. This could be due to a small activity of the repair cycle which is able to operate even under low-light intensities (Vasilikiotis and Melis, 1994; Tikkanen et al., 2008). However, upon the increase in light intensity the operation of PSII repair cycle accelerates significantly which results in the mobilization of the sub-population of PSII core proteins, thus contributing to the rise in the total mobile fraction observed in my measurements. This finding may be compared to the previous result obtained in a cyanobacterium, where pre-illumination with bright red light resulted in the mobilization of up to about 50% of chlorophyll fluorescence (Sarcina et al., 2006). In the cyanobacterium the authors could be confident that this mobilized fraction consists of PSII core complexes, since these contribute to the most of the chlorophyll fluorescence (Sarcina et al., 2001).

In contrast to my findings with intact chloroplasts, the experiments performed by Prof. Helmut Kirchhoff revealed that photoinhibitory pre-illumination had no effect on the mobility of chlorophyll-proteins in isolated grana membranes (Table 2). There are several possible explanations for this discrepancy (Figure 8.1). Mobilisation after photoinhibition may require some stromal factor that is absent from the isolated grana membranes preparation (Figure 8.1.Arrow 1). My results indicate that this stromal factor is likely to be the kinase that phosphorylates the damaged PSII core proteins (see the next paragraph for details), helps in the

disassembly of the photosynthetic supercomplexes and facilitates their migration to stroma lamellae regions where the repair process occurs. Alternatively, mobilisation may only be possible if there is adjacent membrane space available in the stroma lamellae (Figure 8.1.Arrow 2). This idea would indicate a progressive increase in diffusion space in the grana as complexes escape into the stroma lamellae, starting with the complexes closest to the grana-stroma lamellae assembly. Obviously this would not occur in the isolated grana membranes. Finally, there might be a diffusion barrier or ‘gatekeeper’ structure at the grana-stroma lamellae junctions (Figure 8.1.Arrow 3). In this case, movements of protein between grana and the stroma lamellae, and exchange between grana, would not be directly related to mobility within the appressed grana membrane. Again, this idea would explain why there was no-photoinhibition-induced mobilisation of complexes in isolated grana membranes (Table 2). The mobile fraction of chlorophyll fluorescence within isolated grana membranes is considerably higher than the fraction that diffuses between grana in intact chloroplasts (Table 2). This might suggest a partial barrier to exchange between the grana and the stroma lamellae. However, it must be considered that the forces acting on protein complexes in isolated grana membranes could be different from those in the intact system.

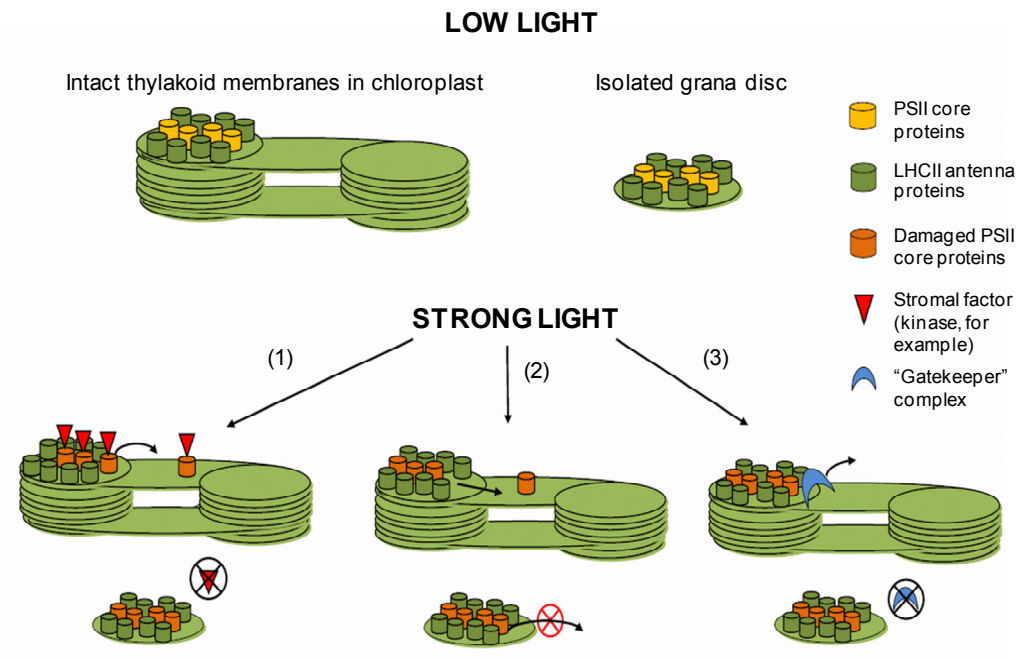


Figure 8.1. Model proposing possible explanations for the differences in the mobility of chlorophyll-proteins upon photoinhibitory illumination in intact chloroplasts where grana are interconnected with stroma lamellae vs. isolated grana patches. (1) Mobilization after photoinhibition requires some stromal factor, which is absent from the isolated grana membrane preparation. (2) Mobilization of chlorophyll-protein complexes is only possible if there is adjacent membrane space available in the stroma lamellae. (3) Escape of chlorophyll-proteins from the grana is controlled by a "gatekeeper" complex at the grana-stroma lamellae junctions. For more detailed description of these three possible situations see the text.

The reasons for the increased protein mobility in photoinhibited chloroplasts could be provided after the analysis of freeze-fracture electron micrographs. I could detect no drastic changes in PSII organisation within the grana (Figure 4.5), suggesting that PSII mobilisation is not a consequence of changes in the large-scale supramolecular interactions. However, photoinhibition caused a small but significant decrease in the mean size of PSII complexes in the grana, most likely due to a loss of part of the strongly associated light-harvesting antenna as the observations made in the LHC mutants of *Arabidopsis* suggest (Figures 6.5 – 6.6). Furthermore, the significant increase in the mean distance between complexes was found after photoinhibition

(Figure 4.6.B). This suggests a loss of PSII complexes from the grana (presumably caused by the escape to the stroma lamellae) which is reflected in the decreased number of PSII particles on the EFs fracture faces (Figure 4.6.A). Progressive loss of PSII complexes from the grana would make the system more fluid. This, in turn, results in the increased protein mobility as the studies on isolated grana membranes with the altered lipid-to-protein ratio show (Kirchhoff et al., 2008).

To further explore the factors required for mobilisation of chlorophyll-proteins after photoinhibition, I performed FRAP measurements in *Arabidopsis* mutants. Most biochemical approaches suggest indirectly that the PSII repair cycle is induced upon phosphorylation of damaged D1 polypeptides in the PSII core and this serves as a trigger for their migration into the stroma thylakoids (Aro et al., 2005; Tikkanen et al., 2008). However, direct experimental data supporting this hypothesis are largely lacking. By taking advantage of my FRAP measurements in the intact thylakoid membrane system, I decided to test this hypothesis using the *stn8* and *stn7stn8* mutants of *Arabidopsis* lacking STN8 or both STN7 and STN8 protein kinases, respectively. These enzymes have been previously shown to be engaged in specific phosphorylation of either LHCII antenna complexes (STN7) (Bellafiore et al., 2005) or PSII core proteins (STN8) (Vainonen et al., 2005). As a consequence, the two investigated mutants have either strongly decreased (*stn8*) or even completely lack the PSII core protein phosphorylation (*stn7stn8*) and are the most suitable to study the role of this process in photoinhibition and the PSII repair cycle (Tikkanen et al., 2008). Although protein phosphorylation by STN7 and STN8 is not absolutely required for the PSII repair cycle (Bonardi et al., 2005) but dynamics of this process are impaired in the absence of these proteins due to impairment of the disassembly of PSII-LHCII supercomplexes (Tikkanen et al., 2008). Recently

Fristedt et al. (2009) further proposed that protein migration in the *stn7stn8* mutant is impaired by an increase in the diameter of the grana discs. My results on the *stn8* and *stn7stn8* mutants are consistent with these models (Figure 4.4). Firstly, they revealed that the mobility of chlorophyll-proteins in dark-adapted intact chloroplasts is slightly lower in the mutant plants than in the wild-type (Figure 4.4). Secondly, if phosphorylation genuinely triggers the migration of photodamaged complexes into the stroma lamellae, one might expect to observe no increase in the mobility of chlorophyll-proteins after photoinhibitory treatment in the mutant plants. Indeed, this was the case in the *stn8* and *stn7stn8* mutants (Figure 4.4) in contrast to the effect seen in wild-type *Arabidopsis* (Figure 4.4) and spinach (Figure 4.2, Table 2). To my knowledge, this is the first direct experimental evidence showing that PSII phosphorylation facilitates the exchange of chlorophyll-proteins between the grana and the stroma lamellae suggesting that phosphorylation switches the thylakoid membrane system to a more fluid state. To further confirm this observation an alternative approach could be used which involves the investigation of tobacco mutants which bear mutations in the N-terminal threonine of the D1 core subunit (chapter VII). This particular threonine serves as a phosphorylation site required for the activity of STN8 kinase (Bennett, 1977; Bennett, 1984). The study on the mentioned mutants has already begun and so far the FRAP measurements have been performed on the dark-adapted intact leaves (Figure 7.4). As predicted, the sizes of mobile fractions in the mutant plants were not significantly different than the wild-type (Figure 7.4) suggesting that the phosphorylation of PSII core does not influence the mobility of chlorophyll-proteins under low-light illumination. The next step for future experiments would be to test the mobility in these mutants after

photoinhibitory treatment and compare these results with the data obtained for the *stn8* and *stn7stn8* mutants of *Arabidopsis* which are presented in this thesis.

#### **8.4. Dynamic and structural changes of PSII and LHCII protein complexes within the grana membranes during photoprotective energy dissipation: the role of xanthophyll composition and the PsbS protein**

Apart from the effect of photoinhibitory illumination on the mobility and macromolecular organisation of PSII-LHCII protein complexes the structural and dynamic changes that underlie the transition between the light harvesting and photoprotective states of the thylakoid membrane were also investigated in this thesis. This was possible by employing thin-section and freeze-fracture electron microscopy techniques and combining them with the FRAP measurements on intact spinach chloroplasts isolated in different de-epoxidation states with or without NPQ (chapter V, section 2). Some indirect evidences suggesting that the qE component of NPQ involves a structural change within the thylakoid membrane have been provided previously by a range of spectroscopic methods. qE is characterized by a series of absorption and fluorescence changes (Horton et al., 1991; Ruban et al., 1991; Ruban et al., 1992; Ruban et al., 1993; Bilger and Bjorkman, 1994; Miloslavina et al., 2008), that have been shown to depend upon the composition of pigments within the LHC antenna system (Johnson et al., 2009; Johnson and Ruban, 2009). Changes in the molecular configuration and interactions between pigments upon qE formation have also been demonstrated using resonance Raman, circular dichroism (CD), linear dichroism (LD) and two-photon excitation spectroscopy (Ruban et al., 1997; Ruban et al., 2007; Bode et al., 2009). The similarities between



these qE-related spectroscopic signatures and those observed when purified LHCs adopt quenched states upon aggregation *in vitro*, has led to the suggestion that changes in LHC conformation and/ or organization underlie qE *in vivo* (Horton et al., 1991). The finding that aggregation-induced quenching can be modulated by low pH and xanthophyll cycle carotenoids, provided a further link between these phenomena (reviewed in Horton et al., 2005). Yet, direct structural evidence to support the suggestion that changes in LHC conformation and/or organisation underlie qE *in vivo* remains largely absent. Recently, Betterle et al. (2009) reported that in negatively-stained detergent-isolated grana membranes, derived from light treated *Arabidopsis* leaves, a PsbS-dependent change in the distance between PSII core complexes occurs, implying a reorganization of the PSII-LHCII macrostructure, may indeed be present during illumination. This was supported by biochemical evidence that showed a fragment of the C<sub>2</sub>S<sub>2</sub>M<sub>2</sub> supercomplex, consisting of the LHCII M-trimer, CP24 and CP29 (B4C subcomplex) is dissociated by light treatment (Betterle et al., 2009). In the current work, direct structural evidence has been provided that these changes in the ultrastructure of the thylakoid membrane and in the organisation of PSII and LHCII complexes within it are genuinely associated with NPQ formation. However, in contrast to the study of Betterle et al., (2009), where the observed changes in PSII organisation took ~30-60 minutes to form and relax, the changes identified here are shown to occur within 5 minutes of illumination and dark relaxation consistent with their involvement in rapidly reversible qE-type quenching. Given the extent and nature of the observed qE-related changes in PSII nearest neighbour distance which are very similar to those observed by Betterle et al., (2009), it is likely that this previous study was hampered by the slower isolation method which involved isolation and detergent solubilisation of thylakoids from

leaves prior to their study by electron microscopy. Indeed, these limitations were already acknowledged by the authors (Betterle et al., 2009). The rapid isolation method and freeze-fracture technique used here not only allows probing of the involvement of the changes in PSII organization in rapidly relaxing NPQ, but also provide information on the size of the PSII supercomplex *in vivo* and on the fate of LHCII. The size of the PSII EFs particles in freeze-fractured intact spinach chloroplasts was shown to be dependent upon the extent of NPQ (Figure 5.7.C, Table 5). The size of the EFs PSII particle decreased from  $\sim 200 \text{ nm}^2$  in the Dark Vio chloroplasts, which is too small to represent a  $\text{C}_2\text{S}_2$  supercomplex but is consistent with a PSII core dimer together with 2-3 minor antenna proteins (Dekker and Boekema, 2005), to  $\sim 125 \text{ nm}^2$  in the Light Zea chloroplasts (Figure 5.7.C). The data therefore suggest that NPQ involves some alteration in binding of a part of the minor antenna complexes to the PSII core dimer resulting in it no longer fracturing with the EFs face. This structural evidence that a change in minor antenna and PSII core interactions is involved in qE supports the biochemical evidence obtained by Betterle et al., (2009) who found that levels of an antenna subcomplex containing CP29, CP24 and the LHCII M-trimer (B4C), that is a building block of the  $\text{C}_2\text{S}_2\text{M}_2$  supercomplex, are reduced following light treatment. In addition to changes in PSII nearest neighbour distances, clustering and size, an increased clustering of LHCII particles was observed under qE conditions (Figure 5.8.C). The direct observation of closer LHCII association upon qE formation *in vivo* represents a landmark in the study of the process, since it provides an explanation for the consistently observed spectroscopic link between qE and LHCII aggregation induced quenching *in vitro* (Horton et al., 1991; Ruban et al., 1992; Ruban et al., 1997; Ruban et al., 2007; Miloslavina et al., 2008; Johnson and Ruban, 2009; Liao et al., 2010).

The relationship between the PSII and LHCII clustering and NPQ show that the extent of the reorganization of PSII and LHCII upon qE formation is enhanced by the presence of zeaxanthin (Figure 5.8.C). This effect of de-epoxidation on the qE-related structural change is consistent with the results of Betterle et al., (2009) who found that the dissociation of the B4C antenna subcomplex was reduced in the *npq1* mutant lacking zeaxanthin. It is interesting to note that quenching sustained in the absence of  $\Delta pH$  in the Dark Zea chloroplasts (Table 5), which is often referred to as a non-photoinhibitory component of 'qI', appears to share the same structural basis as qE. Both qE in Light Vio chloroplasts and the qI in the Dark Zea chloroplasts were characterized by similar levels of PSII and LHCII clustering and changes in PSII size (Figures 5.7 and 5.8.C). This observation lends support to the suggestion of Horton et al., (1991) that de-epoxidation and protonation cooperatively drive the structural change that underlies NPQ formation and that qE and qI are merely different manifestations of the same structural phenomena. Such a conclusion would explain the plentitude of data from titration studies on chloroplasts and on isolated LHCII, which demonstrated that zeaxanthin enhances the pH sensitivity of the quenching process (Horton et al., 1991; Ruban and Horton, 1999). Indeed, zeaxanthin has been shown *in vitro* to have structural effects on LHC proteins enhancing the tendency for aggregation in LHCII (Ruban et al., 1997) and shifting the isoelectric point of CP26 from ~4.8 to 5.1 (Dall'Osto et al., 2005). It has been shown that the chlorophyll excited state lifetime in leaves and in LHCs is modulated by the collective hydrophobicity of the bound xanthophyll compliment (Ruban and Johnson, 2010). The replacement of violaxanthin with zeaxanthin within LHCs was suggested to increase the hydrophobicity of the structure, thus shifting the pKa's of lumenal acidic residues to higher values (Ruban and Johnson, 2010).

This hydrophobic effect on amino acid pKa is well documented in the literature (Li et al., 2004; Thurlkill et al., 2006) and may explain the mentioned alteration in the sensitivity of qE to  $\Delta$ pH in the presence of zeaxanthin, and the enhancement in the observed structural change. It is worth noticing that a similar effect of zeaxanthin-enhanced clustering of PSII and LHCII complexes and the increased amount of semi-crystalline arrays was observed in the *npq2* and *lut2npq2* mutants of *Arabidopsis* which exhibit the elevated levels of zeaxanthin within the light-harvesting antenna complexes (Figures 5.19 and 5.20). Interestingly, the *lut* mutants (*lut2* in particular) which lack the internal luteins in LHCII antenna exhibited the same tendency of reduced distances between PSII and LHCII particles (Figures 5.19 and 5.20). This might be due to the accumulation of the xanthophyll cycle pigments (especially antheraxanthin and zeaxanthin) in the absence of lutein (Pogson et al., 1996). These data are consistent with the observations made in the Dark Zea spinach chloroplasts suggesting that the accumulation of zeaxanthin in the membrane in dark and the resulting change in the hydrophobicity of LHC complexes may serve as a prerequisite for the formation of NPQ state and aggregation of LHC antenna as observed in intact spinach chloroplasts subjected to light adaptation.

Murakami and Packer (1970b) showed that formation of  $\Delta$ pH was associated with an increased hydrophobicity and reduction in the thickness of the thylakoid membrane and a reduced lumenal volume. Unlike the change in lumenal volume, that could be mimicked by incubating thylakoids in concentrated sucrose and was thus a purely osmotic effect, the increased hydrophobicity and decreased thickness was concluded to result from a protonation-induced structural change. In the present study it was shown that the change in membrane thickness is correlated with the extent of NPQ rather than  $\Delta$ pH *per se*, since the thickness of Light Zea membranes

was significantly less than in Light Vio membranes despite identical levels of  $\Delta\text{pH}$  in the two types of chloroplast (Figure 5.5). This observation is consistent with the fact that the change in light-minus-dark recovery absorption difference spectrum, the best known of which is  $\Delta A_{535}$ , that was correlated with the reduction in membrane thickness (Murakami and Packer, 1970a), also correlates with NPQ rather than  $\Delta\text{pH}$  (Horton et al., 1991; Iliesiu et al., 2011). The extent of the change in membrane thickness is directly related to the extent of clustering of PSII and LHCII (Figures 5.5, 5.7.A and 5.8.C), suggesting that the two phenomena may have a common origin. Previously it has been demonstrated using LD spectroscopy that upon qE formation *in vivo* and upon LHCII aggregation *in vitro* the xanthophylls adopt a more parallel orientation with respect to the plane of the membrane (Ruban et al., 1997). This ‘condensed’ state of LHCII formed upon its aggregation may thus be the origin of the reduction in membrane thickness associated with qE. Alternatively the protonation and increased hydrophobicity of the thylakoid membrane upon qE formation may affect the binding of the negative-stain, thus making the membranes appear thinner than they actually are. According to Daum et al., the thylakoid membrane is approximately 40 Å thick as determined by cryo-EM data (Daum et al., 2010), whereas the thickness of single end membranes measured in this study was at ~6-8 Å. Thus, the ‘thickness’ of the membranes is likely to be exaggerated by the fact the negative-stain might also stain certain membrane extrinsic domains of LHCII and PSII which cannot be distinguished at this resolution. The differences observed in the volume of the lumen upon  $\Delta\text{pH}$  formation, which are related to purely osmotic effects rather than qE, are more controversially discussed in the literature. Murakami and Packer (1970a, 1970b) described reductions in the luminal volume in the light using thin-section negative-

stain EM in both leaves, algae and in isolated thylakoids (i.e. broken chloroplasts). Consistent with these observations is the work of Pfeiffer and Krupinska (2005) who used freeze-substitution cryo-EM to observe similar changes in barley leaves. Certainly the lumenal volume which is reported here for the light treated chloroplasts is consistent with recent cryo-EM data on light-adapted chloroplasts from pea (Daum et al., 2010). Nonetheless, another study has reported either that  $\Delta\text{pH}$  is associated with a light-induced swelling of the lumen (Majeran et al., 2001). The conclusions of this study were largely based on the *ac46* mutant of the green algae *Chlamydomonas* mutant, which possessed a defective ATP synthase, resulting in extreme proton accumulation in the lumen. In contrast, the wild-type showed either no or very little swelling in the light indicating that *ac46* may be disrupted in normal osmoregulation as a result of the mutation (Majeran et al., 2001). Further studies may be needed to resolve the swelling versus shrinkage argument.

Similarly to the FRAP experiments performed on photoinhibited chloroplasts I tested the mobility of chlorophyll-proteins upon the formation of NPQ and the different de-epoxidation states within the LHCII antenna complexes. The results suggest that qE formation in intact spinach chloroplasts is associated with a decrease in the mobility of photosynthetic complexes (Figure 5.11), which can be correlated with the extent of the increase in clustering of LHCII and PSII (Figures 5.9 – 5.10). It is worth noticing that a completely different effect was observed in the case of photoinhibited chloroplasts where the size of mobile fraction increased as well as the spacing between the PSII particles. Photoinhibition and qE therefore appear to have opposing effects with regards to both PSII clustering and chlorophyll-protein mobility. It is thus likely that the reduced chlorophyll-protein mobility in qE state is a direct result of the altered packing of PSII and LHCII proteins within the

membrane (see section 6 for further details). The results obtained on the spinach chloroplasts (Figure 5.9) indicate also that the mobility of chlorophyll-proteins decreases upon the de-epoxidation of violaxanthin into zeaxanthin. This observation is further confirmed in the xanthophyll mutants of *Arabidopsis* which exhibit the similar pattern (Figure 5.17). This would again suggest that the accumulation of zeaxanthin in the thylakoid membranes changes their hydrophobicity leading to a decreased fluidity and diffusion of the membrane components which allows for the formation of PSII and LHCII clusters observed in the NPQ state.

The PsbS protein is required for rapid formation of the photoprotective state in plants. The level of qE is strongly related to the level of PsbS protein – mutants of *Arabidopsis thaliana* deficient in PsbS such as *npq4* exhibit a significantly decreased level of qE (although not completely absent) while overexpression of the protein in the *L17* plants results in a great enhancement of this component of NPQ (Horton et al., 2008; Kiss et al., 2008). It is postulated that the protein is involved in sensing the formation of  $\Delta pH$  and could have a facilitating role in the conformational change of LHCII which underlies qE (Horton et al., 2005). Despite the fact that PsbS is not a constituent of the PSII-LHCII supercomplex, the recent discoveries brought some evidence that this protein can actually participate in controlling the macro-organization of photosynthetic complexes in thylakoid membranes. Teardo et al. (2007) showed that not only PsbS can reversibly associate either with the PSII core or the LHCII antenna but also interact with complexes located in stroma lamellae suggesting the possibility of its lateral diffusion within the membrane. The results obtained by Kiss et al. (2008) proved directly that the level of PsbS regulates reorganization of LHCII-PSII during thylakoid restacking and, what is more, it facilitates removal of the LHCII-PSII complex from thylakoid membranes by

detergent. It is then clear that the presence or absence of the protein as well as the changes in its functionality may affect the overall dynamics of the thylakoid membrane components – the main research problem addressed in this thesis. Indeed, I observed that the level of PsbS influenced directly the recovery of chlorophyll fluorescence by mobilizing photosynthetic complexes to a greater extent in the *L17* mutants and immobilizing them in the *npq4* lines in a dark-adapted state (Figure 5.14). This is in agreement with the previous studies (Kiss et al., 2008) suggesting the possible role of the protein in facilitating the diffusion of thylakoid membrane components. This facilitation could be achieved by directly changing the membrane fluidity as it has been previously shown in isolated grana patches (Kirchhoff et al., 2008). In fact, my study shows that PsbS in the dark-adapted state acts as a “lubricant” of the system: it decreases the tendency of PSII to self-organise into semi-crystalline arrays (as observed also by Kereïche et al., (2010)) and increases the mobile population of complexes. However, after the light adaptation the PsbS protein was found to act as a kinetic catalyst of the structural change by promoting greater clustering of PSII-LHCII supercomplexes and a decreased mobility of chlorophyll-proteins (Figures 5.13 – 5.14). The amount of PsbS therefore seems to allow for a rapid transition between the light harvesting and photoprotective states of plant photosynthesis. Moreover, my results suggest that mobilisation of photosynthetic complexes under the influence of PsbS is also related to its functionality in the qE state. Replacement of glutamate with glutamine at both putative protonation sites in the luminal loop of PsbS in the *E122QE226Q* mutants resulted in the mobility of chlorophyll-proteins and PSII organisation being more like the *npq4* than *L17* chloroplasts despite the great abundance of the protein being almost 2.5 times higher than in WT plants (Kiss et al., 2008). Interestingly, with regards to the effect of PsbS



protein on facilitating the re-assembly of the PSII-LHCII macrostructure during restacking the *E122QE226Q* mutant behaved more like *L17* plants (Kiss et al., 2008). Assuming that PsbS genuinely acts as a “membrane lubricant” by affecting its fluidity it is possible that this effect might happen only when the protein is in a native form and the membranes are fully stacked. This mechanism of PsbS action could not be excluded, especially when taking into account the evidence that NPQ proceeds via conformational changes in the subunits of PSII antenna (Pascal et al., 2005; Ruban et al., 2007). It is believed that this conformational change in LHCII is driven by protonation of PsbS, which induces monomerization of the protein and its subsequent detachment from PSII complexes resulting in the aggregation of LHCII and qE formation (Bergantino et al., 2003; Kiss et al., 2008). It is possible that PsbS could co-exist in two distinct states (dimer vs. monomer) even in the dark in plants possessing the protein in its native form (WT and *L17* mutants). In this case, at least some fraction of PsbS population would migrate from the PSII cores and interact with the other photosynthetic complexes as suggested by (Teardo et al., 2007). This effect would be more enhanced when the protein is over-expressed as in the *L17* lines explaining why the observed mobility is increased in my study. However, when the protein is not entirely functional as in the *E122QE226Q* double mutant plants it would remain mostly in the dimeric form attached to the PSII-LHCII supercomplex-enriched regions. As a consequence, despite being much more abundant than in the wild type it would not affect the mobility of chlorophyll-proteins to the same extent as in the *L17* mutants. Another explanation would relate the PsbS-dependent mobility of chlorophyll-proteins to the plant capability of performing NPQ. Both *npq4* and *E122QE226Q* mutants are very inefficient in qE which is only partially reversible (Kiss et al., 2008) and both exhibit reduced mobility of photosynthetic

complexes when compared to the *L17* lines where PsbS is over-expressed but fully functional at the same time. Irrespective of its exact location PsbS appears to be an elegant response of evolution to the conundrum of how to maintain the membrane crowded with light-harvesting complexes in a sufficiently fluid state to the proper functioning of dynamic membrane-wide processes and thus performs a function similar to that suggested to PufX in purple bacterial membranes (Siebert et al., 2004).

The information revealed by this study and the work of Betterle et al., (2009) into the structural basis of qE formation *in vivo* allows us to produce (together with Dr. Matthew Johnson and Professors Alexander Ruban and Conrad Mullineaux) the next step in a working model describing the structural changes (Figure 8.2). The left of Figure 8.2 depicts the lateral organisation of the PSII-LHCII supercomplexes within the grana thylakoid membranes in the dark and in low light states. Most of the PSII and LHCII units are organized into C<sub>2</sub>S<sub>2</sub>M<sub>2</sub> supercomplexes in *Arabidopsis* (Dekker and Boekema, 2005). There is evidence that these supercomplexes are stabilised by the binding of Mg<sup>2+</sup> ions at the lumenal surface (Dekker et al., 2002). Additional LHCII trimers (L-trimers) are dispersed amongst the C<sub>2</sub>S<sub>2</sub>M<sub>2</sub> supercomplexes. Upon ΔpH formation in excess light PsbS and certain LHC proteins are protonated displacing bound Mg<sup>2+</sup> (Barber et al., 1974; Walters et al., 1994; Li et al., 2004) and LHC-bound violaxanthin is converted to zeaxanthin by violaxanthin de-epoxidase (VDE). Together de-epoxidation and protonation co-operatively drive a conformational change within LHC units, which may depend on or be catalyzed in some way by PsbS as previously suggested (Horton et al., 2000; Dominici et al., 2002). The protonated zeaxanthin-binding conformation of LHCs is suggested to be more hydrophobic leading to the observed aggregation of LHCII within the

membrane, leading to the dissociation of the larger C<sub>2</sub>S<sub>2</sub>M<sub>2</sub> supercomplexes and thus the reduced size of the PSII EFs particle (Figure 8.2, right).

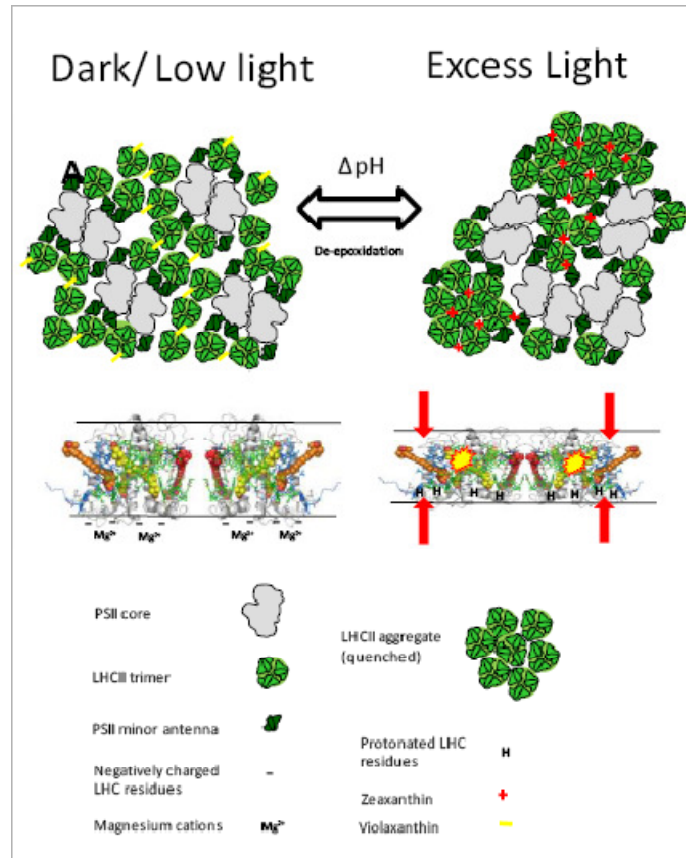


Figure 8.2. Model describing the changes in the ultrastructure and the macro-organisation of PSII-LHCII supercomplexes in the thylakoid membranes upon the switch from light-harvesting (low light) to the photoprotective state (high light). For more detailed explanation see description in text. Figure obtained from Dr Matthew Johnson, with permission.

While we cannot be sure of the exact identity of which of the minor antenna is dissociated from PSII and which remains attached, we suggest the most likely to be detached is CP24. CP24 is the most loosely bound to the supercomplex (Dekker and Bokema, 2005) and its dissociation would explain the reduced levels of the B4C subcomplex observed in high light (Betterle et al., 2009). LD spectroscopy suggests that the conformation of LHCII associated with the aggregated state of is somewhat

condensed (Ruban et al., 1997), thus explaining the increased hydrophobicity and reduced thickness of the thylakoid membrane observed under qE conditions here and by Murakami and Packer (1970b). We suggest that the condensed state of LHC proteins induced by protonation is the primary structural factor underlying the formation of internal dissipative pigment interactions, which may potentially be explained by any of the current xanthophyll-chlorophyll or chlorophyll-chlorophyll quenching models (Ruban et al., 2007; Ahn et al., 2008; Bode et al., 2009; Müller et al., 2010). The other feature, which is left deliberately unclear within our model, is the extent to which LHCII is functionally ‘detached’ from PSII. (Holzwarth et al., 2009) have suggested that based on time-resolved fluorescence data on *Arabidopsis* leaves that PSII and LHCII aggregates are functionally separated preventing energy transfer between them. However, another time-resolved fluorescence and fluorescence excitation spectroscopy study by Johnson and Ruban (2009) found no evidence of a ‘detached’ LHCII component during qE. Certainly the extremely crowded nature of the thylakoid grana membranes, which have a protein density of ~80% (Kirchhoff, 2008), does not appear to lend itself to large spatial separation of PSII and aggregated LHCII. However, since Förster energy transfer has a  $1/R^6$  distance dependency it is likely that large separations are unnecessary to facilitate energetic uncoupling. Further studies are needed to clarify these elements.

## **8.5. The role of light-harvesting antennae in controlling the mobility and the organisation of photosynthetic complexes in the thylakoid membranes**

One of the most important and intriguing research questions referring to the dynamics of thylakoid membrane components is which of the various chlorophyll-protein complexes in the grana are mobile and how the way they are organized in the membrane influences the size of ‘mobile fractions’ i.e. the proportion of chlorophyll fluorescence that can exchange between grana, due to chlorophyll-proteins escaping from one granum and diffusing through the stromal lamellae to another granum. Previous studies performed on individual light-harvesting antenna mutants of *Arabidopsis* indicated clearly that both minor and major antenna complexes contribute significantly to the specific supramolecular organisation of PSII-LHCII supercomplexes in the native thylakoid membranes (Yakushevskaya et al., 2003, Ruban et al., 2003; Kovács et al., 2006; Damkjaer et al., 2009). In the current work I decided to perform, for the first time, a comprehensive study on all light harvesting antenna mutants of *Arabidopsis* (including *chlorina* mutant deficient in formation of stable LHCII) by probing the dynamic and structural changes in the membrane upon the loss of individual light-harvesting antenna complexes.

My data show that the most vulnerable to changes in the mobility of chlorophyll fluorescence were mutants deficient in CP26 and CP24 minor antenna (*asLhcb5* and *koLhcb6*, respectively) which both exhibited a decreased size of the calculated mobile fractions (Figure 6.12.B). This finding corresponded to the significant alterations in the organisation of PSII and LHCII particles that were observed in freeze-fracture electron micrographs obtained from the intact

chloroplasts of the mutant plants. These dramatic changes could be explained given the role these proteins play in a formation of stable  $C_2S_2M_2$  supercomplexes allowing for a proper maintenance of high quantum efficiency (Yakushevskaya et al., 2003). CP26 is the minor antenna complex that is located specifically near CP43 and one of the trimers of major LHCII at both tips of the PSII-LHCII supercomplex (Yakushevskaya et al., 2003). Although CP26 is not required directly for energy transfer from LHCII to the PSII core it plays a crucial role in the assembly of PSII into the supercomplex and controls the macroorganization of supercomplexes in the thylakoid membrane. It has been shown before (Yakushevskaya et al., 2003) and further confirmed in my study that the absence of the CP26 subunits reduces the stability of PSII-LHCII supercomplexes and causes the grana to be more vulnerable to detergents (Figure 6.16.B). The alteration in the basic  $C_2S_2M_2$  supercomplexes is permanent and not compensated by any other complex suggesting that the presence of CP26 is indispensable for the optimum functioning of the thylakoid membrane (Yakushevskaya et al., 2003). Additionally, it has been suggested that CP26 may be engaged in promoting the membrane adhesion by decreasing locally the electrostatic repulsion of approaching thylakoids in the presence of electrostatic screening by cations allowing in this way van der Waals attraction forces between thylakoids to take effect (Król et al., 1995). Indeed, this is reflected in my results and could explain why the lack of CP26 dramatically slows down the kinetics of re-stacking of the thylakoid membranes upon the addition of  $Mg^{2+}$  to the chloroplast suspension (Figure 6.16.E). Moreover, the removal of CP26 minor antenna from the tips of the  $C_2S_2M_2$  supercomplexes (Yakushevskaya et al., 2003) leads to a greater packing of supercomplexes in the membrane which increases the already high level of macromolecular crowding (Kirchhoff, 2008). In my opinion, this would be a primary

cause of the reduced mobility that I observed in my FRAP measurements. A similar great decrease in chlorophyll fluorescence recovery was also measured in the *koLhcb6* mutants lacking CP24 minor antenna. Minor monomeric antenna CP24 is involved in the macro-organization of PSII serving a role in binding the “M” trimer to the core complexes (Dekker and Boekema, 2005). Lack of this protein results in impaired formation of C<sub>2</sub>S<sub>2</sub>M<sub>2</sub> supercomplexes and disrupts the functions of the PSII antenna. CP24-deficient plants showed a reduced connectivity between PSII centers, a decrease in maximum photochemical yield, inhibition of NPQ and state transitions (Kovács et al., 2006). This could be again the explanation of the much faster kinetics of solubilisation and a significant reduction in the amount of re-stacked membranes after Mg<sup>2+</sup> cations were added to the chloroplast suspension of the mutant plants (Figures 6.15-6.16). In addition, the results obtained from the CP24-depleted plants in this study support Kirchhoff’s idea that the problem with protein overcrowding in the membrane can be overcome solely by the very precise design of PSII reaction centers via supercomplex formation and supramolecular ordering of supercomplexes (Kirchhoff, 2008). Hence, any alterations of this specific organization should contribute to the changes in the overall dynamics of thylakoid membrane proteins which is the case as observed in the *koLhcb6* mutant plants. Since CP24 binds only a small fraction of thylakoid chlorophyll (less than 3%, (Dainese et al., 1990)) it seems that the absence of this protein would not have such a significant decrease in the mobility of chlorophyll fluorophores but it is rather a change in the entire organisation of photosynthetic proteins that contributes to the observed effect.

An interesting result was obtained in the case of mutants deprived of CP29 minor antenna proteins (*asLhcb4*). CP29 is normally located in a close proximity to the CP24 in the C<sub>2</sub>S<sub>2</sub>M<sub>2</sub> supercomplex (Yakushevskaya et al., 2003) and accounts for

3-8% of the chlorophyll content of thylakoid membranes (Green, 1982). The absence of this protein has a particularly detrimental consequence leading not only to the deficiency of CP24 (Andersson et al., 2001) but results also in the impaired formation of the entire supercomplex by releasing the strongly bound LHCII trimers (Yakushevskaya et al., 2003). This could explain why the *asLhcb4* mutants do not form any semi-crystalline arrays and the spacing between the PSII and LHCII particles is greatly enhanced (Figures 6.2 and 6.9). Because the PSII and LHCII particles are distributed more randomly in the membrane and do not exist in a form of the strongly-associated supercomplexes the thylakoids of the CP29-depleted plants are consequently the most vulnerable to detergents among all the minor antenna mutants (Figure 6.15.C). Interestingly, these plants showed also the greatest amount of the cation-mediated stacking of the thylakoids (Figure 6.15.D, Table 13). This would suggest that the absence of CP29 minor antenna and the resulting absence of the PSII-LHCII supercomplexes would promote significant stacking under these conditions. This confirms the view that the lateral segregation of protein complexes is likely to be an important factor that sustains the grana and stroma division (Dekker and Boekema, 2005). It should be pointed out that, similarly to the *koLhcb5* mutants, the lack of CP29 does not result in its replacement by another complex indicating its unique role in the oligomeric structure of PSII. Although the supercomplexes are not formed when CP29 is missing, I observed that the mean mobile fraction of chlorophyll fluorescence remained at a similar level as in the wild-type samples (Figure 6.12.B). It may seem unexpected as the more random distribution of PSII and LHCII particles in the grana membranes should most likely contribute to the changes in the dynamic properties of the membrane components (Kirchhoff, 2008). However, by taking into account the fact that the thylakoid membranes in the *asLhcb4* mutants



lack both CP29 and CP24 minor antenna (Andersson et al., 2001) it is possible that there would be actually more free space for the other complexes to diffuse and exchange between neighbouring grana which is large enough to compensate for the absence of supramolecular order. Indeed, there is some evidence that plants deficient in CP29 could possess PSII photosystems that are more labile than in the wild type (Andersson et al., 2001). However, my data indicate that this is not an effect that would substantially change the overall dynamics of all chlorophyll-proteins in the intact thylakoid membranes.

It is worth noticing that the use of minor antenna mutants in my study allowed to prove, for the first time, that the minor light-harvesting antenna are strongly associated with the PSII core dimers and are integral components of the particles present in EFs fracture faces. The suggestion that the particles on EFs fracture faces do not consist only of PSII dimeric cores but a part of the attached light-harvesting antenna complexes may also fracture with the EFs face has been put forward long time ago by Armond et al. (1977) who examined the freeze-fracture electron micrographs of plastid membranes from plants grown under intermediate light. Here it was possible to show directly that the sizes of individual EFs particles correspond most likely to a PSII core dimer ( $\sim 150 \text{ nm}^2$ ) with 2-3 minor antenna ( $\sim 30\text{-}40 \text{ nm}^2$ ) giving a total size of approximately  $200 \text{ nm}^2$  as observed in the electron micrographs (Figure 6.5) (Hankamer et al., 1997, Boekema et al., 1995, Caffari et al., 2009). This would suggest that the observed decrease in the EFs particle sizes which occurred in the qE state (Figure 5.7.C) and after photoinhibition (section 7, chapter IV) was due to the weakened affinity of the minor antenna for the PSII core dimer, resulting in them fracturing with the PFs faces.

Mutants lacking major trimeric light harvesting complexes LHCII (*asLhcb2*) showed also a slightly reduced mobility of chlorophyll fluorescence in the grana membranes, although the effect was not as pronounced as in the case of the *asLhcb5* and *koLhcb6* minor antenna mutants (Figure 6.12). It is somehow unexpected when taking into account the fact that Lhcb2 proteins are the most abundant in LHCII complexes and together with Lhcb1 and Lhcb3 bind about 60% of the total chlorophyll content of thylakoid membranes (Kovács et al., 2006). Because my FRAP measurements probe the mobility of chlorophyll-proteins it seems natural to suspect that the absence of the Lhcb2 apoprotein would severely reduce the size of calculated mobile fractions. In fact, as discussed before, the observed mobile fraction under low light intensities most likely belongs to a subpopulation of LHCII which might participate in state transitions and exchange between the PSII in the grana and PSI in the stroma lamellae regions (Allen, 2003). Moreover, LHCII antenna are the site where non-photochemical quenching (NPQ) occurs under light stress conditions (Ruban et al., 2007) which, as shown in the current work, involves structural rearrangement of the supercomplexes and enhanced clustering upon the formation of qE state. This suggests strongly that the dynamics and lateral diffusion of LHCII is required for this phenomenon. Why then the absence of the major Lhcb2 apoprotein exerts a relatively insignificant change in the overall dynamics of photosynthetic complexes in the thylakoid membrane? This could be well explained by the findings published first by Andersson et al. (2003) and Ruban et al. (2003). They indicate clearly that the lack of major LHCII antenna apoproteins results in an increase of the relative levels of other light harvesting proteins, in particular CP26, associated with PSII and Lhca4, associated with PSI. Under these conditions, a normally minor and monomeric complex, CP26, is organised into trimers and replace the lacking major

LHCII (Ruban et al., 2003). This could be the cause of the observed decrease in the average size of PSII particles from EFs fracture faces. It seems likely that in the absence of Lhcb2 apoproteins monomeric CP26 would lose its association with the PSII core and the trimers of these proteins would fracture now in the PFs faces as native trimers of LHCII usually do. What is more, depletion of the key LHCII polypeptides does not change the abundance and structure of PSII supercomplexes and the overall macro-organisation of PSII and LHCII particles is almost indistinguishable from the one found in the wild-type plants (Ruban et al, 2003). This was also confirmed in the analysis of freeze-fracture electron micrographs obtained in my study. In my opinion, this was most likely the reason why the reduction in the size of mobile fraction was not so significant as it would be expected. This suggests strongly that it is the overall organization of photosynthetic complexes that is crucial for their dynamics rather than a simple contribution of either the abundance or the absence of individual proteins. However, it should be stressed that although the general photosystem II macro-organisation is retained in the *asLhcb2* mutant plants the PSII-LHCII supercomplexes seem to be less stable and more vulnerable to detergent solubilisation as the results shown in Figure 6.15 suggest. In addition, my study confirmed the view that the major trimeric LHCII are not essential for grana stacking (Andersson et al., 2003, Dekker and Boekema, 2005) although their absence significantly slows down the process of re-stacking after the addition of  $Mg^{2+}$  (Figures 6.15-6.16).

The mutant that exhibited the least significant differences in the mobility of its photosynthetic complexes compared to the wild-type was *koLhcb3*. These plants do not express apoproteins encoded by the Lhcb3 genes, and thus do not form “M” trimers of LHCII as they consist most likely of Lhcb1 and Lhcb3 gene products

(Dekker and Boekema, 2005). Unlike Lhcb1 and Lhcb2, Lhcb3 does not possess the N-terminal phosphorylation site, and is therefore less likely to be phosphorylated and detach from PSII during state transitions suggesting that Lhcb3 does not belong to the mobile fraction of LHCII. It is less abundant than both Lhcb1-2 (accounting for ~11% of the apoprotein content of LHCII *in vivo* (Jackowski et al., 2001)) and the depletion of Lhcb3 is accompanied by overexpression of the two latter apoproteins (Damkjaer et al., 2009). It is proposed that Lhcb3 is not involved in light adaptation of photosynthesis and its main function is as an intermediary in light energy transfer from the main Lhcb1-2 antenna to the photosystem II core (Standfuss and Kühlbrandt, 2004) or that the protein acts as a modulator of the rate of state transitions by changing the level of phosphorylation of LHCII in both State 1 and State 2 (Damkjaer et al., 2009). In fact, *koLhcb3* mutants are very similar to the wild-type in respect of their growth, maximum photochemical yield and non-photochemical quenching (Damkjaer et al., 2009). It is reflected also in the results obtained in my study which show hardly any changes in the mobility of chlorophyll fluorophores in plants depleted in Lhcb3 proteins, together with no noticeable changes revealed in the overall organisation of PSII-LHCII supercomplexes. Although the previous findings indicated that the absence of Lhcb3 apoprotein results in the rotation of the M-trimer relative to its native position in the wild-type PSII macrostructure (Damkjaer et al., 2009) but this type of structural alteration is unlikely to be detected in my freeze-fracture electron micrographs. However, it is possible that the rotation of the M-trimer and its changed polypeptide composition increases its ability to migrate to PSI during state transitions in the mutant plants. Indeed, an enhanced degree of detergent-induced solubilization of *koLhcb3* membranes compared with the wild type suggests a somewhat looser association of

the PSII macrostructure (Figures 6.15-616). Nonetheless, in my opinion, the structural changes observed in the *koLhcb3* are still relatively insignificant and this is the major reason why the mobility of chlorophyll-proteins is practically unaffected upon the loss of the Lhcb3 apoproteins.

The most dramatic change in the mobility of chlorophyll-proteins was observed in the case of *chl* mutant of *Arabidopsis thaliana*. However, while all the investigated mutants lacking both minor and major antenna proteins exhibited either decreased or unchanged dynamics of chlorophyll fluorescence, the *chl* mutant showed a considerable rise in the size of calculated mobile fraction by almost 50% comparing to the wild type chloroplasts (Figure 6.12.C). These plants possess a recessive mutation on chromosome 1 leading to chlorophyll b not being synthesized which, in turn, has severe implications on the formation and stability of major and minor LHCII antenna complexes (Murray and Kohorn, 1991). In fact, the mutant does not form functional LHCII (although the level of translatable LHCII mRNA remains unchanged (Murray and Kohorn, 1991)) that could efficiently harvest light energy and transfer it to the PSII core reaction centers. The only photosynthetic proteins found in the mutant plants are the PSII core complexes and some of the monomeric LHC antenna (mainly CP26) (Havaux et al., 2007; Dall'Osto et al., 2010). This is strongly reflected in the yellow green colour of the leaves under all light intensities and slower growth and senescence than the wild type (Murray and Kohorn, 1991). The chlorophyll content is dramatically reduced but all the major polypeptides, and thus complexes of the wild-type thylakoids are present in the mutant, with the only exception of major and minor LHCII (Murray and Kohorn 1991; Havaux et al. 2007). Despite the fact that the chloroplasts are slightly lighter in appearance, the thylakoid membranes are still intact and do form appressed grana that

are visible either on thin-section electron micrographs (Murray and Kohorn, 1991) or confocal micrographs obtained in this study (Figure 8.3). This might be due to the presence of CP26 monomeric antenna which were suggested to take part in the stacking in a similar way as the major trimeric LHCII (Król et al., 1995).

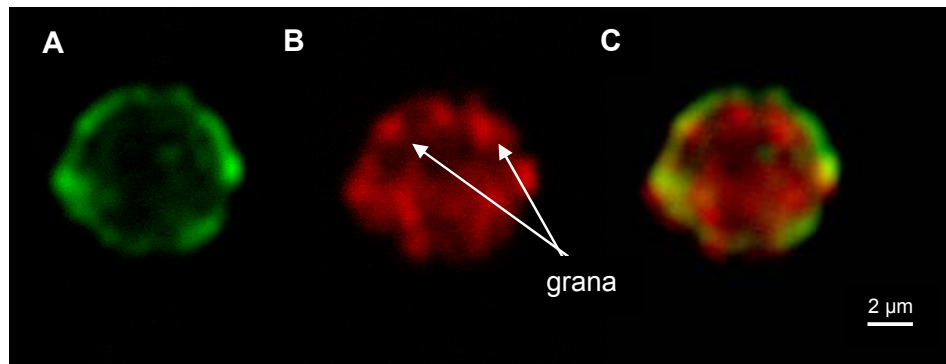


Figure 8.3. Confocal images of the intact chloroplast isolated from *chl* mutant of *Arabidopsis*. (A). Fluorescence of BODIPY FL C<sub>12</sub> showing intactness of the chloroplast envelope. (B). Autofluorescence of chlorophyll. Note the presence of grana membranes as indicated by arrows. (C). Merged (A) and (B).

However, it seems that the grana structure in the mutant plants is significantly less stable than in the wild-type and the protein-protein interactions within the thylakoid membranes are much weakened which is why I observed the highest degree of solubilisation and the lowest degree of re-stacking as shown in Figure 6.15.C-D. FRAP measurements on the intact chloroplasts isolated from the *chl* mutant plants revealed that the fluorescence recovery of the bleached grana was much faster and more complete on the timescale of experiment duration indicating greater mobilization of chlorophyll-proteins than in native membranes of wild-type chloroplasts. Since LHCII antenna proteins in those plants are missing and this is compensated by the elevated PSII core protein content (Murray and Kohorn, 1991) the most probable source of the observed increase in the size of mobile fractions are

PSII photosystems. It is clear that the macro-organisation of photosynthetic complexes is severely disrupted under these specific conditions leading to a much random distribution of the particles and the existence of spaces which are devoid of protein complexes (Figure 6.3.B) but at the same time the regions with enhanced particle density could be observed (Figure 6.3.C). This was not the case in the chlorophyll b-deficient mutant of barley which exhibited a significant increase in PSII density and the formation of semi-crystalline arrays could still be observed (Simpson, 1979). In my study the overall density of photosystems occupying EFs fracture faces was not significantly changed although a slight tendency of enhanced clustering and closer nearest-neighbour distances was detected (Figure 6.10, Table 8). Given the fact that the relative sizes of the EFs fracture faces were larger than in the wild-type (indicating the existence of bigger grana as found previously in the *chlorina* mutants of barley (Simpson, 1979)) the total protein content of PSII might be elevated and this would explain the increase in abundance of bands corresponding to the PSII core complex reported by Murray and Kohorn (1991). Nevertheless, the freeze-fracture electron micrographs obtained from *chl* mutant in my study revealed the presence of large spaces within the grana regions completely devoid of any particles (Figure 6.3). This suggests that there might be more free space available for protein diffusion than in the wild-type membranes and that the exchange of chlorophyll-proteins (PSII, in particular) between the neighbouring grana would occur more easily. In this case, the macromolecular crowding and specific organization of supercomplexes would be no longer a limiting factor preventing from the protein movement which indicates that these elements are crucial in controlling the dynamics of the thylakoid membrane components.

There are numerous reports indicating that the loss of individual light-harvesting antenna impairs the formation of the photoprotective state under high irradiances (e.g. Andersson et al., 2001, Yakushevskaya et al., 2003, Kovács et al., 2006, Damkjaer et al., 2009). As found in the current study, the NPQ formation is associated with a structural change in the thylakoid membrane ultrastructure and the macro-organisation of photosynthetic complexes. This results in the decreased level of protein diffusion after the photoprotective state is established. Here, in the studies performed on the light-harvesting antenna mutants, I confirm this observation by finding a strong relationship which exists between the degree of protein diffusion in a dark-adapted state and the efficiency of qE formation after high light illumination (Figure 6.14). This suggests strongly that in order to be able to undergo the described structural change in the NPQ state the membrane must be already fluid enough under low light to allow these changes to occur once the light intensity increases. This is the reason why the highest amount of NPQ could be formed only in the plants which have the highest level of protein mobility in a dark-adapted state. Consequently, a low level of protein diffusion under low light adaptation resulting from the enhanced packing of photosynthetic complexes makes it harder for the structural change to occur upon the increase in light intensity and therefore the photoprotective state is much less efficient in such plants. This confirms the recent finding by Haferkamp et al. (2010) who showed that in overcrowded isolated grana thylakoids the efficiency of light-harvesting by PSII is significantly decreased, most likely due to excited state quenching in LHCII.



## **8.6. Mobility of chlorophyll-proteins is dependent on the macromolecular crowding in the thylakoid membranes**

The results presented in this thesis indicate explicitly that the diffusion of chlorophyll-proteins within the grana membranes and their exchange between the neighbouring grana is very much restricted to only <25% (dependent on different physiological conditions) of their total population. The remaining fraction of photosynthetic complexes appears either completely immobile or the protein movement is confined to a limited space and therefore cannot be measured by FRAP technique which aims at detecting a long-range diffusion (over a micron or more) (Mullineaux et al., 1997; Mullineaux, 2004). As mentioned before, one of the key factors which can hinder free protein diffusion in a membrane preventing them from diffusing at their theoretical limit includes protein-protein interactions and collisions with other molecules. This is the case of thylakoid membranes which belong to the most crowded biological membranes in nature with lots of interactions present between individual photosynthetic complexes which are required for maintaining the optimal efficiency of light-harvesting and transfer the absorbed energy to the reaction centers (Kirchhoff, 2008). This dense macromolecular crowding can be clearly seen in the freeze-fracture electron micrographs obtained in my study. The quantitative analysis of the distribution of PSII and LHCII particles in the fracture faces allowed me to detect even subtle changes in the macromolecular organisation of PSII-LHCII supercomplexes that occur in the intact membrane under different conditions and upon different mutations in the thylakoid membrane components. These changes can be directly correlated with the sizes of mobile fractions that were measured in intact chloroplasts following the FRAP approach (Figures 5.10 and 6.13). The image that emerges from these linear relationships is

that the degree of macromolecular crowding directly influences the amount of chlorophyll-proteins able to diffuse out of the grana on a timescale of a few minutes. This suggests that one of the major factors controlling the dynamics of the thylakoid membrane proteins is their distribution and the level of packing in the membrane area reflecting the level of protein-protein interactions. This is in agreement with the study of Kirchhoff et al (2008) who have shown that the ‘dilution’ of the isolated grana membranes with additional lipids and a breakdown of a protein network by incubation with low-salt buffers leads to a considerable increase in the mobility of chlorophyll-proteins. In my study I extended this finding to a much more relevant system *in vivo*: the thylakoid membrane network in intact chloroplasts. This allowed me to test also the effect of grana stacking in restricting the mobility of thylakoid membrane proteins. Removal of  $Mg^{2+}$  cations from the chloroplast suspension buffer resulted in the unstacking of the thylakoid membranes leading to destabilization of protein-protein interactions (by reduction in electrostatic screening of negative surface charges as reported e.g. by Barber (1982), Harrison and Allen (1992), Kirchhoff et al. (2004)) and a randomized distribution of photosynthetic complexes (due to the absence of spatial segregation into grana and stroma lamellae regions) (Izawa and Good, 1966; Murakami and Packer, 1971; Staehelin, 1976). Under these conditions there was a noticeable increase in the size of mobile fraction of chlorophyll-proteins (Figure 4.8) suggesting strongly that the concentration of pigment-proteins within the grana regions significantly restricts their movement. However, as mentioned in the chapter I, such concentrations of fluorophores in a limited membrane space could be beneficial since it increases significantly the probability that the light photons will be captured with the greatest possible efficiency which was required in a course of evolution to optimise photosynthesis

process in shade environments after plants colonised the land (Mullineaux, 2005; Kirchhoff, 2008).

# **Chapter IX**

## **Summary and future work**

In this study I employed confocal FRAP technique combined with the freeze-fracture electron microscopy to visualise the mobility and distribution of photosynthetic complexes in the intact thylakoid membranes of higher plants. Firstly, I showed that the FRAP experiments can be successfully applied for measuring the mobile fractions of chlorophyll-proteins in the grana membranes of isolated intact chloroplasts and that this mobility genuinely reflects the lateral diffusion of proteins and their exchange between the neighbouring grana. Secondly, I provided direct evidence that the dynamic changes in the distribution of photosynthetic complexes are involved in the two high-light related physiological phenomena, namely photoinhibition and non-photochemical quenching. My study indicates that these two phenomena work in opposing ways with regards to the level of mobility of chlorophyll-proteins with the higher mobile fraction and greater spacing between the complexes observed in the photoinhibited membranes and the lower mobile fraction accompanied by the noticeable clustering of PSII and LHCII particles in the photoprotective state. Thirdly, my work allowed to identify some key elements that are responsible for controlling the mobility under different physiological conditions such as: (1) requirement of phosphorylation of PSII core complexes after photoinhibition, (2) PsbS protein enhancing the membrane fluidity in a dark-adapted state and decreasing it after light treatment, (3) different xanthophyll composition of light-harvesting antenna with particular attention being paid to zeaxanthin which decreases the size of mobile fraction by enhancing the membrane hydrophobicity, thus promoting the clustering of photosynthetic complexes upon qE formation (4) the degree of macromolecular crowding and the organisation of PSII-LHCII supercomplexes in the grana membranes which is dependent strongly on individual light-harvesting proteins, the minor antenna complexes in particular.

Lastly, I developed a new approach of studying the mobility of photosynthetic complexes in a completely *in vivo* environment by performing FRAP experiments on individual chloroplasts in intact leaves. Using a better optics of a confocal microscope allowed me to visualise individual grana membranes within a single chloroplast inside a plant cell without a need for image processing and made it possible to generate a two-dimensional ‘bleaching hole’ confined to the particular area of an investigated chloroplast. The sizes of mobile fractions obtained from such experiments were similar to the sizes obtained from FRAP measurements performed on isolated chloroplasts confirming that the new approach can be successfully applied to study the diffusion of thylakoid membrane proteins in intact leaves. This opens up a range of new research questions regarding the dynamics of photosynthetic complexes which could be addressed following this approach, for example:

1. Using transgenic tobacco mutants with the altered phosphorylation site in the D1 subunit of PSII core complex it will be possible to determine fully the role of phosphorylation cycle in the PSII repair and turnover during photoinhibition. This study, which is complementary to the one presented in the chapter IV, has already begun (see chapter VII for details) but further experiments are needed, especially under photoinhibitory conditions.
2. Mobility of photosynthetic complexes can be monitored throughout the whole plant life cycle from the early-growth stage when the thylakoid membranes and the photosynthetic apparatus are assembled together until the stage of leaf senescence in which the photosynthetic membranes and their components are disintegrated following a programmed cell death.

3. Protein movements can be investigated in details during the biogenesis and assembly of the thylakoid membranes, for example by GFP-tagging and their visualization under a confocal microscope following a change in their distribution upon the greening of the etiolated leaves.
4. The study of dynamics of photosynthetic complexes can be extended to plant species which are adapted to different habitats, for example plants from shade and high-light environments, plants grown in cold and hot climates etc. including the plants with C4 and CAM type of photosynthesis. In the latter case, three different types of chloroplasts can be investigated and compared at the same time (chloroplasts from stomata guard cells plus mesophyll and bundle sheath cells) allowing to assess the extent to which diffusion of thylakoid membrane proteins is influenced by a different type of metabolism that is characteristic for each cell type.

## References

- Adir, N., Zer, H., Shochat, S., and Ohad, I.** (2003). Photoinhibition - a historical perspective. *Photosynth Res* **76**, 343-370.
- Ahn, T., Avenson, T., Ballottari, M., Cheng, Y., Niyogi, K., Bassi, R., and Fleming, G.** (2008). Architecture of a charge-transfer state regulating light harvesting in a plant antenna protein. *Science* **320**, 794-797.
- Allen, J.** (2003). Botany. State transitions--a question of balance. *Science* **299**, 1530-1532.
- Allen, J., and Forsberg, J.** (2001). Molecular recognition in thylakoid structure and function. *Trends Plant Sci* **6**, 317-326.
- Anderson, J.** (1975). The molecular organization of chloroplast thylakoids. *Biochim Biophys Acta* **416**, 191-235.
- Andersson, B., and Anderson, J.M.** (1980). Lateral heterogeneity in the distribution of chlorophyll-protein complexes of the thylakoid membranes of spinach chloroplasts. *Biochim Biophys Acta* **593**, 427-440.
- Andersson, J., Walters, R., Horton, P., and Jansson, S.** (2001). Antisense inhibition of the photosynthetic antenna proteins CP29 and CP26: implications for the mechanism of protective energy dissipation. *Plant Cell* **13**, 1193-1204.
- Andersson, J., Wentworth, M., Walters, R., Howard, C., Ruban, A., Horton, P., and Jansson, S.** (2003). Absence of the Lhcb1 and Lhcb2 proteins of the light-harvesting complex of photosystem II - effects on photosynthesis, grana stacking and fitness. *Plant J* **35**, 350-361.



- Armond, P.A., Staehelin, L.A., and Arntzen, C.J.** (1977). Spatial relationship of photosystem I, photosystem II, and the light-harvesting complex in chloroplast membranes. *J Cell Biol* **73**, 400-418.
- Aro, E., Suorsa, M., Rokka, A., Allahverdiyeva, Y., Paakkarinen, V., Saleem, A., Battchikova, N., and Rintamäki, E.** (2005). Dynamics of photosystem II: a proteomic approach to thylakoid protein complexes. *J Exp Bot* **56**, 347-356.
- Aro, E.M., Virgin, I., and Andersson, B.** (1993). Photoinhibition of Photosystem II. Inactivation, protein damage and turnover. *Biochim Biophys Acta* **1143**, 113-134.
- Baena-González, E., and Aro, E.** (2002). Biogenesis, assembly and turnover of photosystem II units. *Philos Trans R Soc Lond B Biol Sci* **357**, 1451-1459; discussion 1459-1460.
- Baena-Gonzalez, E., Barbato, R., and Aro, E.** (1999). Role of phosphorylation in the repair cycle and oligomeric structure of photosystem II. *Planta* **208**, 196-204.
- Bailey, S., Horton, P., and Walters, R.** (2004). Acclimation of *Arabidopsis thaliana* to the light environment: the relationship between photosynthetic function and chloroplast composition. *Planta* **218**, 793-802.
- Bailey, S., Walters, R., Jansson, S., and Horton, P.** (2001). Acclimation of *Arabidopsis thaliana* to the light environment: the existence of separate low light and high light responses. *Planta* **213**, 794-801.
- Barbato, R., Friso, G., Rigoni, F., Dalla Vecchia, F., and Giacometti, G.** (1992). Structural changes and lateral redistribution of photosystem II during donor side photoinhibition of thylakoids. *J Cell Biol* **119**, 325-335.

- Barber, J.** (1982). Influence of surface-charges on thylakoid structure and function. *Annu Rev Plant Physiol and Plant Mol Biol* **33**, 261-295.
- Barber, J.** (2003). Photosystem II: the engine of life. *Q Rev Biophys* **36**, 71-89.
- Barber, J.** (2007). Biological solar energy. *Philos Transact A Math Phys Eng Sci* **365**, 1007-1023.
- Barber, J., and Andersson, B.** (1992). Too much of a good thing: light can be bad for photosynthesis. *Trends Biochem Sci* **17**, 61-66.
- Barber, J., Mills, J., and Nicolson, J.** (1974). Studies with cation specific ionophores show that within the intact chloroplast  $Mg^{++}$  acts as the main exchange cation for  $H^+$  pumping. *FEBS Lett* **49**, 106-110.
- Bassi, R., Croce, R., Cugini, D., and Sandonà, D.** (1999). Mutational analysis of a higher plant antenna protein provides identification of chromophores bound into multiple sites. *Proc Natl Acad Sci U S A* **96**, 10056-10061.
- Bellafiore, S., Barneche, F., Peltier, G., and Rochaix, J.** (2005). State transitions and light adaptation require chloroplast thylakoid protein kinase STN7. *Nature* **433**, 892-895.
- Ben-Shem, A., Frolow, F., and Nelson, N.** (2003). Crystal structure of plant photosystem I. *Nature* **426**, 630-635.
- Bennett, J.** (1977). Phosphorylation of chloroplast membrane polypeptides. *Nature* **269**, 344-346.
- Bennett, J.** (1980). Chloroplast phosphoproteins. Evidence for a thylakoid-bound phosphoprotein phosphatase. *Eur J Biochem* **104**, 85-89.
- Bennett, J.** (1983). Regulation of photosynthesis by reversible phosphorylation of the light-harvesting chlorophyll a/b protein. *Biochem J* **212**, 1-13.

- Bennett, J.** (1984). Thylakoid protein phosphorylation: in vitro and in vivo. *Biochem Soc Trans* **12**, 771-774.
- Bergantino, E., Segalla, A., Brunetta, A., Teardo, E., Rigoni, F., Giacometti, G., and Szabo, I.** (2003). Light- and pH-dependent structural changes in the PsbS subunit of photosystem II. *Proc Natl Acad Sci U S A* **100**, 15265-15270.
- Berner, R.** (1997). Paleoclimate - The rise of plants and their effect on weathering and atmospheric CO<sub>2</sub>. *Science* **276**, 544-546.
- Betterle, N., Ballottari, M., Zorzan, S., de Bianchi, S., Cazzaniga, S., Dall'Osto, L., Morosinotto, T., and Bassi, R.** (2009). Light-induced Dissociation of an Antenna Hetero-oligomer Is Needed for Non-photochemical Quenching Induction. *J Biol Chem* **284**, 15255-15266.
- Bilger, W., and Bjorkman, O.** (1994). Relationships among violaxanthin deepoxidation, thylakoid membrane conformation, and nonphotochemical chlorophyll fluorescence quenching in leaves of cotton (*Gossypium hirsutum* L.). *Planta* **193**, 238-246.
- Blackwell, M., Gibas, C., Gygax, S., Roman, D., and Wagner, B.** (1994). The plastoquinone diffusion coefficient in chloroplasts and its mechanistic implications. *Biochim Biophys Acta* **1183**, 533-543.
- Bode, S., Quentmeier, C.C., Liao, P.N., Hafi, N., Barros, T., Wilk, L., Bittner, F., and Walla, P.J.** (2009). On the regulation of photosynthesis by excitonic interactions between carotenoids and chlorophylls. *Proc Natl Acad Sci U S A* **106**, 12311-12316.
- Boekema, E., van Breemen, J., van Roon, H., and Dekker, J.** (2000). Arrangement of photosystem II supercomplexes in crystalline macrodomains

within the thylakoid membrane of green plant chloroplasts. *J Mol Biol* **301**, 1123-1133.

**Boekema, E.J., van Roon, H., Calkoen, F., Bassi, R., and Dekker, J.P.** (1999).

Multiple types of association of photosystem II and its light-harvesting antenna in partially solubilized photosystem II membranes. *Biochemistry* **38**, 2233-2239.

**Boekema, E.J., Hankamer, B., Bald, D., Kruij, J., Nield, J., Boonstra, A.F.,**

**Barber, J., and Rögner, M.** (1995). Supramolecular structure of the photosystem II complex from green plants and cyanobacteria. *Proc Natl Acad Sci U S A* **92**, 175-179.

**Bonardi, V., Pesaresi, P., Becker, T., Schleiff, E., Wagner, R., Pfannschmidt, T.,**

**Jahns, P., and Leister, D.** (2005). Photosystem II core phosphorylation and photosynthetic acclimation require two different protein kinases. *Nature* **437**, 1179-1182.

**Branton, D., Bullivant, S., Gilula, N.B., Karnovsky, M.J., Moor, H.,**

**Mühlethaler, K., Northcote, D.H., Packer, L., Satir, B., Satir, P., Speth, V., Staehlin, L.A., Steere, R.L., and Weinstein, R.S.** (1975). Freeze-etching nomenclature. *Science* **190**, 54-56.

**Brumfeld, V., Charuvi, D., Nevo, R., Chuartzman, S., Tsabari, O., Ohad, I.,**

**Shimoni, E., and Reich, Z.** (2008). A note on three-dimensional models of higher-plant thylakoid networks. *Plant Cell* **20**, 2546-2549; author reply 2549-2551.

**Buick, R.** (2008). When did oxygenic photosynthesis evolve? *Philos Trans R Soc*

*Lond B Biol Sci* **363**, 2731-2743.

- Caffarri, S., Kouril, R., Kereiche, S., Boekema, E., and Croce, R.** (2009). Functional architecture of higher plant photosystem II supercomplexes. *EMBO J* **28**, 3052-3063.
- Chapman, A.** (2009). Numbers of living species in Australia and the World. In A report for the Australian Biological Resources Study, (Toowoomba: Australian Biodiversity Information Services), pp. 1-84.
- Chapman, R.L., and Staehelin, L.A.** (1986). Freeze-fracture (-etch) electron microscopy. In *Ultrastructure Techniques for Microorganisms*, H.C. Aldrich and W.J. Todd, eds (New York: Plenum Press), pp. 213-240.
- Chuartzman, S., Nevo, R., Shimoni, E., Charuvi, D., Kiss, V., Ohad, I., Brumfeld, V., and Reich, Z.** (2008). Thylakoid membrane remodeling during state transitions in Arabidopsis. *Plant Cell* **20**, 1029-1039.
- Cole, N.B., Smith, C.L., Sciaky, N., Terasaki, M., Edidin, M., and Lippincott-Schwartz, J.** (1996). Diffusional mobility of Golgi proteins in membranes of living cells. *Science* **273**, 797-801.
- Consoli, E., Croce, R., Dunlap, D., and Finzi, L.** (2005). Diffusion of light-harvesting complex II in the thylakoid membranes. *EMBO Rep* **6**, 782-786.
- Croce, R., Canino, G., Ros, F., and Bassi, R.** (2002). Chromophore organization in the higher-plant photosystem II antenna protein CP26. *Biochemistry* **41**, 7334-7343.
- Crouchman, S., Ruban, A., and Horton, P.** (2006). PsbS enhances nonphotochemical fluorescence quenching in the absence of zeaxanthin. *FEBS Lett* **580**, 2053-2058.

- Dainese, P., Hoyer-Hansen, G., and Bassi, R.** (1990). The resolution of chlorophyll a/b binding proteins by a preparative method based on flat bed isoelectro focusing. *Photochem Photobiol* **51**, 511-519.
- Dall'Osto, L., Caffarri, S., and Bassi, R.** (2005). A mechanism of nonphotochemical energy dissipation, independent from PsbS, revealed by a conformational change in the antenna protein CP26. *Plant Cell* **17**, 1217-1232.
- Dall'Osto, L., Cazzaniga, S., Havaux, M., and Bassi, R.** (2010). Enhanced photoprotection by protein-bound vs free xanthophyll pools: a comparative analysis of chlorophyll b and xanthophyll biosynthesis mutants. *Mol Plant* **3**, 576-593.
- Daum, B., Nicastro, D., Austin, J., McIntosh, J.R., and Kühlbrandt, W.** (2010). Arrangement of photosystem II and ATP synthase in chloroplast membranes of spinach and pea. *Plant Cell* **22**, 1299-1312.
- Dekker, J., and Boekema, E.** (2005). Supramolecular organization of thylakoid membrane proteins in green plants. *Biochim Biophys Acta* **1706**, 12-39.
- Dekker, J.P., Germano, M., van Roon, H., and Boekema, E.J.** (2002). Photosystem II solubilizes as a monomer by mild detergent treatment of unstacked thylakoid membranes. *Photosynth Res* **72**, 203-210.
- Dias, N., and Stein, C.A.** (2002). Antisense oligonucleotides: basic concepts and mechanisms. *Mol Cancer Ther* **1**, 347-355.
- Dobrikova, A., Petkanchin, I., and Taneva, S.** (2002). Temperature-induced changes in the surface electric properties of thylakoids and photosystem II membrane fragments. *Colloids and Surfaces A-Physicochemical and Engineering Aspects* **209**, 185-192.

- Dominici, P., Caffarri, S., Armenante, F., Ceoldo, S., Crimi, M., and Bassi, R.** (2002). Biochemical properties of the PsbS subunit of photosystem II either purified from chloroplast or recombinant. *J Biol Chem* **277**, 22750-22758.
- Drepper, F., Carlberg, I., Andersson, B., and Haehnel, W.** (1993). Lateral diffusion of an integral membrane protein: Monte Carlo analysis of the migration of phosphorylated light-harvesting complex II in the thylakoid membrane. *Biochemistry* **32**, 11915-11922.
- Eshaghi, S., Andersson, B., and Barber, J.** (1999). Isolation of a highly active PSII-LHCII supercomplex from thylakoid membranes by a direct method. *FEBS Lett* **446**, 23-26.
- Fristedt, R., Granath, P., and Vener, A.V.** (2010). A protein phosphorylation threshold for functional stacking of plant photosynthetic membranes. *PLoS One* **5**, e10963.
- Fristedt, R., Willig, A., Granath, P., Crèvecoeur, M., Rochaix, J., and Vener, A.** (2009). Phosphorylation of photosystem II controls functional macroscopic folding of photosynthetic membranes in Arabidopsis. *Plant Cell* **21**, 3950-3964.
- Funk, C., Adamska, I., Green, B.R., Andersson, B., and Renger, G.** (1995). The nuclear-encoded chlorophyll-binding photosystem II-S protein is stable in the absence of pigments. *J Biol Chem* **270**, 30141-30147.
- Garab, G., and Mannella, C.A.** (2008). Reply: On Three-dimensional models of higher-plant thylakoid networks: Elements of consensus, Controversies, and Future Experiments. *Plant Cell* **20**, 2549-2551.
- Garber, M.P., and Steponkus, P.L.** (1976). Alterations in Chloroplast Thylakoids during Cold Acclimation. *Plant Physiol* **57**, 681-686.

- Gounaris, K., Brain, A., Quinn, P., and Williams, W.** (1984). Structural reorganization of chloroplast thylakoid membranes in response to heat-stress. *Biochim Biophys Acta* **766**, 198-208.
- Green, B.R.** (1982). Protein synthesis by isolated *Acetabularia* chloroplasts. Synthesis of the two minor chlorophyll a complexes in vitro. *Eur J Biochem* **128**, 543-546.
- Habeeb, A., and Hiramoto, R.** (1968). Reaction of proteins with glutaraldehyde. *Arch Biochem Biophys* **126**, 16-26.
- Haferkamp, S., and Kirchhoff, H.** (2008). Significance of molecular crowding in grana membranes of higher plants for light harvesting by photosystem II. *Photosynth Res* **95**, 129-134.
- Haferkamp, S., Haase, W., Pascal, A.A., van Amerongen, H., and Kirchhoff, H.** (2010). Efficient light harvesting by photosystem II requires an optimized protein packing density in Grana thylakoids. *J Biol Chem* **285**, 17020-17028.
- Hankamer, B., Nield, J., Zheleva, D., Boekema, E., Jansson, S., and Barber, J.** (1997). Isolation and biochemical characterisation of monomeric and dimeric photosystem II complexes from spinach and their relevance to the organisation of photosystem II in vivo. *Eur J Biochem* **243**, 422-429.
- Harrison, M.A., and Allen, J.F.** (1992). Protein phosphorylation and Mg<sup>2+</sup> influence light harvesting and electron transport in chloroplast thylakoid membrane material containing only the chlorophyll-a/b-binding light-harvesting complex of photosystem II and photosystem I. *Eur J Biochem* **204**, 1107-1114.
- Havaux, M., Dall'Osto, L., Cuiné, S., Giuliano, G., and Bassi, R.** (2004). The effect of zeaxanthin as the only xanthophyll on the structure and function of



the photosynthetic apparatus in *Arabidopsis thaliana*. *J Biol Chem* **279**, 13878-13888.

**Havaux, M., Dall'osto, L., and Bassi, R.** (2007). Zeaxanthin has enhanced antioxidant capacity with respect to all other xanthophylls in *Arabidopsis* leaves and functions independent of binding to PSII antennae. *Plant Physiol* **145**, 1506-1520.

**Heslop-Harrison, J.** (1963). Structure and morphogenesis of lamellar systems in grana-containing chloroplasts. I. Membrane structure and lamellar architecture. *Planta* **60**, 243-260.

**Holzwarth, A.R., Miloslavina, Y., Nilkens, M., and Jahns, P.** (2009). Identification of two quenching sites active in the regulation of photosynthetic light-harvesting studied by time-resolved fluorescence. *Chem Phys Lett* **483**, 262-267.

**Horton, P., Ruban, A., and Walters, R.** (1996). Regulation of light harvesting in green plants. *Annu Rev Plant Physiol Plant Mol Biol* **47**, 655-684.

**Horton, P., Ruban, A.V., and Wentworth, M.** (2000). Allosteric regulation of the light-harvesting system of photosystem II. *Philos Trans R Soc Lond B Biol Sci* **355**, 1361-1370.

**Horton, P., Wentworth, M., and Ruban, A.** (2005). Control of the light harvesting function of chloroplast membranes: the LHCII-aggregation model for non-photochemical quenching. *FEBS Lett* **579**, 4201-4206.

**Horton, P., Johnson, M., Perez-Bueno, M., Kiss, A., and Ruban, A.** (2008). Photosynthetic acclimation: does the dynamic structure and macro-organisation of photosystem II in higher plant grana membranes regulate light harvesting states? *FEBS J* **275**, 1069-1079.

- Horton, P., Ruban, A., Rees, D., Pascal, A., Noctor, G., and Young, A.** (1991). Control of the light-harvesting function of chloroplast membranes by aggregation of the LHCII chlorophyll-protein complex. *FEBS Lett* **292**, 1-4.
- Ilioaia, C., Johnson, M.P., Duffy, C.D., Pascal, A.A., van Grondelle, R., Robert, B., and Ruban, A.V.** (2011). Origin of absorption changes associated with photoprotective energy dissipation in the absence of zeaxanthin. *J Biol Chem* **286**, 91-98.
- Iwai, M., Yokono, M., Inada, N., and Minagawa, J.** (2010). Live-cell imaging of photosystem II antenna dissociation during state transitions. *Proc Natl Acad Sci U S A* **107**, 2337-2342.
- Izawa, S., and Good, N.** (1966). Effect of Salts and Electron Transport on the Conformation of Isolated Chloroplasts. II. Electron Microscopy. *Plant Physiol* **41**, 544-552.
- Jackowski, G., Kacprzak, K., and Jansson, S.** (2001). Identification of Lhcb1/Lhcb2/Lhcb3 heterotrimers of the main light-harvesting chlorophyll a/b-protein complex of Photosystem II (LHC II). *Biochim Biophys Acta* **1504**, 340-345.
- Jansson, S.** (1994). The light-harvesting chlorophyll a/b-binding proteins. *Biochim Biophys Acta* **1184**, 1-19.
- Jansson, S.** (1999). A guide to the Lhc genes and their relatives in Arabidopsis. *Trends Plant Sci* **4**, 236-240.
- Johnson, M.P., and Ruban, A.V.** (2009). Photoprotective energy dissipation in higher plants involves alteration of the excited state energy of the emitting chlorophyll(s) in the light harvesting antenna II (LHCII). *J Biol Chem* **284**, 23592-23601.

- Johnson, M., and Ruban, A.** (2010). Arabidopsis plants lacking PsbS protein possess photoprotective energy dissipation. *Plant J* **61**, 283-289.
- Johnson, M., Davison, P., Ruban, A., and Horton, P.** (2008). The xanthophyll cycle pool size controls the kinetics of non-photochemical quenching in *Arabidopsis thaliana*. *FEBS Lett* **582**, 262-266.
- Johnson, M., Havaux, M., Triantaphylidès, C., Ksas, B., Pascal, A., Robert, B., Davison, P., Ruban, A., and Horton, P.** (2007). Elevated zeaxanthin bound to oligomeric LHCII enhances the resistance of *Arabidopsis* to photooxidative stress by a lipid-protective, antioxidant mechanism. *J Biol Chem* **282**, 22605-22618.
- Johnson, M., Perez-Bueno, M., Zia, A., Horton, P., and Ruban, A.** (2009). The zeaxanthin-independent and zeaxanthin-dependent qE components of nonphotochemical quenching involve common conformational changes within the photosystem II antenna in *Arabidopsis*. *Plant Physiol* **149**, 1061-1075.
- Kanervo, E., Suorsa, M., and Aro, E.** (2005). Functional flexibility and acclimation of the thylakoid membrane. *Photochem Photobiol Sci* **4**, 1072-1080.
- Kasahara, M., Kagawa, T., Oikawa, K., Suetsugu, N., Miyao, M., and Wada, M.** (2002). Chloroplast avoidance movement reduces photodamage in plants. *Nature* **420**, 829-832.
- Kereïche, S., Kiss, A., Kouril, R., Boekema, E., and Horton, P.** (2010). The PsbS protein controls the macro-organisation of photosystem II complexes in the grana membranes of higher plant chloroplasts. *FEBS Lett* **584**, 759-764.
- Kirchhoff, H.** (2008). Molecular crowding and order in photosynthetic membranes. *Trends Plant Sci* **13**, 201-207.

- Kirchhoff, H., Mukherjee, U., and Galla, H.** (2002). Molecular architecture of the thylakoid membrane: Lipid diffusion space for plastoquinone. *Biochemistry* **41**, 4872-4882.
- Kirchhoff, H., Tremmel, I., Haase, W., and Kubitscheck, U.** (2004). Supramolecular photosystem II organization in grana thylakoid membranes: evidence for a structured arrangement. *Biochemistry* **43**, 9204-9213.
- Kirchhoff, H., Haferkamp, S., Allen, J., Epstein, D., and Mullineaux, C.** (2008). Protein diffusion and macromolecular crowding in thylakoid membranes. *Plant Physiol* **146**, 1571-1578.
- Kirchhoff, H., Haase, W., Wegner, S., Danielsson, R., Ackermann, R., and Albertsson, P.A.** (2007). Low-light-induced formation of semicrystalline photosystem II arrays in higher plant chloroplasts. *Biochemistry* **46**, 11169-11176.
- Kiss, A., Ruban, A., and Horton, P.** (2008). The PsbS protein controls the organization of the photosystem II antenna in higher plant thylakoid membranes. *J Biol Chem* **283**, 3972-3978.
- Kovács, L., Damkjaer, J., Kereiche, S., Illoaia, C., Ruban, A., Boekema, E., Jansson, S., and Horton, P.** (2006). Lack of the light-harvesting complex CP24 affects the structure and function of the grana membranes of higher plant chloroplasts. *Plant Cell* **18**, 3106-3120.
- Król, M., Spangfort, M.D., Huner, N.P., Oquist, G., Gustafsson, P., and Jansson, S.** (1995). Chlorophyll a/b-binding proteins, pigment conversions, and early light-induced proteins in a chlorophyll b-less barley mutant. *Plant Physiol* **107**, 873-883.

- Kyle, D., Staehelin, L., and Arntzen, C.** (1983). Lateral mobility of the light-harvesting complex in chloroplast membranes controls excitation energy distribution in higher plants. *Arch Biochem Biophys* **222**, 527-541.
- Lambrev, P.H., Tsonev, T., Velikova, V., Georgieva, K., Lambreva, M.D., Yordanov, I., Kovács, L., and Garab, G.** (2007). Trapping of the quenched conformation associated with non-photochemical quenching of chlorophyll fluorescence at low temperature. *Photosynth Res* **94**, 321-332.
- Lenn, T., Leake, M., and Mullineaux, C.** (2008). Clustering and dynamics of cytochrome bd-I complexes in the Escherichia coli plasma membrane in vivo. *Mol Microbiol* **70**, 1397-1407.
- Li, X.P., Gilmore, A.M., and Niyogi, K.K.** (2002a). Molecular and global time-resolved analysis of a psbS gene dosage effect on pH- and xanthophyll cycle-dependent nonphotochemical quenching in photosystem II. *J Biol Chem* **277**, 33590-33597.
- Li, X.P., Muller-Moule, P., Gilmore, A.M., and Niyogi, K.K.** (2002b). PsbS-dependent enhancement of feedback de-excitation protects photosystem II from photoinhibition. *Proc Natl Acad Sci U S A* **99**, 15222-15227.
- Li, X.P., Gilmore, A.M., Caffarri, S., Bassi, R., Golan, T., Kramer, D., and Niyogi, K.K.** (2004). Regulation of photosynthetic light harvesting involves intrathylakoid lumen pH sensing by the PsbS protein. *J Biol Chem* **279**, 22866-22874.
- Liao, P.N., Bode, S., Wilk, L., Hafi, N., and Walla, P.J.** (2010). Correlation of electronic carotenoid-chlorophyll interactions and fluorescence quenching with the aggregation of native LHCI and chlorophyll deficient mutants. *Chem Phys* **373**, 50-55.

- Lippincott-Schwartz, J., Snapp, E., and Kenworthy, A.** (2001). Studying protein dynamics in living cells. *Nat Rev Mol Cell Biol* **2**, 444-456.
- Liu, Z., Yan, H., Wang, K., Kuang, T., Zhang, J., Gui, L., An, X., and Chang, W.** (2004). Crystal structure of spinach major light-harvesting complex at 2.72 Å resolution. *Nature* **428**, 287-292.
- Long, S., Humphries, S., and Falkowski, P.** (1994). Photoinhibition of photosynthesis in nature. *Annu. Rev. Plant Physiol. Plant Mol. Biol.* **45**, 633-662.
- Luciński, R., and Jackowski, G.** (2006). The structure, functions and degradation of pigment-binding proteins of photosystem II. *Acta Biochim Pol* **53**, 693-708.
- Majeran, W., Olive, J., Drapier, D., Vallon, O., and Wollman, F.A.** (2001). The light sensitivity of ATP synthase mutants of *Chlamydomonas reinhardtii*. *Plant Physiol* **126**, 421-433.
- McCain, D.C.** (1998). Chloroplast movement can be impeded by crowding. *Plant Sci* **135**, 219-225.
- Miller, K.R., Miller, G.J., and McIntyre, K.R.** (1976). The light-harvesting chlorophyll-protein complex of photosystem II. Its location in the photosynthetic membrane. *J Cell Biol* **71**, 624-638.
- Miloslavina, Y., Wehner, A., Lambrev, P.H., Wientjes, E., Reus, M., Garab, G., Croce, R., and Holzwarth, A.R.** (2008). Far-red fluorescence: a direct spectroscopic marker for LHCII oligomer formation in non-photochemical quenching. *FEBS Lett* **582**, 3625-3631.
- Mitchell, R., Spillmann, A., and Haehnel, W.** (1990). Plastoquinol diffusion in linear photosynthetic electron transport. *Biophys J* **58**, 1011-1024.

- Müller, P., Li, X.P., and Niyogi, K.K.** (2001). Non-photochemical quenching. A response to excess light energy. *Plant Physiol* **125**, 1558-1566.
- Müller, M.G., Lambrev, P., Reus, M., Wientjes, E., Croce, R., and Holzwarth, A.R.** (2010). Singlet energy dissipation in the photosystem II light-harvesting complex does not involve energy transfer to carotenoids. *Chem Phys Chem* **11**, 1289-1296.
- Mullineaux, C.** (2004). FRAP analysis of photosynthetic membranes. *J Exp Bot* **55**, 1207-1211.
- Mullineaux, C.** (2005). Function and evolution of grana. *Trends Plant Sci* **10**, 521-525.
- Mullineaux, C.** (2008). Factors controlling the mobility of photosynthetic proteins. *Photochem Photobiol* **84**, 1310-1316.
- Mullineaux, C., and Emlyn-Jones, D.** (2005). State transitions: an example of acclimation to low-light stress. *J Exp Bot* **56**, 389-393.
- Mullineaux, C., Tobin, M., and Jones, G.** (1997). Mobility of photosynthetic complexes in thylakoid membranes. *Nature* **390**, 421-424.
- Mullineaux, C.W., and Sarcina, M.** (2002). Probing the dynamics of photosynthetic membranes with fluorescence recovery after photobleaching. *Trends Plant Sci* **7**, 237-240.
- Murakami, S., and Packer, L.** (1970a). Light-induced changes in the conformation and configuration of the thylakoid membrane of *Ulva* and *Porphyra* chloroplasts in vivo. *Plant Physiol* **45**, 289-299.
- Murakami, S., and Packer, L.** (1970b). Protonation and chloroplast membrane structure. *J Cell Biol* **47**, 332-351.

- Murakami, S., and Packer, L.** (1971). The role of cations in the organization of chloroplast membranes. *Arch Biochem Biophys* **146**, 337-347.
- Murray, D., and Kohorn, B.** (1991). Chloroplasts of *Arabidopsis thaliana* homozygous for the *ch-1* locus lack chlorophyll b, lack stable LHCPII and have stacked thylakoids. *Plant Mol Biol* **16**, 71-79.
- Mustárdy, L., and Garab, G.** (2003). Granum revisited. A three-dimensional model--where things fall into place. *Trends Plant Sci* **8**, 117-122.
- Mustárdy, L., Buttle, K., Steinbach, G., and Garab, G.** (2008). The three-dimensional network of the thylakoid membranes in plants: quasihelical model of the granum-stroma assembly. *Plant Cell* **20**, 2552-2557.
- Napier, J., and Barnes, S.** (1995). The isolation of intact chloroplasts. *Methods Mol Biol* **49**, 355-360.
- Navari-Izzo, F., Quartacci, M., Pinzino, C., Rascio, N., Vazzana, C., and Sgherri, C.** (2000). Protein dynamics in thylakoids of the desiccation-tolerant plant *Boea hygropica* during dehydration and rehydration. *Plant Physiol* **124**, 1427-1436.
- Nelson, N., and Ben-Shem, A.** (2004). The complex architecture of oxygenic photosynthesis. *Nar Rev Mol Cell Biol* **5**, 971-982.
- Nield, J., and Barber, J.** (2006). Refinement of the structural model for the Photosystem II supercomplex of higher plants. *Biochim Biophys Acta* **1757**, 353-361.
- Nield, J., Funk, C., and Barber, J.** (2000a). Supermolecular structure of photosystem II and location of the PsbS protein. *Philos Trans R Soc Lond B Biol Sci* **355**, 1337-1344.



- Nield, J., Orlova, E.V., Morris, E.P., Gowen, B., van Heel, M., and Barber, J.** (2000b). 3D map of the plant photosystem II supercomplex obtained by cryoelectron microscopy and single particle analysis. *Nat Struct Biol* **7**, 44-47.
- Niyogi, K.K., Grossman, A.R., and Björkman, O.** (1998). Arabidopsis mutants define a central role for the xanthophyll cycle in the regulation of photosynthetic energy conversion. *Plant Cell* **10**, 1121-1134.
- Niyogi, K.K., Shih, C., Soon Chow, W., Pogson, B.J., Dellapenna, D., and Björkman, O.** (2001). Photoprotection in a zeaxanthin- and lutein-deficient double mutant of Arabidopsis. *Photosynth Res* **67**, 139-145.
- Niyogi, K.K., Li, X.P., Rosenberg, V., and Jung, H.S.** (2005). Is PsbS the site of non-photochemical quenching in photosynthesis? *J Exp Bot* **56**, 375-382.
- Noctor, G., Rees, D., Young, A., and Horton, P.** (1991). The relationship between zeaxanthin, energy-dependent quenching of chlorophyll fluorescence and the transthylakoid pH-gradient in isolated chloroplasts. *Biochim Biophys Acta* **1057**, 320-330.
- Paolillo, D.J.** (1970). The three-dimensional arrangement of intergranal lamellae in chloroplasts. *J Cell Sci* **6**, 243-255.
- Pascal, A., Liu, Z., Broess, K., van Oort, B., van Amerongen, H., Wang, C., Horton, P., Robert, B., Chang, W., and Ruban, A.** (2005). Molecular basis of photoprotection and control of photosynthetic light-harvesting. *Nature* **436**, 134-137.
- Pérez-Bueno, M., Johnson, M., Zia, A., Ruban, A., and Horton, P.** (2008). The Lhcb protein and xanthophyll composition of the light harvesting antenna

controls the DeltapH-dependency of non-photochemical quenching in *Arabidopsis thaliana*. FEBS Lett **582**, 1477-1482.

**Peter, G.F., and Thornber, J.P.** (1991). Biochemical composition and organization of higher plant photosystem II light-harvesting pigment-proteins. J Biol Chem **266**, 16745-16754.

**Pfeiffer, S., and Krupinska, K.** (2005). New insights in thylakoid membrane organization. Plant Cell Physiol **46**, 1443-1451.

**Pogson, B., McDonald, K.A., Truong, M., Britton, G., and DellaPenna, D.** (1996). *Arabidopsis* carotenoid mutants demonstrate that lutein is not essential for photosynthesis in higher plants. Plant Cell **8**, 1627-1639.

**Porra, R.J., Thompson, W.A., and Kriedemann, P.E.** (1989). Determination of accurate extinction coefficients and simultaneous equations for assaying chlorophylls a and b extracted with four different solvents: verification of the concentration of chlorophyll standards by atomic absorption spectroscopy. Biochimica et Biophysica Acta **975**, 384-394.

**Rees, D., Noctor, G., Ruban, A.V., Crofts, J., Young, A., and Horton, P.** (1992). pH dependent chlorophyll fluorescence quenching in spinach thylakoids from light treated or dark adapted leaves. Photosynth Res **31**, 11-19.

**Reits, E., and Neefjes, J.** (2001). From fixed to FRAP: measuring protein mobility and activity in living cells. Nat Cell Biol **3**, 145-147.

**Rintamäki, E., Kettunen, R., and Aro, E.** (1996). Differential D1 dephosphorylation in functional and photodamaged photosystem II centers. Dephosphorylation is a prerequisite for degradation of damaged D1. J Biol Chem **271**, 14870-14875.

- Robert, B., Horton, P., Pascal, A., and Ruban, A.** (2004). Insights into the molecular dynamics of plant light-harvesting proteins in vivo. *Trends Plant Sci* **9**, 385-390.
- Rose, R.J., and Possingham, J.V.** (1976). The localization of (3H) thymidine incorporation in the DNA of replicating spinach chloroplasts by electron-microscope autoradiography. *J Cell Sci* **20**, 341-355.
- Ruban, A.** (2009). Plants in light. *Commun Integr Biol* **2**, 50-55.
- Ruban, A., and Johnson, M.** (2009). Dynamics of higher plant photosystem cross-section associated with state transitions. *Photosynth Res* **99**, 173-183.
- Ruban, A.V., and Johnson, M.P.** (2010). Xanthophylls as modulators of membrane protein function. *Arch Biochem Biophys* **504**, 78-85.
- Ruban, A., and Horton, P.** (1999). The xanthophyll cycle modulates the kinetics of nonphotochemical energy dissipation in isolated light-harvesting complexes, intact chloroplasts, and leaves of spinach. *Plant Physiol* **119**, 531-542.
- Ruban, A., Wentworth, M., and Horton, P.** (2001). Kinetic analysis of nonphotochemical quenching of chlorophyll fluorescence. 1. Isolated chloroplasts. *Biochemistry* **40**, 9896-9901.
- Ruban, A.V., Young, A.J., and Horton, P.** (1993). Induction of Nonphotochemical Energy Dissipation and Absorbance Changes in Leaves (Evidence for Changes in the State of the Light-Harvesting System of Photosystem II in Vivo). *Plant Physiol* **102**, 741-750.
- Ruban, A.V., Rees, D., Pascal, A., and Horton, P.** (1992). Mechanism of Delta pH-dependent dissipation of absorbed excitation energy by photosynthetic membranes. II Relationships between LHClI aggregation in vitro and qE in isolated thylakoids. *Biochim Biophys Acta* **1102**, 39-44.

- Ruban, A.V., Rees, D., Noctor, G.D., Young, A., and Horton, P.** (1991). Long wavelength chlorophyll species are associated with amplification of high-energy-state excitation quenching in higher plants. *Biochim Biophys Acta* **1059**, 355-360.
- Ruban, A.V., Calkoen, F., Kwa, S.L.S., van Grondelle, R., Horton, P., and Dekker, J.P.** (1997). Characterisation of the aggregated state of the light harvesting complex of photosystem II by linear and circular dichroism spectroscopy. *Biochim Biophys Acta* **1321**, 61-70.
- Ruban, A., Wentworth, M., Yakushevskaya, A., Andersson, J., Lee, P., Keegstra, W., Dekker, J., Boekema, E., Jansson, S., and Horton, P.** (2003). Plants lacking the main light-harvesting complex retain photosystem II macro-organization. *Nature* **421**, 648-652.
- Ruban, A., Berera, R., Iliaia, C., van Stokkum, I., Kennis, J., Pascal, A., van Amerongen, H., Robert, B., Horton, P., and van Grondelle, R.** (2007). Identification of a mechanism of photoprotective energy dissipation in higher plants. *Nature* **450**, 575-578.
- Sarcina, M., and Mullineaux, C.W.** (2004). Mobility of the IsiA chlorophyll-binding protein in cyanobacterial thylakoid membranes. *J Biol Chem* **279**, 36514-36518.
- Sarcina, M., Tobin, M., and Mullineaux, C.** (2001). Diffusion of phycobilisomes on the thylakoid membranes of the cyanobacterium *Synechococcus* 7942. Effects of phycobilisome size, temperature, and membrane lipid composition. *J Biol Chem* **276**, 46830-46834.

- Sarcina, M., Bouzovitis, N., and Mullineaux, C.** (2006). Mobilization of photosystem II induced by intense red light in the Cyanobacterium *Synechococcus* sp PCC7942. *Plant Cell* **18**, 457-464.
- Sarcina, M., Murata, N., Tobin, M.J., and Mullineaux, C.W.** (2003). Lipid diffusion in the thylakoid membranes of the cyanobacterium *Synechococcus* sp.: effect of fatty acid desaturation. *FEBS Lett* **553**, 295-298.
- Shimoni, E., Rav-Hon, O., Ohad, I., Brumfeld, V., and Reich, Z.** (2005). Three-dimensional organization of higher-plant chloroplast thylakoid membranes revealed by electron tomography. *Plant Cell* **17**, 2580-2586.
- Siebert, C.A., Qian, P., Fotiadis, D., Engel, A., Hunter, C.N., and Bullough, P.A.** (2004). Molecular architecture of photosynthetic membranes in *Rhodospira rubra* sphaeroides: the role of PufX. *EMBO J* **23**, 690-700.
- Simpson, D.J.** (1979). Freeze-fracture studies on barley plastid membranes. III. Location of the light-harvesting chlorophyll-protein. *Carlsberg Res Commun* **44**, 305-336.
- Simpson, D.J.** (1982). Freeze-fracture studies on barley plastid membranes V. *Viridis-n<sup>34</sup>*, a Photosystem I mutant *Carlsberg Res Commun* **47**, 215-225.
- Stachelin, L.A.** (1976). Reversible particle movements associated with unstacking and restacking of chloroplast membranes in vitro. *J Cell Biol* **71**, 136-158.
- Stachelin, L.** (2003). Chloroplast structure: from chlorophyll granules to supra-molecular architecture of thylakoid membranes. *Photosynth Res* **76**, 185-196.
- Stachelin, L.A., and Arntzen, C.J.** (1983). Regulation of chloroplast membrane function: protein phosphorylation changes the spatial organization of membrane components. *J Cell Biol* **97**, 1327-1337.

- Staelin, A.L., and van der Staay, G.W.M.** (1996). Structure, Composition, Functional Organization and Dynamic Properties of Thylakoid Membranes. In *Oxygenic photosynthesis: The light reactions*, D.R. Ort and C.F. Yocum, eds (Dordrecht: Kluwer Academic Publishers), pp. 11-30.
- Standfuss, J., and Kühlbrandt, W.** (2004). The three isoforms of the light-harvesting complex II: spectroscopic features, trimer formation, and functional roles. *J Biol Chem* **279**, 36884-36891.
- Stocking, C., and Franceschi, V.** (1982). Some Properties of the Chloroplast Envelope as Revealed by Electrophoretic Mobility Studies of Intact Chloroplasts. *Plant Physiol* **70**, 1255-1259.
- Svab, Z., and Maliga, P.** (1993). High-frequency plastid transformation in tobacco by selection for a chimeric *aadA* gene. *Proc Natl Acad Sci USA* **90**, 913-917
- Szabó, I., Bergantino, E., and Giacometti, G.M.** (2005). Light and oxygenic photosynthesis: energy dissipation as a protection mechanism against photo-oxidation. *EMBO Rep* **6**, 629-634.
- Teardo, E., de Laureto, P., Bergantino, E., Dalla Vecchia, F., Rigoni, F., Szabò, I., and Giacometti, G.** (2007). Evidences for interaction of PsbS with photosynthetic complexes in maize thylakoids. *Biochim Biophys Acta* **1767**, 703-711.
- Thorneycroft, D., Sherson, S.M., and Smith, S.M.** (2001). Using gene knockouts to investigate plant metabolism. *J Exp Bot* **52**, 1593-1601.
- Thurlkill, R.L., Grimsley, G.R., Scholtz, J.M., and Pace, C.N.** (2006). pK values of the ionizable groups of proteins. *Protein Sci* **15**, 1214-1218.

- Tikkanen, M., Nurmi, M., Kangasjärvi, S., and Aro, E.** (2008). Core protein phosphorylation facilitates the repair of photodamaged photosystem II at high light. *Biochim Biophys Acta* **1777**, 1432-1437.
- Tremmel, I., Weis, E., and Farquhar, G.** (2005). The influence of protein-protein interactions on the organization of proteins within thylakoid membranes. *Biophys J* **88**, 2650-2660.
- Vainonen, J., Hansson, M., and Vener, A.** (2005). STN8 protein kinase in *Arabidopsis thaliana* is specific in phosphorylation of photosystem II core proteins. *J Biol Chem* **280**, 33679-33686.
- van Oort, B., van Hoek, A., Ruban, A., and van Amerongen, H.** (2007). Aggregation of light-harvesting complex II leads to formation of efficient excitation energy traps in monomeric and trimeric complexes. *FEBS Lett* **581**, 3528-3532.
- van Roon, H., van Breemen, J.F., de Weerd, F.L., Dekker, J.P., and Boekema, E.J.** (2000). Solubilization of green plant thylakoid membranes with n-dodecyl-alpha,D-maltoside. Implications for the structural organization of the Photosystem II, Photosystem I, ATP synthase and cytochrome b6 f complexes. *Photosynth Res* **64**, 155-166.
- Vasilikiotis, C., and Melis, A.** (1994). Photosystem II reaction center damage and repair cycle: chloroplast acclimation strategy to irradiance stress. *Proc Natl Acad Sci U S A* **91**, 7222-7226.
- Walters, R.** (2005). Towards an understanding of photosynthetic acclimation. *J Exp Bot* **56**, 435-447.

- Walters, R.G., Ruban, A.V., and Horton, P.** (1994). Higher plant light-harvesting complexes LHCIIa and LHCIIc are bound by dicyclohexylcarbodiimide during inhibition of energy dissipation. *Eur J Biochem* **226**, 1063-1069.
- Wehrmeyer, W.** (1964). Zur Klärung der strukturellen Variabilität der Chloroplastengrana des Spinats in Profil und Aufsicht. *Planta* **62**, 272-293.
- Weis, E.** (1985). Light- and temperature-induced changes in the distribution of excitation energy between Photosystem I and Photosystem II in spinach leaves *Biochim Biophys Acta* **807**, 118-126.
- Wettstein von, D.** (1959). The formation of plastid structures. *Brookhaven Symp. Biol.* **11**, 138-159.
- Xie, X.S., and Trautman, J.K.** (1998). Optical studies of single molecules at room temperature. *Annu Rev Phys Chem* **49**, 441-480.
- Yakushevskaya, A., Jensen, P., Keegstra, W., van Roon, H., Scheller, H., Boekema, E., and Dekker, J.** (2001). Supermolecular organization of photosystem II and its associated light-harvesting antenna in *Arabidopsis thaliana*. *Eur J Biochem* **268**, 6020-6028.
- Yakushevskaya, A., Keegstra, W., Boekema, E., Dekker, J., Andersson, J., Jansson, S., Ruban, A., and Horton, P.** (2003). The structure of photosystem II in *Arabidopsis*: localization of the CP26 and CP29 antenna complexes. *Biochemistry* **42**, 608-613.



## Visualizing the mobility and distribution of chlorophyll proteins in higher plant thylakoid membranes: effects of photoinhibition and protein phosphorylation

Tomasz K. Gorol<sup>1</sup>, Matthew P. Johnson<sup>1</sup>, Anthony P.R. Brain<sup>2</sup>, Helmut Kirchhoff<sup>3</sup>, Alexander V. Ruban<sup>1</sup> and Conrad W. Mullineaux<sup>1,\*</sup>

<sup>1</sup>School of Biological and Chemical Sciences, Queen Mary University of London, Mile End Road, London E1 4NS, UK,

<sup>2</sup>Centre for Ultrastructural Imaging, Kings College, University of London, New Hunt's House, Guy's Campus, London SE1 1UL, UK, and

<sup>3</sup>Institute of Biological Chemistry, Washington State University, Pullman, WA 99164-6340, USA

Received 29 January 2010; revised 25 February 2010; accepted 8 March 2010; published online 8 April 2010.

\*For correspondence (fax 44 20 8983 0773; e-mail c.mullineaux@qmul.ac.uk).

### SUMMARY

The diffusion of proteins in chloroplast thylakoid membranes is believed to be important for processes including the photosystem-II repair cycle and the regulation of light harvesting. However, to date there is very little direct information on the mobility of thylakoid proteins. We have used fluorescence recovery after photobleaching in a laser-scanning confocal microscope to visualize in real time the exchange of chlorophyll proteins between grana in intact spinach (*Spinacia oleracea* L.) and Arabidopsis chloroplasts. Most chlorophyll proteins in the grana appear immobile on the 10-min timescale of our measurements. However, a limited population of chlorophyll proteins (accounting for around 15% of chlorophyll fluorescence) can exchange between grana on this timescale. In intact, wild-type chloroplasts this mobile population increases significantly after photoinhibition, consistent with a role for protein diffusion in the photosystem-II repair cycle. No such increase in mobility is seen in isolated grana membranes, or in the Arabidopsis *stn8* and *stn7 stn8* mutants, which lack the protein kinases required for phosphorylation of photosystem II core proteins and light-harvesting complexes. Furthermore, mobility under low-light conditions is significantly lower in *stn8* and *stn7 stn8* plants than in wild-type Arabidopsis. The changes in protein mobility correlate with changes in the packing density and size of thylakoid protein complexes, as observed by freeze-fracture electron microscopy. We conclude that protein phosphorylation switches the membrane system to a more fluid state, thus facilitating the photosystem-II repair cycle.

**Keywords:** chloroplast, thylakoid membrane, fluorescence microscopy, freeze-fracture electron microscopy, photoinhibition, protein phosphorylation.

### INTRODUCTION

Thylakoid membranes are densely packed with proteins. For example, the protein complexes occupy about 80% of the membrane area of grana thylakoid membranes (Kirchhoff *et al.*, 2002, 2008b). This dense macromolecular crowding may cause problems. Protein diffusion is crucial for the function of most biological membranes, but the dense packing of thylakoids must lead to a severe reduction in the mobility of protein complexes (Kirchhoff *et al.*, 2004). Nevertheless, it is clear that some proteins in the grana must be mobile under some conditions. Two well-characterized examples are the redistribution of LHCl light-harvesting

complexes during state transitions (Allen and Forsberg, 2001), and the migration of photosystem I (PSI) reaction centres as part of the PSII repair cycle (Tikkanen *et al.*, 2008). In both cases, protein phosphorylation has been implicated in triggering the redistribution of complexes (Allen and Forsberg, 2001; Tikkanen *et al.*, 2008). Fractionation of thylakoid membranes into grana and stroma lamellae shows the redistribution of complexes between the two fractions, over a timescale of a few minutes (Crøpper *et al.*, 1993). However, this biochemical approach does not show how far the complexes migrate. Some authors have argued that

LHCII migrates only a short distance during state transitions, between the grana and the 'grana margins', without ever moving into the stroma lamellae (Allen and Forsberg, 2001). The biochemical approach also only gives a crude indication of the timescale upon which protein movements occur, and it does not distinguish between two possibilities for the relationship between grana structure and protein movement: (i) a subpopulation of proteins can diffuse in and out of the grana, which are relatively stable structures; and (ii) protein escape from the grana membranes requires the partial or complete disassembly of a proportion of the grana.

Freeze-fracture electron microscopy has revealed considerable detail of the distribution of chlorophyll-protein complexes in thylakoid membranes (reviewed by Staehelin, 2003), and has shown quantitative differences in the supra-molecular organization of chlorophyll-protein complexes resulting from state transitions (Staehelin and Arntzen, 1983). Electron tomography also suggests large-scale structural changes in grana during state transitions (Chauzmann *et al.*, 2008). However, electron microscopic techniques can only give part of the story, as the preparation required (fixing and/or freezing) obviously prevents the dynamic tracking of protein movements and membrane rearrangement. Techniques based on fluorescence microscopy offer the best hope of resolving these issues by tracking the movement of protein complexes in real time, albeit with much lower spatial resolution than that achieved with electron microscopy. Fluorescence microscopy in thylakoid membranes is facilitated by the natural fluorescence of the chlorophylls, which allows the distribution of some protein complexes to be visualized without the need for artificial fluorescent tagging (Mullineaux and Sarcina, 2002). Fluorescent tagging with GFP or fluorescent antibodies is likely to perturb the system, particularly in the grana where the tight appression of the membranes will almost certainly exclude any bulky fluorescent tags (Consoli *et al.*, 2005).

Fluorescence recovery after photobleaching (FRAP) has been used to probe the mobility of protein complexes in some photosynthetic membranes (Mullineaux *et al.*, 1997; Mullineaux and Sarcina, 2002). In favourable cases, FRAP is fully quantitative and can be used to measure the diffusion coefficients of photosynthetic complexes. However, this requires a simple, predictable membrane topography, and a membrane that can be assumed to be homogeneous over a distance of a micron or more. This is the case with the thylakoid membranes of some cyanobacteria (Mullineaux *et al.*, 1997; Mullineaux and Sarcina, 2002). Green plant thylakoid membranes are much more difficult systems for FRAP because of their lateral heterogeneity and their complex three-dimensional architecture, which is still not fully understood (Garab and Menella, 2008). Kirchoff *et al.* recently used FRAP to measure the mobility of chlorophyll-protein complexes in isolated grana membranes from spinach (*Spinacia oleracea* L.), taking advantage of the

tendency of these membranes to fuse laterally into larger membrane patches *in vitro* (Kirchoff *et al.*, 2008a). There, most of the chlorophyll proteins are completely immobile, at least on timescales of a few minutes. However, a subpopulation accounting for about 25% of chlorophyll fluorescence is able to diffuse surprisingly fast (diffusion coefficient  $D \sim 0.005 \mu\text{m}^2 \text{sec}^{-1}$ ). It was suggested that this mobile subpopulation might be able to exchange rapidly between the grana and stroma lamellae *in vivo* (Kirchoff *et al.*, 2008a).

Here, we report the extension of the FRAP approach to probe the mobility of chlorophyll proteins in a more physiologically relevant system: the thylakoid membranes of intact spinach and *Arabidopsis* chloroplasts. Because of the complex membrane architecture, we cannot measure diffusion coefficients in this system. However, we can accurately measure the 'mobile fraction': in this case the proportion of chlorophyll fluorescence that can exchange between grana, because of chlorophyll proteins escaping from one granum and diffusing through the stroma lamellae to another granum. This leads to the recovery of fluorescence in a bleached granum. We use a range of control measurements to show that this fluorescence recovery is the result of protein diffusion. Our technique provides a new tool for the direct measurement of the dynamics of plant thylakoid membranes. We show that photoinhibition increases the mobility of chlorophyll proteins, suggesting that mobilization of these proteins is important for the repair cycle. We use *Arabidopsis* mutants lacking the STN7 and STN8 protein kinases (Bonardi *et al.*, 2005) to show that mobilization requires these proteins. Freeze-fracture electron micrographs indicate that changes in protein mobility within the thylakoid system correlate with changes in the packing density and size of the complexes.

## RESULTS

### Visualization of chloroplast intactness

We set out to measure the mobility of chlorophyll proteins in chloroplasts with intact outer envelopes, in order to ensure that our results were as physiologically relevant as possible. We tried several methods for isolating intact chloroplasts, including the use of centrifugation on a Percoll cushion to separate the intact and broken organelles (Napier and Barnes, 1995); however, we never obtained 100% intact organelles in the preparation. As our confocal FRAP measurements are made on individual chloroplasts it is important to assess whether the chloroplast under examination is broken or intact. We found that this could be achieved by staining the preparation with the green lipophilic fluorophore BOPICY FL C<sub>12</sub> which was previously used to stain membranes in the cells of cyanobacteria (Sarcina *et al.*, 2003). In intact chloroplasts the dye only stains the

chloroplast envelope, and does not enter the chloroplast interior: it is visualized as a continuous halo of green fluorescence surrounding the red chlorophyll fluorescence from the thylakoid membranes (Figure 1). In broken chloroplasts the distribution of green fluorescence appears very different: there is only fragmentary staining outside the thylakoid membranes and considerable staining of the thylakoid membranes themselves (Figure 1). We used this method to select intact chloroplasts for our FRAP experiments.

#### FRAP measurements in isolated intact chloroplasts: optimisation and controls

For FRAP it is important to immobilize the sample to ensure that any fluorescence recovery is the result of diffusion within the sample rather than movement of the sample as a whole. Slides coated with polylysine are often used to immobilize bacterial cells (e.g. Lenn *et al.*, 2008), and we found this method to be effective with intact chloroplasts.

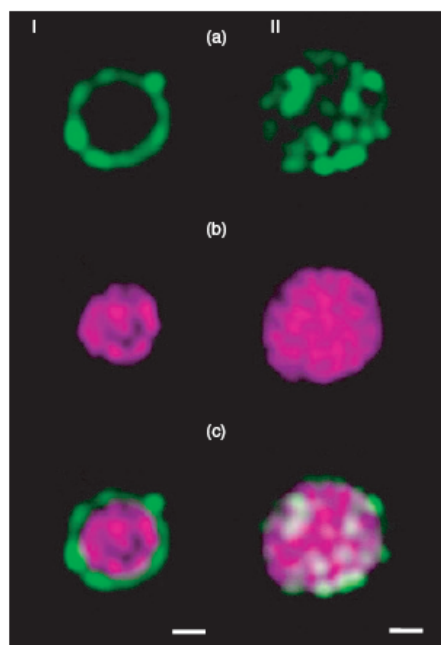


Figure 1. Confocal fluorescence images of intact (I) and broken (II) chloroplasts from spinach (*Spinacia oleracea* L.). Scale bars: 2  $\mu$ m. (a) Green fluorescence from the BODIPY FL C<sub>12</sub> stain. (b) Chlorophyll fluorescence. (c) Merged pseudocolour images (chlorophyll fluorescence shown in magenta; BODIPY FL C<sub>12</sub> fluorescence shown in green).

Most chloroplasts adhered to the polylysine-coated slide and remained immobile during the experiment. Presumably the negatively charged outer membrane (Stocking and Franceschi, 1982) interacts electrostatically with the positively charged polylysine film. In this system there is no direct interaction between the thylakoid membranes and the support, and thus no danger that such interactions might perturb membrane conformation and the mobility of membrane proteins.

For FRAP measurements we first selected intact, immobilized chloroplasts, as described above, and then visualized chlorophyll fluorescence by scanning in two dimensions (see Experimental procedures). At the fixed imaging laser intensity, chlorophyll fluorescence was stable: repeated scans across the same chloroplast did not lead to detectable photobleaching (not shown). The grana within the chloroplasts appeared as bright fluorescent spots (dark spots in the inverted images shown in Figures 2–4). For our measurements it was important to resolve the fluorescence from individual grana as cleanly as possible. Because the grana are tightly packed together, this is problematic at optical resolution. We used a routine deconvolution procedure, taking into account the measured point-spread function (see Experimental procedures), to improve the resolution of individual grana. To photobleach a region of the chloroplast we increased the laser power by a factor of 32, and then scanned the confocal laser spot repeatedly in one dimension across the sample for 5–7 sec. This bleached a line across the chloroplast, which could be visualized by subsequent imaging at a lower laser power (Figures 2–4). Under some conditions we could then observe a partial recovery of fluorescence in the bleached zone over a timescale of a few minutes (Figure 4).

We needed to establish whether or not this fluorescence recovery was the result of the diffusion of chlorophyll protein complexes into the bleached area. The other possibility would be some form of reversible fluorescence quenching allowing fluorescence recovery in the bleached area without any movement of complexes. In geometrically simpler systems (for example isolated, laterally fused grana membranes and the quasi-cylindrical thylakoid membranes of some cyanobacteria), fluorescence redistribution can be clearly visualized. The recovery of fluorescence in the bleached area is matched by a loss of fluorescence in the neighbouring regions of the membrane, leading to a characteristic 'blurring' of the bleached line, which is a clear indication of diffusion (Mullineaux *et al.*, 1997; Kirchhoff *et al.*, 2008a). However, the situation is more complex in intact chloroplasts because of the lateral heterogeneity and intricate geometry of the membrane (Anderson and Andersson, 1982), combined with the small extent of fluorescence quenching, we bleached entire chloroplasts rather than just a line across the chloroplast (Figure 2a). If

Figure 2. Control fluorescence recovery after photobleaching (FRAP) experiments on intact spinach (*Spinacia oleracea* L.) chloroplasts. Fluorescence images are shown in inverted grayscale. Scale bars: 3  $\mu$ m.  
 (a) 'Total bleach' experiment, bleaching out the entire thylakoid membrane area. Note the lack of fluorescence recovery.  
 (b) Bleaching a line across a chloroplast fixed with glutaraldehyde. The circle in the prebleach image shows the region of interest selected for quantitative analysis, and the panel below shows enlarged and contrast-enhanced images of the bleached area (with the position of the granum indicated by the arrow). Fluorescence recovery is minimal.  
 (c) Mobile fractions in experiments of the type shown in (a) and (b), compared with experiments of the type shown in Figure 4. Means of 10 experiments  $\pm$  SEs. Asterisks indicate values significantly different from the control analysed by a one-way ANOVA with Tukey's *post hoc* test,  $P < 0.05$ .

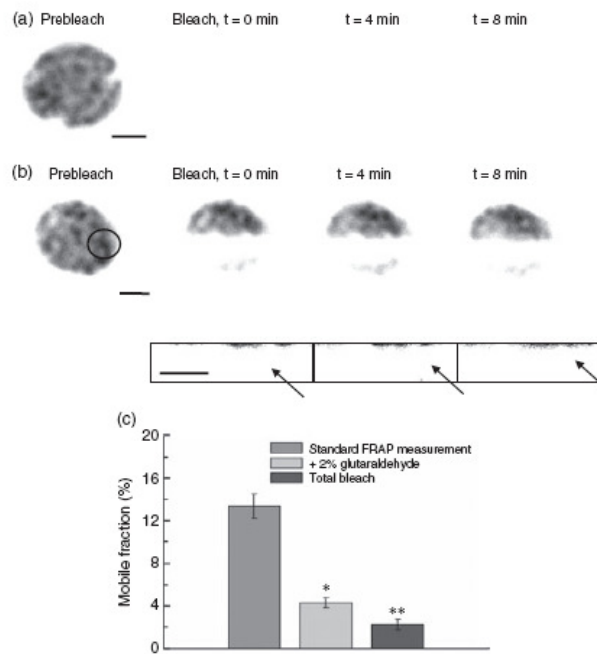
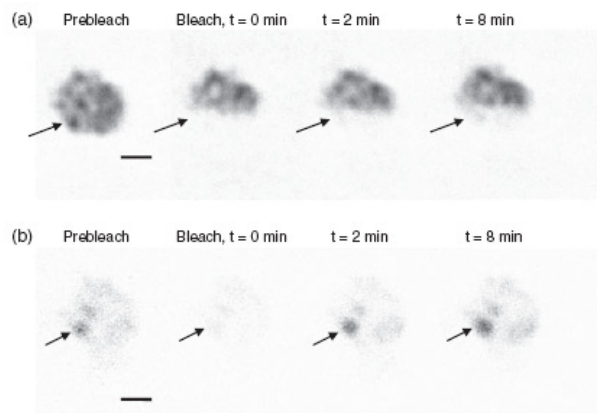


Figure 3. Control fluorescence recovery after photobleaching (FRAP) experiment on a broken spinach (*Spinacia oleracea* L.) chloroplast. Fluorescence images are shown in inverted grayscale. Scale bars: 3  $\mu$ m. The chloroplast was stained with the green lipophilic fluorophore BODIPY FL C<sub>12</sub>. Following photobleaching, fluorescence was monitored simultaneously in (a) the red channel (chlorophyll fluorescence) and (b) the green channel (BODIPY fluorescence). The arrowed granum shows only partial chlorophyll fluorescence recovery, but complete BODIPY fluorescence recovery.



fluorescence recovery resulted from reversible fluorescence quenching, we would still expect to observe it in this experiment. If the recovery resulted from diffusion, we would not expect to see it because bleaching the entire

chloroplast removes the pool of unbleached complexes, the diffusion of which into the bleached area causes the recovery. Fluorescence recovery was very slight in this experiment (Figure 2a). This is strong evidence against any

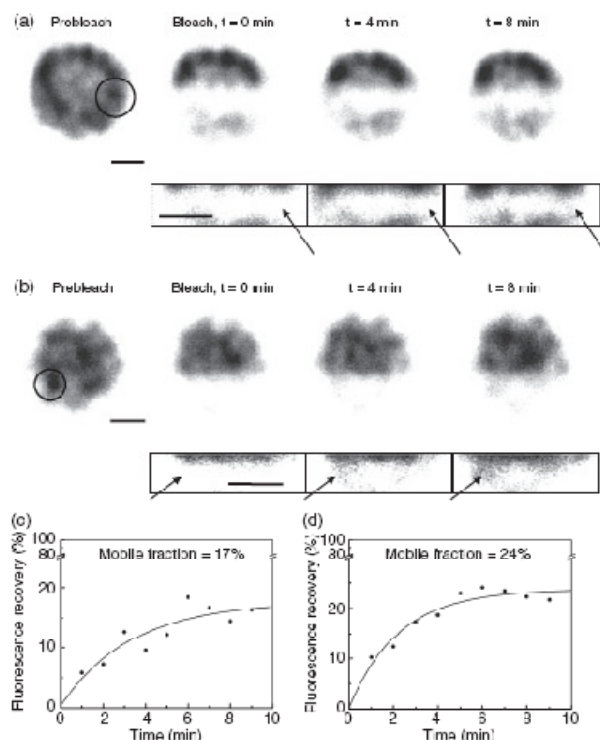


Figure 4. Fluorescence recovery after photobleaching (FRAP) measurements on intact spinach (*Spinacia oleracea* L.) chloroplasts.

(a) Chlorophyll fluorescence image sequence (inverted greyscale) for a dark-adapted chloroplast. The circle indicates the position of an individual grana (used as the region of interest for quantitative data analysis). Scale bars: 2  $\mu$ m. The lower panel shows enlarged and contrast-enhanced images of the bleached area (grana indicated by the arrow).

(b) Similar image sequence for a photoinhibited chloroplast.

(c) Fluorescence recovery curve for the bleached grana in (a).

(d) Fluorescence recovery curve for the bleached grana in (b).

Note the greater mobile fraction and faster recovery of fluorescence in the photoinhibited chloroplast.

significant reversible fluorescence quenching under our conditions. As a second control we used treatment with glutaraldehyde, a very effective protein cross-linker (Habeeb and Hiramoto, 1968). If fluorescence recovery resulted from protein diffusion we would expect it to be strongly inhibited by glutaraldehyde treatment, and indeed we observed very little fluorescence recovery in glutaraldehyde-treated chloroplasts (Figure 2b). Both of the controls shown in Figure 2 suggest that the fluorescence recovery observed results from protein diffusion, as it takes place in isolated grana membranes (Kirchhoff *et al.*, 2008a).

For our purposes it is also important to assess the effect of the bleaching on the grana membrane structure. To do this we carried out FRAP measurements on broken chloroplasts in which the thylakoid membrane system was stained with 4,4-difluoro-5,7-dimethyl-4-hydroxy-3a,4a-diaza-s-indacene-3-dodecanoic acid (BODIPY FL C<sub>12</sub>), as in Figure 1. Following the bleaching, fluorescence recovery was observed simultaneously in the red channel (monitoring chlorophyll fluorescence) and the green channel (monitoring BODIPY

fluorescence) (Figure 3). The recovery of chlorophyll fluorescence in the bleached grana is slow and incomplete; however, there is a complete recovery of BODIPY fluorescence on a timescale of a few minutes (Figure 3). This indicates relatively rapid lipid mobility within the thylakoid membrane system, and it indicates that the basic structure of the grana is not destroyed by photobleaching.

#### Mobility of chlorophyll proteins in intact spinach chloroplasts

Figure 4(a) shows an example of an FRAP measurement in an intact spinach chloroplast. After 8 min the bleached line remains clearly visible; however, there is a partial recovery of fluorescence that we attribute to the long-range diffusion of chlorophyll proteins within the thylakoid membrane system. The fluorescence recovery curve shown in Figure 4(c) is obtained by selecting a region of interest in the images corresponding roughly to one individual grana, the fluorescence of which was strongly decreased during the bleaching. This particular grana shows about 17% fluo-

rescence recovery over about 10 min (Figure 4c). Thus, the mobile fraction of chlorophyll fluorescence is small, but measurable, and fairly consistent under these conditions. There is some variation between measurements, but the mean mobile fraction from measurements on 10 individual chloroplasts is about 13% (Table 1). The controls described above and shown in Figures 2 and 3 indicate that this partial fluorescence recovery is the result of protein diffusion. We considered the possibility that this diffusion might be 'vertical' movement between the different membrane layers of the granum, which may be interconnected (Shimoni *et al.*, 2005). However, the limited resolution of our measurements in the  $x$ ,  $y$  and  $z$  directions (see Experimental procedures) will ensure that the full depth of the granum is bleached. It also means that any 'vertical' movement within the granum will not change the fluorescence signal observed. This means that our measurements do not report on 'vertical' diffusion within a granum: we are not able to assess whether such protein movements occur. The diffusion we observe must result from exchange between grana, with complexes escaping from one granum, diffusing through the stroma lamellae and entering another granum. Our results indicate that a limited pool of chlorophyll-protein complexes is able to exchange between grana on a timescale of a few minutes.

#### Effect of photoinhibition on the mobility of chlorophyll proteins in spinach chloroplasts

Most models for the PSII repair cycle involve the migration of photodamaged PSII reaction centres from the grana to the stroma lamellae for repair (Aro *et al.*, 1993; Tikkanen *et al.*, 2008). Therefore, photoinhibition might be expected to result in an increase in the mobility of chlorophyll-protein complexes within the thylakoid membrane system. To test this possibility we carried out FRAP measurements on photoinhibited spinach chloroplasts (Figure 4b). Intact

**Table 1** Effect of photoinhibition on the mobility of chlorophyll proteins in intact spinach chloroplasts and isolated grana membranes

Sample	Mobile fraction (%)		
	Dark-adapted	Photoinhibited	<i>P</i>
Intact chloroplast	13.3 ± 1.1	18.0 ± 1.3	0.014
Intact chloroplast + nigericin	12.3 ± 1.5	16.4 ± 1.0	0.04
Isolated grana membrane	28.0 ± 3.0	27.0 ± 5.0	0.86

Means (±SEs) from 10 fluorescence recovery after photobleaching (FRAP) measurements on individual chloroplasts or 16–18 measurements on isolated grana (BBY) membranes. In intact chloroplasts the mobile fraction indicates the proportion of chlorophyll proteins that are able to exchange between grana, whereas in isolated grana membranes it indicates the proportion of chlorophyll proteins that is mobile within the granal membrane. *P* values are from Student's *t*-tests for significance of the difference between the mobile fractions in dark-adapted and photoinhibited samples.

chloroplasts were photoinhibited in suspension by illuminating them for 10–15 min with actinic light at approximately 3000  $\mu\text{mol photons m}^{-2} \text{sec}^{-1}$ . During photoinhibition, chlorophyll fluorescence was monitored with a pulsed-amplitude modulation (PAM) fluorometer (Figure 5). The treatment resulted in a decrease of about 50% in the maximal yield of fluorescence with closed PSII reaction centres ( $F_m$ ), which was not reversed, even after 2 h (Figure S1). Photoinhibited chloroplasts were immediately adhered to polylysine-coated slides, and FRAP measurements were carried out as described above. Chlorophyll fluorescence recovery was faster and more complete in photoinhibited chloroplasts (Figure 4b,d), as compared with chloroplasts that had not been photoinhibited (Figure 4a,c). The mean mobile fraction of chlorophyll fluorescence in photoinhibited chloroplasts was significantly increased, as compared with chloroplasts that had not been photoinhibited (Table 1).

#### FRAP measurements in intact spinach chloroplasts in the presence of an uncoupler

As an additional control for our FRAP measurements, we repeated the measurements in the presence of nigericin, an uncoupler that effectively prevents the formation of a transmembrane pH difference ( $\Delta\text{pH}$ ).  $\Delta\text{pH}$  is an indispensable trigger for the induction of qE, a reversible quenching mechanism that converts excess excitation energy to heat (Horton *et al.*, 1996; Ruban *et al.*, 2007). PAM fluorometer measurements (not shown) confirmed the absence of qE in

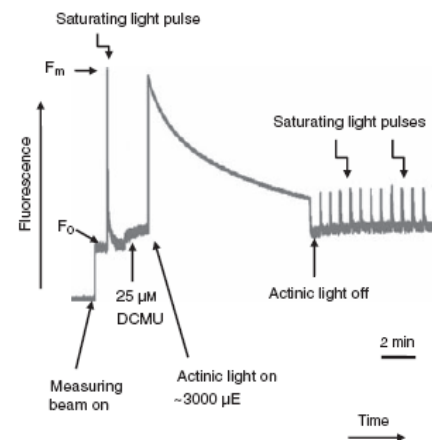


**Figure 5.** Photoinhibition of intact spinach (*Spinacia oleracea* L.) chloroplasts monitored by pulsed-amplitude modulation (PAM) fluorometry. A sample was withdrawn and used for fluorescence recovery after photobleaching (FRAP) measurements (Figure 4) at the end of the actinic illumination.

the presence of nigericin. Mobile fractions calculated from this control did not differ significantly when compared with the corresponding measurements on chloroplasts where nigericin was not added (Table 1). As with chloroplasts in the absence of nigericin (Figure 4; Table 1), we observed a significant increase in the mobile fraction in chloroplasts that were photoinhibited in the presence of nigericin (Table 1). These measurements confirm that changes in the extent of qE are not involved in the fluorescence bleaching and recovery that we observe in our FRAP measurements. They also show that the increase in mobility of chlorophyll proteins that we observe following photoinhibition (Figure 4; Table 1) is not dependent on the induction of qE.

#### Effect of photoinhibition on mobility of chlorophyll proteins in isolated grana membranes

For comparison with our results on intact chloroplasts, we examined the effect of photoinhibition on the mobility of chlorophyll proteins in isolated grana membranes from spinach. These experiments used the system previously described in which isolated grana membranes are adsorbed onto an artificial lipid bilayer support. Membrane fragments tend to fuse together, forming patches large enough for quantitative FRAP measurements of mobile fraction and diffusion coefficient (Kirchhoff *et al.*, 2008a). As previously reported (Kirchhoff *et al.*, 2008a), grana membranes show a mobile fraction of chlorophyll fluorescence of  $28 \pm 3\%$  (SE), which is much higher than that observed in intact chloroplasts. Photoinhibition of the grana membranes was carried out in the same way as described above for intact chloroplasts, with similar effects on chlorophyll fluorescence, as monitored by PAM fluorometry (not shown). However, in contrast to the result in intact chloroplasts, we could not detect a significant increase in the mobility of chlorophyll proteins induced by photoinhibition in isolated grana membranes (Table 1).

#### Mobilization of chlorophyll proteins under photoinhibitory conditions requires protein kinases

Upon photoinhibition, the PSII core proteins, in particular the D1 polypeptide, undergo a rapid light-induced phosphorylation cycle that is connected to the regulation of PSII protein turnover and the repair of damaged proteins (Rintamäki *et al.*, 1996). The *Arabidopsis thaliana stn7* and *stn8* mutants lack the protein kinases required for the phosphorylation of thylakoid membrane proteins (Bonardi *et al.*, 2005). The STN8 protein kinase appears to be primarily responsible for the phosphorylation of PSII core proteins (Bonardi *et al.*, 2005); however, the *stn7 stn8* double mutant shows a more complete loss of capacity for PSII phosphorylation at high light intensities (Tikkanen *et al.*, 2008). As a test for the involvement of PSII phosphorylation in the mobilization of chlorophyll proteins after photoinhibition, we carried out FRAP measurements on intact

chloroplasts from *Arabidopsis* wild type (Col-0), and *stn8* and *stn7 stn8* mutants. Results obtained for wild-type *Arabidopsis* chloroplasts were comparable with those from spinach. Photoinhibition resulted in a small but significant increase in the mobile fraction of chlorophyll fluorescence (Figure 6). However, in the *stn8* and *stn7 stn8* mutants, the mobility of chlorophyll proteins was significantly lower than in the wild type, and there was no increase in the mobile fraction following photoinhibition (Figure 6).

#### Correlation of protein mobility with supramolecular organization

We obtained freeze-fracture electron micrographs from intact spinach chloroplasts that were either dark-adapted or photoinhibited prior to freezing (Figure 7). There were no dramatic changes in PSII organization as a result of photoinhibition (Figure 7), but quantitative analysis of the images indicates that photoinhibition results in a significant decrease in the density of PSII particles in the granal regions, with a concomitant increase in the mean distance between particles (Figure 8). Photoinhibition also induced a small but significant decrease in the mean size of granal PSII particles. Mean PSII dimensions in dark-adapted samples were  $(16.0 \pm 2.4) \times (10.8 \pm 2.0)$  nm, decreasing to  $(14.2 \pm 2.6) \times (9.2 \pm 1.8)$  nm in photoinhibited samples ( $\pm$ SDs,  $P \leq 0.0002$  from a Student's *t*-test).

#### DISCUSSION

Here, we have shown that confocal microscopy and FRAP can be used to probe the mobility of chlorophyll-protein complexes in higher plant thylakoid membranes. We visualized the proteins using the native fluorescence from the chlorophylls. This has the advantage that we are not

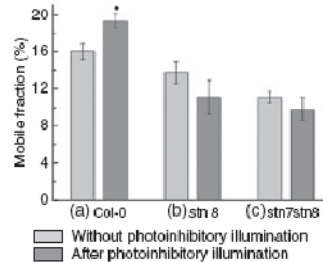


Figure 6. Chlorophyll-protein mobility in intact *Arabidopsis* chloroplasts, with and without photoinhibition. Bars represent mean mobile fractions ( $\pm$ SEs) from 10 measurements. *P*-values are from unpaired Student's *t*-tests. (a) Wild-type (Col-0). Photoinhibition induces a significant increase in the mobile fraction ( $P = 0.013$ ). (b) *stn8* mutant. Photoinhibition does not increase the mobile fraction. (c) *stn7 stn8* mutant. Photoinhibition does not increase the mobile fraction, and mobility in non-photoinhibited chloroplasts is significantly lower than in the wild type ( $P = 0.0001$ ).

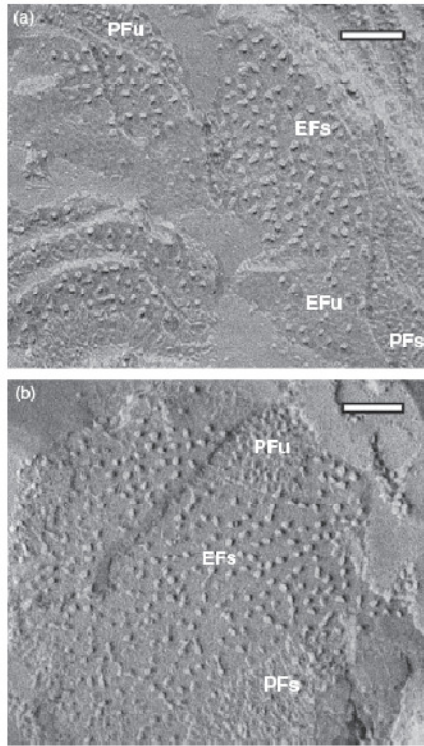


Figure 7. Freeze-fracture electron micrographs from intact spinach (*Spinacia oleracea* L.) chloroplasts (scale bars: 100 nm). (a) Dark-adapted sample. The thylakoid fracture faces EFs, EFu, PFs and PFu have been labelled according to the nomenclature of Branton *et al.* (1975). (b) Photoinhibited sample.

perturbing the membrane structure. It may be the only way that we can track proteins through the grana, where the tight appression of the membranes (Dekker and Boekema, 2005) is likely to exclude extrinsic fluorescent tags such as GFP and antibody-linked fluorophores. At the same time, the approach brings some difficulties.

- (i) We have no direct way to distinguish the different chlorophyll-protein complexes (PSII, LHCII, etc.), which puts obvious limits on the information that we can obtain.
- (ii) Chlorophyll fluorescence yield is influenced by a complex set of quenching mechanisms, including, for example, photochemical quenching by the reaction centres and various mechanisms that dissipate excita-

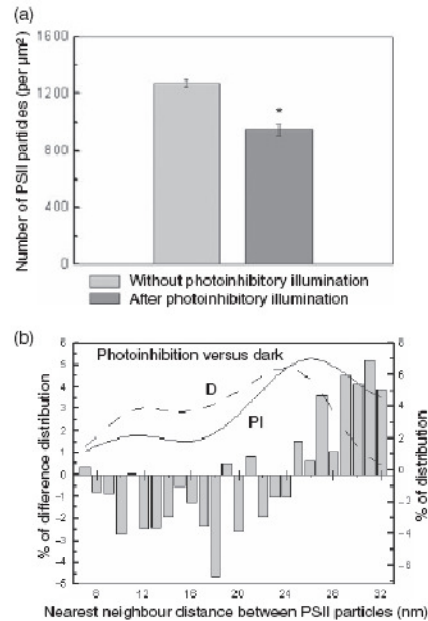


Figure 8. Differences in photosystem II (PSII) density in the grana regions of dark-adapted and photoinhibited spinach (*Spinacia oleracea* L.) chloroplasts revealed in the EFs faces of freeze-fracture electron micrographs, such as those shown in Figure 7. (a) Mean PSII density in  $\mu\text{m}^{-2}$ . Mean  $\pm$  SE ( $n = 30$ ) is shown, and the difference is significant (Student's *t*-test,  $P < 0.001$ ). (b) Nearest-neighbour distances between PSII particles in photoinhibited (PI) and dark (D) states. The lines show the smoothed distributions of nearest-neighbour distances, and the histogram shows the difference between the distributions (PI - D). Note the shift towards greater nearest-neighbour distance in the photoinhibited state.

tion energy as heat (Maxwell and Johnson, 2000). We have to control carefully to make sure that any fluorescence recovery we observe is genuinely the result of protein diffusion, rather than the result of recovery from some reversible quenching process.

- (iii) Problems are caused by the complex three-dimensional structure and lateral heterogeneity of higher-plant thylakoid membranes. This prevents us from quantifying diffusion coefficients, as can be performed in cyanobacteria (Mullineaux *et al.*, 1997; Mullineaux and Sarcina, 2002), and in isolated, laterally fused grana membranes (Kirchhoff *et al.*, 2008a). It also makes it harder to check that fluorescence changes are the result of diffusion. In a simple, homogeneous membrane, diffusion is easily recognizable because of the charac-



teristic redistribution of fluorescence. This is much harder to check in laterally segregated thylakoid membranes, where the fluorescence distribution is very inhomogeneous.

Despite these problems, we are confident that our FRAP measurements do reveal protein movements within the thylakoid membrane system, as the controls shown in Figures 2 and 3 and Table 1 eliminate the other possibilities.

Obviously an FRAP measurement is somewhat disruptive. Bleaching out fluorescence in a region of the membrane will significantly perturb the processes occurring there. This is particularly true of a photosynthetic membrane, where bleaching chlorophyll fluorescence means destroying the function of photosynthetic proteins. However it must be remembered that the bleaching is very localized. Although we damage function in the bleached region, we do not do any damage in the remainder of the chloroplast. The line bleaching used in our experiments generally bleaches out a single granum, but leaves the neighbouring grana unaffected. If we see fluorescence recovery in the bleached area, it indicates that chlorophyll proteins must be able to diffuse within the neighbouring, undamaged regions of the membrane, and escape from unbleached grana.

Our results on intact spinach chloroplasts show a partial fluorescence recovery in bleached grana. Although we cannot quantify the diffusion coefficients within this complex system, we can quantify the mobile fraction. There is variation from chloroplast to chloroplast, but on average about 13% of chlorophyll fluorescence is mobile (Table 1). The simplest explanation for our observation is that a relatively small proportion of grana chlorophyll proteins are mobile to the extent that they are not only able to diffuse within the appressed membrane region of a single granum, but they can also escape from the granum, diffuse through the connecting stroma lamellae, and enter the appressed membranes of another granum. Thus, a limited fraction of chlorophyll proteins are relatively loosely associated with the grana, and are able to exchange between grana on a timescale of a few minutes. This result can be compared with our previous result in isolated spinach grana membranes, where we showed that a fraction of chlorophyll proteins accounting for about 25% of chlorophyll fluorescence is mobile within the grana membrane (Kirchhoff *et al.*, 2008a). The remainder of the chlorophyll proteins appear completely immobile. Our current results extend this finding to a much more intact and physiologically relevant system, suggesting that some of the chlorophyll proteins that are mobile within the grana can also readily migrate into the stroma lamellae. It is clear that the grana and the stroma lamellae are part of a continuous membrane system, although the precise three-dimensional architecture of the system and the nature of the connections between the

granal membranes and the stroma lamellae remain controversial (Sillimoni *et al.*, 2005; Garab and Manela, 2008; Mustárdy *et al.*, 2008). Our results confirm that protein diffusion through these connections is possible. Once in the stroma lamellae, diffusion is likely to be relatively rapid. There is one report using single-particle tracking for the direct visualization of antibody-labelled LHCII (Consoi *et al.*, 2005). Given the large size of the fluorescent tag used, the LHCII visualized would have been excluded from appressed grana membranes, and was probably in the stroma lamellae. The tagged LHCII exhibited a random walk confined to a limited membrane area, with a mean diffusion coefficient of about  $0.003 \mu\text{m}^2 \text{sec}^{-1}$ , rising to about  $0.027 \mu\text{m}^2 \text{sec}^{-1}$  for phospho-LHCII (Consoi *et al.*, 2005). Our results confirm that there is at least some long-range diffusion within the thylakoid membrane system. Thus, models for state transitions and PSII repair that involve the migration of LHCII and PSII core complexes out of the grana and into the bulk phase of the stroma lamellae are plausible.

Our experiments indicate that grana are relatively stable structures *in vivo*. Even after considerable photodamage (photobleaching an entire granum), some chlorophyll proteins diffuse back into the same region of the sample, and there is rapid and complete diffusion of a lipophilic fluorophore back into the granum (Figure 3). This indicates that the location of the granum does not change. High-resolution studies using cryo-electron tomography suggest considerable effects of illumination and adaptation on grana structure (Chauvannet *et al.*, 2008). Such changes would probably not be detectable at optical resolution. However, our studies indicate that grana remain in place: they do not totally disintegrate or reform, even after drastic light exposure.

To further investigate the mobility of chlorophyll proteins in intact chloroplasts, we measured the effect of a pre-illumination to induce photoinhibition. Such a treatment will initiate the PSII repair cycle, the operation of which is essential for maintaining efficient photosynthesis under most conditions (Long *et al.*, 1984). Most models for the PSII repair cycle involve the migration of photodamaged PSII complexes out of the grana and into the stroma lamellae for repair (Aro *et al.*, 1993; Deena-Gonzalez and Aro, 2002). Thus, we might expect a photoinhibitory pre-treatment to mobilize the thylakoid membrane system, causing an increase in the mobile fraction in our measurements. We found this to be the case: a photoinhibitory pre-illumination significantly increases the mean mobile fraction from about 13% to about 18%. This suggests that an additional population of chlorophyll proteins is able to escape from the grana under these conditions. A simple interpretation would be that the mobile fraction under low light conditions consists of a subpopulation of LHCII (Dreyer *et al.*, 1993; Allen and Foreberg, 2001). After photoinhibition, a proportion of PSII complexes may also

become mobile. The result may be compared with previous findings in a cyanobacterium, where pre-illumination with bright red light results in the mobilization of up to approximately 50% of the chlorophyll fluorescence (Sarcina *et al.*, 2006). In the cyanobacterium we can be confident that the mobilized fraction does consist of PSII core complexes, as these contribute most of the chlorophyll fluorescence (Sarcina *et al.*, 2006).

In contrast to our finding with intact chloroplasts, we found that photoinhibitory pre-illumination has no effect on the mobility of chlorophyll proteins in isolated grana membranes (Table 1). There are several possible explanations for this discrepancy. Mobilization after photoinhibition may require some stromal factor that is absent from the isolated grana membrane preparation. Alternatively, mobilization may only be possible if there is adjacent membrane space available in the stroma lamellae. This idea would envisage a progressive increase in diffusion space in the grana as complexes escape into the stroma lamellae, starting with the complexes closest to the grana-stroma lamellae connections. Obviously this would not occur in the isolated grana membranes. Finally, there might be a diffusion barrier or 'gatekeeper' structure at the grana-stroma lamellae junctions. In this case, movement of proteins between grana and the stroma lamellae, and exchange between grana, would not be directly related to mobility *within* the appressed grana membrane. Again, this idea would explain why we saw no photoinhibition-induced mobilization of complexes in isolated grana membranes. The mobile fraction of chlorophyll fluorescence *within* isolated grana membranes is considerably higher than the fraction that diffuses *between* grana in intact thylakoids (Table 1). This might suggest a partial barrier to exchange between the grana and the stroma lamellae; however, it must be considered that the forces acting on complexes in isolated grana membranes could be different from those in the intact system. Freeze-fracture electron micrographs (Figure 7) provide some clues to the reasons for the increased protein mobility in photo-inhibited thylakoids. We could detect no drastic changes in PSII organization within the grana, suggesting that PSII mobilization is not a consequence of changes in the large-scale supramolecular interactions. Photoinhibition causes a small but significant decrease in the mean size of PSII complexes in the grana (perhaps because of a loss of part of the light-harvesting antenna), and it significantly increases the mean distance between complexes. This suggests a loss of PSII complexes from the grana (presumably caused by the escape to the stroma lamellae). Progressive loss of PSII complexes from the grana would make the system more fluid: studies on isolated grana membranes show that protein mobility is increased in a more 'dilute' system (Kirchhoff *et al.*, 2003a).

We used Arabidopsis mutants to further explore the factors required for mobilization of chlorophyll-protein

complexes after photoinhibition. Arabidopsis mutant studies have shown that STN7 and STN8 protein kinases are required for the phosphorylation of PSII components (PSI core proteins and LHCII) (Bonardi *et al.*, 2005). Protein phosphorylation by STN7 and STN8 is not absolutely required for the PSII repair cycle (Bonardi *et al.*, 2005). However, the dynamics of the repair cycle are impaired in the absence of these proteins, and this effect seems to be related to impairment of the disassembly of PSII supercomplexes (Tikkanen *et al.*, 2008). Therefore, it was suggested that PSII phosphorylation enables the disassembly of PSII supercomplexes, facilitating the migration of damaged PSII complexes into the stroma lamellae for repair (Tikkanen *et al.*, 2008). Fristedt *et al.* (2009) further propose that protein migration in the *stn7 stn8* mutant is impaired by an increase in the diameter of the grana discs. Our results on the Arabidopsis *stn8* and *stn7 stn8* mutants (Figure 6) are consistent with these models. Firstly, we find that the mobility of chlorophyll proteins in intact chloroplasts is lower in the *stn8* and *stn7 stn8* mutants than in the wild type. In both mutants, the mobile fraction of chlorophyll fluorescence is significantly lower than in the wild type (Figure 6). Secondly, we find that in *stn8* and *stn7 stn8* there is no increase in the mobile fraction following photoinhibition (Figure 5), in contrast to the effect seen in wild-type Arabidopsis (Figure 6) and spinach (Figure 4, Table 1). This provides direct evidence that PSII phosphorylation facilitates the exchange of chlorophyll proteins between the grana and the stroma lamellae. Phosphorylation switches the thylakoid membrane system to a more fluid state.

## EXPERIMENTAL PROCEDURES

### Plant material

Spinach leaves were purchased fresh from a local supermarket and kept overnight at 4°C in the dark prior to use. Wild-type (WT) *A. thaliana* (L.) ecotype Columbia (Col-0) plants, and the *stn8* and *stn7 stn8* mutant plants were grown in a Conviron plant growth room with an 8-h photoperiod at a light intensity of 200  $\mu\text{mol photons m}^{-2} \text{sec}^{-1}$  and a day/night temperature of 22/8°C, respectively. Mature rosette leaves from 10- to 12-week-old plants were dark adapted for 30 min prior to use for experiments.

### Isolation of intact chloroplasts and grana membranes

Intact chloroplasts were isolated from spinach and Arabidopsis leaves using a modification of the procedure described by Croucher *et al.* (2005). Fresh, dark-adapted leaves were homogenized in ice-cold grinding buffer (450 mM sorbitol, 20 mM Tricine, 10 mM EDTA, 10 mM NaHCO<sub>3</sub>, 5 mM MgCl<sub>2</sub> and 0.1% BSA at pH 8.4) with a Polytron (Kinematica GmbH, <http://www.kinematica.ch>). The homogenate was then filtered through four layers of muslin followed by four layers of muslin and one layer of cotton wool. The filtrate was centrifuged for 30 sec at 4000 *g* and 4°C. The chloroplast-enriched pellet was then washed twice and finally resuspended with a small volume of the buffer containing 300 mM sorbitol, 20 mM Tricine, 5 mM MgCl<sub>2</sub> and 2.5 mM EDTA, pH 7.5, and put on ice until use. The washing step was carried out with the resuspension medium. Chlorophyll concentration was determined

according to the method described by Porra *et al.* (1989). Isolated grana membranes were prepared from spinach leaves following a procedure described previously (Kirchhoff *et al.*, 2008a).

#### Control experiments with glutaraldehyde and nigericin

For the glutaraldehyde control, chloroplasts were resuspended in resuspending buffer containing 2% glutaraldehyde (Aqar Scientific Ltd, <http://www.aqarscientific.com>) and incubated for 30 min at 4°C in the dark, followed by centrifugation (60 sec at 5000 g). The clean pellet was then resuspended in the resuspending buffer, and chlorophyll content was measured. For the nigericin control, 4 µM nigericin (Sigma-Aldrich, <http://www.sigmaaldrich.com>) was added to the chloroplast suspension at a chlorophyll concentration of 10 µg ml<sup>-1</sup> prior to FRAP measurements.

#### Photoinhibitory treatment of intact chloroplasts and isolated grana membranes

Photoinhibition in intact chloroplasts and grana membranes was induced by high light exposure and monitored by PAM fluorescence measurements (Walz-101 PAM fluorometer; Walz, <http://www.walz.com>), as presented in Figure 5. In brief, the chloroplast suspension or grana membranes (at a chlorophyll concentration of 10 and 10 µg ml<sup>-1</sup>, respectively) was illuminated with a high intensity of light (3000 µmol photons m<sup>-2</sup> sec<sup>-1</sup>) for approximately 10–15 min at room temperature following saturating light pulses at 30-sec intervals for about 5 min. Prior to illumination, 25 µM 3-(3,4-dichlorophenyl)-1,1-dimethylurea (DCMU; Sigma-Aldrich) was added to eliminate the photochemical contribution to fluorescence quenching. The decrease in variable fluorescence ( $F_v/F_m$ ) after photoinhibitory treatment was more than 50%, and did not recover significantly, even after 2 h (Figure S1). Photoinhibited chloroplasts and grana membranes were immediately used for FRAP measurements.

#### Sample preparation for FRAP

Prior to experiments, chloroplast suspensions were diluted in resuspending buffer containing 5 µM BODIPY FL C12 (Invitrogen, <http://www.invitrogen.com>) to a final chlorophyll concentration of 10 µg ml<sup>-1</sup>. A glass slide was sealed with a coverslip using vacuum grease, so as to form a flow chamber. A 60-µl volume of 0.5% aqueous solution of polylysine (Sigma-Aldrich) was applied to the chamber, washed with the resuspending buffer, followed by the application of 60 µl of the chloroplast suspension. After 5 min of incubation the chloroplasts that were not immobilized were washed out with resuspending buffer. Isolated grana membranes were immobilized by adsorption onto an artificial lipid bilayer, as described previously (Kirchhoff *et al.*, 2008a).

#### FRAP measurements

The FRAP measurements were carried out with a Nikon PCM2000 laser-scanning confocal microscope, as previously described (Kirchhoff *et al.*, 2008a), using a 60× oil-immersion objective (numerical aperture 1.4). Images were recorded with pixel dimensions of 28 nm. The 468-nm line of a 100-mW Argon laser (Spectra-Physics, part of Newport, <http://www.newport.com>) was used for exciting both chlorophyll and BODIPY fluorescence. BODIPY fluorescence was selected with a 505-nm dichroic mirror and an interference filter with a transmission range of 500–527 nm. Chlorophyll fluorescence was selected with a Schott RG665 red glass filter transmitting above about 665 nm. Chloroplasts were visualized using a 20-µm confocal pinhole giving a point-spread in the z-direction of about 1.3 µm (full width at half maximum). For FRAP, a line was bleached across the sample by

withdrawing neutral density filters to increase the laser power by a factor of 32. The laser was then scanned repeatedly in one dimension for 5–7 sec. Laser power was then reduced again, and 10 post-bleaching images were recorded at 60-sec intervals. For the total bleaching control, the entire sample was bleached out by increasing the laser power and scanning across the entire field of view in xy mode for 15–20 sec.

#### Image processing and FRAP data analysis

In the intact chloroplast measurements, confocal images were converted to greyscale and deconvolved using the DeconvolutionJ plug-in of the public domain NIH ImageJ software (<http://rsb.info.nih.gov/ij/>) using 2D deconvolution based on the Wiener filter. The regularization parameter (gamma) was 0.0001. The point-spread function was determined by the visualization of 0.175-µm diameter fluorescence microspheres (PS-Speck Microscope Point Source kit; Invitrogen, Molecular Probes, <http://www.invitrogen.com>) with the same microscope set-up. The point-spread function in the xy plane was 0.76 µm (full width at half-maximum), and was reduced to 0.68 µm after deconvolution. The images were aligned to correct for the slight drift with time during the FRAP series using ImagePro Plus software (Media Cybernetics, <http://www.mediacy.com>), and then analysed with ImageJ. An individual granum was selected as a region of interest and the fluorescence intensity of that region was measured in pre- and post-bleach images. Simultaneously, the fluorescence in unbleached regions in post-bleach images was normalized to the same total fluorescence as in pre-bleach images. Mobile fractions were determined by fluorescence recovery curves, as presented in Figures 3 and 4, according to the following equation (Reits and Neeffjes, 2001):

$$R = (F_{\infty} - F_0) / (F_1 - F_0),$$

where  $R$  is the mobile fraction,  $F_{\infty}$  is the fluorescence intensity in the bleached region after full recovery,  $F_0$  is the fluorescence intensity just after bleaching (time 0) and  $F_1$  is the fluorescence intensity in the pre-bleach image.  $F_0$  values were normalized to 0 in all measurements, and an exponential curve was plotted to the experimental points in Origin (OriginLab, <http://www.originlab.com>). Mathematical analysis and calculations of diffusion coefficients for BBY membranes were performed as described previously (Kirchhoff *et al.*, 2008a).

#### Freeze-fracture electron microscopy

Freshly prepared spinach chloroplast suspensions were concentrated and rapidly frozen as a thin film by rapid immersion in slushy liquid nitrogen (-210°C) using Bal-Tech double rodless carriers, and were then fractured at -150°C in a Peltax E7000 freeze-fracture device. Realices were prepared by shadowing with platinum and carbon, cleared with bleach and examined with an FEI Tecnai T12 electron microscope at 120 000× magnification. The PSI particle average density and distance measurements ( $n \approx 2000$ ) were conducted using PIXAVATOR IA 4.2 (Intelligent Perception, <http://nperc.com>) and the Delaunay Voronoi plug-in of the ImageJ software. Measurements of PSI particle sizes were carried out with ImagePro Plus software.

#### ACKNOWLEDGEMENTS

TKG is supported by a Biotechnology and Biological Sciences Research Council (BBSRC) studentship. Part of the work was supported by a Royal Society International Joint Project grant to CWM and TK, and a BBSRC research grant to AVR. Equipment used for the project was purchased with Wellcome Trust and BBSRC grants to

CWM. We thank Prof. Dario Leister (LMU München) for the gift of the *Arabidopsis str6* and *str7 str8* mutants.

#### SUPPORTING INFORMATION

Additional Supporting Information may be found in the online version of this article:

**Figure S1.** Pulsed-amplitude modulation (PAM) fluorescence measurement on intact spinach chloroplasts subjected to high-intensity illumination ( $3000 \mu\text{E m}^{-2} \text{sec}^{-1}$ ) in the presence of  $25 \mu\text{M}$  3-(3,4-dichlorophenyl)-1,1-dimethylurea (DCMU). As in Figure 5, but with an extended timescale.

Please note: As a service to our authors and readers, this journal provides supporting information supplied by the authors. Such materials are peer-reviewed and may be re-organized for online delivery, but are not copy-edited or typeset. Technical support issues arising from supporting information (other than missing files) should be addressed to the authors.

#### REFERENCES

Albertsson, P.-Å. (2001) A quantitative model of the domain structure of the photosynthetic membrane. *Trends Plant Sci.* **6**, 340–354.

Allen, J.F. and Fersberg, J. (2001) Molecular recognition in thylakoid structure and function. *Trends Plant Sci.* **6**, 217–225.

Anderson, J.M. and Andersson, B. (1992) The architecture of photosynthetic membranes – lateral and transverse organization. *Trends Biochem. Sci.* **7**, 200–202.

Aro, E.-M., Virgisi, I. and Andersson, B. (1993) Photoinhibition of Photosystem II. Inactivation, protein damage and turnover. *Biochim. Biophys. Acta*, **1145**, 113–134.

Baena González, E. and Aro, E.-M. (2002) Biogenesis, assembly and turnover of photosystem II units. *Philos. Trans. R. Soc. Lond. B Biol. Sci.* **357**, 1451–1460.

Bonardi, V., Pasarelli, P., Boscar, T., Schläpff, E., Wagner, R., Pfander, M., T. Johns, P. and Lédor, D. (2005) Photosystem II acroporphorylation and photosynthetic acclimation require two different protein kinases. *Nature*, **437**, 1170–1182.

Erastov, D., Bullivent, S., Gilula, N.B. et al. (1975) Freeze etching of membranes. *Solano*, **100**, 54–56.

Chauvancin, S.G., Navo, R., Shimen, E., Charuv, D., Kiss, V., Ohad, I., Rumberg, V. and Reich, Z. (2005) Thylakoid membrane remodeling during state transitions in *Arabidopsis*. *Plant Cell*, **17**, 1029–1039.

Conson, F., Orza, R., Dunlap, D.D. and Finzi, I. (2005) Diffusion of light harvesting complex II in the thylakoid membrane. *EMBO Rep.* **6**, 782–786.

Craichmin, S., Rubin, A. and Horton, P. (2005) PsbS enhances non-photochemical fluorescence quenching in the absence of zeaxanthin. *FEBS Lett* **580**, 2053–2058.

Dekker, J.P. and Boekema, E.J. (2005) Supramolecular organization of thylakoid membrane proteins in green plants. *Biochim. Biophys. Acta*, **1706**, 12–39.

Dreyer, F., Carberg, L., Andersson, B. and Hanel, W. (1993) Lateral diffusion of an integral membrane protein: Monte Carlo analysis of the migration of phosphorylated light-harvesting complex II in the thylakoid membrane. *Biochemistry* **32**, 11915–11922.

Frisé, R., Willip, A., Granth, P., Crèvecoeur, M., Rochaix, J.-D. and Vener, A.V. (2009) Phosphorylation of Photosystem II controls functional macroscopic folding of photosynthetic membranes in *Arabidopsis*. *Plant Cell*, **21**, 3950–3964.

Garab, G. and Maréchal, C.A. (2009) Reply: on three-dimensional models of higher-plant thylakoid networks: elements of consensus, controversies and future experiments. *Plant Cell*, **20**, 2549–2551.

Habeeb, A.F.S.A. and Hiramoto, R. (1968) Reaction of proteins with glutaraldehyde. *Arch. Biochem. Biophys.* **126**, 16–26.

Horton, P., Ruban, A.V. and Walters, R.G. (1996) Regulation of light-harvesting in green plants. *Annu. Rev. Plant Physiol. Plant Mol. Biol.* **47**, 655–684.

Kirchheff, H., Mukherjee, U. and Galia, H.J. (2002) Molecular architecture of the thylakoid membrane: lipid diffusion space for plastoquinone. *Biochemistry*, **41**, 4872–4882.

Kirchheff, H., Tremmel, L., Haase, W. and Kubitschek, U. (2004) Supramolecular photosystem II organization in grana thylakoid membranes: evidence for a structured arrangement. *Biochemistry*, **43**, 9204–9212.

Kirchheff, H., Häferkamp, S., Allen, J.F., Epstein, D.B.A. and Mullineux, C.W. (2008a) Protein diffusion and macromolecular crowding in thylakoid membranes. *Plant Physiol.* **146**, 1571–1578.

Kirchheff, H., Lenhart, S., Büchel, C., Chi, L. and Nield, J. (2008b) Probing the organization of Photosystem II in photosynthetic membranes by steric force microscopy. *Biochemistry*, **47**, 431–440.

Lena, T., Leake, M.C. and Mullineux, C.W. (2008) Clustering and dynamics of cytochrome *b6-f* complexes in the *Escherichia coli* plasma membrane *in vivo*. *Mol. Microbiol.* **74**, 1397–1407.

Long, S.P., Humphries, S. and Falkowski, P.G. (1994) Photoinhibition of photosynthesis in nature. *Annu. Rev. Plant Physiol. Plant Mol. Biol.* **45**, 633–662.

Maxwell, K. and Johnson, G.N. (2000) Chlorophyll fluorescence – a practical guide. *J. Exp. Bot.* **51**, 655–668.

Mullineux, C.W. and Sarcina, M. (2002) Probing the dynamics of photosynthetic membranes with fluorescence recovery after photobleaching. *Trends Plant Sci.* **7**, 237–240.

Mullineux, C.W., Tolán, M.J. and Jones, G.R. (1997) Mobility of photosynthetic complexes in thylakoid membranes. *Nature*, **390**, 421–424.

Mustardy, L., Bettle, K., Steinbach, G. and Garab, G. (2008) The three-dimensional network of the thylakoid membranes in plants: a quantitative model of the grana-strucure assembly. *Plant Cell*, **20**, 2552–2557.

Napier, J.A. and Barnes, S.A. (1995) The isolation of intact chloroplasts. *Methods Mol. Biol.* **49**, 355–360.

Purra, R.J., Thompson, W.A. and Kriedemann, P.E. (1989) Determination of accurate extinction coefficients and simultaneous equations for assaying chlorophyll *a* and chlorophyll *b* extracted with 4 different solvents – verification of the concentration of chlorophyll standards by atomic absorption spectroscopy. *Biochim. Biophys. Acta*, **975**, 304–304.

Reis, L.A.J. and Neefjes, J.J. (2001) From fixed to FRAP: measuring protein mobility and activity in living cells. *Nat. Cell Biol.* **3**, 140–147.

Rintamäki, E., Kettunen, R. and Aro, E.-M. (1996) Differential D1 dephosphorylation in functional and photo-damaged Photosystem II centers. Dephosphorylation is a prerequisite for degradation of damaged D1. *J. Biol. Chem.* **271**, 14870–14875.

Ruban, A.V., Barera, R., Hloala, C., van Stekum, I.H.M., Kennis, J.T.M., Pascal, A.A., van Amerongen, H., Robert, B., Horton, P. and van Groenendijk, R. (2007) Identification of a mechanism of photoprotective energy dissipation in higher plants. *Nature*, **450**, 575–578.

Sarcina, M., Murata, N., Tobin, M.J. and Mullineux, C.W. (2003) Lipid diffusion in the thylakoid membranes of the cyanobacterium *Synechococcus* sp.: effect of fatty acid desaturation. *FEBS Lett* **553**, 295–298.

Sarcina, M., Bouzonville, N. and Mullineux, C.W. (2006) Mobilization of Photosystem II induced by intense red light in the cyanobacterium *Synechococcus* sp. PCC6802. *Plant Cell*, **18**, 457–464.

Shimada, F., Rav-Hon, O., Ohad, I., Rumberg, V. and Reich, Z. (2005) Three-dimensional organization of higher-plant chloroplast thylakoid membranes revealed by electron tomography. *Plant Cell*, **17**, 2580–2586.

Staelin, L.A. (2003) Chloroplast structure from chlorophyll granules to supra-molecular architecture of thylakoid membranes. *Photosynth. Res.* **78**, 195–196.

Staelin, L.A. and Amtzen, C.J. (1983) Regulation of chloroplast membrane function: protein phosphorylation changes the spatial organization of membrane components. *J. Cell Biol.* **97**, 1327–1337.

Stocking, C.R. and Franceschi, V.R. (1982) Some properties of the chloroplast envelope as revealed by electrophoretic mobility studies of intact chloroplasts. *Plant Physiol.* **70**, 1255–1259.

Tikkanen, M., Nurmi, M., Kangasjärvi, S. and Aro, E.-M. (2008) Core protein phosphorylation facilitates the repair of photodamaged photosystem II at high light. *Biochim. Biophys. Acta*, **1777**, 1432–1437.

